BNL-72336-2004
FORMAL REPORT

Proceedings of RIKEN BNL Research Center Workshop Volume 61

RIKEN-TODAI Mini-Workshop on "Topics in Hadron Physics at RHIC"

March 23-24, 2004

Organizers:

H. En'yo, H. Hamagaki, T. Hatsuda, Y. Watanabe, and K. Yazaki

Location:

Nishina Memorial Hall of RIKEN, Wako, Saitama, Japan

RIKEN BNL Research Center

Building 510A, Brookhaven National Laboratory, Upton, NY 11973-5000, USA

DISCLAIMER

This report was prepared as an account of work sponsored by an agency of the United States Government. Neither the United States Government nor any agency thereof, nor any of their employees, nor any of their contractors, subcontractors or their employees, makes any warranty, express or implied, or assumes any legal liability or responsibility for the accuracy, completeness, or any third party's use or the results of such use of any information, apparatus, product, or process disclosed, or represents that its use would not infringe privately owned rights. Reference herein to any specific commercial product, process, or service by trade name, trademark, manufacturer, or otherwise, does not necessarily constitute or imply its endorsement, recommendation, or favoring by the United States Government or any agency thereof or its contractors or subcontractors. The views and opinions of authors expressed herein do not necessarily state or reflect those of the United States Government or any agency thereof.

FOR UNCLASSIFIED, UNLIMITED STI PRODUCTS

Available electronically at-

OSTI:

http://www.osti.gov/bridge

Available for a processing fee to U.S. Department of Energy and its contractors, in paper from-

U.S. Department of Energy
Office of Scientific and Technical Information
P.O. Box 62
Oak Ridge, TN 37831
(865) 576-8401
Facsimile: (865) 576-5728
E-mail: reports@adonis.osti.gov

National Technical Information Service (NTIS):

Available for sale to the public from-

U.S. Department of Commerce
National Technical Information Service
5285 Port Royal Road
Springfield, VA 22131
(800) 553-6847
Facsimile: (703) 605-6900
Online ordering: http://www.ntis.gov/ordering.htm

Printed on recycled paper

Preface to the Series

The RIKEN BNL Research Center (RBRC) was established in April 1997 at Brookhaven National Laboratory. It is funded by the "Rikagaku Kenkyusho" (RIKEN, The Institute of Physical and Chemical Research) of Japan. The Center is dedicated to the study of strong interactions, including spin physics, lattice QCD, and RHIC physics through the nurturing of a new generation of young physicists.

During the first year, the Center had only a Theory Group. In the second year, an Experimental Group was also established at the Center. At present, there are four Fellows and eight Research Associates in these two groups. During the third year, we started a new Tenure Track Strong Interaction Theory RHIC Physics Fellow Program, with six positions in the first academic year, 1999-2000. This program had increased to include ten theorists and one experimentalist in academic year, 2001-2002. With five fellows having already graduated, the program presently has eleven theorists and three experimentalists. Of these eleven RHIC Physics Fellows, five have been awarded/offered tenured positions, and this will be their final year in the program.

Beginning in 2001 a new RIKEN Spin Program (RSP) category was implemented at RBRC. These appointments are joint positions of RBRC and RIKEN and include the following positions in theory and experiment: RSP Researchers, RSP Research Associates, and Young Researchers, who are mentored by senior RBRC Scientists. A number of RIKEN Jr. Research Associates and Visiting Scientists also contribute to the physics program at the Center.

RBRC has an active workshop program on strong interaction physics with each workshop focused on a specific physics problem. Each workshop speaker is encouraged to select a few of the most important transparencies from his or her presentation, accompanied by a page of explanation. This material is collected at the end of the workshop by the organizer to form proceedings, which can therefore be available within a short time. To date there are sixty proceeding volumes available.

The construction of a 0.6 teraflops parallel processor, dedicated to lattice QCD, begun at the Center on February 19, 1998, was completed on August 28, 1998. A 10 teraflops QCDOC computer in under development and expected to be completed this year.

N. P. Samios, Director
April 1, 2004

*Work performed under the auspices of U.S.D.O.E. Contract No. DE-AC02-98CH10886.

CONTENTS

Preface to the Series i

Introduction
H. En'yo, H. Hamagaki, T. Hatsuda, Y. Watanabe and K. Yazaki 1

Program of RIKEN-TODAI Mini-Workshop 3

Workshop Participants 5

What is the Experimental Evidence for the Color Glass Condensate?
Larry McLerran 7

Tensor Method for Pentaquark Baryons:
Mass, Decay Modes and Ideal Mixing
Su Houng Lee 33

On the Role of Strange Quark Mass in QCD Phase Diagram
--BCS-BEC Crossover in Color-Flavor Locked Phase?--
Hiroaki Abuki 61

Novel Phases of High Density Quark Matter and
Their Roles in Physical Systems
M. Tachibana 99

Color Ferromagnetism and Quantum Hall State of Gluon
M. Ohtani 117

Relation Between the Chiral and Deconfinement
Phase Transitions
Yoshitaka Hatta 135

Mode Coupling Theory for the Dynamic Aspect
Of the Chiral Phase Transition
K. Ohnishi 153

The Effect of Memory on Relation in ϕ^4 Theory
Takashi Ikeda 165

Glueball Properties Near the QCD Phase Transition
Noriyoshi Ishii 181

Thermal Effects on Quark-Gluon Mixed Condensate
$g(\bar{q}\sigma_{\mu\nu}G_{\mu\nu}q)$ From Lattice QCD
Takumi Doi 211

Detailed Lattice QCD Study of the Three-quark Potentials: The Ground-state and the Excited-state of the Static 3Q System
Toru T. Takahashi 235

Polarized Parton Distributions and Their Uncertainties
M. Hirai 257

Comment on π^0 Double Spin Asymmetry at RHIC
K. Sudoh 275

Chiral Doubling of Heavy-Light Hadrons in the Vector Manifestation
Chihiro Sasaki 289

Additional RIKEN BNL Research Center Proceeding Volumes 309

Contact Information

Introduction

The RIKEN-TODAI Mini-Workshop on "Topics in Hadron Physics at RHIC" was held on March 23rd and 24th, 2004 at the Nishina Memorial Hall of RIKEN, Wako, Saitama, Japan, sponsored by RIKEN (Institute of Physical and Chemical Research) and TODAI (University of Tokyo). The workshop was planned when we learned that two distinguished theorists in hadron physics, Professors L. McLerran and S.H. Lee, would be visiting TODAI and /or RIKEN during the week of March 22-26. We asked them to give key talks at the beginning of the workshop and attend the sessions consisting of talks by young theorists in RIKEN, TODAI and other institutes in Japan and they kindly agreed on both. Considering the JPS meeting scheduled from March 27 through 30, we decided to have a one-and-half-a-day workshop on March 23 and 24.

The purpose of the workshop was to offer young researchers an opportunity to learn the forefront of hadron physics as well as to discuss their own works with the distinguished theorists.

We had a session consisting of two one-hour talks by Profs. McLerran and Lee and three sessions each consisting of four half-an-hour talks by young theorists. The titles of the two main talks are given below.

L. McLerran (RBRC)	"What is the experimental evidence for the Color Glass Condensate ?"
S. H. Lee (Yonsei Univ.)	"Tensor method in pentaquark baryons – Mass, decay modes and ideal mixing –"

Although the workshop was announced only at the beginning of March, we had totally 31 participants including 18 graduate students and young postdocs.

The main talks were both inspiring and pedagogical, discussing the frontiers of hadron physics. The talks by young theorists were also well prepared and excellent. Discussions during the talks were active and fruitful. Profs. McLerran and Lee told us after the workshop that they had been very much impressed not only by the excellent presentations but also by the advanced contents of the talks of young speakers.

We are grateful to RIKEN for the financial support which enabled us to organize this workshop. It was held as an activity related to the collaboration with the RIKEN-BNL Research Center and we thank the director of the Center, Professor N. Samios, for the approval of publishing this proceedings as a volume of the RBRC Workshop Proceedings Series and general support. We are obliged to all the participants for making the workshop exciting and fruitful.

Special thanks are due to Ms.N. Kiyama , who did most of the administrative works and took care of drinks and snacks during the breaks, and Drs. M. Hirai, M. Ohtani and K. Sudoh for general assistance.

Hideto En'yo, Hideki Hamagaki, Tetsuo Hatsuda
Yasushi Watanabe and Koichi Yazaki

RIKEN,
May, 2004

Program of RIKEN-TODAI Mini-workshop

March 23 (Tue)

Session 1	Main lectures Chair: T. Hatsuda (Tokyo)
10:00-10:10	H. En'yo (RIKEN) Openning address
10:10-11:10	L. McLerran (RBRC) "What is the experimental evidence for the Color Glass Condensate ?"
11:10-12:10	S. H. Lee (Yonsei) "Tensor method for pentaquark baryons"
12:10-13:30	Lunch
Session 2	Various phases in QCD Chair: K. Iida (RIKEN)
13:30-14:00	H. Abuki (YITP) "On the role of strange quark mass in QCD phase diagram –BCS-BEC crossover in color-flavor locked phase ?–"
14:00-14:30	M. Tachibana(RIKEN) "Novel phases of high density quark matter and their roles in physical systems "
14:30-15:00	M. Ohtani(RIKEN) "Color ferromagnetism and quantum hall states in quark matter"
15:00-15:30	Y. Hatta (Kyoto) "Relation between the chiral and deconfinement phase transitions"
15:30-16:00	Coffee
Session 3	Dynamical aspects of the QCD plasma Chair: H. Fujii (Tokyo)
16:00-16:30	K. Ohnishi (Tokyo) "Mode coupling theory for the dynamic aspect of the chiral phase transition"
16:30-17:00	T. Ikeda (RBRC) "The effect of memory on relaxation in ϕ^4 theory"
17:00-17:30	N. Ishii (Titech) "Glueball properties near QCD phase transition"
17:30-18:00	T. Doi (Titech) "Thermal effects on quark-gluon mixed condensate from lattice QCD"

March 24 (Wed)

Session 4	Hard QCD, hadron spectroscopy Chair: K. Yazaki (RIKEN)
10:00-10:30	T. Takahashi (YITP) "Detailed lattice QCD study of the three-quark potentials: the ground-state and the excited-state of the static 3Q system"
10:30-11:00	M. Hirai (RIKEN) "Polarized parton distributions and their uncertainties"
11:00-11:30	K. Sudoh (RIKEN) "Comment on π^0 double spin asymmetry at RHIC"
11:30-12:00	C. Sasaki (Nagoya) "Chiral doubling of heavy-light hadrons in the vector manifestation"

End of workshop

List of Participants

Abuki, Hiroaki (YITP)
Akiba, Yasuyuki (RIKEN)
Doi, Takumi (Tokyo Institute of Technology)
En'yo, Hideto (RIKEN/RBRC)
Fujii, Hirotsugu (University of Tokyo)
Hatsuda, Tetsuo (University of Tokyo)
Hatta, Yoshitaka (Kyoto University)
Hirai, Masanori (RIKEN)
Iida, Kei (RIKEN)
Ikeda, Takashi (RBRC)
Ishii, Noriyoshi (Tokyo Institute of Technology)
Kohama, Akihisa (RIKEN)
Kojo, Toru (Kyoto University)
Lee, Suhoung (Yonsei University)
Mao, Yajun (Peking University)
Matsuura, Taeko (University of Tokyo)
Mawatarai, Kentaro (Kobe University)
McLerran, Larry (RBRC)
Nisida, Yusuke (University of Tokyo)
Ohnishi, Kazuaki (University of Tokyo)
Ohta, Shigemi (KEK)
Ohatani, Munehisa (RIKEN)
Sasaki, Chihiro (Nagoya University)
Sasaki, Syoichi (University of Tokyo)
Sudoh, Kazutaka (RIKEN)
Suzuki, Katsuhiko (Numazu College of Technology)
Tachibana, Motoki (RIKEN)
Takahashi, Toru (YITP)
Taketani, Atsushi (RIKEN)
Torii, Hisayuki (RIKEN)
Watanabe, Yasushi (RIKEN/RBRC)
Yazaki, Koichi (Tokyo Woman's Christian University/RIKEN)

What Is The Experimental Evidence For The Color Glass Condensate?

Larry McLerran

What is the Experimental Evidence for the Color Glass Condensate?

Larry McLerran

Nuclear Theory and Riken Brookhaven Research Center
BNL PO Box 5000
Upton NY 11973

Abstract

I discuss the Color Glass Condensate as a theory of the high energy limit of QCD. I disucss the experimental evidence concerning this hypothesis from HERA and RHIC.

What is the Evidence for the Color Glass Condensate? Motivation:

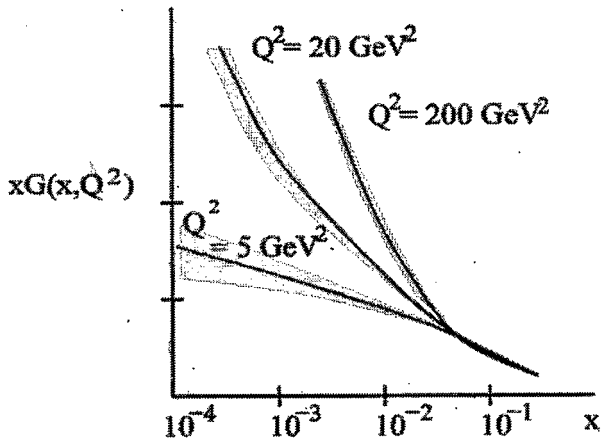

G,L,R
M,Q
M,V
BFKL

HERA

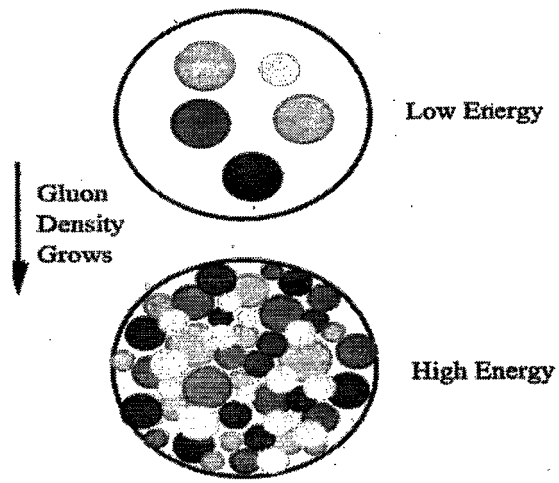

I,L,M

Density high →
Separation small →
$\alpha_S << 1$

1

What is Color Glass Condensate?

Glue at large x generates
glue at small x

Glue at small x is classical field
Time dilation → glassy
High phase space density → condensate

Phase space density ρ
Negative mass term $\sim -\rho$
Repulsive interactions $\sim \alpha_S \rho^2$

$$\rho = \frac{1}{\pi R^2} \frac{dN}{dy d^2 p_T} \sim \frac{1}{\alpha_S}$$

Separation of longitudinal scales
Renormalization Group
Limiting Fragmentation

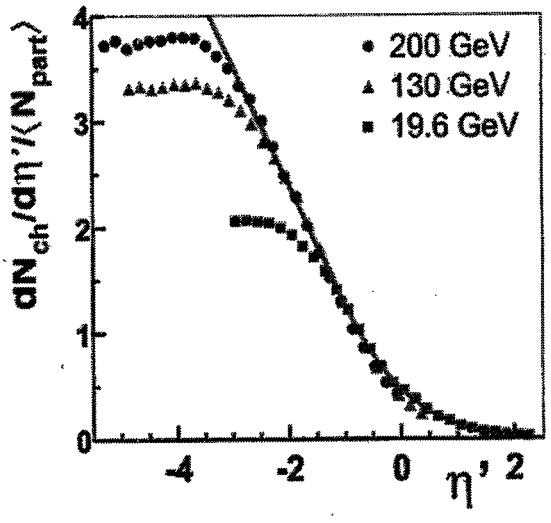

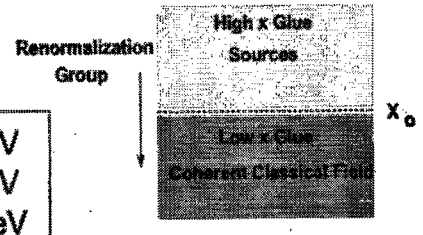

Total multiplicity is
$\sim N_Q + N_{\bar{Q}} + N_G$
for projectile evaluated at
$Q^2 \sim Q^2_{sat}(x_{target})$

Jalilian-Marian

2

Theory (Not Model) of CGC

Mathematically similar to a spin glass

$$Z = \int_{X_0} [dA][d\rho] \; exp\,(iS[A,\rho] - \chi[\rho])$$

ρ is the source
X_0 is the cutoff in x
$\chi[\rho]$ is the weight function
for the fields

M,V; K;B
JIMWLK; F;

$\chi[\rho]$ satisfies RG equation
derived from QCD

JIMWLK equation
Equaivalent in limits to
DGLAP, BFKL and BK equations

$\chi[\rho]$ quadratic is MV model

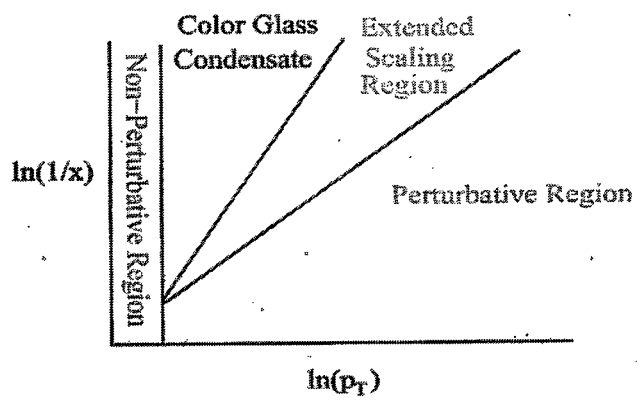

3

Why CGC is Important:

It is a new universal type of matter.

Matter:
Separation of gluons is
small compared to size.

New:
Can only be probed
at high energy and it is produced
in heavy ion collisions.

Universal:
Independent of hadron
Fundamental
(Universality also applies in scaling region)

It is a theory of:

The origin of glue and sea quarks
in hadrons.

The origin and nature of cross
sections and particle production

The distribution of valence quantum
numbers at small x

Provides initial conditions for
the QGP as produced in heavy ion collisions.

4

Infinite Momentum Frame:

In rest frame

Valence quarks
and occasional glue
and sea quarks

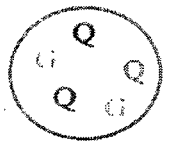

Nucleon is made of
states with 3 quarks
3 quarks with one gluon
3 quarks with two gluons
.....
3 quarks with 1000 gluons
.....

In infinite momentum frame

Wall of lots and
lots of glue at near
light speed

At low energy:
3 quarks and few gluons

At high energy:
Lots of gluons

Description is frame independent:

Mueller-Kovchegov Duality:
Infinite momentum frame multigluon
states are important.

Target rest frames:
Coherent multiple scattering.

Dipole Model Included in CGC Framework
Iancu-Mueller

5

What does the gluon wall look like?

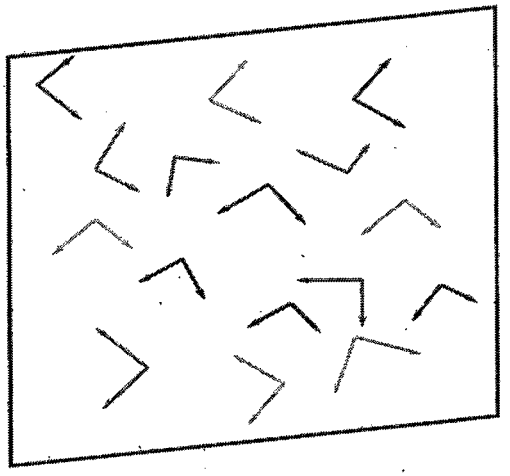

On sheet $x^- = t - z$ is small
Independent of $x^+ = t + z$
$F^{i+} \sim \partial/\partial x^- A^i$ is big.
F^{i-} and F^{ij} are small
$F^{i\pm} \sim E^i \pm \epsilon^{ij} B^j$

$\vec{E} \perp \vec{B} \perp \vec{z}$
Fields random in color

The density of gluons per unit area:

$$\frac{1}{\pi R^2}\frac{dN}{dy} \sim \frac{1}{\alpha_S} Q^2_{sat}(x)$$

6

Experimental Evidence: HERA

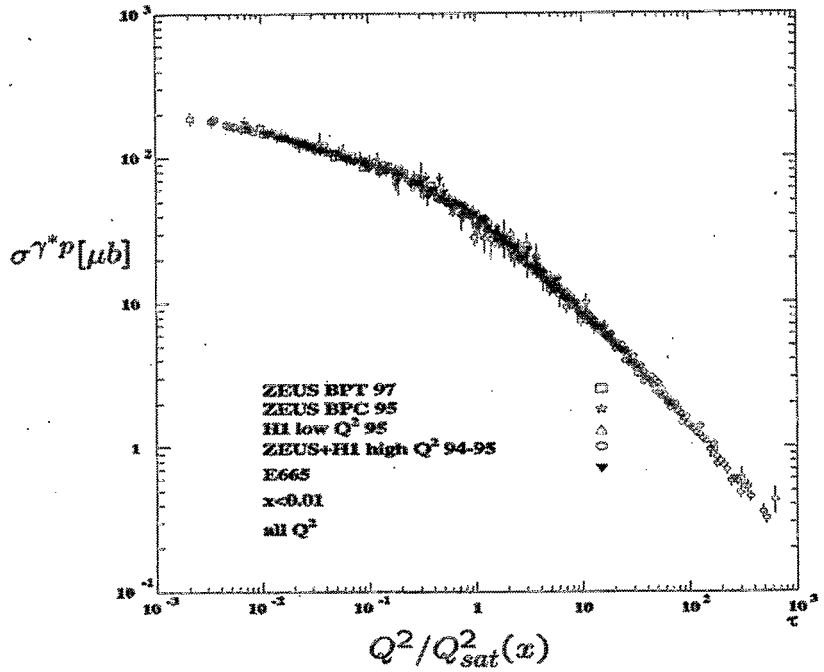

$\sigma \sim F(Q^2/Q^2_{sat}(x))$

$Q^2_{sat}(x)$ dependence on x computed by Mueller and Triantafyllopoulos

First observed by G-B,K,S. Geometric scaling shown to be property of CGC by IIM

For $Q^2 << Q^2_{sat}$ trivial

Works til $Q^2 \sim Q^4_{sat}/\Lambda^2$

Needs $x \leq 10^{-2}$

7

Experimental Evidence:

F_2 for $x < 10^{-2}$ and $Q^2 < 50\ GeV^2$

Must include computable deviations from geometric scaling

3 parameters: R, x_0, λ

$$N(x, r_T) = N_0 (r_T^2 Q_{sat}^2)^\gamma exp\left\{-\frac{1}{2\kappa\lambda ln(1/x)} ln^2(1/r_T^2 Q_{sat}^2)\right\}$$

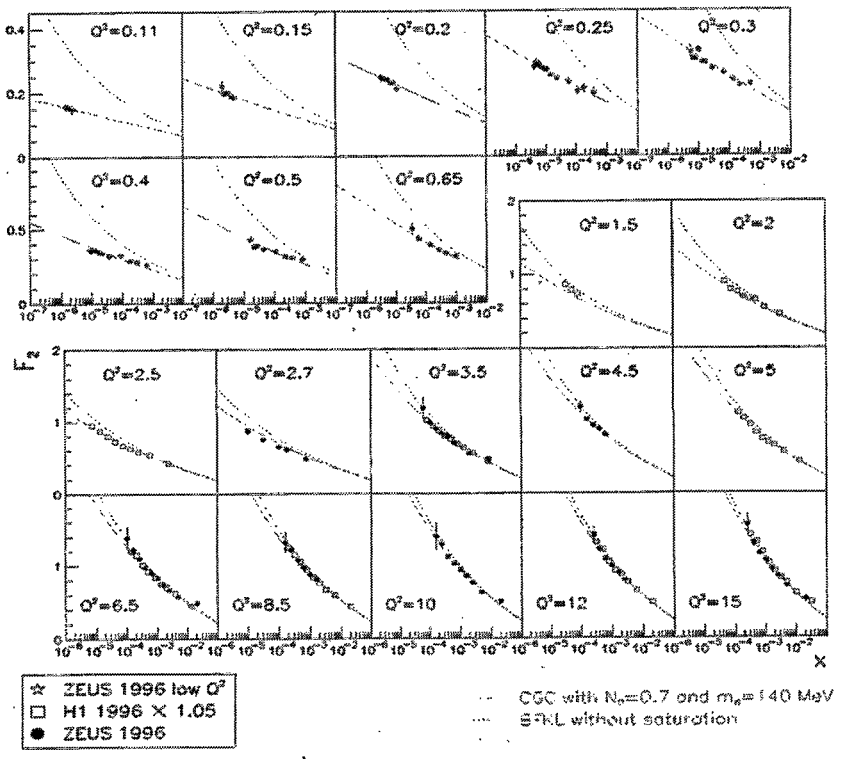

8

Experimental Evidence:

F_2 for $x < 10^{-2}$ and $Q^2 < 50GeV^2$

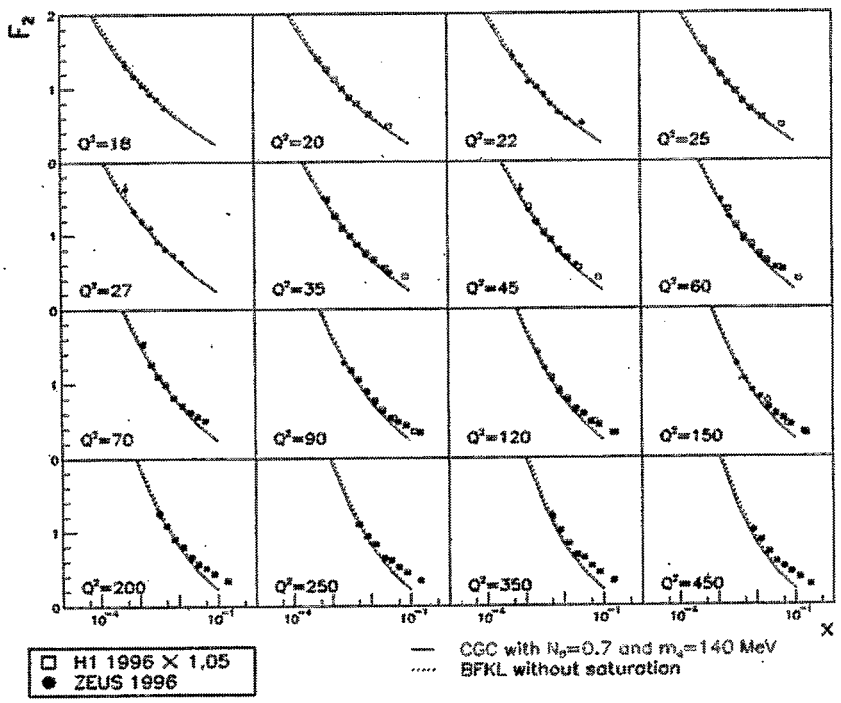

Early work by Golec-Biernat, Wustoff, Stasto
Kwiecinski, Kowalski, Bartels, Teaney.
Work above by Iancu, Itakura and Munier

9

Experimental Evidence:

Diffraction and Quasi-Elastic

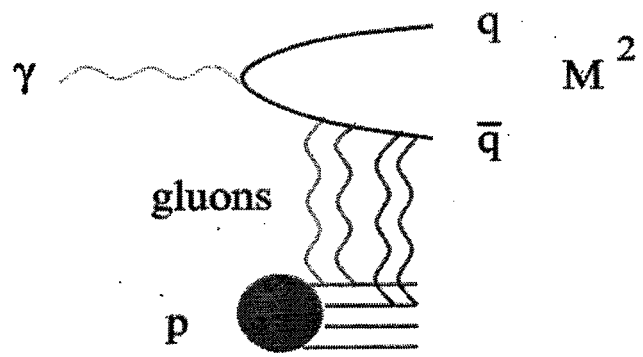

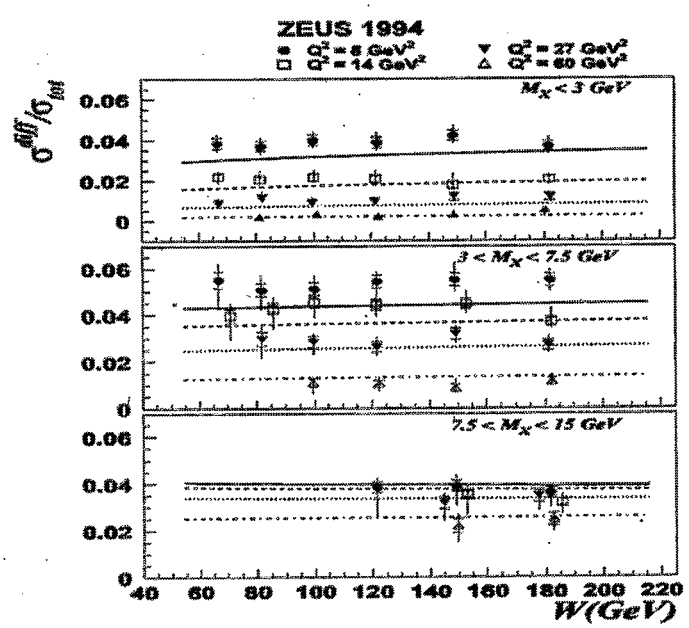

G-B, W; M,H; K,M; G-B,B; K,T;

10

Experimental Evidence:

Diffraction and Quasi-Elastic

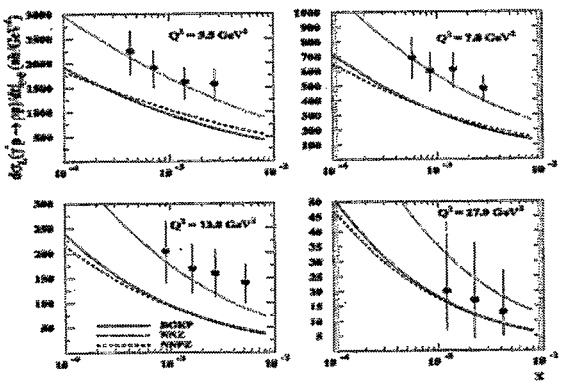

$\gamma^* p \to \rho p$

Some sensitivity to ρ wavefunction

Mueller, Munier and Stasto

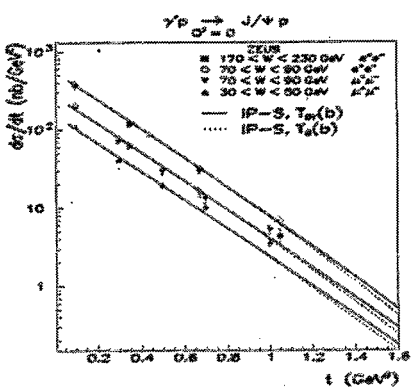

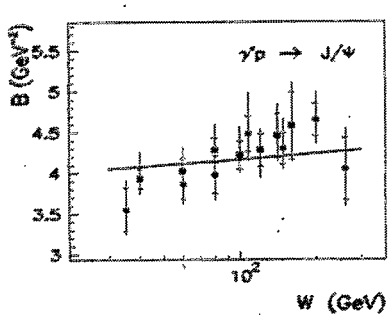

$\gamma^* p \to J/\Psi p$; Teaney and Kowalski

11

Experimental Evidence:

Qualitative Understanding of Hadronic σ^{tot}

The total hadronic cross section:

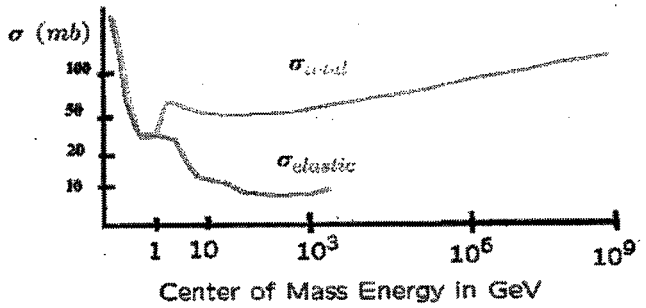

F,I,I,M
K,W

Nucleon becomes dark at some impact parameter b when the probability to scatter is of order one

The number of gluons increases as

$$(x_0/x_{min})^\lambda$$

$$x_{min} \sim \Lambda_{QCD}/E$$

The impact parameter distribution is

$$exp(-2m_\pi b).$$

$$(x_0/x_{min})^\lambda exp(-2m_\pi b) \sim 1$$

or

$$\sigma \sim b^2 \sim ln^2(1/x_{min}) \sim ln^2(E)$$

Froissart Bound Saturation

11a

Heavy Ion Collisions

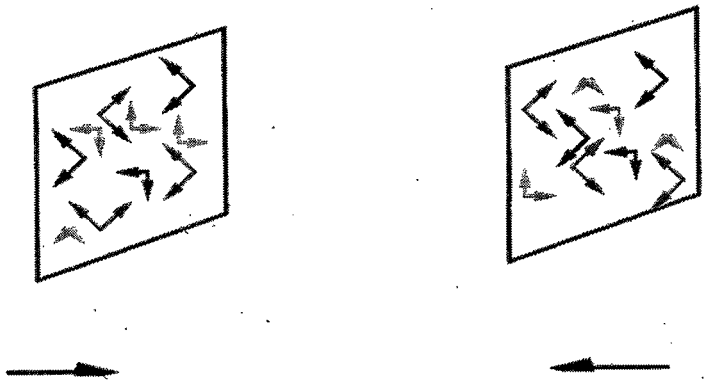

M,K,W; G, M; Krasnitz, Nara, Venugopalan

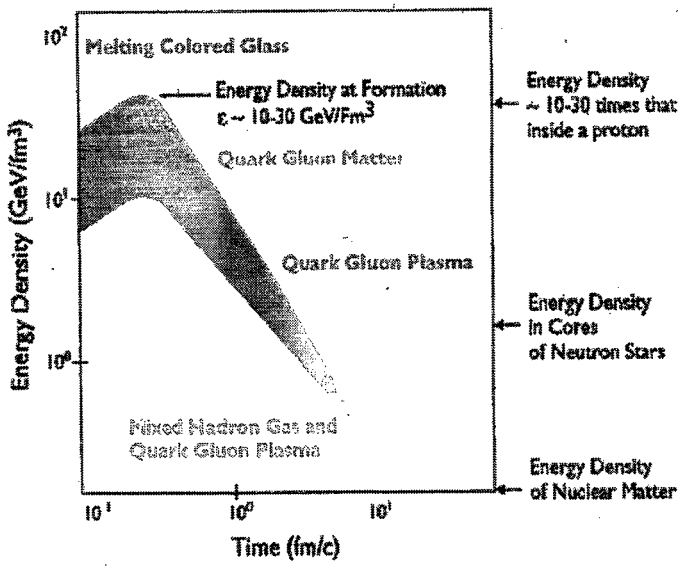

12

Evidence from Heavy Ions:

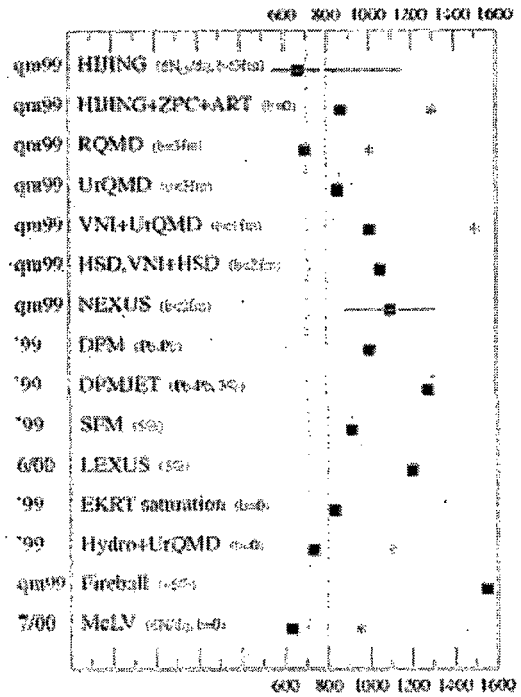

Krasnitz and Venugopalan

CGC is only theory which allows consistent computation of multiplicity

$$\frac{1}{\pi R^2}\frac{dN}{dyd^2p_T} \sim \frac{1}{\alpha_S}\frac{Q_{sat}^4}{p_T^4}$$

for $p_T >> Q_{sat}$

For $p_T \leq Q_{sat}$, the distribution softens and becomes integrable:

$$\frac{dN}{dy} \sim \frac{1}{\alpha_S}Q_{sat}^2$$

13

Global Features of Heavy Ion Collisions

dN/dη vs Centrality at η=0

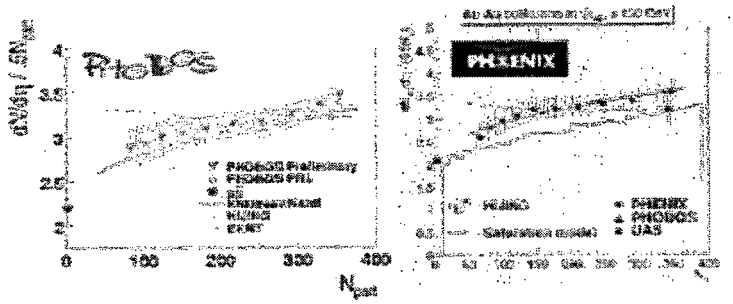

Kharzeev and Nardi

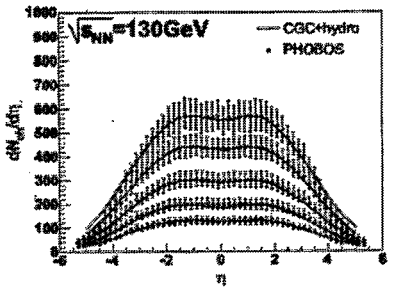

$$\frac{1}{N_{part}}\frac{dN}{dy} \sim \frac{1}{\alpha_S}$$

CGC initial conditions ala Kharzeev, Levin and Nardi lead to good rapidity and p_T distributions
Nara and Hirano

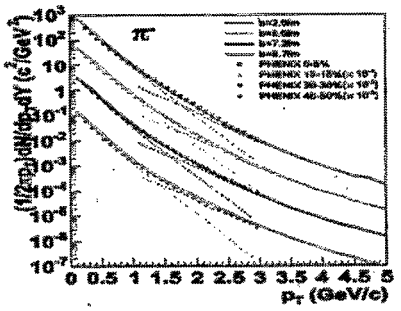

Not so much processing of dN/dy

14

AA and dA Collisions: Probing the Nuclear Wavefunction

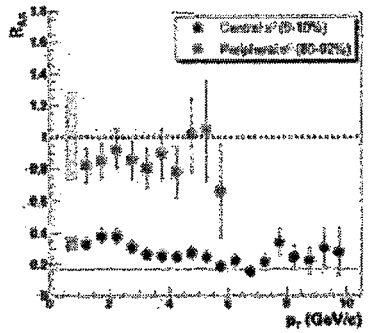

Heavy Ion Experiments at central rapidities give evidence of strong suppression relative to incoherent scattering

Is it an initial state effect (CGC) or final state (QGP)

Gluons and quarks come from $x \sim 10^{-1}$
Not small x

Some features of data look like geometrical scaling: K,L, M

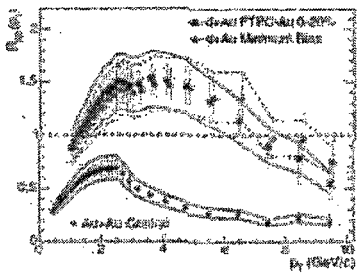

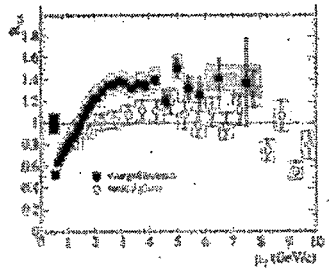

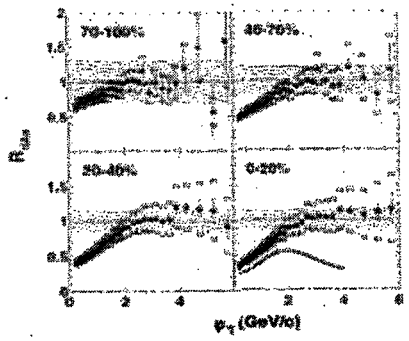

Conclusively established: Jet quenching at central rapidity is largely a final state effect (QGP).

15

dA Collisions and Shadowing:

What about the rapidity dependence of R_{dA}?

Cronin enhancement at nuclear rapidity

Small effect at zero rapidity

Forward rapidity? $x \sim 10^{-3}$.

Quantum evolution plus classical rescattering for CGC give suppression

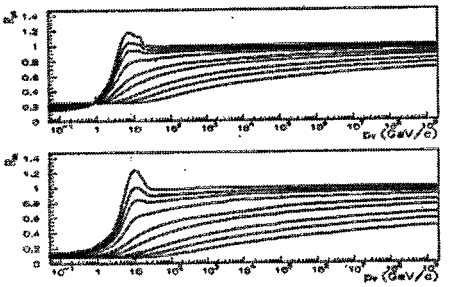

Centrality and rapidity dependence different

Very rapid evolution in Color Glass Condensate

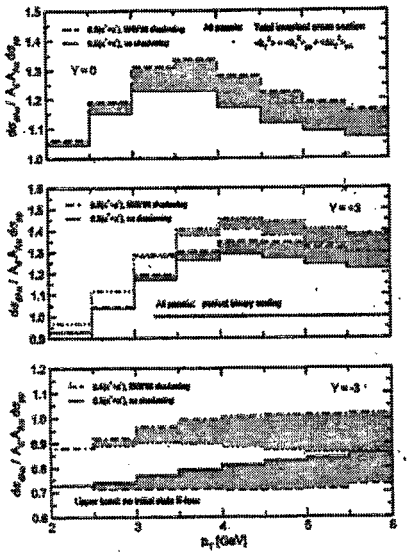

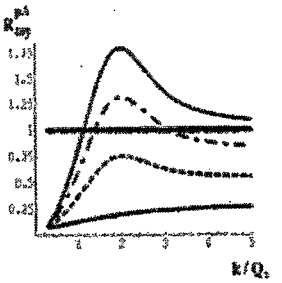

K,K

A,A,K,S,W

Classical multiple scattering gives Cronin enhancement

More matter at small x bigger Cronin enhancement

G,V,W

16

dA Collisions: Data

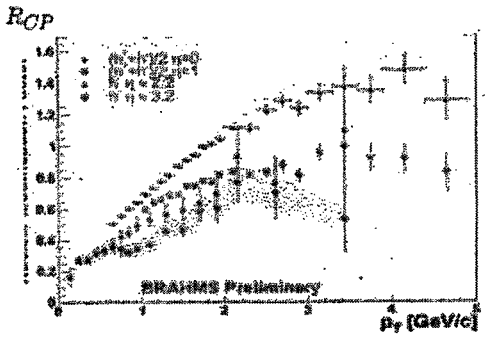

Brahms shows Cronin enhancement turn into suppression in deuteron fragmentation region

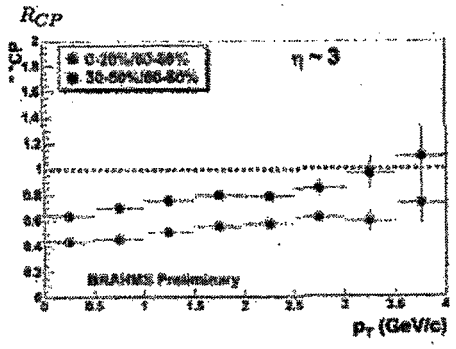

Brahms shows suppression increase as function of centrality

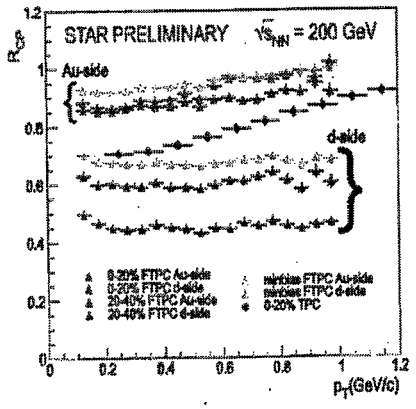

At lower p_T star shows suppression increase as one goes to fragementation region of deuteron

17

dA Data: More

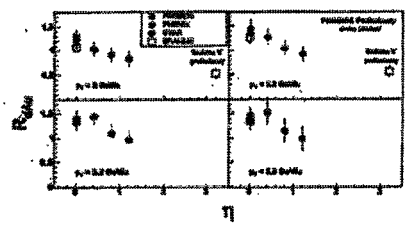

Phobos data at fixed p_T as function of rapidity.

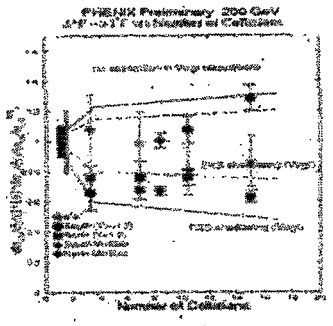

Phenix data for R_{dAu} of J/Ψ as function of centrality for different rapidities

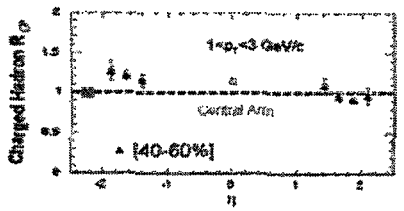

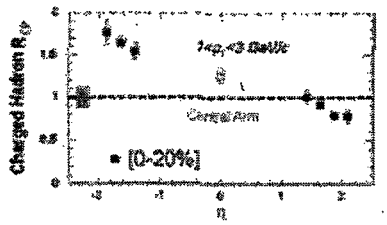

Phenix R_{dAu} for stopped hadrons and charm decays with $1\ GeV < p_T < 3\ GeV$ as function of rapidity and centrality

18

dA: What does it mean?

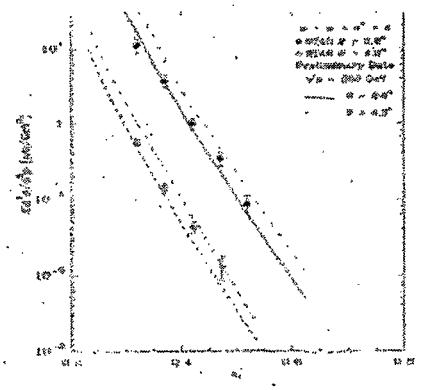

Perturbative QCD for single particle inclusive should work at p_T of several GeV

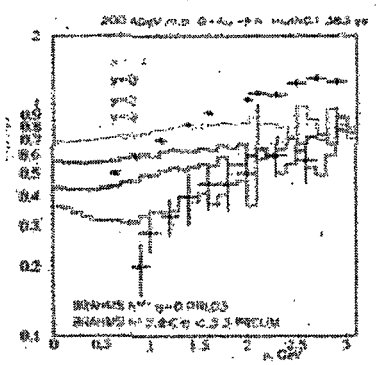

M. Gyulassy, QM2004

If Hijing with shadowing fits the forward data it is off by about a factor of two for the central data!

If this is "corrected" for multiple scattering one can arrange it to fit the central region but then it is almost a factor of 2 too large in the forward region! Accardi; Leval et. al. QM2004

But surely someone will find some shadowing computation

CGC provides a first principles theory of shadowing. It is falsifiable!

19

Does Color Glass Describe Brahms Data?

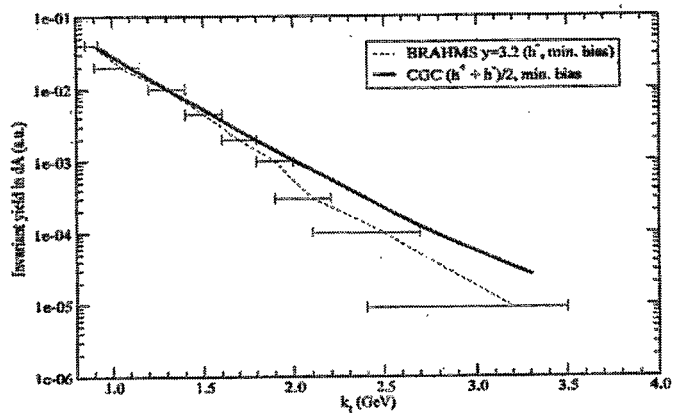

Jamal Jalilian-Marian:
Use CGC fits to DIS
and saturation momentum determined
from RHIC multiplicity measurements
No free parameter

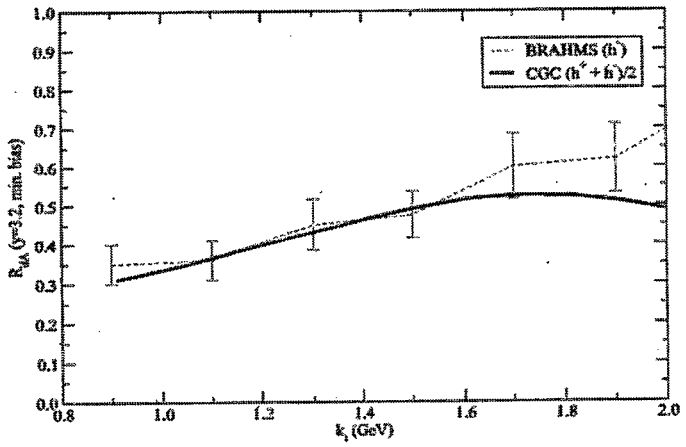

19a

Summary

"This is nothing short of a major discovery"
"it's going to trigger a real revolution in nuclear physics"
D. Kharzeev

Revolutions:

A re-allignment of relationships between large groups of people

Friends try to kill one another
Sometimes successfully!

Has bad consequences if you are not successful!

Perhaps the most famous scientific revolution:
The Copernican Revolution:

Ptolemaic theory could describe data much better than Copernican long after Copernican was accepted.

Copernicus had a simple intellectual framework.

It unified a large amount of different phenomena.

It was falsifiable.

20

Tensor Method for Pentaquark Baryons: Mass, Decay Modes and Ideal Mixing

Su Houng Lee

Tensor method for Pentaquark Baryons: Mass, Decay modes and Ideal mixing

Su Houng Lee
Department of Physics
Yonsei University
Seoul 120-749, Krea

This talk consists of two parts. In the first part, I will start by listing the experiments that reported observing the pentaquark states. Then I will discuss the soliton approach for the pentaquark, which motivated the experimental search for pentaquark states, and also discuss the criticisms related to the validity of the soliton approach. Then I will discuss other approaches on pentaquark states.

In the second part of my talk, I will introduce the tensor method based on SU(3) flavor symmetry. From constructing invariants composed of anti decuplet, decuplet and octet representations, I will rederive the mass formula for the pentaquark states, which follows from the SU(3) symmetry, and also discuss possible interaction terms. I will also discus why ideal mixing and fall apart decay naturally follows from an effective OZI rule. The simple tensor method provides specific ratios and selection rules from which one can experimentally test and discriminate between octet and decuplet pentaquark states.

Hadronic world

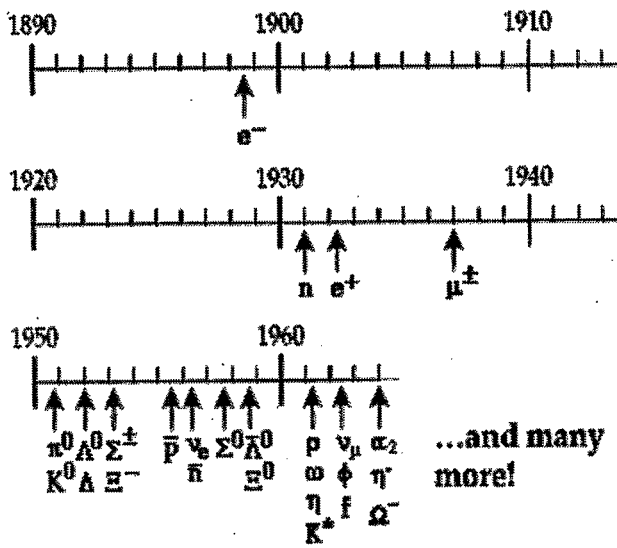

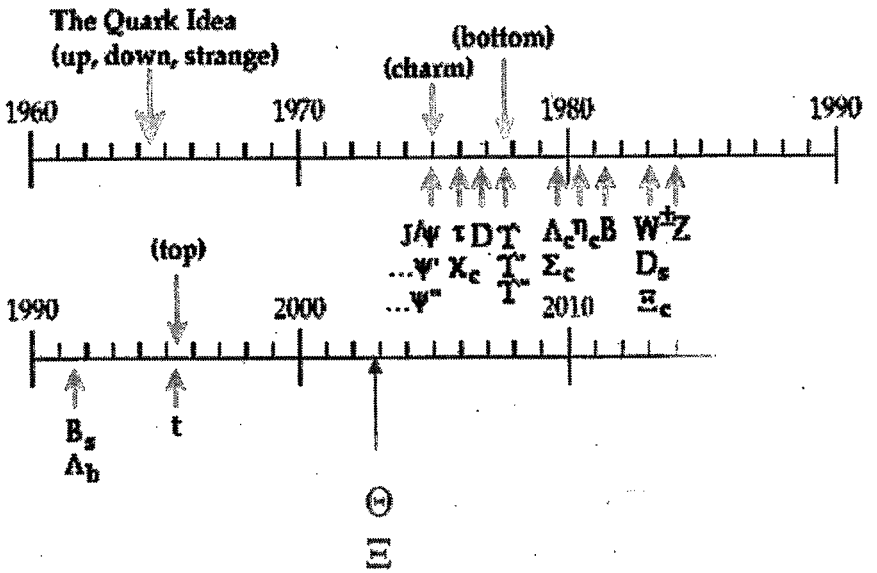

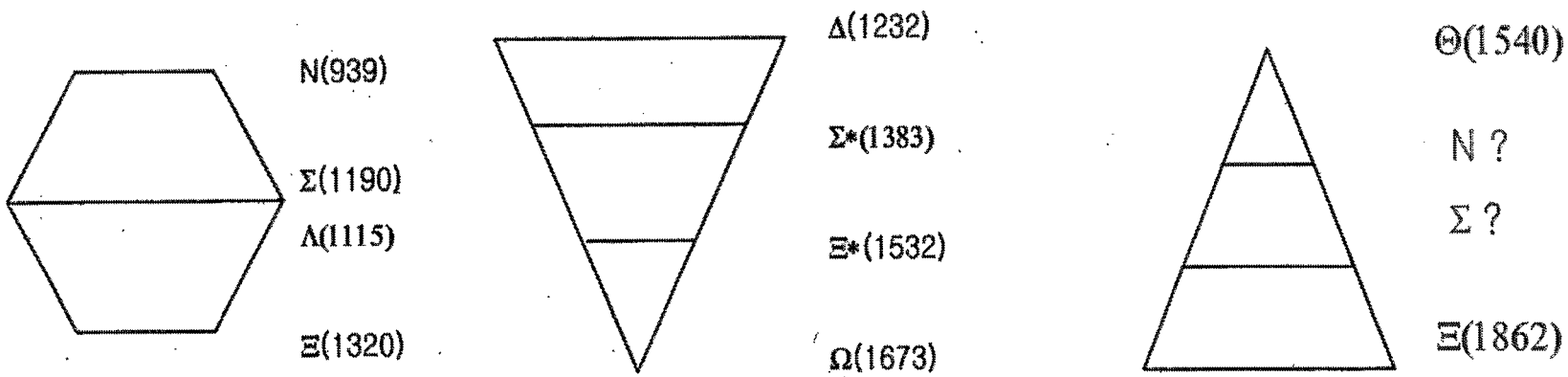

Experimental Summary

1. LEPS found Θ+ in K+ n invariant mass: Y=2 state with : uudd bar(s)
2. Class finds no Θ++ in K+ P invariant mass: anti-decuplet

$$\mathbf{3} \otimes \mathbf{3} \otimes \mathbf{3} \otimes \mathbf{3} \otimes \overline{\mathbf{3}} = \mathbf{35} + (3)\mathbf{27} - (2)\overline{\mathbf{10}} + (4)\mathbf{10} - (8)\mathbf{8} + (3)\mathbf{1},$$

Basic reaction	$M(\Theta^+)$ in MeV	$\Gamma(\Theta^+)$ in MeV	Collaboration/Reference
$\gamma n \to K^+K^-n$	1540 ± 10	≤ 25	LEPS [1]
$K^+Xe \to K^0pXe'$	1539 ± 2	≤ 9	DIANA [2]
$\gamma d \to K^+K^-pn$	1542 ± 5	≤ 21	CLAS [3]
$\gamma p \to K^+K^0_Sn$	$1540 \pm 4 \pm 2$	≤ 25	SAPHIR [4]
$\gamma p \to \pi^+K^-K^+n$	1537 ± 10	≤ 31	CLAS [5]
$\nu_\mu(\bar{\nu}_\mu) + A \to \mu^-(\mu^+)pK^0_SX$	1533 ± 5	≤ 20	BBCN [6]
$\gamma p \to \pi^+K^-K^+n$	1555 ± 10	≤ 26	CLAS [7]
$ed \to pK^0_sX$	$1526 \pm 2 \pm 2.5$	≤ 7.5	HERMES [8]

TABLE I: Summary of the experimental data for the $\Theta^+(1540)$ baryon.

3. NA49 hep-ex/0310014 : found Ξ*(1862) in Ξ- π- (ddss bar(u)) with width< 18 MeV
4. H1 hep-ex/04031017: found Θc0(3099) in D* p (uudd bar(c)) with width= 12+-3 MeV (not D p, due to experimental diff?)

Solition Model: original prediction (Diaknov, Petrov, Polyakov 97)

1. SU(3) solition $L_{Kin}(U^2)+L_{Skyrme}(U^4)+L_{W-Z}$

$$U(x,t)=R(t)\begin{pmatrix}\exp(i\pi\cdot r) & 0\\ 0 & 1\end{pmatrix}R^{\dagger}(t)$$

2. Hamiltonian $H^{Rot}=\frac{1}{2I_1}\sum_{A=1}^{3}\hat{J}'^2_A+\frac{1}{2I_2}\sum_{A=4}^{7}\hat{J}'^2_A$

$$E_{10}-E_8=\frac{3}{2I_1},\quad E_{\overline{10}}-E_8=\frac{3}{2I_2}$$

$$J'_8=-\frac{N_c B}{2\sqrt{3}}$$

-> only SU(3) representations containing Hypercharge= N_c /3 are allowed

moreover, the number of states at S=0 must determine the spin of the representation because I=J in the SU(2) solition

3. Anti decuplet mass: including $O(m_s N_c)$ and $O(m_s N_c^0)$ splitting

splitting within anti-decuplet: fixed by splitting within octet and decuplet and

splitting among representation: fixed by N(1710) to be a member of anti decuplet

4. Anti decuplet width: including $O(1/N_c)$ correction

Solition Model: comparison with experiment

	Solition model		experiment		Quark model		SU(3)	
MeV	mass	width	mass	width	Wave function	Total strange quark	mass	width
Θ	1530	15X2	1535	<10 or 1	$uudd\bar{s}$	1	1535	Γ
$N_{\underline{10}}$	1710	40			$\sqrt{\frac{1}{3}}uudd\bar{d}+\sqrt{\frac{2}{3}}uuds\bar{s}$	4/3	1644	
$\Sigma_{\underline{10}}$	1890	70			$\sqrt{\frac{2}{3}}uuds\bar{d}+\sqrt{\frac{1}{3}}uuss\bar{s}$	5/3	1753	
$\Xi_{\underline{10}}$	2070	>140	1862	<18	$uuss\bar{d}$	2	1862	3.5 Γ
	Only s= ½ antidecuplet				s= ½ 1+½ antidecuplet			
$\Theta_{\underline{c}}$	2700		3099	<12				10 Γ

Tokyo 2004

Solition Model for antidecuplet: why it is an artifact of large N_c

(T. Cohen 03)

1. Solition picture is valid at large N_c:

Semi-classical quantization is valid for slow rotation: ie. Valid for describing excitations of order 1/N_c, so that it does not mix and breakdown with vibrational modes of order 1

2. Lowest representation at large N_c (p,q)

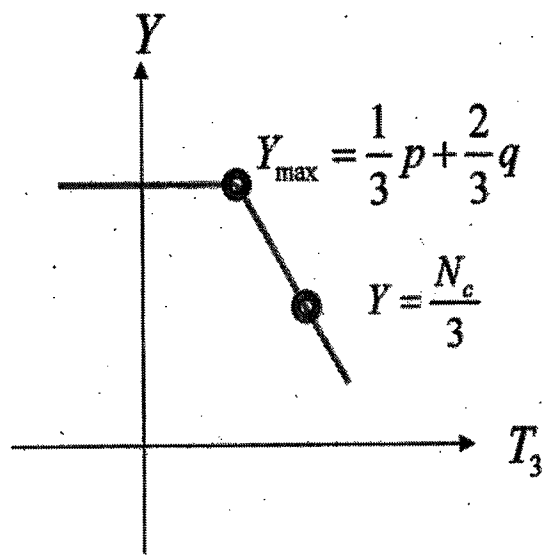

Qunatization constraint requires $Y_{\max} \geq \frac{N_c}{3}$

1. Octet $(1, \frac{N_c - 1}{2})$
2. Decuplet $(3, \frac{N_c - 3}{2})$
3. Anti decuplet $(0, \frac{N_c + 3}{2})$

(lowest representation containing s=1) $Y = \frac{N_c B}{3} + S$

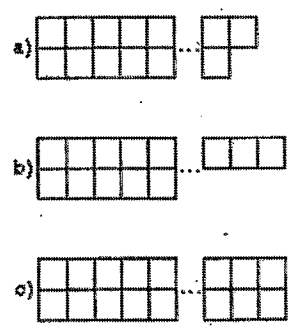

$$H^{Rot} = \frac{1}{2I_1}\sum_{A=1}^{3}\hat{J}'^2_A + \frac{1}{2I_2}\sum_{A=4}^{7}\hat{J}'^2_A \qquad E_{10} - E_8 = \frac{3}{2I_1}, \quad E_{\overline{10}} - E_8 = \frac{3+N_c}{4I_2}$$

Bound state approaches for SU(3) solition

1. SU(2) solition+ Kaon $L_{Kin}(U^2)+L_{Skyrme}(U^4)+L_{W-Z}$

2. Successful for hyperon (attractive anti-kaon) but repulsion for kaon (no pentaquark) from WZ term

3. But found to give bound state for chamed meson (uudd bar(c)) with mass 2700 MeV

   But H1 found $\Theta_c^0 \rightarrow D^* + p$ at 3099 MeV ?

4. Nowak, Praszalowics hep-ph/0403184

   1. for heavy-light meson: chiral partners exist : BaBar (D_s*), CLEO, Belle

      $(0^-,0^+)$ $(1^-,1^+)$ with mass 350 -400 MeV apart

   2. H1 observed chiral partner of ground state Θ_c(pD)

   3. If this is right -> there should be ground state charmed pentaquark at 2700 MeV and the theta pentaquark ?

Tensor notation of flavor SU(3)

What are model dependent results and what are the consequences of SU(3) ?

1. Fundamental representation $\square$ $\qquad q^i \to U^i_j q^j$

2. Octet representation $\qquad B^i{}_j \to U^i{}_a B^a{}_b U^{\dagger b}{}_j$

3. Anti-decuplet representation 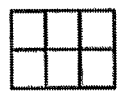

$$\mathcal{P}_{ijk} \to P_{abc} U^{\dagger a}{}_i U^{\dagger b}{}_j U^{\dagger c}{}_k,$$

4. Construction of effective Lagrangian

contract each index of representation with delta and epsilon

$$\varepsilon_{ijk} \overline{P}^{ilm} B^j_l M^k_m$$

$$\delta^j_m U^i_j U^{\dagger m}_l = \delta^i_l$$

$$\varepsilon_{ijk} U^i_l U^j_m U^k_n = \varepsilon_{lmn}$$

SU(3) mass formulas (m_s)

- QCD mass term

$$H_{QCD} = \bar{q}\begin{pmatrix} m_u & 0 & 0 \\ 0 & m_d & 0 \\ 0 & 0 & m_s \end{pmatrix} q = \bar{q}^i Y_i^j q_j$$

- In Hadronic world, there are no quarks and Hadrons form higher irreducible representation of SU(3)

- Octet representation mass term

$$H_{Octet} = a\bar{B}_i^j Y_j^l B_l^i + b\bar{B}_i^j Y_l^i B_j^l + c\bar{B}_i^j B_j^i$$

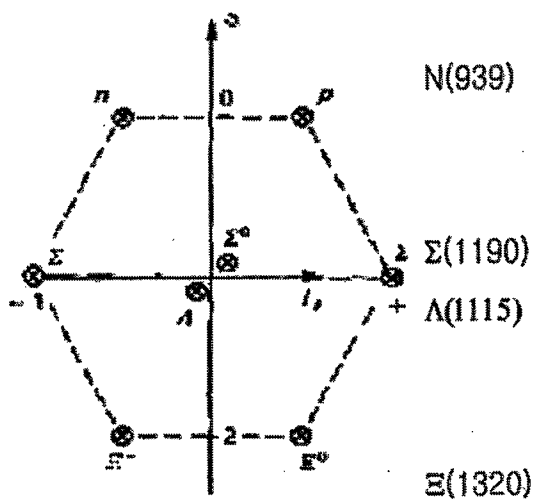

4 masses– 3 parameters
Gell-Mann Okubo mass formula

$$3M_\Lambda + M_\Sigma = 2(M_N + M_\Xi)$$

3x1115+1190=2x(939+1320)

4535 MeV =4518 MeV

SU(3) mass formula

- Decuplet representation mass term

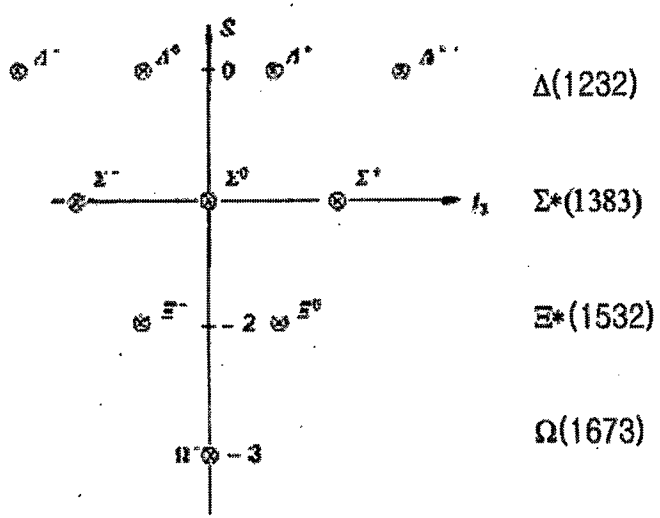

$$H_{Decuplet} = a\overline{T}^{ijk} Y_k^l T_{lij} + c\overline{T}^{ijk} T_{ijk}$$

4 masses−2 parameters

$$M_\Omega - M_{\Xi^*} = M_{\Xi^*} - M_{\Sigma^*} = M_{\Sigma^*} - M_\Delta$$

140 MeV 150 MeV 150 MeV

Mass formula for anti-decuplet

hep-ph/0310117 , Y. Oh, H. Kim , SHL

- $\Theta^+(uudd\bar{s})$ is an isosinglet; a member of anti-decuplet

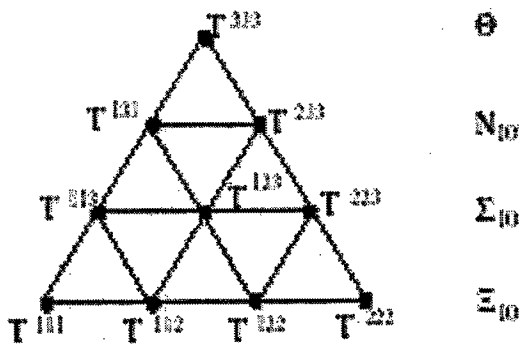

$$H_{Anti-decuplet} = a\bar{T}^{ijk}Y_k^l T_{lij} + c\bar{T}^{ijk}T_{ijk}$$

again 2 parameters

$$M_{\Xi_{10}} - M_{\Sigma_{10}} = M_{\Sigma_{10}} - M_{N_{10}} = M_{N_{10}} - M_{\Theta}$$

Since $M_{\Theta} = 1540$ MeV, $M_{\Xi_{3/2}} = 1862$ MeV

We will have

$$M_{N_{10}} = 1647 \text{ MeV}, \quad M_{\Sigma_{10}} = 1755 \text{ MeV}$$

SU(3) symmetric interaction is not so bad to begin with

$$L = g_1 \overline{B_i^j} P_j^l B_l^i + g_2 \overline{B_l^i} P_j^l B_i^j$$

Janssen et al., EPJA 11 (2001) 105, PRC 67 (2003) 052201, PRC 66 (2002) 035202,
Benhold et al., Phys.Rev.C36:438-440,1987.
Nijmegen potential uses SU(3)symmetry for NN, YN interactions.

For Decuplet meson Baryon, only one term is possible

$$L = g\varepsilon_{ilm} \overline{D^{ijk}} P_j^l M_k^m$$

$$\Gamma(\Delta \to N\pi) = \frac{3G_0^2}{2\pi(M_\Delta + M_N)^2}|\vec{p}|^3 \frac{M_N}{M_\Delta} \cdot \frac{1}{5} = 110\,MeV \ vs.\ 110\,MeV\ (exp.),$$

$$\Gamma(\Sigma^* \to \Lambda\pi) = \frac{3G_0^2}{2\pi(M_{\Sigma^*} + M_\Lambda)^2}|\vec{p}|^3 \frac{M_\Lambda}{M_{\Sigma^*}} \cdot \frac{1}{10} = 35\,MeV \ vs.\ 35\,MeV\ (exp.),$$

$$\Gamma(\Sigma^* \to \Sigma\pi) = \frac{3G_0^2}{2\pi(M_{\Sigma^*} + M_\Sigma)^2}|\vec{p}|^3 \frac{M_\Sigma}{M_{\Sigma^*}} \cdot \frac{1}{15} = 5.3\,MeV \ vs.\ 4.8\,MeV\ (exp.),$$

$$\Gamma(\Xi^* \to \Xi\pi) = \frac{3G_0^2}{2\pi(M_{\Xi^*} + M_\Xi)^2}|\vec{p}|^3 \frac{M_\Xi}{M_{\Xi^*}} \cdot \frac{1}{10} = 8.6\,MeV \ vs.\ 10\,MeV\ (exp.),$$

Diakonov, Petrov, Polyakov (97)

Search for remaining anti-decuplet states

- Very small hadronic interaction

  Y. Oh, H. Kim, SH Lee (hep-ph/0310117)

$$L_{10\text{-}8\text{-}8} = -ig\varepsilon_{ilm}\overline{T}^{ijk}M^l_j B^m_k$$

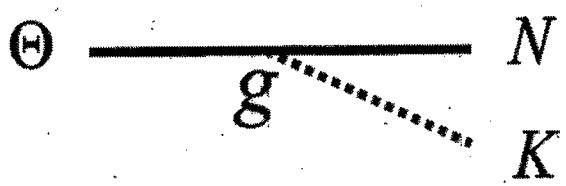

$$\Gamma_{\Xi_{10}} = 3.5\times\Gamma_{\Theta} < 18\ \text{MeV}$$

- Forbiden decay

$$L_{\overline{10}\text{-}8\text{-}10} = g\varepsilon_{ijl}\varepsilon_{mno}\overline{T}^{ijk}M^l_k D^{mno} = 0$$

Θ^+		$\bar{N}^+$		$\bar{N}^0$		$\bar{\Sigma}^+$	
K^+n	$\sqrt{6}$	π^+n	$\sqrt{2}$	π^0n	1	$\pi^+\Lambda$	$\sqrt{3}$
K^0p	$-\sqrt{6}$	π^0p	1	π^-p	$-\sqrt{2}$	$\pi^+\Sigma^0$	-1
		ηp	$-\sqrt{3}$	ηn	$\sqrt{3}$	$\pi^0\Sigma^+$	1
		$K^+\Lambda$	$\sqrt{3}$	$K^+\Sigma^-$	$\sqrt{2}$	$\eta\Sigma^+$	$-\sqrt{3}$
		$K^+\Sigma^0$	-1	$K^0\Lambda$	$-\sqrt{3}$	$K^+\Xi^0$	$-\sqrt{2}$
		$K^0\Sigma^+$	$-\sqrt{2}$	$K^0\Sigma^0$	-1	$\bar{K}^0p$	$\sqrt{2}$
$\bar{\Sigma}^0$		$\bar{\Sigma}^-$		$\Xi^+_{3/2}$		$\Xi^0_{3/2}$	
$\pi^+\Sigma^-$	1	$\pi^0\Sigma^-$	1	$\pi^+\Xi^0$	$-\sqrt{6}$	$\pi^+\Xi^-$	$-\sqrt{2}$
$\pi^0\Lambda$	$\sqrt{3}$	$\pi^-\Lambda$	$-\sqrt{3}$	$\bar{K}^0\Sigma^+$	$\sqrt{6}$	$\pi^0\Xi^0$	-2
$\pi^-\Sigma^+$	-1	$\pi^-\Sigma^0$	-1			$\bar{K}^0\Sigma^0$	2
$\eta\Sigma^0$	$-\sqrt{3}$	$\eta\Sigma^-$	$\sqrt{3}$			$K^-\Sigma^+$	$\sqrt{2}$
$K^+\Xi^-$	-1	$K^0\Xi^-$	$\sqrt{2}$				
$K^0\Xi^0$	1	K^-n	$-\sqrt{2}$				
$\bar{K}^0n$	-1						
K^-p	1						
$\Xi^-_{3/2}$		$\Xi^{--}_{3/2}$					
$\pi^0\Xi^-$	-2	$\pi^-\Xi^-$	$\sqrt{6}$				
$\pi^-\Xi^0$	$\sqrt{2}$	$K^-\Sigma^-$	$-\sqrt{6}$				
$\bar{K}^0\Sigma^-$	$-\sqrt{2}$						
$K^-\Sigma^0$	2						

N(1710) ->Δπ

Hence can not be a pure anti-decuplet

Pentaquark Baryons can mix (Follow the quark picture of Jaffe and Wilczek)

Previous scenario is possible but expect to have a pentaquark octet

$$3 \otimes 3 \otimes 3 \otimes 3 \otimes \overline{3}$$

$$\rightarrow (\overline{3} \oplus 6) \otimes (\overline{3} \oplus 6) \otimes \overline{3}$$

$$\rightarrow \quad \overline{6} \otimes \overline{3} = 1\overline{0} + 8$$

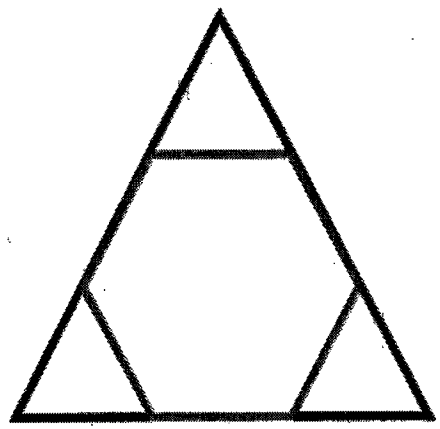

Mixing in Vector Meson Octet

Vector meson octet mass formula

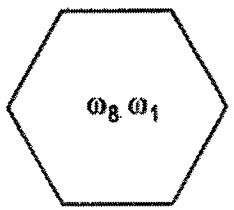

K* (892)

ρ(770),

K*

$$H_{Octet} = a\bar{M}_i^j Y_j^l M_l^i + b\bar{M}_i^j Y_l^i M_j^l + c\bar{M}_i^j M_j^i$$

$$3M_{\omega_8}^2 + M_\rho^2 = 4(M_{K^*}^2)$$

$$\rightarrow \quad M_{\omega_8} = 900 \text{ MeV} \quad ??$$

$$\omega_8 = \overset{\omega}{\frac{1}{\sqrt{3}}\frac{1}{\sqrt{2}}(\bar{u}u + \bar{d}d)} - \overset{\varphi}{\sqrt{\frac{2}{3}}\bar{s}s}, \qquad \tan\theta_{\mathrm{w}} = \frac{1}{\sqrt{2}}, \text{ mixing angle from wave function}$$

$$M_8^2 \approx \frac{1}{3}M_\omega^2 + \frac{2}{3}M_\varphi^2, \qquad \tan\theta_{\mathrm{M}} \approx \frac{1}{\sqrt{2}} \text{ mixing angle from mass}$$

Ideal mixing : $\omega_1, \omega_8 \rightarrow \omega, \varphi$

$$\tan^2(\theta_{\mathrm{w}} - \theta_M) \approx 10^{-3}$$

When is Angle from Mass or wave function equal?

1. Angle from diagonalizing mass matrix

$$H=\begin{pmatrix} E_8 & \Delta \\ \Delta & E_1 \end{pmatrix} \rightarrow \begin{pmatrix} \phi \\ \omega \end{pmatrix}=\begin{pmatrix} \cos\theta_M & \sin\theta_M \\ -\sin\theta_M & \cos\theta_M \end{pmatrix}\begin{pmatrix} \psi_8 \\ \psi_1 \end{pmatrix} \rightarrow \frac{E_8-E_1}{\Delta}=\frac{\cos^2\theta_M-\sin^2\theta_M}{2\cos\theta_M\sin\theta_M}$$

2. Angle from wave function

$$\psi_8=\cos(\theta_W)\phi-\sin(\theta_W)\omega$$
$$\psi_1=\cos(\theta_W)\omega+\sin(\theta_W)\phi,$$

when does $\theta_W=\theta_M$?

Hint from looking at correlator,

$$\frac{<\psi_8,\psi_8>-<\psi_1,\psi_1>}{<\psi_8,\psi_1>} \rightarrow \frac{(\cos^2\theta_W-\sin^2\theta_W)[<\phi,\phi>-<\omega,\omega>]}{2\cos\theta_W\sin\theta_W[<\phi,\phi>-<\omega,\omega>]},$$

hence, $\theta_M=\theta_W$ when $<\phi,\omega>=0$ $\rightarrow$ OZI rule

In terms of quarks, ideal mixing

1. OZI rule

$$<\bar{u}u,\bar{u}u>,<\bar{d}d,\bar{d}d>\neq<\bar{s}s,\bar{s}s> \quad >> \quad <\bar{u}u,\bar{s}s>$$

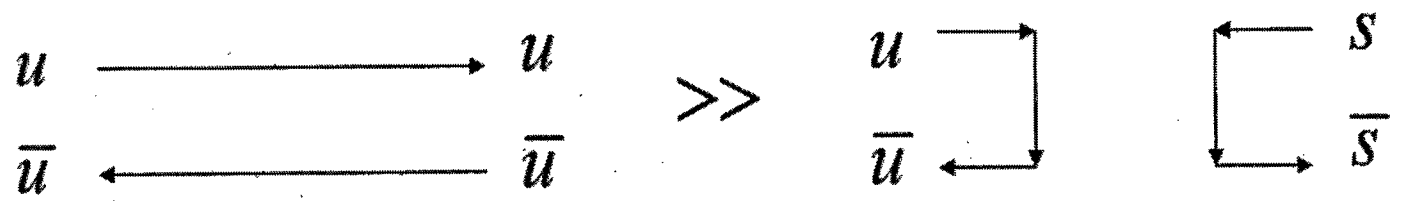

2. No mixing in pseudo scalar

$$<\bar{u}u,\bar{u}u>,<\bar{d}d,\bar{d}d>,<\bar{s}s,\bar{s}s>= \text{dominated by instantons}$$

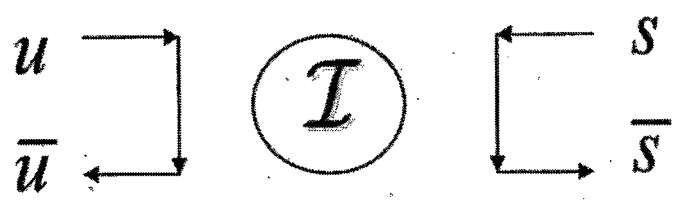

For pentaquark ?

1. Very small pseudo scalar component, hence everything can be assumed to be dominated by connected diagrams; But really an assumption

   a) Mass: Ideal mixing (Jaffe, Wilczek)

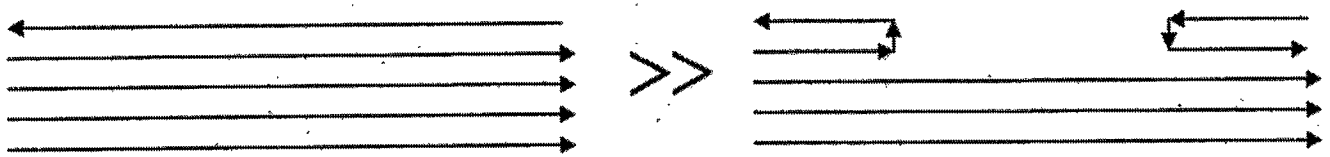

   b) Decay width: Fall apart decay (Close, Dudek)

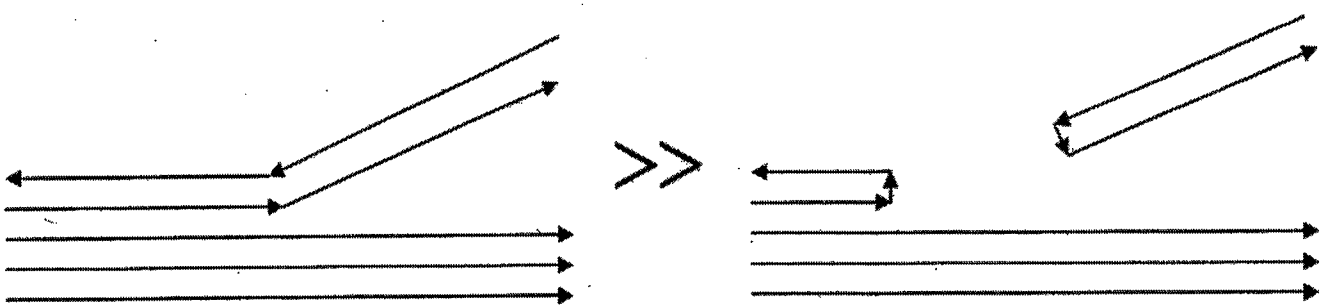

Mass in Ideal mixing scenario of pentaquarks

$$\bar{6} \otimes \bar{3} = 1\bar{0} \oplus 8$$

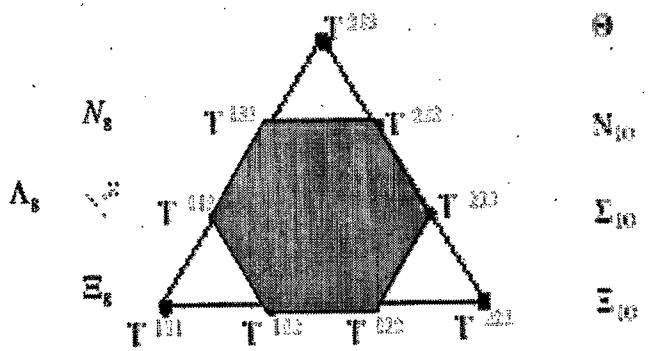

8 masses−3−2 parameters

$$M_{N_q} + 2M_{N_s} = 2M_\Theta + M_{\Xi_{10}}$$

$$2M_{\Sigma_q} + M_{\Sigma_s} = M_\Theta + 2M_{\Xi_{10}}$$

$$3M_{\Lambda_8} = M_{\Sigma_q} + M_{N_q} + 2M_{\Xi_8} - M_{\Xi_{10}}$$

$1\bar{0}$

$$\Theta_{10} = uudd\bar{s}$$

$$N_{10} = \sqrt{\frac{1}{3}}uudd\bar{d} + \sqrt{\frac{2}{3}}uuds\bar{s}$$

$$\Sigma_{10} = \sqrt{\frac{2}{3}}uuds\bar{d} + \sqrt{\frac{1}{3}}uuss\bar{s}$$

$$\Xi_{10} = uuss\bar{d}$$

8

$$N_8 = \sqrt{\frac{2}{3}}uudd\bar{d} - \sqrt{\frac{1}{3}}uuds\bar{s}$$

$$\Sigma_8 = \sqrt{\frac{1}{3}}uuds\bar{d} - \sqrt{\frac{2}{3}}uuss\bar{s}$$

$$\Xi_8 = ussd\bar{d}$$

$1\bar{0}$+8

$$N_q = uudd\bar{d}$$

$$\Theta_{10} = uudd\bar{s}$$

$$\Sigma_q = uuds\bar{d}$$

$$N_s = uuds\bar{s}$$

$$\Xi_{10} = uuss\bar{d}$$

$$\Sigma_s = uuss\bar{s}$$

1. One possible scenario hep-ph/0310117 , Y. Oh, H. Kim , SHL

$$M_{\Xi_8} = M_{\Xi_{10}} = 1862 \text{ MeV}$$

$$M_{\Lambda_8} = M_{\Sigma_q}$$

$$M_{N_q} = 1440 \text{ MeV}$$

then

$$M_{N_s} = 1751 \text{ MeV}$$

$$M_{\Lambda_8} = M_{\Sigma_q} = 1651 \text{ MeV}$$

$$M_{\Sigma_s} = 1962 \text{ MeV}$$

Tensor method for decay modes for Ideally mixed pentaquarks

hep-ph/040235, SHL, H. Kim , Y. Oh

$$\overline{6}\otimes\overline{3}=1\overline{0}\oplus 8, \qquad S^{ij}\otimes\overline{q}^{k}=T^{ijk}\oplus S^{[ij,k]}$$

For the octet field, $\quad S^{[ij,k]}=\varepsilon^{ljk}P_l^i+\varepsilon^{lik}P_l^i$

$$L_{8\text{-}8\text{-}8}=(d+f)P_j^iM_i^lB_l^j+(d-f)P_j^iB_i^lM_l^j$$

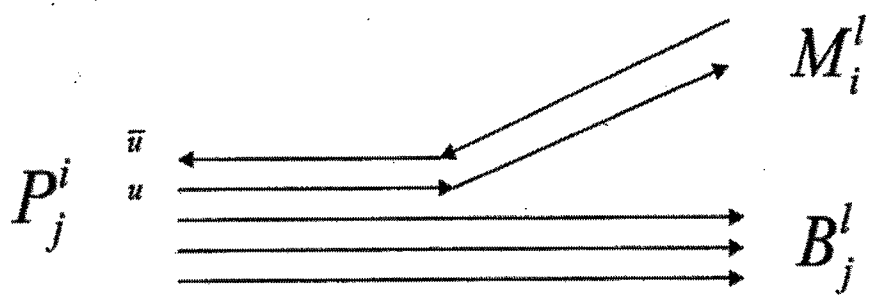

$\propto g$

$$L=-ig\varepsilon_{ilm}(\overline{T}^{ijk}+S^{[ij,k]})M_j^lB_k^m \quad \rightarrow f/d=1/3$$

where $\quad S^{[ij,k]}=\varepsilon^{ljk}P_l^i+[i\leftrightarrow j]$

Decay modes for Ideally mixed pentaquarks

All the pentaquarks are Narrow: Close, Dudek hep-ph/0401192, hep-ph/040235, Y. Oh, H. Kim , SHL

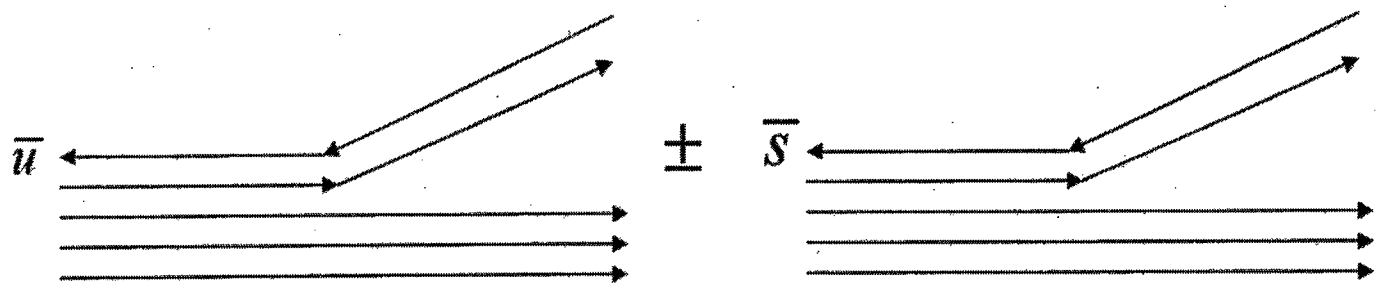

The difference between octet and anti decuplet decays are just additive

$$L = -ig(\bar{\Sigma}_5^O KN + \bar{\Sigma}_5^O \pi\Sigma)$$
$$-ig(\bar{\Sigma}_5^A KN - \bar{\Sigma}_5^A \pi\Sigma)$$

Detection of octet Pentaquark Baryons ?

$$3 \otimes 3 \otimes 3 \otimes 3 \otimes \bar{3}$$

$$\rightarrow (\bar{3} \oplus 6) \otimes (\bar{3} \oplus 6) \otimes \bar{3}$$

$$\rightarrow \quad \bar{6} \otimes \bar{3} = 1\bar{0} + 8$$

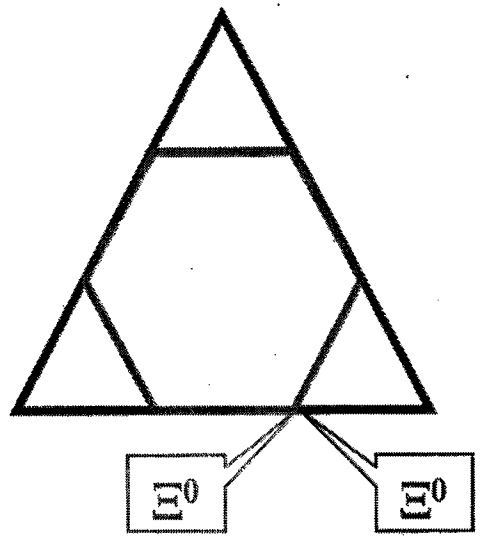

NA49 observed Pentaquark from

$$\Xi^0_{1\bar{0}}(1862) \rightarrow \Xi^-_8(1321) + \pi^+$$

Future experiments could observe octet Pentaquark from

$$\Xi^0_8(1862 \pm \delta) \rightarrow ? \rightarrow \Xi^-_{10}{}^*(1530) + \pi^+, \quad \text{with large width but ,}$$

$$\Xi^0_{1\bar{0}}(1862) \not\rightarrow \Xi^-_{10}{}^*(1530) + \pi^+$$

Octet pentaquark exists without large mixing with anti decuplet pentaquark

If none is observed, look at branching ratios into octet decayand see if there is octet component

Pentaquark anti-decuplet decay

Θ^+		$\tilde{N}^+$		$\tilde{N}^0$		$\tilde{\Sigma}^+$	
K^+n	$\sqrt{6}$	π^+n	$\sqrt{2}$	π^0n	1	$\pi^+\Lambda$	$\sqrt{3}$
K^0p	$-\sqrt{6}$	π^0p	1	π^-p	$-\sqrt{2}$	$\pi^+\Sigma^0$	-1
		ηp	$-\sqrt{3}$	ηn	$\sqrt{3}$	$\pi^0\Sigma^+$	1
		$K^+\Lambda$	$\sqrt{3}$	$K^+\Sigma^-$	$\sqrt{2}$	$\eta\Sigma^+$	$-\sqrt{3}$
		$K^+\Sigma^0$	-1	$K^0\Lambda$	$-\sqrt{3}$	$K^+\Xi^0$	$-\sqrt{2}$
		$K^0\Sigma^+$	$-\sqrt{2}$	$K^0\Sigma^0$	-1	$\bar{K}^0p$	$\sqrt{2}$

$\tilde{\Sigma}^0$		$\tilde{\Sigma}^-$		$\Xi^+_{3/2}$		$\Xi^0_{3/2}$	
$\pi^+\Sigma^-$	1	$\pi^0\Sigma^-$	1	$\pi^+\Xi^0$	$-\sqrt{6}$	$\pi^+\Xi^-$	$-\sqrt{2}$
$\pi^0\Lambda$	$\sqrt{3}$	$\pi^-\Lambda$	$-\sqrt{3}$	$\bar{K}^0\Sigma^+$	$\sqrt{6}$	$\pi^0\Xi^0$	-2
$\pi^-\Sigma^+$	-1	$\pi^-\Sigma^0$	-1			$\bar{K}^0\Sigma^0$	2
$\eta\Sigma^0$	$-\sqrt{3}$	$\eta\Sigma^-$	$\sqrt{3}$			$K^-\Sigma^+$	$\sqrt{2}$
$K^+\Xi^-$	-1	$K^0\Xi^-$	$\sqrt{2}$				
$K^0\Xi^0$	1	K^-n	$-\sqrt{2}$				
$\bar{K}^0n$	-1						
K^-p	1						

$\Xi^-_{3/2}$		$\Xi^{--}_{3/2}$	
$\pi^0\Xi^-$	-2	$\pi^-\Xi^-$	$\sqrt{6}$
$\pi^-\Xi^0$	$\sqrt{2}$	$K^-\Sigma^-$	$-\sqrt{6}$
$\bar{K}^0\Sigma^-$	$-\sqrt{2}$		
$K^-\Sigma^0$	2		

Pentaquark octet decay

Ξ^-_8		Ξ^0_8		N^+_8		N^0_8	
$\pi^-\Xi^0$	-1	$\pi^+\Xi^-$	-1	π^0p	$\sqrt{2}$	π^0n	$-\sqrt{2}$
$\pi^0\Xi^-$	$\frac{1}{\sqrt{2}}$	$\pi^0\Xi^0$	$-\frac{1}{\sqrt{2}}$	π^+n	2	π^-p	2
$\eta_8\Xi^-$	$-\sqrt{\frac{3}{2}}$	$\eta_8\Xi^0$	$-\sqrt{\frac{3}{2}}$	η_8p	0	η_8n	0
$\bar{K}^0\Sigma^-$	-2	$K^-\Sigma^+$	2	$K^+\Sigma^0$	$\frac{1}{\sqrt{2}}$	$K^0\Sigma^0$	$-\frac{1}{\sqrt{2}}$
$K^-\Sigma^0$	$-\sqrt{2}$	$\bar{K}^0\Sigma^0$	$-\sqrt{2}$	$K^0\Sigma^+$	1	$K^+\Sigma^-$	1
$K^-\Lambda$	0	$\bar{K}^0\Lambda$	0	$K^+\Lambda$	$-\sqrt{\frac{3}{2}}$	$K^0\Lambda$	$-\sqrt{\frac{3}{2}}$

Σ^0_8		Σ^+_8		Σ^-_8		Λ^0_8	
$\pi^+\Sigma^-$	$\frac{1}{\sqrt{2}}$	$\pi^+\Sigma^0$	$-\frac{1}{\sqrt{2}}$	$\pi^-\Sigma^0$	$\frac{1}{\sqrt{2}}$	$\pi^-\Sigma^+$	$\sqrt{\frac{3}{2}}$
$\pi^-\Sigma^+$	$-\frac{1}{\sqrt{2}}$	$\pi^0\Sigma^+$	$\frac{1}{\sqrt{2}}$	$\pi^0\Sigma^-$	$-\frac{1}{\sqrt{2}}$	$\pi^+\Sigma^-$	$\sqrt{\frac{3}{2}}$
$\pi^0\Lambda$	$\sqrt{\frac{3}{2}}$	$\eta_8\Sigma^+$	$\sqrt{\frac{3}{2}}$	$\eta_8\Sigma^-$	$\sqrt{\frac{3}{2}}$	$\pi^0\Sigma^0$	$\sqrt{\frac{3}{2}}$
$\eta_8\Sigma^0$	$\sqrt{\frac{3}{2}}$	$\pi^+\Lambda$	$\sqrt{\frac{3}{2}}$	$\pi^-\Lambda$	$\sqrt{\frac{3}{2}}$	$\eta_8\Lambda$	$-\sqrt{\frac{3}{2}}$
K^-p	$\frac{1}{\sqrt{2}}$	$K^+\Xi^0$	2	$K^0\Xi^-$	-2	$K^+\Xi^-$	0
$\bar{K}^0n$	$-\frac{1}{\sqrt{2}}$	$\bar{K}^0p$	1	K^-n	1	$K^0\Xi^0$	0
$K^+\Xi^-$	$-\sqrt{2}$					K^-p	$-\sqrt{\frac{3}{2}}$
$K^0\Xi^0$	$-\sqrt{2}$					$\bar{K}^0n$	$-\sqrt{\frac{3}{2}}$

Ideally mixed Pentaquark Nucleon and sigma decay modes, which are expected to be also narrow

N^+_{qq}		N^+_{ss}		N^0_{qq}		N^0_{ss}	
$\pi^+ n$	$-\sqrt{6}$	$K^+\Lambda$	$-\frac{3}{\sqrt{2}}$	$\pi^0 n$	$\sqrt{3}$	$K^0\Sigma^0$	$-\sqrt{\frac{3}{2}}$
$\pi^0 p$	$-\sqrt{3}$	$K^+\Sigma^0$	$\sqrt{\frac{3}{2}}$	$\pi^- p$	$-\sqrt{6}$	$K^+\Sigma^-$	$\sqrt{3}$
$\eta_{qq} p$	$\sqrt{3}$	$K^0\Sigma^+$	$\sqrt{3}$	η_{qq}	$\sqrt{3}$	$K^0\Lambda$	$-\frac{3}{\sqrt{2}}$
		$\eta_{ss} p$	$-\sqrt{3}$			$\eta_{ss} n$	$-\sqrt{3}$
Σ^+_{qq}		Σ^+_{ss}		Σ^-_{qq}		Σ^-_{ss}	
$\pi^+\Sigma^0$	$\sqrt{\frac{3}{2}}$	$K^+\Xi^0$	$\sqrt{6}$	$\pi^-\Sigma^0$	$-\sqrt{\frac{3}{2}}$	$K^0\Xi^-$	$-\sqrt{6}$
$\pi^0\Sigma^+$	$-\sqrt{\frac{3}{2}}$	$\eta_{ss}\Sigma^+$	$-\sqrt{6}$	$\pi^0\Sigma^-$	$\sqrt{\frac{3}{2}}$	$\eta_{ss}\Sigma^-$	$-\sqrt{6}$
$\eta_{qq}\Sigma^+$	$\sqrt{\frac{3}{2}}$			$\eta_{qq}\Sigma^-$	$\sqrt{\frac{3}{2}}$		
$\pi^+\Lambda$	$-\frac{3}{\sqrt{2}}$			$\pi^-\Lambda$	$-\frac{3}{\sqrt{2}}$		
$\bar{K}^0 p$	$-\sqrt{3}$			$K^- n$	$-\sqrt{3}$		
Σ^0_{qq}		Σ^0_{ss}					
$\pi^+\Sigma^-$	$-\sqrt{\frac{3}{2}}$	$K^+\Xi^-$	$-\sqrt{3}$				
$\pi^-\Sigma^+$	$\sqrt{\frac{3}{2}}$	$K^0\Xi^0$	$-\sqrt{3}$				
$\eta_{qq}\Sigma^0$	$\sqrt{\frac{3}{2}}$	$\eta_{ss}\Sigma^0$	$-\sqrt{6}$				
$\pi^0\Lambda$	$-\frac{3}{\sqrt{2}}$						
$K^- p$	$-\sqrt{\frac{3}{2}}$						
$\bar{K}^0 n$	$\sqrt{\frac{3}{2}}$						

Summary

1. If one finds s=3/2 anti-deuplet pentaquark -> soliton picture is ruled out.

2. If one finds charmed pentaquark at 2700 MeV -> supports bound state approach for solitions and chiral doubling

3. If octet pentaquark is observed -> stongly supports diquark picture.

4. Should look for remaining potentially narrow states. Starting with no mixing.

5. By looking at $\Xi 0$ Idecay in more detail, can learn if there is other octet pentaquark states and some idea about ideal mixing.

On The Role of Strange Quark Mass In QCD Phase Diagram
--BCS-BEC Crossover in Color-Flavor Locked Phase?--

Hiroaki Abuki

On the role of strange quark mass in QCD phase diagram

– *BCS-BEC crossover in color-flavor locked phase?* –

Hiroaki Abuki

Yukawa Institute for Theoretical Physics, Kyoto University, Kyoto, Japan

Abstract

We revisited the unlocking transition from the color-flavor locked (CFL) phase to the two-flavor pairing (2SC) phase paying a special attention to the multiplicity of the gap parameters. By deriving the exact formula of the effective potential for 5-gap parameters, we show that the CFL phase is much robuster against the increase of the strange quark mass than is predicted by the kinematical criterion for the unlocking. As temperature is decreased, the CFL phase gets stronger against the strange quark mass. However, we could not conclude at which point the CFL state gets unlocked to the 2SC state just on $T = 0$ for some numerical difficulties and also for the limit of the adopted model. Even a possibility of surviving CFL pairs for all finite value of strange quark mass manifests itself at zero temperature. In this case, the 2SC phase may be realized only as the asymptotic limit of the *distorted* CFL state as $M_s \to \infty$. In contrast to this ambiguous situation at zero temperature, we can find a clear 2nd order phase transition from the CFL to the 2SC at finite temperature. At low temperature, we found the distorted CFL state even for the region $M_s > \mu_r$ and more detailed analyses indicate a power law scaling relation between the strange quark density ρ_s and the unlocking critical temperature T_c in this region: $T_c \sim \rho_s^\alpha$. These two facts strongly suggest that the CFL state undergoes the smooth crossover from the weak coupling BCS-like state to the Bose-Einstein condensed state of bound the CFL diquarks as one increases (decreases) strange quark mass (density).

On the role of strange quark mass in QCD phase diagram

BCS-BEC crossover in Color-Flavor Locked Phase?

Hiroaki Abuki (YITP, Kyoto Univ., Japan)

based on H. Abuki, arXiv:hep/0401245

1. Quark pairing phenomena in QCD
2. 2SC pairing and CFL pairing
3. Dynamical effect of strange mass
4. Unlocking transition revisited
5. Asymptotic Smooth Unlocking?
6. BCS-BEC crossover in the CFL phase?
7. Summary and future problems

Quark pairing phases in QCD

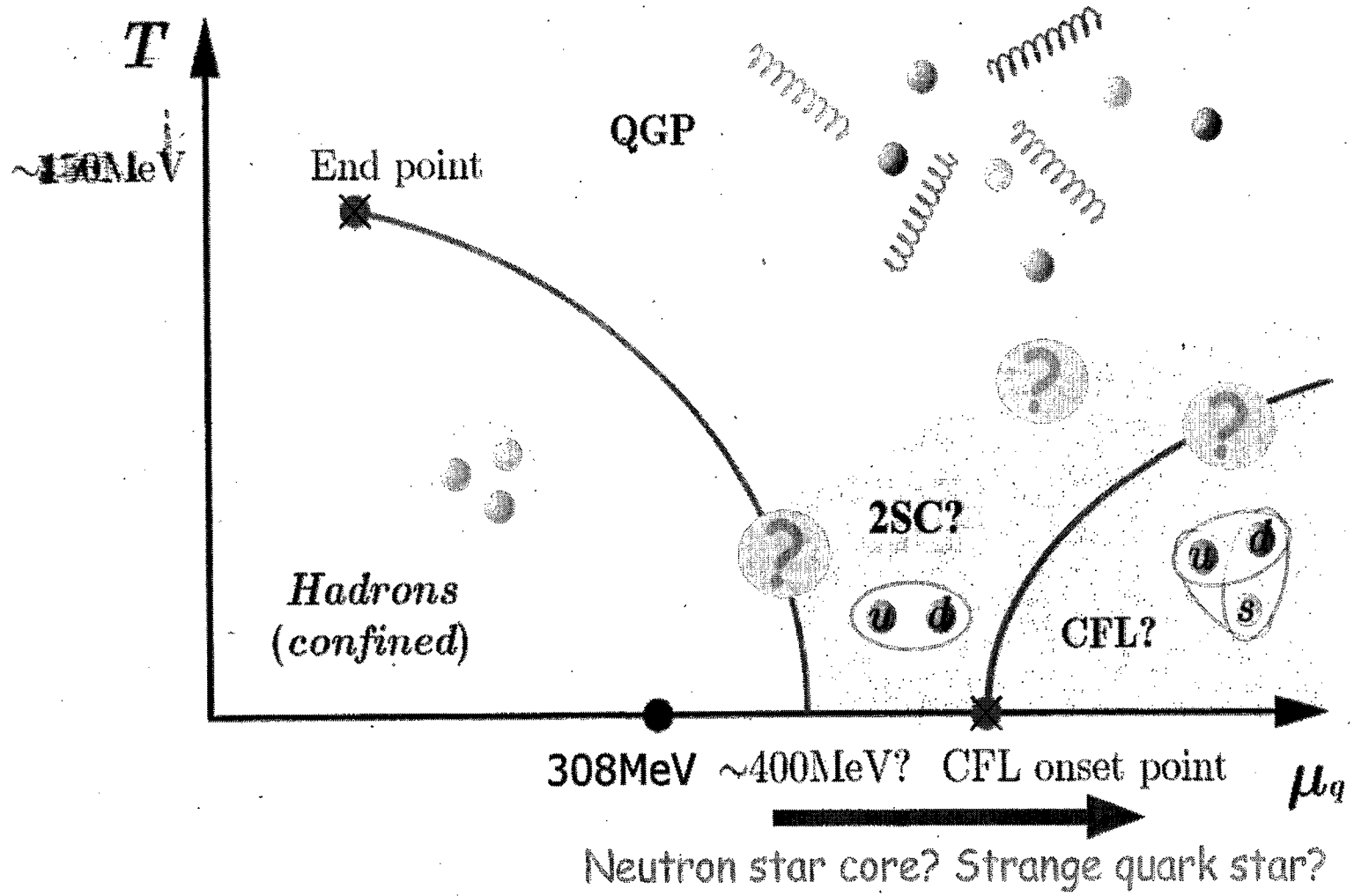

(i) 2SC	(ii) pure CFL
Bailin-Love, '80 Iwasaki-Iwado, '95, etc…	M. Alford, K. Rajagopal, F. Wilczek, Nucl.Phys.B537, '99
Order : $\left\langle q_i^a q_j^b \right\rangle_{2CS} = \Delta \varepsilon^{ab,g} \varepsilon_{s,ij}$	$\left\langle q_i^a q_j^b \right\rangle_{CFL} \simeq \Delta_A \varepsilon^{abL} \varepsilon_{Lij}$
Rank : 4	9 (full rank)
Gapless modes : 5 (sr, sb, sg, ug, dg)	0
Symmetry : $SU(2)_c \times SU(2)_f$	$SU(3)_{C+V}$: δ_i^a remains invariant

Gaps, Quasiquarks and Multiplets:

Δ, $SU(2)_f \times SU(2)_c$ doublet^2 (4) $= \left[2_{(r,b)}, 2_{(u,d)} \right]$	$\begin{cases} \Delta_1 \simeq 2\Delta_A, \ SU(3)_{C+V} \text{ singlet } (1) \\ \Delta_8 \simeq -\Delta_A, \ SU(3)_{C+V} \text{ octet } (8) \end{cases}$
Correlation works between 4 quarks out of 9	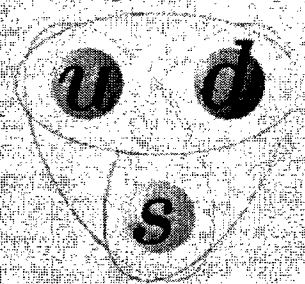 *Correlation works among all 9 quarks*

The role of the strange quark mass and unlocking transition

pure CFL → **pure 2SC**

$$\left\langle q_i^a q_j^b \right\rangle_{\mathrm{CFL}} \simeq \Delta_A \varepsilon^{abL} \varepsilon_{Lij} \longrightarrow \left\langle q_i^a q_j^b \right\rangle_{\mathrm{2CS}} = \Delta \varepsilon^{ab,g} \varepsilon_{s,ij}$$

$$M_s^2 / \mu = 0 \qquad\qquad M_s^2 / \mu = \infty$$

Unlocking *transition?*

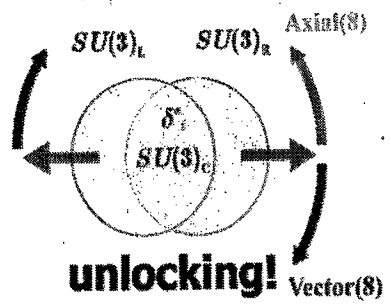

1. Is there sharp *phase separation*?
2. If there actually is a phase transition
   i. the *critical value* of $[M_s^2/\mu]_{crit.}$?
   ii. the *order* of phase transition?
3. The *nature, mechanism* of unlocking?

Trials in Past:

M. Alford et al., Nucl. Phys. B558,'99;
T. Schaefer, F.Wilczek, Phys. Rev. D60,'99.

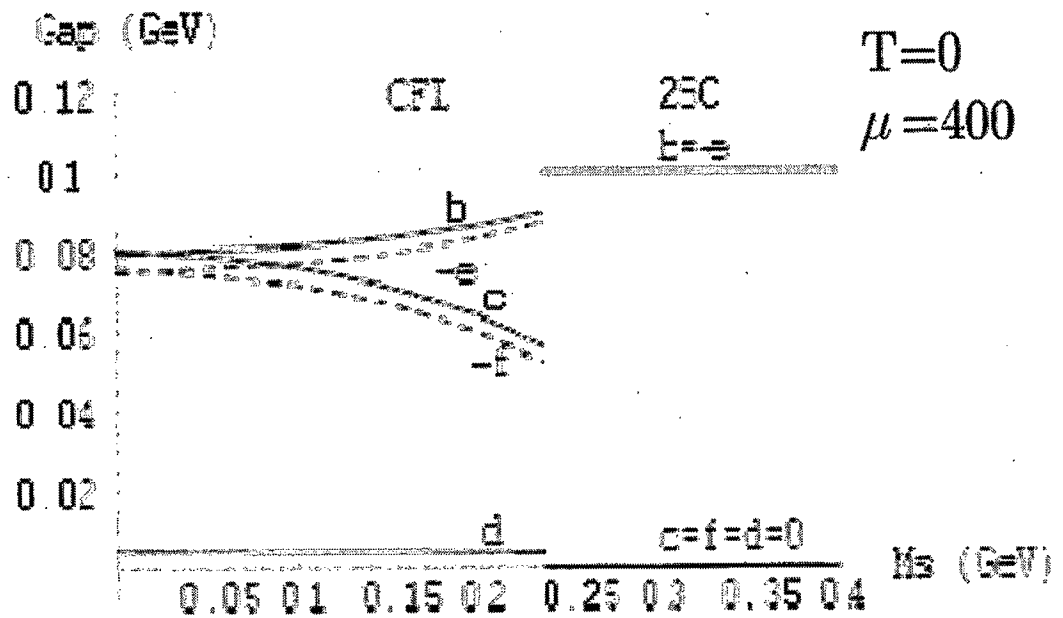

T=0
μ=400

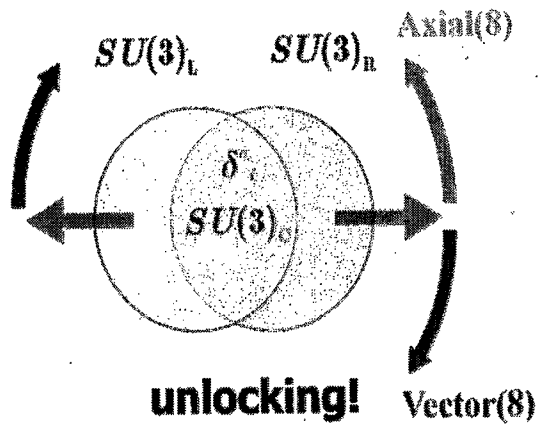

From: M. Alford et al, NPB558

1. Is there sharp phase separation? : Yes
2. If there actually is a phase transition
   i. The critical value of $[M_s^2/\mu]_{crit.}$? : $[M_s^2/\mu]_{crit.} \sim \Delta_8$
   ii. the order of phase transition? : 1st order

Trials in Past:

M. Alford et al., Nucl. Phys. B558,'99;
T. Schaefer, F.Wilczek, Phys. Rev. D60,'99.

3. The ***nature, mechanism*** of unlocking?

: kinematical one rather than dynamical

$p_F^{u,d}$
p_F^{s}

$$\langle us - su \rangle_{\mathrm{CFL}} = \langle ds - sd \rangle_{\mathrm{CFL}} \to 0$$

$$p_F^{u,d} - p_F^{s} \cong \frac{M_s^2}{4\mu} \begin{cases} \leq \Delta_8 & \text{: CFL (smallest gap in CFL)} \\ \geq \Delta_8 & \text{: Unlocked into 2SC} \end{cases}$$

Kinematical criterion works well ! However...

Does Color-Flavor Unlocking need to be revisited?

1. **T. Schaefer and F.Wilczek, Phys. Rev. D60,'99**

   ? 1. Based on the expansion in $R = M_s^2/2p_F$

   ✓ 2. Constructing effective potential

2. **M. Alford et al., Nucl. Phys. B558,'99;**

   ✓ 1. Non-perturbative treatment of M_s

   ? 2. Constructing effective potential (Wrong construction!!)

Can we really neglect the dynamical effect of strange quark mass even after eliminating these ambiguities?

What about dynamical effect of strange quark mass?

$$\left\langle q_i^a q_j^b \right\rangle_{CFL} = \Delta_A \varepsilon^{abL} \varepsilon_{Lij} + \Delta_S S_{ij}^{ab} = \frac{1}{2} \sum_{\alpha,\beta=1}^{9} \Delta_{\alpha\beta} \left(\lambda_\alpha\right)_{ai} \left(\lambda_\beta\right)_{bj}$$

$$\Delta_{\alpha\beta} = \begin{pmatrix} \Delta_8 E_8 & \\ & \Delta_1 \end{pmatrix} \quad : \quad \textit{Pure}\ \textbf{CFL (Chiral limit)}$$

$$\Rightarrow \Delta_{\alpha\beta} = \begin{pmatrix} \Delta_8^3 E_3 & & & \\ & \Delta_8^2 E_4 & & \\ & & \Delta_8^1 & \\ & & & \Delta_1^1 \end{pmatrix} \quad : \quad \textit{Distorted}\ \textbf{CFL}\ (m_s \le m_s^c)$$

$9 = 3 + 2^2 + 1 + 1$

$$\Rightarrow \Delta_{\alpha\beta} = \begin{pmatrix} \Delta E_3 & & & \\ & 0 E_4 & & \\ & & -\Delta/3 & -\sqrt{2}\Delta/3 \\ & & -\sqrt{2}\Delta/3 & -2\Delta/3 \end{pmatrix} \quad : \quad 2SC\ (m_s \ge m_s^c)$$

$4 = 3 + 1 = 2 + 2$

Gap equations

$$\Delta_{\alpha\beta} = \begin{pmatrix} \Delta_8^3 E_3 & & & \\ & \Delta_8^2 E_4 & & \\ & & \Delta_8^1 & \Delta \\ & & \Delta & \Delta_1^1 \end{pmatrix}$$

: **Minimal interpolating State between 2SC and pure CFL**

$$R \begin{pmatrix} \Delta_8^1 & \Delta \\ \Delta & \Delta_1^1 \end{pmatrix} R^T = \begin{pmatrix} \chi_1 & 0 \\ 0 & \chi_2 \end{pmatrix} \text{ with } |\chi_1| > |\chi_2|$$

States are distinguished by value of $(\Delta_{83}, \Delta_{82}, \chi_1, \chi_2)$

[illegible]	[illegible]	[illegible]
[illegible]	[illegible]	[illegible]
[illegible]	[illegible]	[illegible]
[illegible]	[illegible]	[illegible]

Effective potential for multi-gap parameters

Pauli trick has to be carefully done in the case that many couplings enters in gap parameter space

$$g^2 \frac{\partial \Omega_{eff}}{\partial \Delta_i} \neq \left[\Delta_i - g^2 K_i[\vec{\Delta}]\right]$$

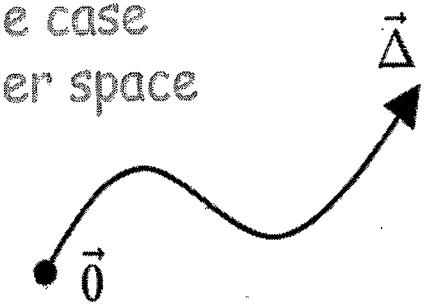

Which is wrong point in Ref: M. Alford et al., NPB558,'99;

$$g^2 \frac{\partial \Omega_{eff}}{\partial \Delta_i} = \sum C^{ij} \left[\Delta_j - g^2 K_j[\vec{\Delta}]\right] : \textit{linear combination}$$

C^{ij} *relate condensates* $\phi \sim \langle qq \rangle$ *and gap parameters* Δ *as*

$$\textit{symbolically } g^2 \phi^i = \sum C^{ij} \Delta_j, \quad (g^2 tr(S(\Sigma)\Sigma) \sim C^{ij} \Delta_i \Delta_j)$$

$$\Omega_{eff}(\vec{\Delta}) = \frac{1}{2g^2} C^{ij} \Delta_i \Delta_j - \int_0^1 dt \; C^{ij} \Delta_i K_j[t\vec{\Delta}]$$

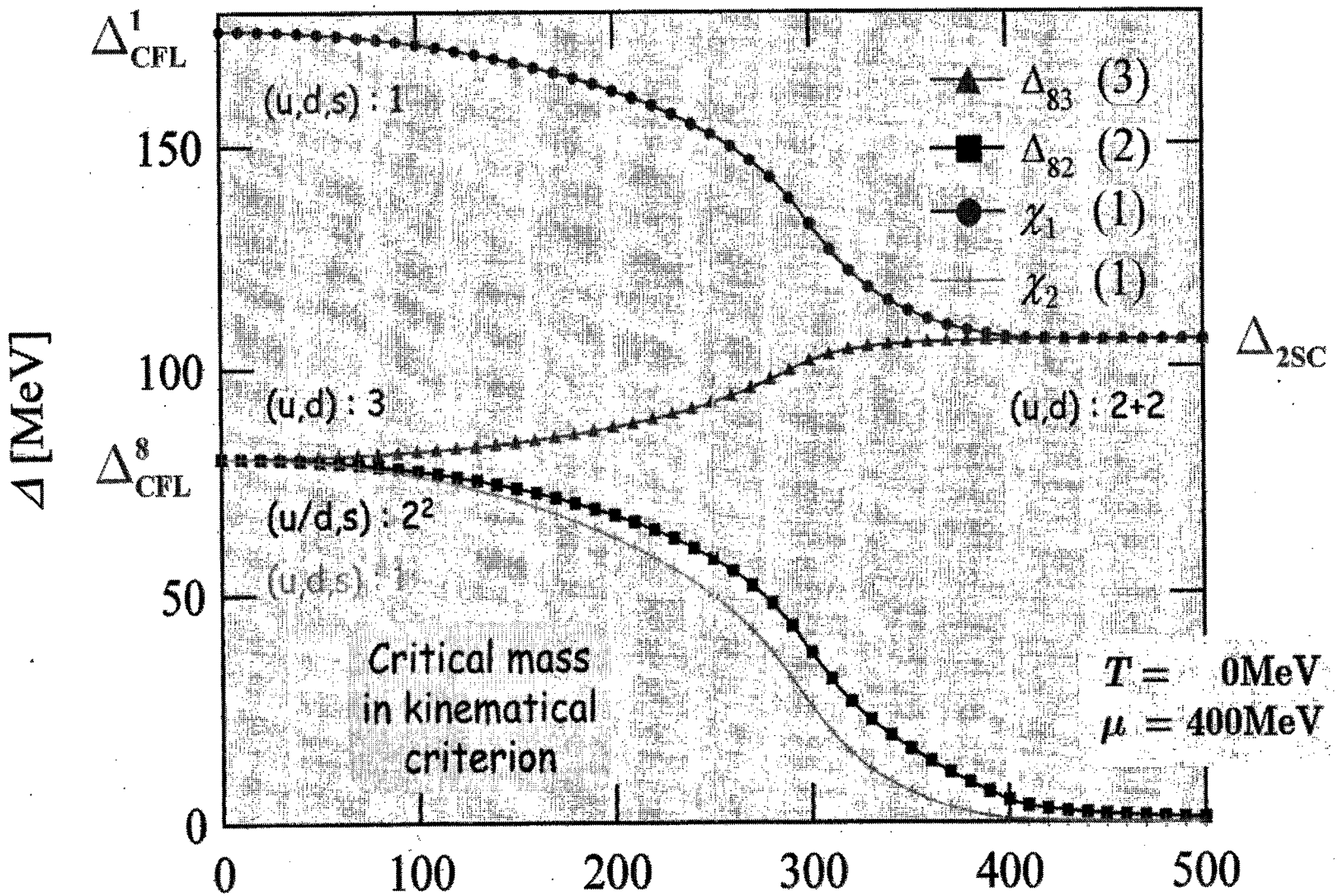

1. Asymptotic smooth Unlocking: No sharp unlocking for finite value of M_s
2. Continuous 2nd order transition at some critical value : $M_s^c > \mu$

Effective potential in multi-gap parameter space

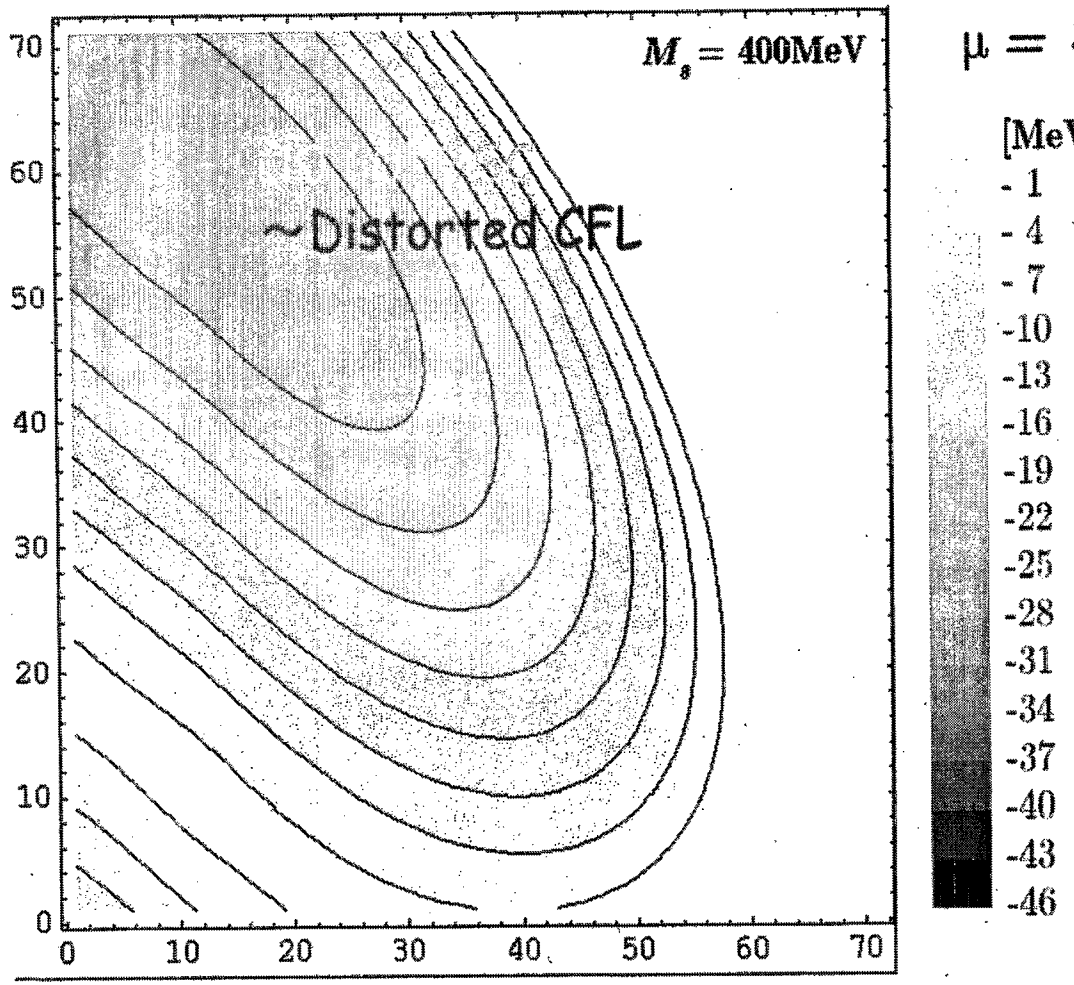

$\mu = 400$ MeV, $T = 0$ MeV

2SC is saddle point: always a solution of gap equation

Distorted CFL state moves towards the 2SC state and Condensation energy gets reduced

CFL state disappears into 2SC state as $M_s \to \mu$

2nd order transition?

Phase Diagram in (T, Ms) plane

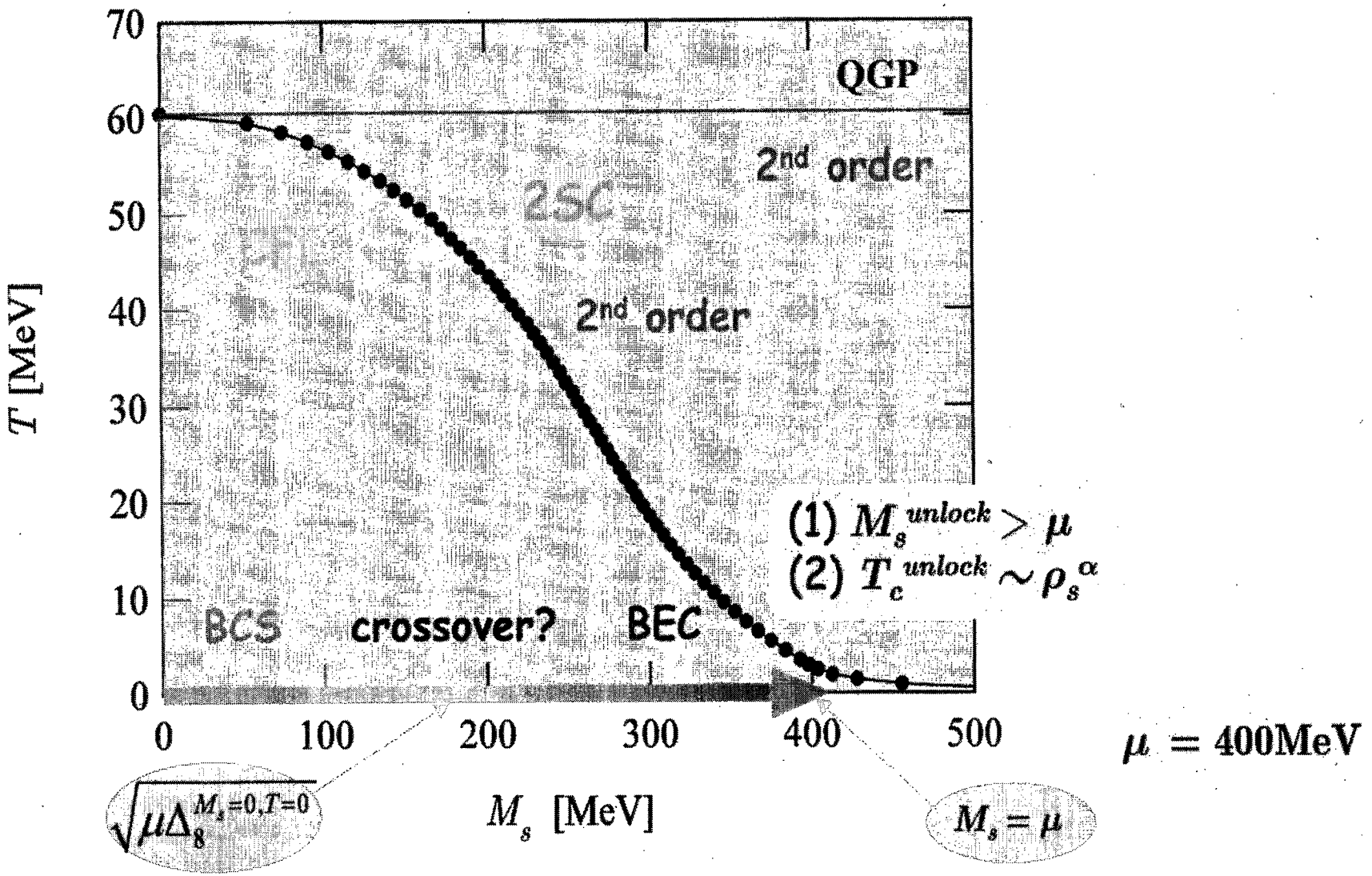

What is BCS/BEC crossover?

In non-relativistic case : BEC (strong, dilute limit) ⇔ BCS,(weak, dense)

Weak coupling gap equation :

$$\Delta(p) = \sum_k V(p,k)\left[1 - 2n_F(\varepsilon_k)\right]\frac{\Delta(k)}{2\varepsilon_k[\Delta]}, \text{ with } \begin{cases} \varepsilon_k[\Delta] \equiv \sqrt{E_k^2 + \Delta(k)^2} \\ E_k = \left(\hbar^2 k^2 / 2m - \mu\right) \\ f_F(\varepsilon) = 1/(1 + e^{\varepsilon/T}) \end{cases}$$

is equivalent to the following wave equation :

$$\frac{p^2}{m}\varphi(p) - (1 - 2n_p)\sum_k V(p,k)\varphi(p) = 2\mu\varphi(p), \text{ with } \begin{cases} \varphi(p) = \langle a_p a_{-p} \rangle_{\text{BCS}} \\ n(p) = \langle a_p^+ a_p \rangle_{\text{BCS}} \end{cases}$$

This is (Pauli-blocked) 2-body Schodinger (BS) equation
If $2\mu < 0$ in dilute limit $\rho \to 0$, this signals
appearance of Bound state! (BEC)

What is BCS/BEC crossover?

C.A.R. Sa de Melo et al., Phys. Rev. Lett. 71. 3202, '93

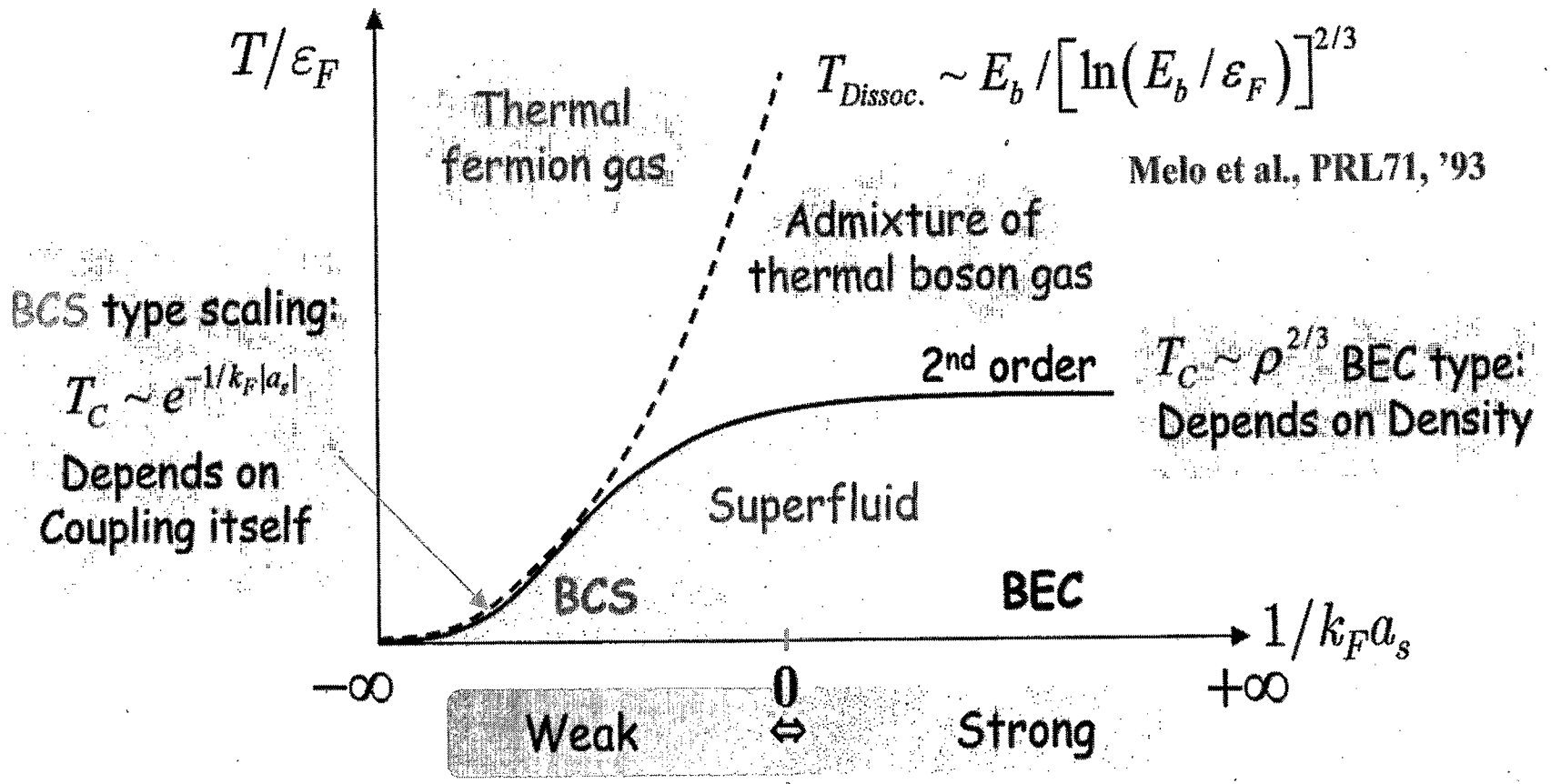

Possible relation to precursory pseudo gap phase?

Kitazawa-Koide-Kunihiro-Nemoto, PRD65, '02; arXiv: hep-ph/0309026 '03

Phase diagram for Ms=400MeV

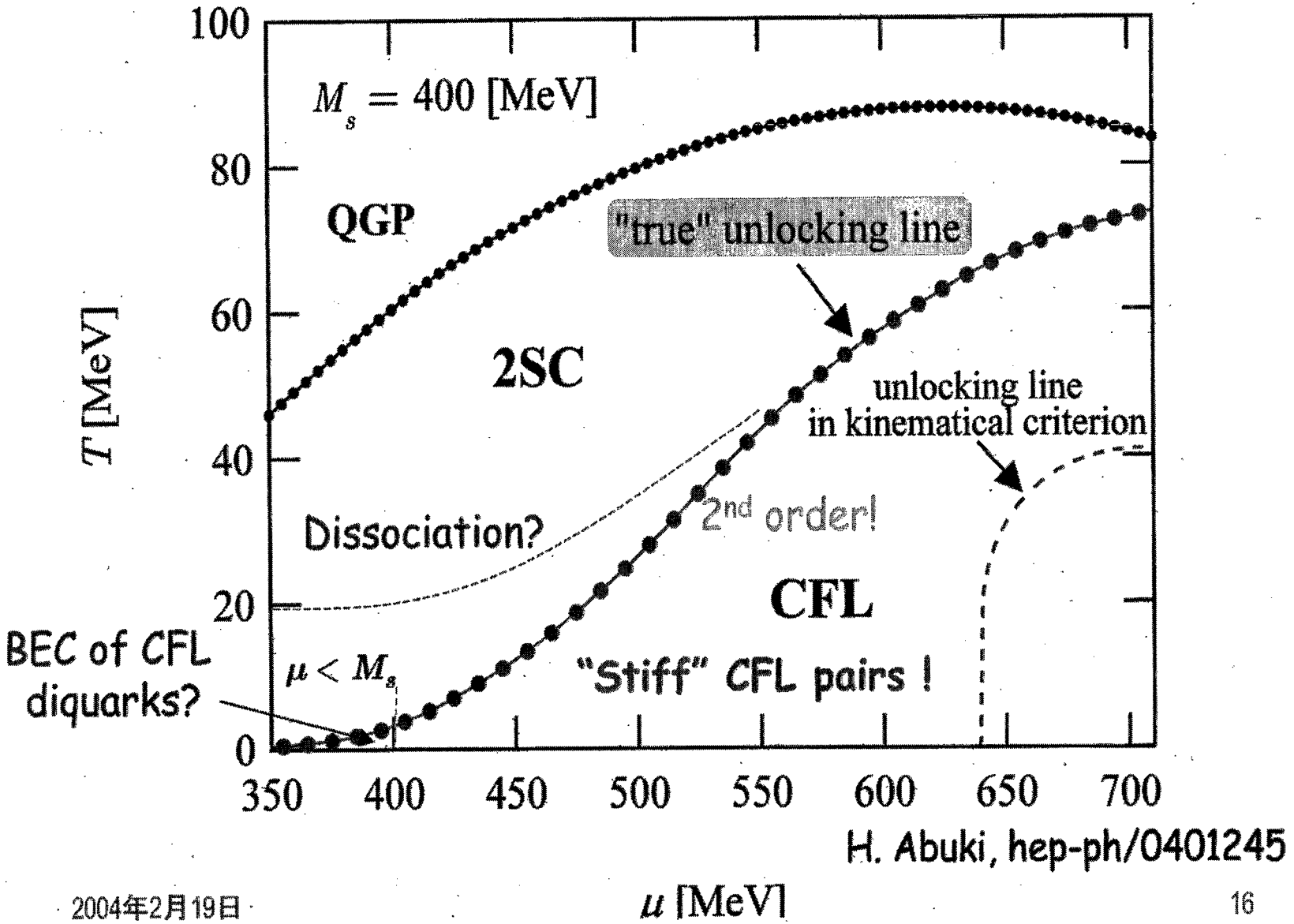

H. Abuki, hep-ph/0401245

Summary

Color-Flavor Unlocking is revisited in more complete way than was taken in work in past

1. Is there sharp phase separation ?
2. If there actually is a phase transition,
   the critical value of $[M_s^2/\mu]_{crit.}$?
   the order of phase transition?
3. The nature, mechanism of unlocking?

(1a) Unlocking is of continuous 2nd order at finite T

(1b) Asymptotic smooth change realizes for T=0 ?

(2) CFL is tough (stiff) against Ms !

$[M_s^2/\mu]_{crit.}(\mathrm{T}=0) > \mu$ and $T_c^{unlock} \sim \rho_s^{\alpha}$

(3) An interesting possibility of BCS-BEC crossover in the relativistic CFL superfluid

Future problems

1. **Imposing Electric & Color Neutralities :**

   This is shown to strongly <u>disfavor naive 2SC state!</u>

   M. Alford and K. Rajagopal, JHEP206. 031,'02 : **Model independent analysis**

   A.W. Steiner, S.Reddy and M.Prakash, Phys. Rev. D66, '02 : **NJL model**

2. **Chiral condensate and in medium Strange quark mass.**

3. **Study the BCS-BEC crossover in more detail.**

   (1) The interaction between bosons

   (2) Time-dependent diquark fluctuation modes?

   & Gross-Pitaevski equation in BEC region?

   (3) Discuss the thermodynamic properties in crossover

   in detail, and seek for Astrophysical consequences...

Fermi surface and Cooper instability

Our starting point : there is Large Fermi sphere

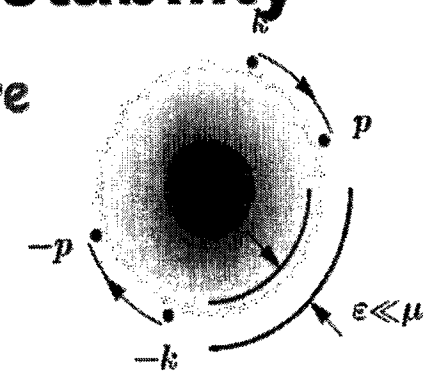

- Pauli-Blocking
- Low Energy Modes with Large Density of State

Results in non-perturbative IR dynamics

$-1/g^2 +$ = 1PI vertex

$$\Gamma^{(2)}(p) = -\Delta_F^{-1}(p)$$

low p RPA mode is *tachyonic* at T=0 !

negative curvature of effective potential

Cooper instability !

leads to reorganization of Fermi ball
into BCS state with non-vanishing ee condensate

BCS mechanism $\Delta \sim \omega_D e^{-1/Ng^2}$

Attraction in color-antitriplet channel

$$\sum_{\alpha}(\lambda_\alpha/2)_{ab}(\lambda_\alpha/2)_{cd} = -\frac{N+1}{2N}(\delta_{ab}\delta_{cd}-\delta_{ad}\delta_{bc}) + \frac{N-1}{2N}(\delta_{ab}\delta_{cd}+\delta_{ad}\delta_{bc})$$

$\bar{3}_c$(anti-triplet) Attraction!

6_c(sextet) Repulsive

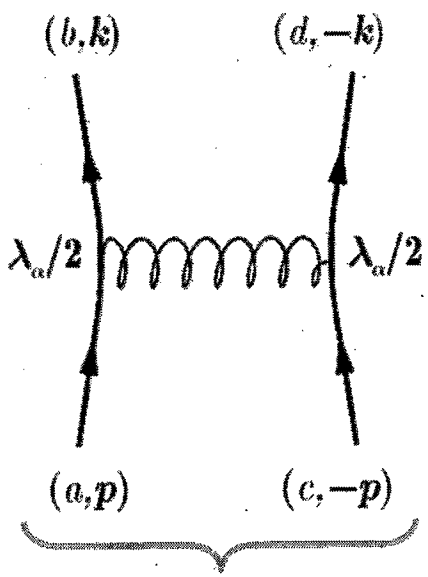

Attraction in anti-triplet channels

Dynamical Formation of $\langle q_a q_b \rangle \approx \varepsilon_{abc}\Delta^c$?

Bailin and Love, Phys. Rept. 107, 325 (1984)

- Ginzburg-Landau Approach
- Phenomenological IR cut off
- Small gap (a few hundred keV)

Proposed pairing patterns in QCD (1)

2SC (2 flavor ansatz)

1. **Color** Attractive anti-symmetric channel

   ε_{abc} : **Color anti-triplet**

2. **Dirac** attractive in total $J=0$ (8 Dirac operator)
   and aligned chirality $(m/\mu \ll 0)$ (4 Dirac operator)

   $\{C\gamma_5,\ C\gamma_5\gamma_0\vec{\gamma}\cdot\hat{q}\}$: **Parity (+)** Favored by instanton

   $\{C,\ C\gamma_0\vec{\gamma}\cdot\hat{q}\}$: **Parity (−)** ??? ???

3. **Flavor** Anti-symmetric (purely from Pauli principle)

   ε_{ij} : $SU(2)_f$ **flavor singlet**

Proposed pairing patterns in QCD (2)

CFL (Color-Flavor Locking)

M. Alford, K. Rajagopal, F. Wilczek, **Nucl.Phys.B537:443-458,1999**

1. **Dirac structure is the same as in 2SC**

$$\left\{C\gamma_5,\ C\gamma_5\gamma_0\vec{\gamma}\cdot\hat{q}\right\}:\ J=0^+ \text{ and aligned chirarity}$$

anti-symmetric with respect to spinor indices

2. **CFL ansatz for Flavor and Color structure**

$$\left\langle q_i^a q_j^b\right\rangle_{\mathrm{CFL}} = \Delta_A \varepsilon^{abI}\varepsilon_{Iij} + \Delta_S\left(\delta_i^a\delta_j^b + \delta_j^a\delta_i^b\right)$$

$$\left(\bar{3}_c\times\bar{3}_f\right) \qquad \left(6_c\times 6_f\right)$$

(Attractive) (Repulsive) in naïve OGE level

symmetric under $(a,i)\Leftrightarrow(b,j)$ Pauli principle is OK.

c.f. ***B*-phase in He^3**

Symmetry of CFL

$$\underbrace{\left\langle q_{Li}^{a} q_{Lj}^{b} \right\rangle_{\mathrm{CFL}} = \underbrace{\sum_{I} \Delta_{A} \varepsilon^{abI} \varepsilon_{Iij}}_{SU(3)_{\mathrm{C+R}}} = -\left\langle q_{Ri}^{a} q_{Rj}^{b} \right\rangle_{\mathrm{CFL}}}_{\text{Invariant under } SU(3)_{\mathrm{C+L}}}$$

$$\underbrace{SU(3)_c \times SU(3)_L \times SU(3)_R}_{\supset U(1)_{\mathrm{EM}}} \times U(1)_B \to \underbrace{SU(3)_{C+V}}_{\supset \tilde{U}(1)_{\mathrm{EM}}}$$

- color symmetry is broken : 8 massive gluons
- chiral symmetry is broken : octet NG bosons
- baryon number is broken : superfluid mode (H)

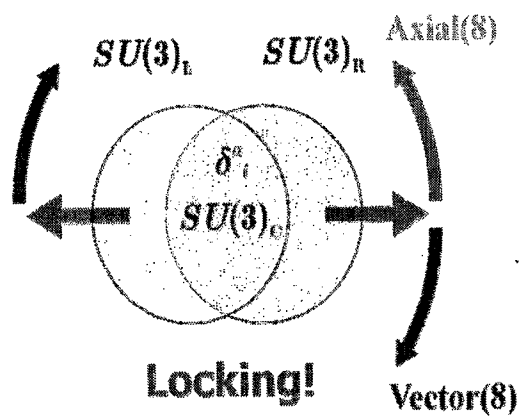

Analogy with He^3 system

$$\langle \psi_\alpha(\vec{q})\psi_\beta(-\vec{q})\rangle = \sum_{a,i} \hat{q}_i \left[\sigma^a \sigma_2\right]_{\alpha\beta} d^i_a$$

: General L=1,S=1 state
with 3×3 matrix d^i_a (a:spin,i:spatial)

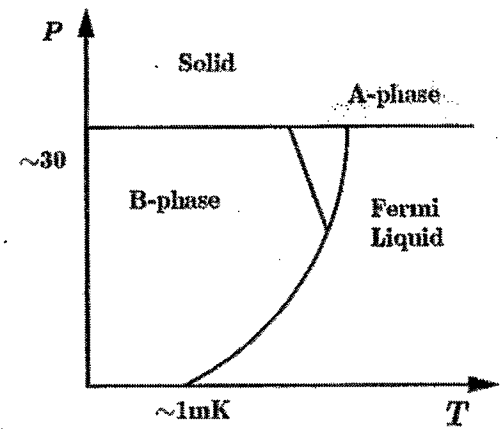

B-phase (BW state;Balian-Werthaner)

$d^i_a = \Delta_{BW}\delta^i_a$ (S and L are locked!!) ⟷ CFL

- Gap is equal on the entire Fermi surface

A-phase(ABM state;Anderson-Morel)

$d^i_a = \Delta_{ABM}\delta^3_a (e_1 + ie_2)_i$ ⟷ 2SC

- Gap is zero at South and North poles

Solution of NJL gap equation: What about the unlocking for

$$T = 0?$$

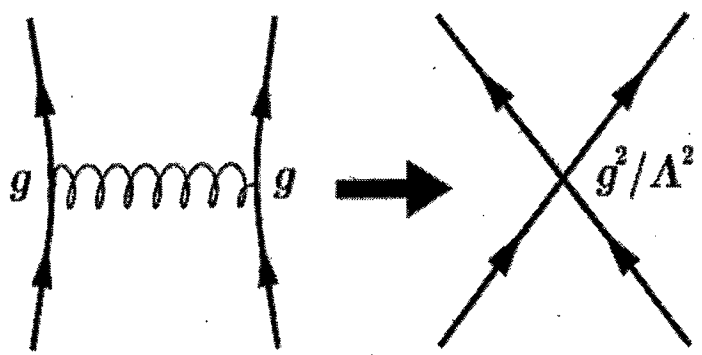

Solution of NJL gap equation: What about the unlocking for

$$T \neq 0?$$

Gap equations

$$\Delta_{\alpha\beta} = \begin{pmatrix} \Delta_8^3 E_3 & & & \\ & \Delta_8^2 E_4 & & \\ & & \Delta_8^1 & \Delta \\ & & \Delta & \Delta_1^1 \end{pmatrix}$$

: **Minimal interpolating State between 2SC and pure CFL**

$$\begin{cases} \Delta_8^3 = \frac{1}{12}\left(5K_{83}\left[\Delta_8^3\right] - 2K_{11}\left[\Delta_8^1,\Delta,\Delta_1^1\right] - K_{81}\left[\Delta_8^1,\Delta,\Delta_1^1\right] - 2\sqrt{2}K\left[\Delta_8^1,\Delta,\Delta_1^1\right]\right) \\ \Delta_8^2 = \frac{1}{12}\left(2K_{82}\left[\Delta_8^2\right] - 2K_{11}\left[\Delta_8^1,\Delta,\Delta_1^1\right] + 2K_{81}\left[\Delta_8^1,\Delta,\Delta_1^1\right] + \sqrt{2}K\left[\Delta_8^1,\Delta,\Delta_1^1\right]\right) \\ \Delta_8^1 = \frac{1}{12}\left(-K_{81}\left[\Delta_8^1,\Delta,\Delta_1^1\right] - 2K_{11}\left[\Delta_8^1,\Delta,\Delta_1^1\right] + 2\sqrt{2}K\left[\Delta_8^1,\Delta,\Delta_1^1\right] - 3K_{83}\left[\Delta_8^3\right] + 8K_{82}\left[\Delta_8^2\right]\right) \\ \Delta_1^1 = \frac{1}{6}\left(-K_{81}\left[\Delta_8^1,\Delta,\Delta_1^1\right] - 3K_{83}\left[\Delta_8^3\right] - 4K_{82}\left[\Delta_8^2\right]\right) \\ \Delta = \frac{1}{12}\left(-2K\left[\Delta_8^1,\Delta,\Delta_1^1\right] + \sqrt{2}K_{81}\left[\Delta_8^1,\Delta,\Delta_1^1\right] + \sqrt{2}\left(2K_{82}\left[\Delta_8^2\right] - 3K_{83}\left[\Delta_8^3\right]\right)\right) \end{cases}$$

Detail of kernel

$$K_{83}[\Delta]=\int\frac{d^3q}{(2\pi)^3}\frac{1}{4}\left(\tanh\left(\frac{E_{0+}[\Delta]}{2T}\right)\frac{\Delta}{E_{0+}[\Delta]}+\tanh\left(\frac{E_{0-}[\Delta]}{2T}\right)\frac{\Delta}{E_{0-}[\Delta]}\right)\bar{g}^2(q,k)\left[g_{\mu\nu}D_{\mu\nu}(q-k)\right]$$

$$K_{82}[\Delta]=\int\frac{d^3q}{(2\pi)^3}\frac{1}{8}\left(\begin{array}{l}+\tanh\left(\frac{E_{0+}[\Delta]}{2T}\right)\frac{\Delta}{E_{0+}[\Delta]}+\tanh\left(\frac{E_{0-}[\Delta]}{2T}\right)\frac{\Delta}{E_{0-}[\Delta]}\\+\tanh\left(\frac{E_{M+}[\Delta]}{2T}\right)\frac{\Delta}{E_{M+}[\Delta]}+\tanh\left(\frac{E_{M-}[\Delta]}{2T}\right)\frac{\Delta}{E_{M-}[\Delta]}\end{array}\right)\bar{g}^2(q,k)\left[g_{\mu\nu}D_{\mu\nu}(q-k)\right]$$

$$K_{81}[\Delta_1,\Delta_2,\Delta_3]=\{\text{ultra super complicated form...}\}$$

$$K_{11}[\Delta_1,\Delta_2,\Delta_3]=\{\text{ultra super complicated form...}\}$$

$$K[\Delta_1,\Delta_2,\Delta_3]=\{\text{ultra super complicated form...}\}$$

$$E_{M\pm}[\Delta]=\sqrt{\left(\sqrt{q^2+M^2}\mp\mu\right)^2+\Delta^2}$$: **Quasi-Quark and Quasi-AntiQuark energy**

Derivation of effective potential

$$\frac{\partial \Omega_{eff}}{\partial g^2} = \frac{1}{g^2}\left\langle H_{\text{int.}} \right\rangle = \frac{1}{2g^2} tr\left[S(\Sigma)\Sigma\right] \quad \textit{with definition}$$

$$\Sigma_{\alpha\beta} = g^2 T_{\gamma\alpha} S^{\gamma\delta} T_{\delta\beta}, \quad S = \begin{pmatrix} \phi^1 E_3 & & & \\ & \phi^2 E_4 & & \\ & & \phi^3 & \phi^4 \\ & & \phi^4 & \phi^5 \end{pmatrix}, \quad \Sigma = \begin{pmatrix} \Delta_1 E_3 & & & \\ & \Delta_2 E_4 & & \\ & & \Delta_3 & \Delta_4 \\ & & \Delta_4 & \Delta_5 \end{pmatrix}.$$

$T_{\gamma\alpha}$ *is quark-gluon vertex in color-flavor mixed base. We have*

$$\frac{\partial \Omega_{eff}}{\partial g^2} = \frac{1}{2g^4} C^{ij} \Delta_i \Delta_j, \quad \textit{with} \quad C = \begin{pmatrix} 3 & 0 & -3 & -6\sqrt{2} & -6 \\ 0 & -8 & 8 & 4\sqrt{2} & -8 \\ -3 & 8 & -5 & 2\sqrt{2} & -2 \\ -6\sqrt{2} & 4\sqrt{2} & 2\sqrt{2} & -12 & 0 \\ -6 & -8 & -2 & 0 & -4 \end{pmatrix}$$

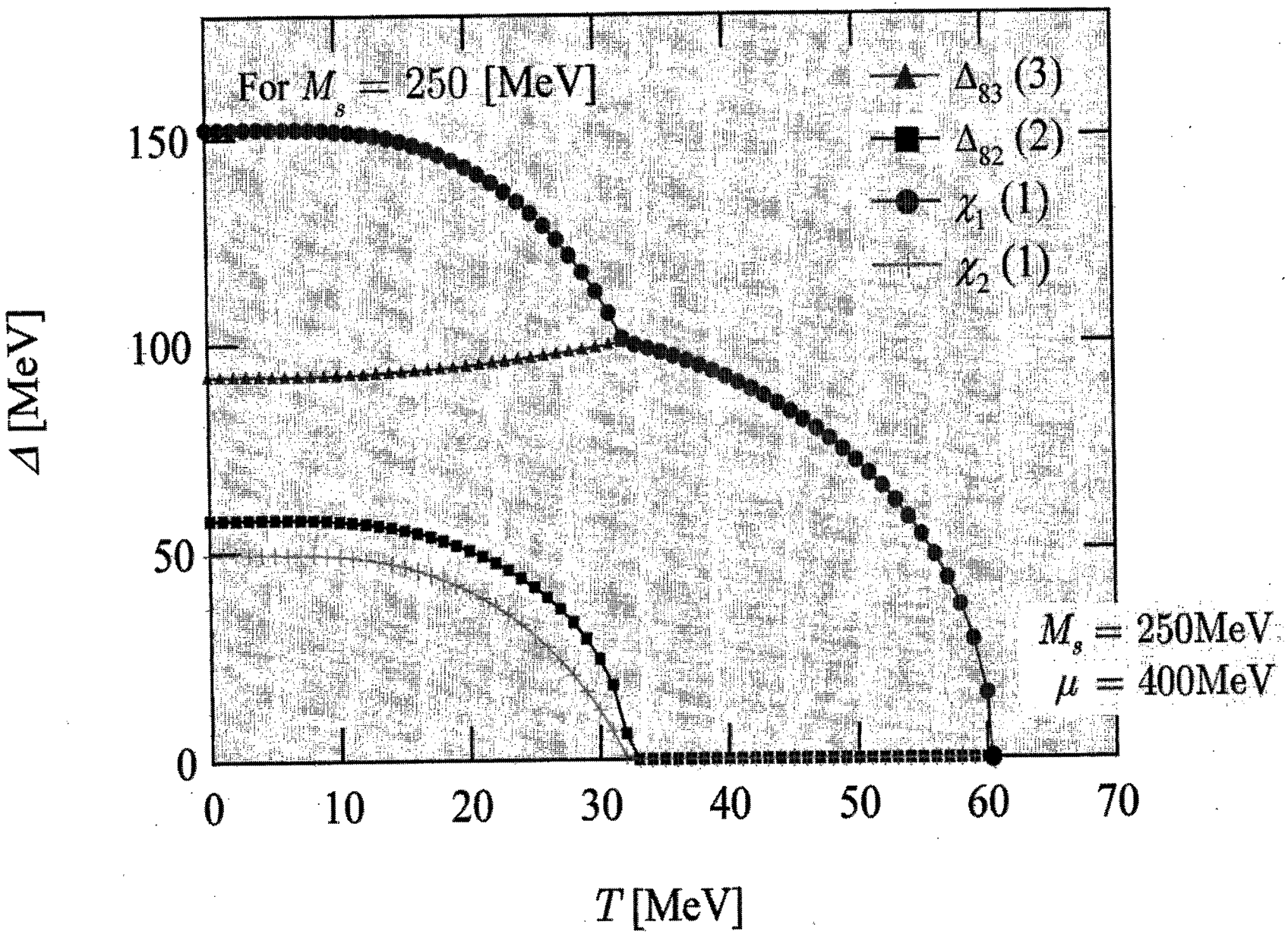
For $M_s = 250$ [MeV]
Δ_{83} (3)
Δ_{82} (2)
χ_1 (1)
χ_2 (1)
$M_s = 250$MeV
$\mu = 400$MeV
Δ [MeV]
T [MeV]
0
50
100
150
0
10
20
30
40
50
60
70

Asymptotic Smooth Unlocking or Continuous 2nd order transition?

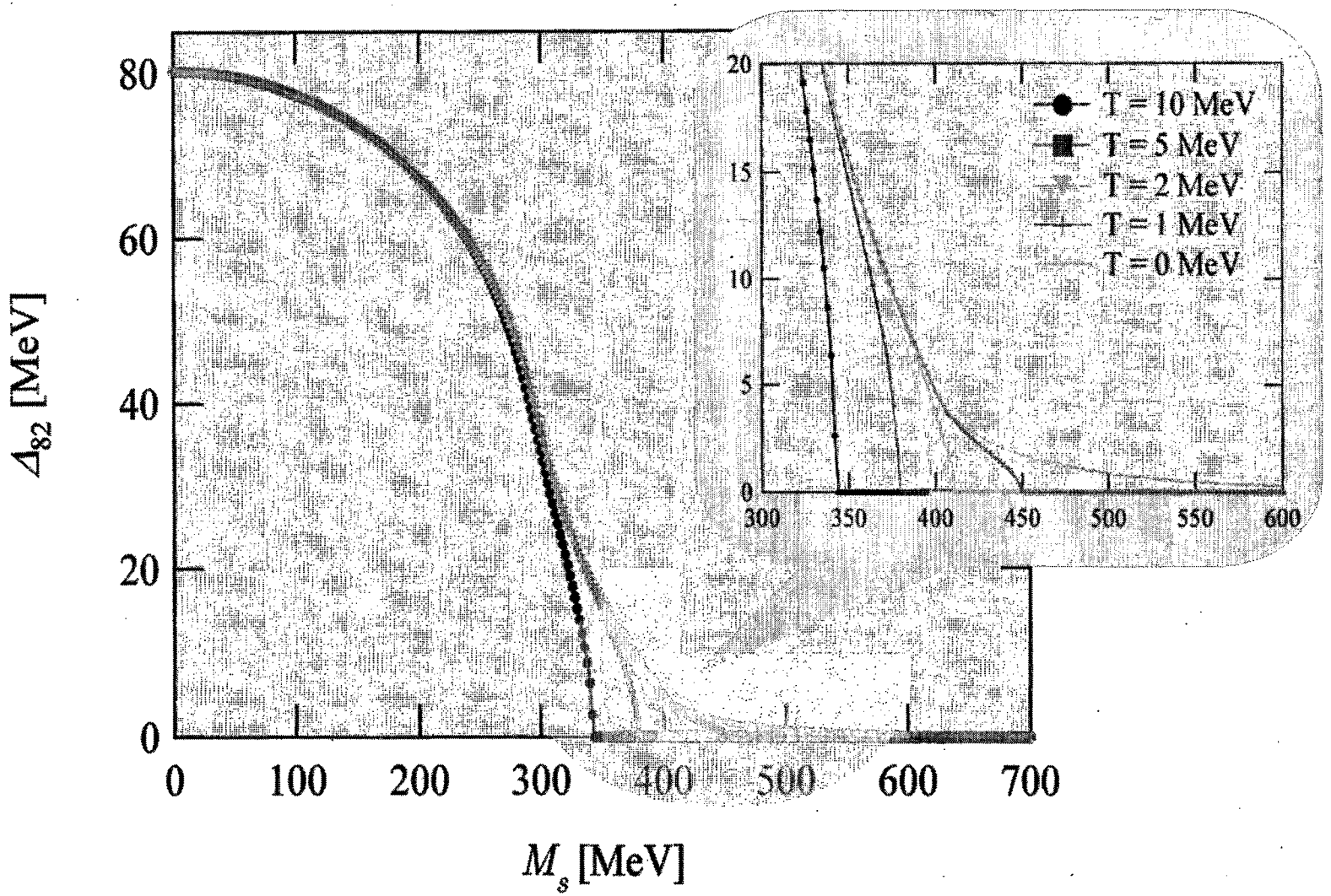

What happens when we goes towards low density?

Pair "wavefunction" : $\varphi(\vec{r}) = \langle q(t,\vec{r})q(t,0)\rangle \underset{\mu r \gg 1}{\rightarrow} N\frac{\sin(\mu r)}{(\mu r)^{3/2}}e^{-\Delta r}$

What about internal structure of Cooper pairs?

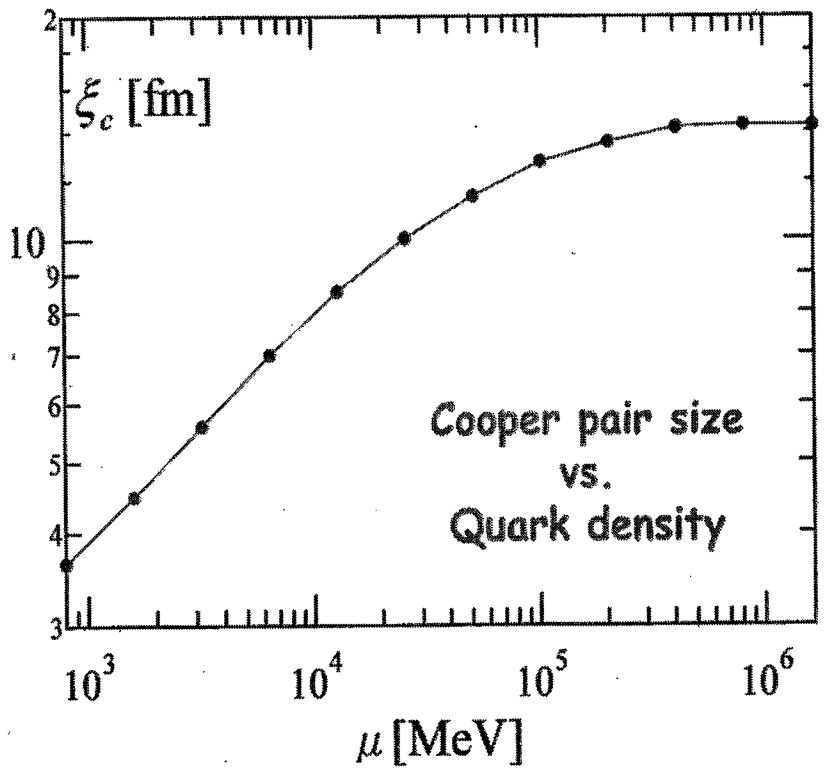

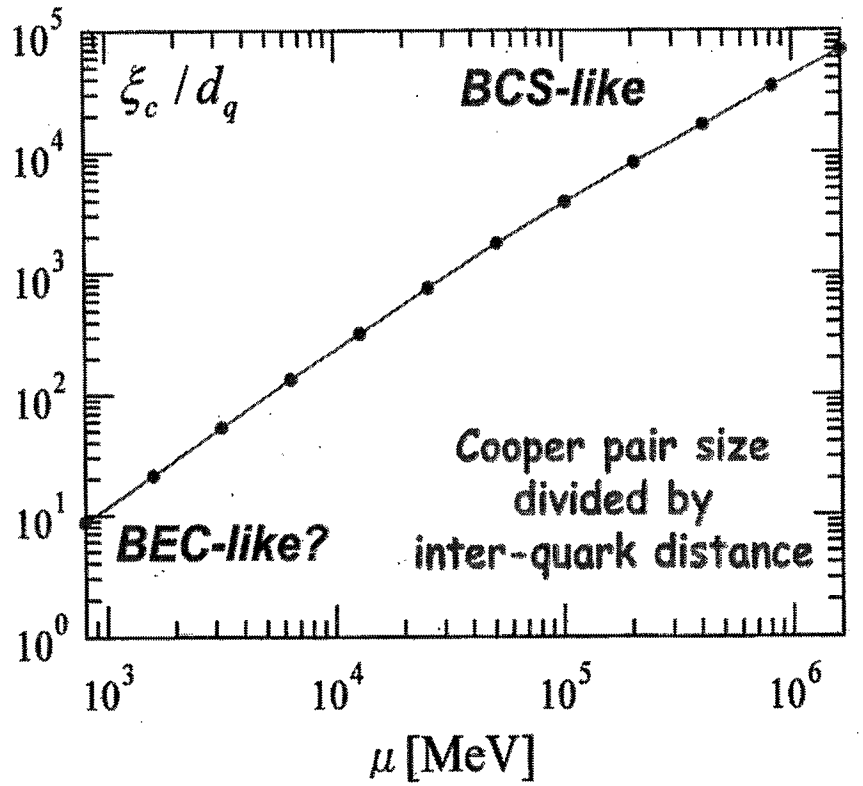

Improved ladder Schwinger-Dyson approach
Abuki-Itakura-Hatsuda, Phys. Rev. D65, (2002)

Tightly bound diquarks at low density?

What is BCS/BEC crossover?

What about the **relativistic** fermion case?

Weak coupling gap equation :

$$\Delta(p) = \sum_k V(p,k)\left[\left(1-2n_F^+\right)\frac{\Delta(k)}{2\varepsilon_k^+[\Delta]} + \left(1-2n_F^-\right)\frac{\Delta(k)}{2\varepsilon_k^-[\Delta]}\right]$$

with $\begin{cases} \varepsilon_k^{\pm}[\Delta] \equiv \sqrt{E_k^{\pm 2} + \Delta(k)^2} \\ E_k^{\pm} = \sqrt{k^2+m^2} \mp \mu \end{cases}$

can be converted into :

$$\begin{cases} \left(-\mu + \sqrt{p^2+m^2}\right)\varphi_+(p) = \sum_k \left(1-2n_p^+\right)V(p,k)\left[\varphi_+(k)+\varphi_-(k)\right] \\ \left(-\mu - \sqrt{p^2+m^2}\right)\varphi_+(p) = \sum_k \left(1-2n_p^-\right)V(p,k)\left[\varphi_+(k)+\varphi_-(k)\right] \end{cases}$$

which is regarded as Pauli - blocked Dirac eigenvalue equation

$\left(i\vec{\alpha}\cdot\vec{\nabla} + m\beta - (1-2n)\hat{V}\right)\varphi(x) = \mu\varphi(x)$ **with** $\vec{\alpha} = \gamma_0\vec{\gamma},\ \beta = \gamma_0$

S-wave scattering length and Phase shift

C.A.R. Sa de Melo et al., Phys. Rev. Lett. 71. 3202, '93

$$q\cot\delta(q) = -\frac{1}{a_s} + O\left(q^2\right)$$

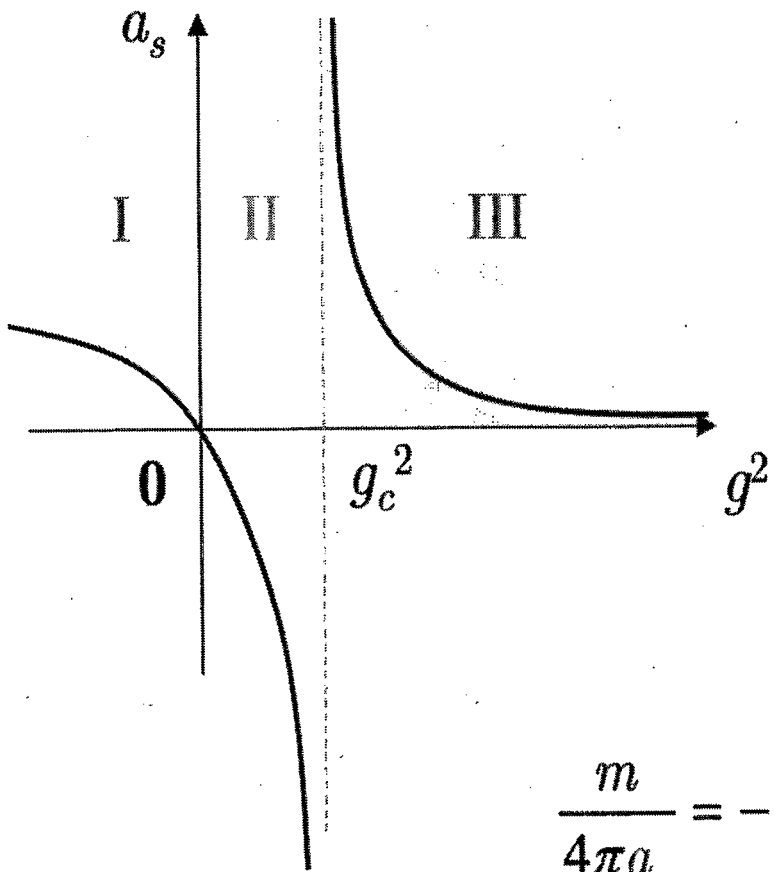

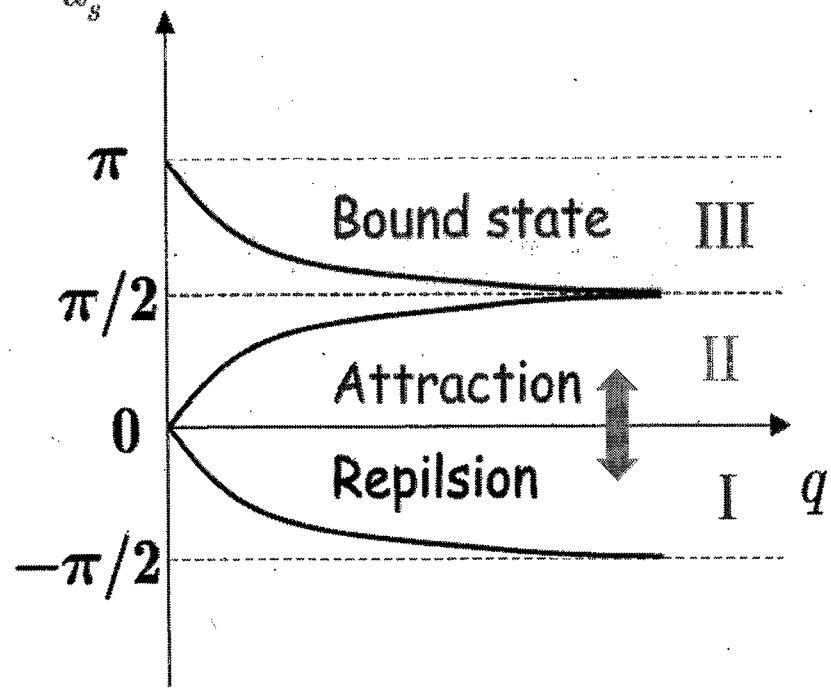

$$\frac{m}{4\pi a_s} = -\frac{1}{g_s^2} + \sum_{\vec{k}} \frac{m}{\vec{k}^2}$$

Novel Phases of High Density Quark Matter and Their Roles in Physical Systems

M. Tachibana

Novel phases of high density quark matter and their roles in physical systems *

M. Tachibana†

Abstract

In this paper, we investigate several interesting aspects of high density quark matter, particularly emphasizing on remarkable phase structures of color superconductivity and their possible roles in physical systems. Firstly thermal color superconducting phase transitions in high density three-flavor quark matter are investigated in the Ginzburg-Landau approach. Effects of nonzero strange quark mass, electric and color charge neutrality, and direct instantons are considered. Weak coupling calculations show that an interplay between the mass and electric neutrality effects near the critical temperature gives rise to three successive second-order phase transitions as the temperature increases. Secondly we show calculations of neutrino interaction rates such as mean free path and emissivity in color-flavor locked quark matter besed on the effective field theory approach, which may play an important role when we consider the issue on neutron star cooling.

*Talk given in RIKEN-TODAI Mini-Workshop on "Topics in Hadron Physics at RHIC"

†The Institute of Physical and Chemical Research (RIKEN)

1 Introduction

Unraveling the phase structure at high baryon density is one of the most challenging problems in quantum chromodynamics (QCD). Among others, color superconductivity in cold dense quark matter has been discussed from various viewpoints [1, 2]. In relation to real systems such as newly born compact stars in stellar collapse, it is important to study the color superconductivity not only as a function of the quark chemical potential μ but also as a function of the temperature T. This is because the possible presence of color superconducting quark matter in a star affects the star's thermal evolution [3]. In this paper, we show some interesting aspects of color superconductivity, especially emphasizing on novel phase structures associated with realistic systems. The content of this paper is as follows. In section 2, we describe thermal phase transition based on the Ginzburg-Landau approach. In section 3 and 4, effective field theory in the CFL phase is introduced, computing the weak interaction rates associated with neutron star cooling.

2 Melting pattern of diquark condensates

In this section, we adopt the Ginzburg-Landau (GL) approach near the transition temperatures, which was previously used to study the massless three-flavor case [4, 5, 6] and is a more advantageous framework to weak coupling calculations than other mean-field approaches [7, 8]. In a realistic situation, the GL potential acquires the following corrections. First of all, nonzero m_s affects the potential through the s quark propagator [8] in such a way as to lower the temperature at which a diquark condensate with s quarks dissolves. This is because the pairing interaction due to one-gluon exchange is effectively diminished by m_s if the pair contains the s quark. Secondly, when quark matter with nonzero m_s is beta equilibrated and neutralized by electrons near the transition temperatures, the chemical potentials between d, s quarks and u quarks differ. Through this chemical potential difference, the GL potential acquires another m_s dependence, which is the essential origin of the dSC phase. Thirdly, the instanton contribution gives an m_s dependence to the GL potential through the effective four-fermion interaction proportional to m_s. We finally note that in weak coupling, color neutrality makes negligible difference in the GL potential near the transition temperatures [4].

We assume that diquark pairing takes place in the color-flavor anti-

symmetric channel with $J^P = 0^+$, which is predicted to be the most attractive channel in weak coupling [9]. In this case, the pairing gap of a quark of color b and flavor j with that of color c and flavor k has the form $\phi_{bcjk} = \epsilon_{abc}\epsilon_{ijk}(\mathbf{d}_a)^i$ [4]. Here the $3\times$ 3 matrix $(\mathbf{d}_a)^i$ transforms as a vector under $G = SU(3)_C \times SU(3)_{L+R} \times U(1)_B$ and belongs to the $(3^*, 3^*)$ representation of $SU(3)_C \times SU(3)_{L+R}$.

For a homogeneous system of massless quarks ($m_{u,d,s} = 0$), the GL potential is invariant under $SU(3)_C \times SU(3)_{L+R}$ and valid near the critical temperature, T_c, common to all states belonging to the channel considered here. This potential reads [4, 10]

$$S = \bar{\alpha}\sum_a |\mathbf{d}_a|^2 + \beta_1(\sum_a |\mathbf{d}_a|^2)^2 + \beta_2 \sum_{ab} |\mathbf{d}_a{}^* \cdot \mathbf{d}_b|^2, \tag{1}$$

where $(\mathbf{d}_a)^i = (d_a^u, d_a^d, d_a^s)$ and the inner product is taken for flavor indices. In the weak coupling regime, the coefficients are [4]

$$\beta_1 = \beta_2 = \frac{7\zeta(3)}{8(\pi T_c)^2} N(\mu) \equiv \beta, \quad \bar{\alpha} = 4N(\mu)t \equiv \alpha_0 t, \tag{2}$$

where $N(\mu) = \mu^2/2\pi^2$ is the density of states at the Fermi surface, and $t = (T - T_c)/T_c$ is the reduced temperature. With the parameters (2), one finds a second order phase transition at $T = T_c$ from the CFL phase ($d_a^i \propto \delta_a^i$) to the normal phase ($d_a^i = 0$) in mean-field theory [4].

Let us now consider the effect of a nonzero m_s in the quark propagator on the GL potential. We assume $m_{u,d} = 0$ for simplicity and consider the high density regime, $m_s \ll \mu$. Near T_c the leading effect of m_s is to modify the quadratic term in the GL potential (1). The corrections to the quartic terms are subleading and negligible. Since m_s affects only us and ds pairings, the correction to the quadratic term has the form

$$\epsilon \sum_a (|d_a^u|^2 + |d_a^d|^2) = \epsilon \sum_a (|\mathbf{d}_a|^2 - |d_a^s|^2). \tag{3}$$

Note that this correction induces an asymmetry in the flavor structure of the CFL phase.

In weak coupling, ϵ can be calculated by including m_s in the Nambu-Gor'kov quark propagator when evaluating the thermodynamic potential. Following Ref. [4], we expand the thermodynamic potential not only in d_a^i but also in m_s up to $\mathcal{O}(m_s^2)$, and obtain

$$\epsilon \simeq \alpha_0 \frac{m_s^2}{4\mu^2} \ln\left(\frac{\mu}{T_c}\right) \sim 2\alpha_0\sigma. \tag{4}$$

Here the dimensionless parameter σ is given by

$$\sigma = \left(\frac{3\pi^2}{8\sqrt{2}}\right)\frac{m_s^2}{g\mu^2}, \tag{5}$$

where g is the QCD coupling constant. As long as $\sigma \ll 1$, which is relevant at asymptotically high density, the following GL analysis near T_c is valid. In the latter estimate in Eq. (4) we use the leading-order result in g, $\ln(T_c/\mu) \sim -3\pi^2/(\sqrt{2}g)$ [9]. This behavior of T_c originates from the long-range color magnetic interaction which prevails in the relativistic regime. As a result of the modification by m_s to $\ln(T_c/\mu)$, ϵ has a positive value such that ud pairing is favored over us and ds pairings. Consequently, the CFL phase becomes asymmetric in flavor space and its critical temperature is lowered, leading to the appearance of the 2SC phase ($d_a^i \propto \delta^{is}$) just below T_c [8]. Note that Eq. (3) has no effect on the 2SC phase. We also note that T_c itself is modified by m_s through the modification of the normal medium as $T_c(1 + \mathcal{O}(g\sigma))$.

We turn to discuss effects of charge neutrality which also depend on m_s as mentioned above. Under beta equilibrium and charge neutrality, the electron chemical potential μ_e and the shift $\delta\mu_i$ of the chemical potential of flavor i from the average (μ) are related by $\delta\mu_i = -q_i\mu_e$, with electric charge q_i. We see from Ref. [4] that the thermodynamic-potential correction due to $\delta\mu_i$ has the form

$$\eta\ (\frac{1}{3}\sum_a |\mathbf{d}_a|^2 - \sum_a |d_a^u|^2). \tag{6}$$

In weak coupling, where one may regard normal quark matter and electrons as noninteracting Fermi gases, μ_e is related to m_s as $\mu_e = m_s^2/4\mu$. This estimate is valid in the vicinity of T_c where corrections to μ_e by a finite pairing gap affect only the quartic terms in the GL potential. By combining this estimate with the weak coupling expression for η/μ_e given in Ref. [4], we obtain

$$\eta \simeq \alpha_0 \frac{m_s^2}{8\mu^2} \ln\left(\frac{\mu}{T_c}\right) \sim \alpha_0\sigma. \tag{7}$$

Since $\eta > 0$, ds pairing is more favorable than ud and us pairings. This feature stems from the modification by $\delta\mu_i$ to the exponential factor of T_c, $\exp[-3\pi^2/(\sqrt{2}g)]$, which tends to increase (decrease) the critical temperature for ij pairing when $\delta\mu_i + \delta\mu_j > 0 (< 0)$.

We consider color neutrality of the system as well. In contrast to the case at $T = 0$, however, it affects only the quartic terms in the GL potential through possible chemical potential differences between colors [4, 11], and in weak coupling its magnitude is suppressed by $\mathcal{O}((T_c/g\mu)^2)$ compared to the leading quartic terms. Thus color neutrality has no essential consequence to the phase transitions considered in this Letter. A major difference between corrections of the charge neutrality and the color neutrality is that the former shifts the quark chemical potentials even in the normal phase, while the latter works only when the pairing occurs. This is why the former is more important than the latter near T_c.

The direct instanton at nonzero m_s, which induces an effective four-fermion interaction between u and d quarks [12], leads to a quadratic term in the GL potential, $\zeta \sum_a |d_a^s|^2$. An explicit weak coupling calculation shows that $\zeta \sim -\alpha_0(m_s/\mu)(\Lambda_{\rm QCD}/\mu)^9(1/g)^{14}$. The negative sign indicates that the instanton favors ud pairing as does one-gluon exchange [see Eq. (3)], but the magnitude of ζ is highly suppressed at high densities. Hereafter we will thus ignore instanton effects.

Since the two effects of nonzero m_s, characterized by Eqs. (3) and (6), favor ud pairing and ds pairing, respectively, the finite temperature transition from the CFL to the normal phase at $m_s = 0$ is expected to be significantly modified. In fact, successive color-flavor unlocking transitions take place instead of a simultaneous unlocking of all color-flavor combinations. To describe this *hierarchical thermal unlocking*, it is convenient to introduce a parameterization,

$$d_a^i = \begin{pmatrix} \Delta_1 & 0 & 0 \\ 0 & \Delta_2 & 0 \\ 0 & 0 & \Delta_3 \end{pmatrix}, \tag{8}$$

where $\Delta_{1,2,3}$ are assumed without loss of generality to be real. We also name the phases for later convenience as

$$\begin{array}{lll} \Delta_{1,2,3} \neq 0 & & : \text{mCFL}, \\ \Delta_1 = 0, & \Delta_{2,3} \neq 0 & : \text{uSC}, \\ \Delta_2 = 0, & \Delta_{1,3} \neq 0 & : \text{dSC}, \\ \Delta_{1,2} = 0, & \Delta_3 \neq 0 & : \text{2SC}, \end{array} \tag{9}$$

where dSC (uSC) stands for superconductivity in which for d (u) quarks all three colors are involved in the pairing.

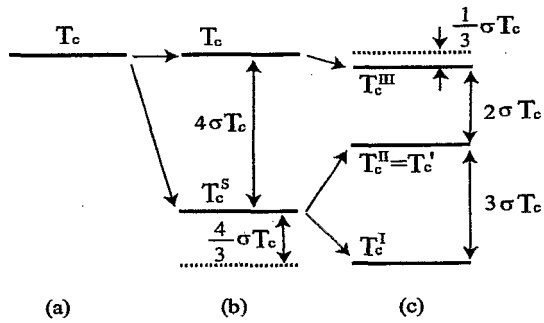

Figure 1: Transition temperatures of the three-flavor color superconductor in weak coupling: (a) all quarks are massless; (b) nonzero m_s in the quark propagator is considered; (c) electric charge neutrality is further imposed. The numbers attached to the arrows are in units of σT_c.

In terms of the parameterization (8), the GL potential with corrections of $\mathcal{O}(m_s^2)$ to the quadratic term, Eqs. (3) and (6), reads

$$\begin{aligned} S &= \bar{\alpha}'(\Delta_1^2+\Delta_2^2+\Delta_3^2) - \epsilon\Delta_3^2 - \eta\Delta_1^2 \\ &+ \beta_1(\Delta_1^2+\Delta_2^2+\Delta_3^2)^2 + \beta_2(\Delta_1^4+\Delta_2^4+\Delta_3^4), \end{aligned} \tag{10}$$

where $\bar{\alpha}' = \bar{\alpha} + \epsilon + \frac{\eta}{3}$.

We proceed to analyse the phase structure dictated by Eq. (10) with the weak coupling parameters (2), (4), and (7) up to leading order in g. In Figs. 1 and 2 the results obtained by solving the coupled algebraic equations, $\partial S/\partial\Delta_{1,2,3} = 0$, are summarized. Figure 1(a) shows the second-order phase transition, CFL $\rightarrow$ normal for $m_s = 0$. Figures 1(b,c) represent how the phase transitions and their critical temperatures bifurcate as we introduce (b) effects of a nonzero m_s in the quark propagator and then (c) effects of charge neutrality. In case (b), two second-order phase transitions arise, mCFL (with $\Delta_1 = \Delta_2$) $\rightarrow$ 2SC at $T = T_c^s \equiv (1-4\sigma)T_c$, and 2SC $\rightarrow$ normal at $T = T_c$. In case (c), there arises three successive second-order phase transitions, mCFL $\rightarrow$ dSC at $T = T_c^{\rm I}$, dSC $\rightarrow$ 2SC at $T = T_c^{\rm II}$, and 2SC $\rightarrow$ normal at $T = T_c^{\rm III}$. Shown in Fig. 2 is the T-dependence of the gaps $\Delta_{1,2,3}$ for case (c). All the gaps are continuous functions of T, but their slopes are discontinuous at the critical points, which reflects the second order nature of the transitions in the mean-field treatment of Eq. (10).

We may understand the bifurcation of the transition temperatures in weak

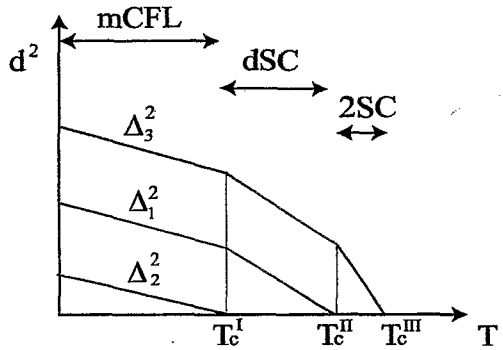

Figure 2: A schematic illustration of the gaps squared as a function of T.

coupling as follows. In the massless case (a), T_c is degenerate between the CFL and 2SC phases, the chemical potential is common to all three flavors and colors, and the CFL phase is more favorable than the 2SC phase below T_c. As one goes from (a) to (b), nonzero m_s sets in, which tends to suppress the pairing interactions including the s quark. The critical temperature for the CFL phase is then lowered, which allows the 2SC phase to appear at temperatures between T_c^s and T_c. As one goes from (b) to (c), charge neutrality sets in, which acts to decrease the chemical potential of u quarks by $(2/3)\mu_e$ and increase that of d and s quarks by $(1/3)\mu_e$. Since $\mu_e > 0$, the average chemical potential of quarks involved in ds pairing increases, while those in ud and us pairings decrease equally. Accordingly, the transition temperatures further change from T_c to $T_c^{\rm III}$ and from T_c^s to $T_c^{\rm I}$ and $T_c^{\rm II}$.

Now we examine in more detail how the color-flavor unlocking in case (c) proceeds with increasing T from the region below $T_c^{\rm I}$.
(i) Just below $T_c^{\rm I}$, we have a CFL-like phase, but the three gaps take different values, with an order $\Delta_3 > \Delta_1 > \Delta_2 \neq 0$ (the mCFL phase). The reason why this order is realized can be understood from the GL potential (10). The ϵ-term and η-term in Eq. (10) tend to destabilize us pairing (Δ_2) relative to ud pairing (Δ_3) and ds pairing (Δ_1). Since $\epsilon > \eta (> 0)$, ds pairing is destabilized more effectively than ud pairing. The value of each gap in the mCFL phase reads

$$\Delta_3^2 = \frac{\alpha_0}{8\beta}\left(\frac{T_c - T}{T_c} + \frac{8}{3}\sigma\right), \tag{11}$$

$$\Delta_1^2 = \frac{\alpha_0}{8\beta}\left(\frac{T_c - T}{T_c} - \frac{4}{3}\sigma\right), \tag{12}$$

$$\Delta_2^2 = \frac{\alpha_0}{8\beta}\left(\frac{T_c - T}{T_c} - \frac{16}{3}\sigma\right). \tag{13}$$

The mCFL phase has only a global symmetry $U(1)_{C+L+R} \times U(1)_{C+L+R}$ in contrast to the global symmetry $SU(3)_{C+L+R}$ in the CFL phase with $m_{u,d,s} = 0$. There are no gapless quark excitations in both mCFL and CFL phases. As T increases, the first unlocking transition, the unlocking of Δ_2 (the pairing between Bu and Rs quarks), takes place at the critical temperature,

$$T_c^{\mathrm{I}} = \left(1 - \frac{16}{3}\sigma\right) T_c. \tag{14}$$

(ii) For $T_c^{\mathrm{I}} < T < T_c^{\mathrm{II}}$, $\Delta_2 = 0$ and

$$\Delta_3^2 = \frac{\alpha_0}{6\beta}\left(\frac{T_c - T}{T_c} + \frac{2}{3}\sigma\right), \tag{15}$$

$$\Delta_1^2 = \frac{\alpha_0}{6\beta}\left(\frac{T_c - T}{T_c} - \frac{7}{3}\sigma\right). \tag{16}$$

In this phase, we have only ud and ds pairings (the dSC phase), and there is a manifest symmetry, $U(1)_{C+L+R} \times U(1)_{C+L+R} \times U(1)_{C+V+B} \times U(1)_{C+V+B}$. By diagonalizing the inverse quark propagator in the Nambu-Gor'kov representation, we find three gapless quark excitations in the color-flavor combinations: Bu, Rs, and a linear combination of Ru and Bs. At $T = T_c^{\mathrm{II}}$, the second unlocking transition, the unlocking of Δ_1 (the pairing between Gs and Bd quarks), takes place at the critical temperature,

$$T_c^{\mathrm{II}} = \left(1 - \frac{7}{3}\sigma\right) T_c. \tag{17}$$

(iii) For $T_c^{\mathrm{II}} < T < T_c^{\mathrm{III}}$, one finds the 2SC phase, which has only ud pairing with

$$\Delta_3^2 = \frac{\alpha_0}{4\beta}\left(\frac{T_c - T}{T_c} - \frac{1}{3}\sigma\right). \tag{18}$$

The 2SC phase has a symmetry $SU(2)_C \times SU(2)_{L+R} \times U(1)_{C+B} \times U(1)_{L+R+B}$ [6]. In this phase the s quark and B quark excitations are gapless. The

final unlocking transition where Δ_3 (the pairing between Rd and Gu quarks) vanishes occurs at

$$T_c^{\mathrm{III}} = \left(1 - \frac{1}{3}\sigma\right) T_c. \tag{19}$$

Above T_c^{III}, the system is in the normal phase.

In Table I, we summarize the symmetry and the gapless quark modes in each phase discussed above. The number of gluons having nonzero Meissner masses, which is related to the remaining color symmetry, is also shown [14]. We note that more gapless quark modes may appear if the system is in the close vicinity of T_c^{I}, T_c^{II}, and T_c^{III} where Δ_2, Δ_1, and Δ_3 are less than $\sim m_s^2/\mu$ [13].

So far, we have studied the phase transitions in the mean-field level. In weak coupling, as shown in Ref. [6] in the massless limit, thermally fluctuating gauge fields could change the order of the transitions described in Figs. 1 and 2. A detailed account on this effect will be reported elsewhere [14]; here we recapitulate the important results. First, the second order transition, mCFL $\rightarrow$ dSC, remains second order even in the presence of the thermal gluon fluctuations. This is because all eight gluons are Meissner screened at $T = T_c^{\mathrm{I}}$ and thus cannot induce a cubic term with respect to the order parameter in the GL potential. On the other hand, the transitions, dSC $\rightarrow$ 2SC and 2SC $\rightarrow$ normal, become weak first order since some gluons, which

Table 1: The symmetry, the gapless quark modes, and the number of Meissner screened gluons in the mCFL, dSC, and 2SC phases. The gapless quark mode (Ru, Bs) denotes the linear combination of Ru and Bs quarks.

	Symmetry	Gapless quark modes	Number of massive gluons
mCFL	$[U(1)]^2$	none	8
dSC	$[U(1)]^4$	Bu, Rs (Ru, Bs)	8
2SC	$[SU(2)]^2 \times [U(1)]^2$	Bu, Bd, Bs, Rs, Gs	5

are massless in the high temperature phase, become Meissner screened in the low temperature phase (Table I).

In summary, we have investigated color-flavor unlockings at finite temperatures taking into account the strange quark mass and charge neutrality in the GL approach. We find three successive unlocking transitions, mCFL $\rightarrow$ dSC $\rightarrow$ 2SC$\rightarrow$ normal, occurring in weak coupling. Most remarkably, the dSC phase appears between the mCFL and 2SC phases. In this phase all eight gluons are Meissner screened and the three quark excitations are gapless. The question of how the phase structure of neutral quark matter obtained near T_c is connected to that at $T = 0$, which approaches the CFL phase in the limit of high density, is an interesting open problem.

3 Effective Field Theory in CFL phase

In this section, we introduce the effective lagrangian in the CFL phase in order to calculate the weak interaction rates related to neutron star cooling. As was already mentioned, in the CFL phase, all nine quarks are massive and all the gluons acquire the Meissner mass. Due to this, the dominant degrees of freedom at low energies such as several tens of MeV are Namubu-Goldstone bosons associated with chiral symmetry breaking as well as U(1) baryon symmetry breaking. There are several articles that describe in detail the effective theory for the Goldstone bosons in Color-Flavor-Locked quark matter [19, 20, 21]. It is possible to parametrize low energy excitations about the CFL ground state in terms of the two fields $B = H/\sqrt{24}f_H$ and $\Sigma = e^{2i\pi/f_\pi}$, representing the Goldstone bosons of broken baryon number H and of broken chiral symmetry, the octet π. Then the leading terms of the effective Lagrangian describing the octet Goldstone boson field π are given by

$$\mathcal{L} = \frac{1}{4}f_\pi^2\Big[Tr\nabla_0\Sigma\nabla_0\Sigma^\dagger - v^2\vec{\nabla}\Sigma\vec{\nabla}\Sigma^\dagger\Big] + f_\pi^2\Big[\frac{a}{2}Tr\tilde{M}(\Sigma+\Sigma^\dagger) + \frac{\chi}{2}TrM(\Sigma+\Sigma^\dagger)\Big]. \tag{20}$$

The decay constant f_π has been computed previously [21] and is proportional to the quark chemical potential μ. ∇_0 includes the Bedaque-Schafer terms[22] and $\tilde{M} = |M|M^{-1}$, where $M = \mathrm{diag}(m_u, m_d, m_s)$. The velocity factor $v = 1/\sqrt{3}$ and $a = 3\frac{\Delta^2}{\pi^2 f_\pi^2}$ [21], where Δ is the gap which is around 100 MeV at μ = 500 MeV.

To incorporate weak interactions, we gauge the chiral Lagrangian in the usual way by replacing the covariant derivative by [23]

$$D_\mu\Sigma = \nabla_\mu\Sigma - \frac{ig}{\sqrt{2}}(W_\mu^+\tau^+ + W_\mu^-\tau^-)\Sigma - \frac{ig}{\cos\theta_W}Z_\mu(\tau_3\Sigma - \sin^2\theta_W[Q,\Sigma]). \quad (21)$$

The fields $W_\mu^\pm, Z_\mu$ describe weak gauge bosons. The charge matrix is diagonal $Q = \mathrm{diag}(\frac{2}{3}, -\frac{1}{3}, -\frac{1}{3})$ as well as weak-isospin matrix $\tau_3 = \frac{1}{2}\mathrm{diag}(1,-1,-1)$ whereas τ^+ and τ^- are the isospin raising and lowering operators which incorporate Cabbibo mixing.

For momenta small compared to f_π we can expand the nonlinear chiral Lagrangian to classify diagrams as the first order (proportional to f_π) and the second order (independent of f_π). The amplitudes for the leading order processes are given by

$$A_{\pi^0\to\nu\bar{\nu}} = \frac{G_F}{\sqrt{2}}f_\pi\tilde{p}_\mu j_Z^\mu, \quad A_{\pi^\pm\to e\nu} = G_F f_\pi\cos\theta_C\tilde{p}_\mu j_W^\mu, \quad A_{K^\pm\to e\nu} = G_F f_\pi\sin\theta_C\tilde{p}_\mu j_W^\mu \quad (22)$$

where $\tilde{p}_\mu = (E, v^2\vec{p})$ is the modified four-momentum of Goldstone boson and j_W^μ and j_Z^μ describe the charged and neutral leptonic currents, respectively. θ_C is the Cabbibo mixing angle. Note that the meson "four-momentá" that appear in the matrix element do not correspond to the on-shell four momenta of the mesons. This is because the covariant derivative contains the in-medium velocity and for the case of kaons, the energy shift arising from the Bedaque-Schafer term.

In addition to the octet Goldstone bosons, the massless Goldstone boson associated with $U(1)_B$ breaking couples to the weak neutral current. Amplitude for processes involving the $U(1)_B$ Goldstone boson H and the neutral current is given by

$$A_{H\to\nu\bar{\nu}} = \frac{4}{\sqrt{3}}G_F f_H\tilde{p}_\mu j_Z^\mu, \quad (23)$$

The decay constant for the $U(1)_B$ Goldstone boson has also been computed in earlier work and is given by $f_H^2 = 3\mu^2/(8\pi^2)$ [21]. Using these amplitudes we shall evaluate some interaction rates associated with thermal evolution of the early born neutron star, *i.e.*, neutrino opacity and neutrino emissivity in the next section.

4 Neutrino Rates

4.1 Neutrino Opacity

Figure 3 shows the resulting neutrino mean free path in a CFL meson plasma as a function of temperature. In the CFL medium, novel Cherenkov like processes such as $\nu \longrightarrow H\nu, \nu \longrightarrow \pi^0\nu$ and $\nu_e \longrightarrow \pi^+ e^-$ are allowed owing to the fact that mesons can have a space like dispersion relation [3]. Especially the massless $U(1)_B$ Goldstone boson H is space like for all momenta. Thus the processes involving H boson become dominant. Since these processes do not have mesons in the initial state they can occur at zero temperature. The neutrino mean free path due to the reaction $\nu \longrightarrow H\nu$ can be calculated analytically and is given by

$$\frac{1}{\lambda_{\nu\to H\nu}(E_\nu)} = \frac{256}{45\pi}\left[\frac{v(1-v)^2(1+\frac{v}{4})}{(1+v)^2}\right] G_F^2 f_H^2 E_\nu^3. \tag{24}$$

Although eq.(24) has no intrinsic temperature dependence, it arises by setting $E_\nu = \pi T$, which corresponds to mean energy of neutrinos in thermal equilibrium.

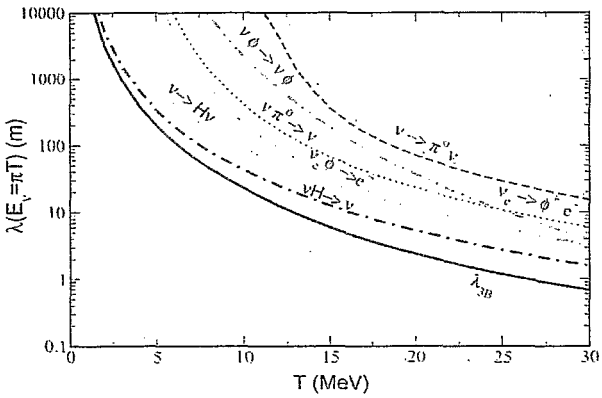

Figure 3: Neutrino mean free path in a CFL meson plasma as a function of temperature

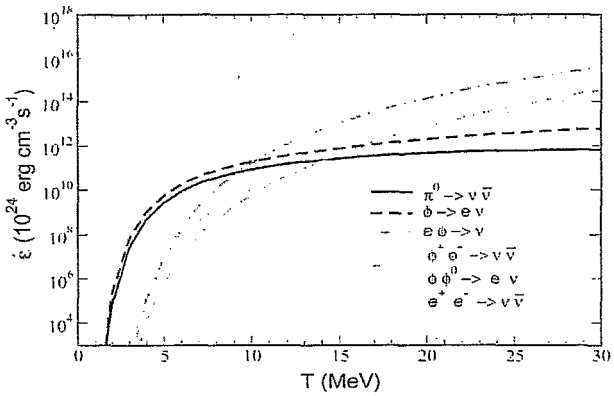

Figure 4: Rate of energy loss due to neutrino emitting reactions

4.2 Neutrino Emissivity

The rate of energy loss due to neutrino emitting reactions is shown in Figure 4. Charged current decays of pions and kaons, and the novel neutral current decay of π^0 are the leading one body processes. In vacuum, the amplitudes for similar processes are proportional to the lepton mass due to angular momentum conservation. However, in the CFL phase, due to the lack of Lorentz invariance, the decay of finite momentum pions and kaons is not suppressed by the electron mass. Thus even the process such as $\pi^0 \to \nu\bar{\nu}$ could happen.

Decay processes can occur only when the meson four momentum is time like. Thus, the one body decay of H boson is forbidden and only low momentum pions and kaons can participate in the decay process. This accounts for the saturation of the one body decay contribution to the emissivity with increasing temperature seen in Figure 4. At high temperature, processes involving two mesons in the initial states become important. This is because these processes do not have momentum threshold unlike those of one body decays.

In summary, we have shown that novel processes in which mesons are either emitted or absorbed from neutrinos occur in the CFL plasma and contribute to neutrino opacity. Absorption of thermal, massless H bosons is the dominant reaction contributing to the opacity for temperatures in the range T = 1-30 MeV. We find that the mean free path for thermal neutrinos at T = 10 MeV is of the order of 10 meters and at T = 5 MeV it is similar to 100 meters. In the table below we compare the neutrino mean free path in CFL matter with those in nuclear matter [24] and unpaired quark matter [25] under similar conditions.

phase	process	λ(T=5 MeV)	λ(T=30 MeV)
Nuclear Matter	$\nu n \to \nu n$	200 m	1 cm
	$\nu_e n \to e^- p$	2 m	4 cm
Unpaired Quarks	$\nu q \to \nu q$	350 m	1.6 m
	$\nu_e d \to e^- u$	120 m	4 m
CFL	λ_{3B}	100 m	70 cm
	$\nu\phi \to \nu\phi$	$\geq$ 10 km	4 m

The findings presented in the table indicate that neutrino mean free path in CFL matter is similar to or shorter than in unpaired quark matter for the whole temperature range. This surprising result arises solely due to

the novel processes involving Cherenkov absorption and radiation of CFL Goldstone bosons. Despite the energy gap in the quark excitation spectrum the opacity remains large and there is no exponential suppression of neutrino cross section even at low temperature. This is in sharp contrast to earlier findings in the two flavor superconducting phase [26]. However, since we expect the specific heat of the CFL phase $C_V \sim T^3$ to be small compared to that of unpaired quark matter, the cooling rates could still differ and needs to be investigated. The early evolution of a newly born neutron star is, in general, a complex process which depends on several macroscopic ingredients and microscopic conditions. In order to gauge how color superconductivity in the neutron star core will impact observable aspects of early evolution the rates computed in this work as well as the thermodynamic properties of the CFL phase need to be included in detailed numerical simulations of core collapse supernova. This is the only reliable means to bridge the gap between theoretical expectation of color superconductivity and observable aspects of core collapse supernova.

Acknowledgments

This work was supported in part by RIKEN Special Postdoctoral Researchers Grant No. A12-52010.

References

[1] D. Bailin and A. Love, Phys. Rep. **107**, 325 (1984); M. Iwasaki and T. Iwado, Phys. Lett. B **350**, 163 (1995); M. Alford, K. Rajagopal, and F. Wilczek, Phys. Lett. B **422**, 247 (1998); R. Rapp, T. Schäfer, E.V. Shuryak, and M. Velkovsky, Phys. Rev. Lett. **81**, 53 (1998).

[2] For reviews, see K. Rajagopal and F. Wilczek, in *Handbook of QCD*, edited by M. Shifman (World Scientific, Singapore, 2001); M.G. Alford, Ann. Rev. Nucl. Part. Sci. **51**, 131 (2001).

[3] S. Reddy, M. Sadzikowski, and M. Tachibana, Nucl. Phys. **A714**, 337 (2003), and references therein.

[4] K. Iida and G. Baym, Phys. Rev. D **63**, 074018 (2001); *ibid.* **66**, 059903(E) (2002).

[5] K. Iida and G. Baym, Phys. Rev. D **66**, 014015 (2002).

[6] T. Matsuura, K. Iida, T. Hatsuda, and G. Baym, Phys. Rev. D (in press); hep-ph/0312042.

[7] A.W. Steiner, S. Reddy, and M. Prakash, Phys. Rev. D **66**, 094007 (2002).

[8] H. Abuki, Prog. Theor. Phys. **110**, 937 (2003).

[9] D.T. Son, Phys. Rev. D **59**, 094019 (1999); D.K. Hong, Nucl. Phys. **B582**, 451 (2000); R.D. Pisarski and D.H. Rischke, Phys. Rev. D **61**, 074017 (2000); W.E. Brown, J.T. Liu, and H.C. Ren, Phys. Rev. D **62**, 054016 (2000).

[10] R.D. Pisarski, Phys. Rev. C **62**, 035202 (2000).

[11] D.D. Dietrich and D.H. Rischke, nucl-th/0312044.

[12] T. Schäfer, Phys. Rev. D **65**, 094033 (2002).

[13] I. Shovkovy and M. Huang, Phys. Lett. B **564**, 205 (2003); M. Huang, and I. Shovkovy, Nucl. Phys. **A729**, 835 (2003); M. Alford, C. Kouvaris, and K. Rajagopal, hep-ph/0311286.

[14] T. Matsuura, K. Iida, M. Tachibana, and T. Hatsuda (unpublished).

[15] M. Alford, K. Rajagopal and F. Wilczek, Phys. Lett. B**422** (1998) 247.

[16] R. Rapp, T. Schafer, E. Shuryak and M. Velkovsky, Phys. Rev. Lett. **81** (1998) 53.

[17] M. Alford, K. Rajagopal and F. Wilczek, Nucl. Phys. **B537** (1999) 443.

[18] For a review, see J. A. Pons et al., Astrophys. J. **513** (1999) 780.

[19] D. K. Hong, M. Rho and I. Zahed, Phys. Lett. B**468** (1999) 261.

[20] R. Casalbuoni and R. Gatto, Phys. Lett. B**464** (1999) 111.

[21] D. Son and M. Stephanov, Phys. Rev. D**61** (2000) 074012; Erratum, *ibid* D**62** (2000) 059902.

[22] P. Bedaque and T. Schafer, Nucl. Phys. **A697** (2002) 802.

[23] R. Casalbuoni, Z. Duan and F. Sannino, Phys. Rev. D**63** (2002) 054042.

[24] S. Reddy, M. Prakash and J. M. Lattimer, Phys. Rev. D**58** (1998) 013009.

[25] N. Iwamoto, Ann. Phys. **141** (1982) 1.

[26] G. W. Cartor and S. Reddy, Phys. Rev. D**62** (2000) 103002.

Color Ferromagnetism and Quantum Hall State of Gluon

M. Ohtani

Color Ferromagnetism and Quantum Hall State of Gluon

M. OHTANI (*RIKEN*), A. IWAZAKI (*Nishogakusha-U*), O. MORIMATSU (*KEK*), T. NISHIKAWA (*KEK*)

Abstract

In non-Abelian gauge theory, the perturbative vacuum is known to be unstable against condensation of a color magnetic field. The spontaneously-generated color magnetic field can be set to be in maximal Abelian subalgebra and off-diagonal gluons involve unstable modes. Since the most unstable modes are uniform in the direction parallel to the magnetic field, the system is effectively reduced to two dimensional one accompanied by the magnetic field, which is analogous to the quantum Hall system of electrons. We propose that these unstable modes compose a quantum Hall state in quark matter to realize a stable color ferromagnetic state.

We show that this state is gapped state and absolutory stable by studying the excitation energy of fluctuation around the state and also the vortex excitation. This state must be supplied with color charge by quark matter and turn out to be energetically favored than color super-conducting phase below a critical chemical potential. These fact implies that the color ferromagnetic state along with quantum Hall state of gluon may arise between hadron phase and color super-conducting phase.

Color Ferromagnetic State

Spontaneous generation of **color magnetic field,** $\langle B \rangle \neq 0$
with a **quantum Hall state of the gluons**

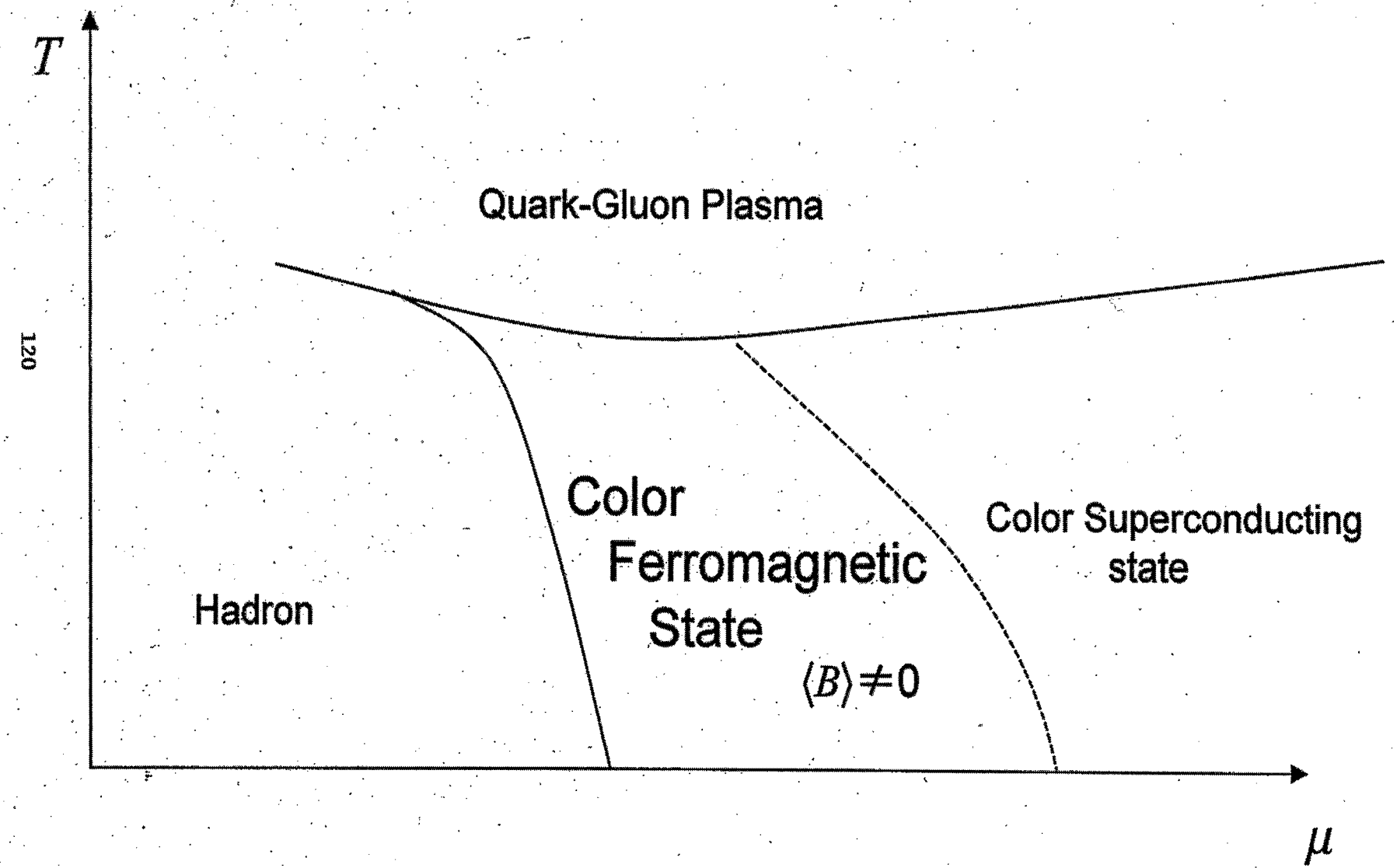

Savvidy state in SU(2) gauge theory

$$\mathcal{L}_{\text{gluon}} = -\tfrac{1}{4}\vec{F}_{\mu\nu}^{2} = -\tfrac{1}{4}(\partial_\mu A_\nu - \partial_\nu A_\mu)^2 - \tfrac{1}{2}\left|(\partial_{[\mu} - igA_\mu)\Phi_{\nu]}\right|^2$$
$$+ig(\partial^\mu A^\nu - \partial^\nu A^\mu)\Phi_\mu^*\Phi_\nu + \frac{g^2}{4}(\Phi_\mu\Phi_\nu^* - \Phi_\mu^*\Phi_\nu)^2$$

color magnetic field : $A_\mu = A_\mu^3$, (color) charged vector field: $\Phi_\mu = \dfrac{A_\mu^1 + iA_\mu^2}{\sqrt{2}}$

★ <u>One loop effective potential</u> for $\boldsymbol{B} = \nabla \times \boldsymbol{A}$, $A^\mu = (0, 0, x_1 B, 0)$

$$V(B) = \frac{1}{2}B^2 + \frac{11g^2B^2}{48\pi^2}\left(\ln\frac{gB}{\Lambda^2} - \frac{1}{2}\right) - \frac{ig^2B^2}{8\pi}$$

$\langle B \rangle \neq 0$

Savvidy PL **B 7 1** (1977) 133

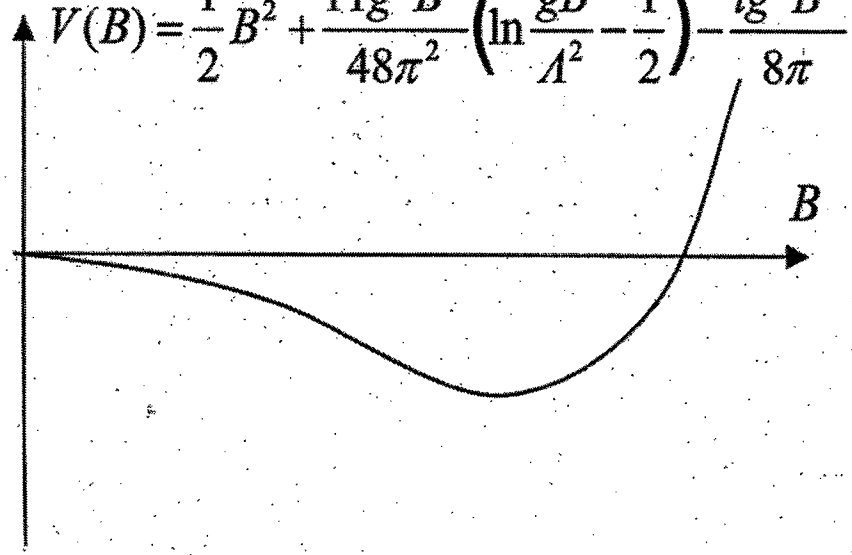

Savvidy state is unstable
due to $\mathrm{Im}V(B) \neq 0$
Nielsen and Olesen, NP **B 144**(1978)376

Instability of Savvidy state

$$D^\mu D_\mu \Phi^\nu + 2ig(\partial^\mu A^\nu - \partial^\nu A^\mu)\Phi_\mu = 0$$

♦ Spectrum of the modes: $E_\pm^2(n,k) = 2gB\left(n + \frac{1}{2} - s_z\right) + k^2$ **"Landau Level"**

(n=0, 1, 2, … ; s_z=± 1: spin ; k=momentum // B)

♦ **Unstable modes : Lowest Landau Level, n=0 with spin parallel to B**

$$E_-^2(n=0,\ |k| < \sqrt{gB}) = k^2 - gB < 0$$

The instability of the Savvidy vacuum

⇐ **unstable modes** of Φ_μ under the magnetic field B

¶ **The most unstable modes are uniform in the direction // B** (∵ k =0)

with (**degeneracy** for each n / **area**) = $gB/2\pi$

The most unstable mode

We extract from $\mathcal{L}_{\text{gluon}}$ only
the most unstable modes: k=0 ⇔ uniform in the direction // B. } effectively ⟹ 2+1dim.

$$\mathcal{L}_{2+1} = |(\partial_\mu - igA_\mu)\phi|^2 + 2gB\,|\phi|^2 - \frac{g^2}{2l_3}|\phi|^4$$

where $\phi \equiv (\Phi_1 - i\Phi_2)\sqrt{\frac{l_3}{2}}$,

" l_3 " length scale of a domain

With LLL condition: $(D_1 + iD_2)\phi = 0$

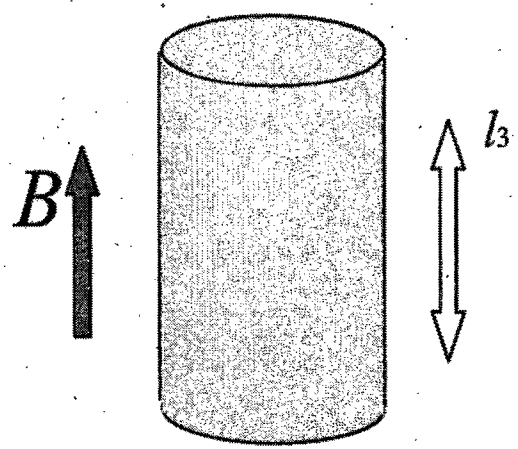

uniform in the direction // B.

The negative mass term $-2gB$

(If A_μ =0 , potential from $\mathcal{L}_{2+1}$ has the typical double well.)

⟹ $\langle\phi\rangle = 0$ is unstable.

Our proposal

[redacted]

Phys. Lett. B **571** (2003) 61; **579** (2004) 347

Gluons in B^{color}

Unstable modes $(k=0)$ of gluons in B^{color}

- effectively 2d
- occupy LL

Electrons in B

2d electrons in semiconductors under strong B

- occupy LL

Quantum Hall state of gluons ?

Absolutely stable state:
Quantum Hall state (QHS)

- finite gap
- incompressible

cf. superconductor

2-dim system with gauge field

If A_μ=0, typical double well potential

The unstable state $\langle\phi\rangle$ =0 decays into the stable state $\langle\phi\rangle = v$

The spatially uniform mode (k=0) condenses.

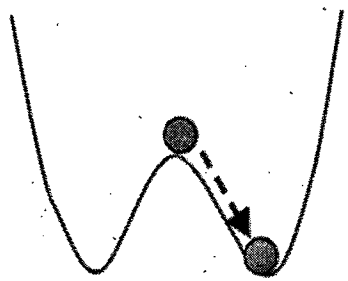

$$\Updownarrow$$

Under $B \neq 0$, the unstable mode couples with $A_\mu(x)$:

$$\mathcal{L}_{2+1} = |(\partial_\mu - igA_\mu)\phi|^2 + 2gB|\phi|^2 - \frac{g^2}{2l_3}|\phi|^4$$

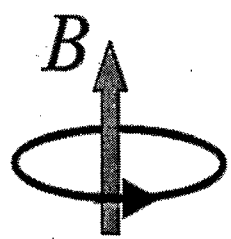

There is no such uniform state as $\langle\phi\rangle = v$.

Chern-Simons theory: useful for 2-dim systems

Chern-Simons theory

Chern-Simons field $a_\mu \rightarrow$ fictitious flux $\rightarrow$ particle statistics in 2-dim

the quantum Hall states are described by *Chern-Simons gauge theory.*

For electrons

$$\mathcal{L} = \Phi^\dagger(i\partial_t - eA_0 - ea_0)\Phi - \frac{1}{2M}|(-i\nabla + e\boldsymbol{A} + e\boldsymbol{a})\Phi|^2 + \frac{\epsilon^{\mu\nu\lambda}e^2}{4\pi m} a_\mu \partial_\nu a_\lambda + \ldots$$

$$\Longrightarrow \quad m\Phi^\dagger\Phi = \frac{\nabla \times \boldsymbol{a}}{2\pi/e} \; ; \text{ permutation phase: } \exp\left[\frac{i}{2}\oint e\,\boldsymbol{a}\cdot \mathrm{d}\boldsymbol{x}\right] \rightarrow \exp(im\pi)$$

$\therefore m$: odd integer for fermion

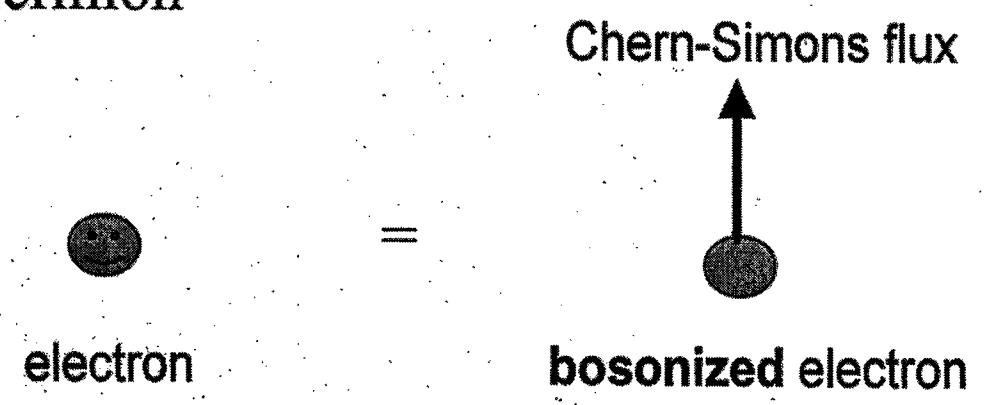

Chern-Simons gauge theory for the Quantum Hall states of gluons.

Chern-Simons flux a_μ

(# of flux:even for boson)

original gluons = composite boson ϕ_c

$$\mathcal{L}_{CS} = |(\partial_\mu - igA_\mu + ia_\mu)\phi_c|^2 + 2gB|\phi_c|^2 - \frac{g^2}{2l_3}|\phi_c|^4 + \frac{1}{4\pi m}\epsilon^{\mu\nu\lambda}a_\mu\partial_\nu a_\lambda \ ; \ m : \text{even}$$

★ Quantum Hall states : $\langle\phi_c\rangle = v_c$, $a_i = gA_i$

(Chern-Simons gauge field cancels the magnetic field.)

$\Downarrow$

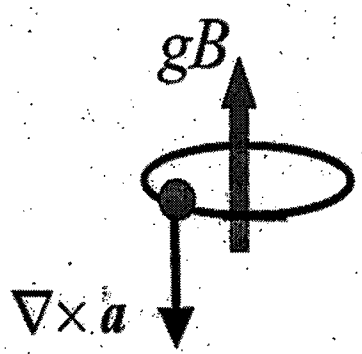

bosons feel totally
no gauge flux to form
a uniform & stable state

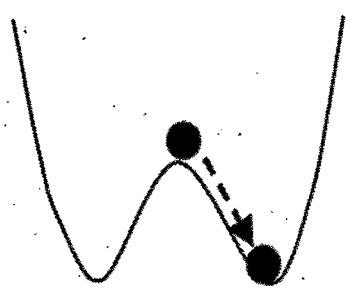

Quantum Hall state in quark matter

★ The state $\langle \phi_c \rangle = v_c$, $a_i = gA_i$ corresponds to

QHS with filling $1/m$ $\leftarrow$ Hall conductance $= \dfrac{1}{m}\dfrac{g^2}{h}$

★ **The color charge density** of the condensed gluons: $\rho_c = \dfrac{gB}{2\pi m}$

$$\Downarrow$$

Quark matter is a supplier of the color charge.

"In the quark matter, Color ferromagnetic state is stabilized by the formation of gluons quantum Hall state."

Color ferro and color superconductivity

Ebert *et al*, Phys. Rev. **D65** (2002) 054024

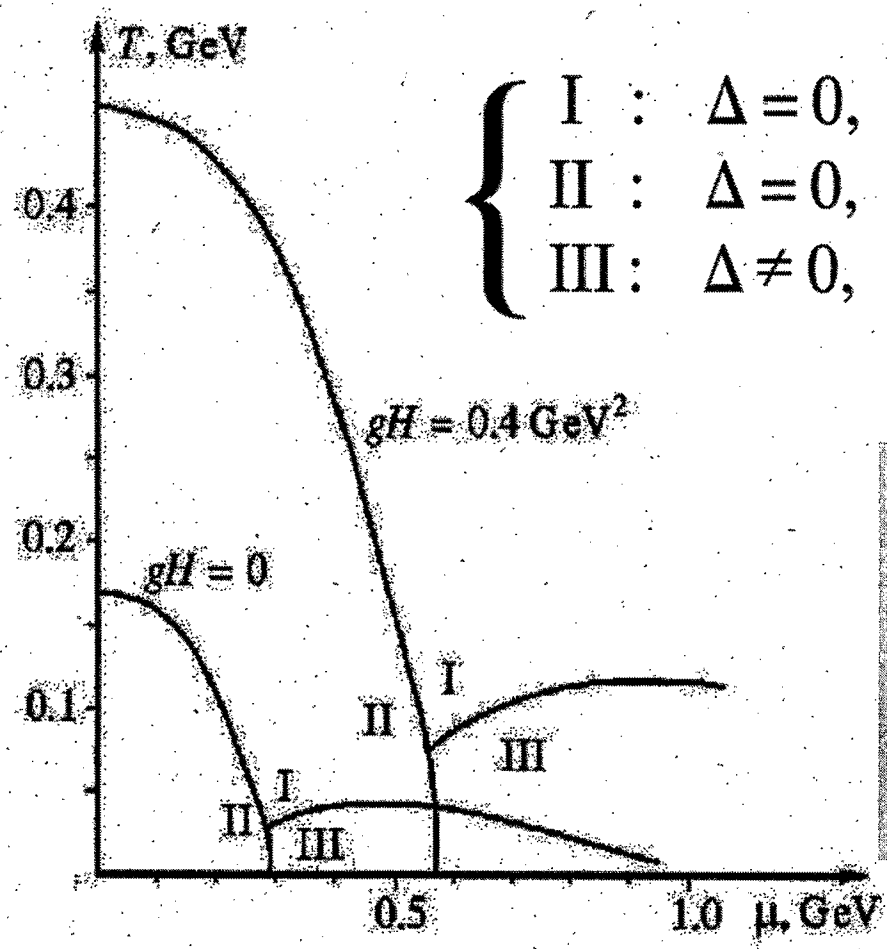

$$\begin{cases} \text{I} : & \Delta = 0, \ \sigma = 0 & \cdots \text{QGP} \\ \text{II} : & \Delta = 0, \ \sigma \neq 0 & \cdots \text{Hadron} \\ \text{III} : & \Delta \neq 0, \ \sigma = 0 & \cdots \text{Color Super} \end{cases}$$

color magnetic field

⇕ against

color super cond.

Comparison of the quark energy in various states
— where the ferromagnetic state is realized in the phase diagram

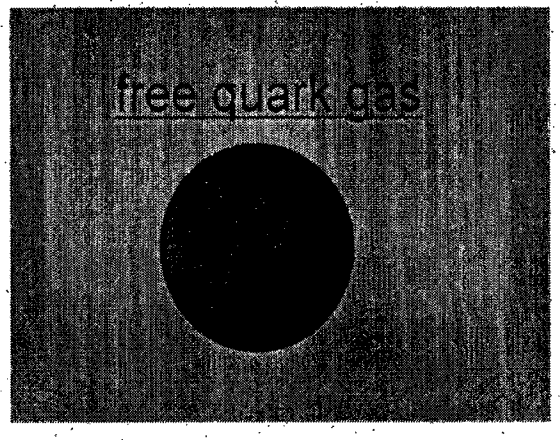

(for any μ)

$\geq$

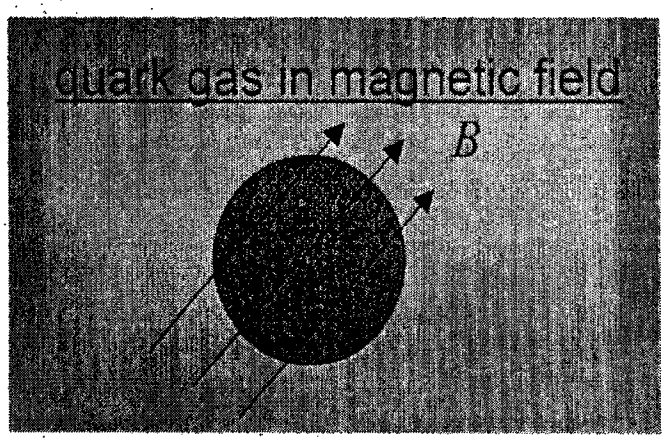

(for any μ) $\vee$

$\wedge$ (for $\mu < \sqrt{2gB}$)

$\vee$ (for $\mu > \sqrt{2gB}$)

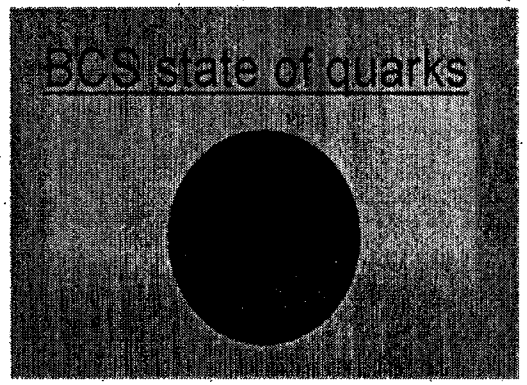

if gap energy $\sim O$(100MeV)

$\Rightarrow$ μ_c = 200 ~ 500 MeV

Color ferromagnetic state can be realized between hadron phase and color super conducting phase

Vortex excitation

QHS of e^- : quasi-particles w/ a fractional charge
$\Rightarrow$ vortex excitation in QHS of gluon

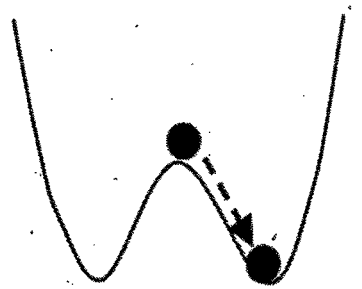

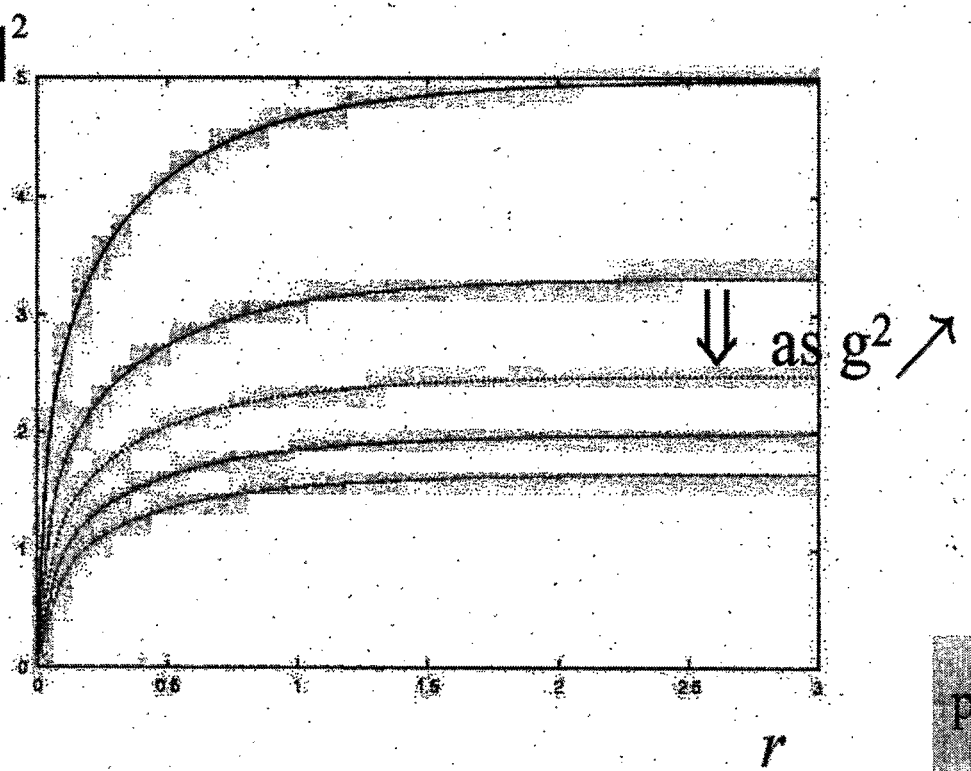

$\Downarrow$ as $g^2 \nearrow$

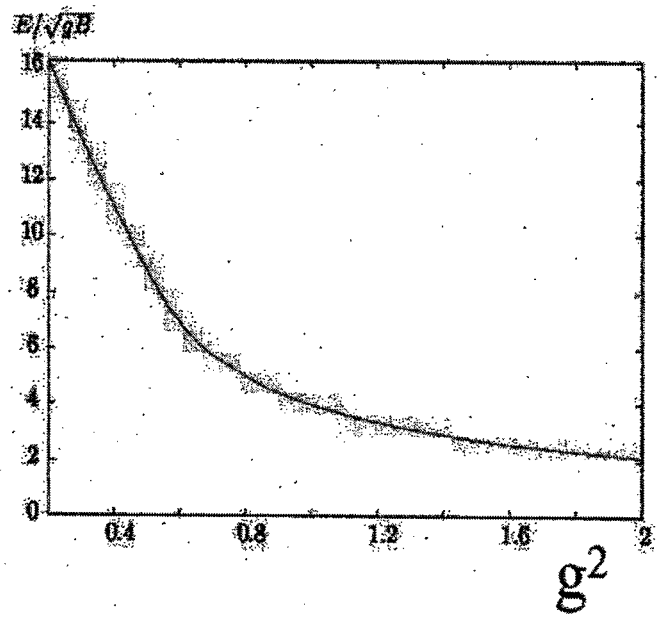

pair creation of vortices for low density

Implications of color ferro with QHS

- Comparison with electron QHS:
  quantum Hall plateau, Anderson localization by Impurities,
  quasi particles with a rational (fractional) charge, → Quark dynamics
  incompressibility → EoS in N★…

- **Real observable magnetic field**
  is induced in quark matter
  owing to the rotational motions of quarks.

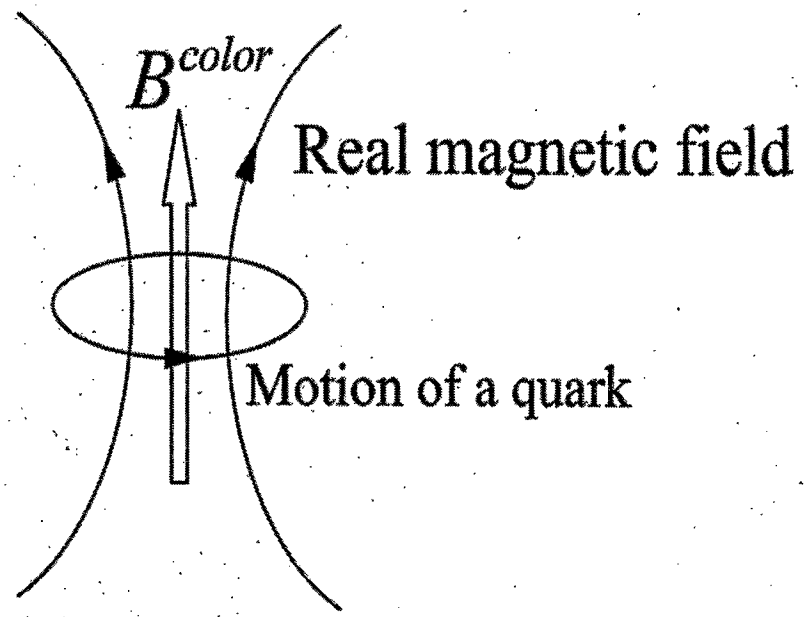

"Such a phase of the quark matter produced by heavy ion collisions may be detected by observing the strong magnetic field"

Summary

- Color ferromagnetic state can exist in quark matter matter accompanying a quantum Hall state of gluons. gluons.
- The state lies between hadron phase and color superconducting phase.
- (Anti-)Vortex excitations will break the state for low density.
- If the state is realized in the quark matter produced produced by heavy ion collisions, real magnetic field field might be observed.

Relation Between the Chiral and Deconfinement Phase Transitions

Yoshitaka Hatta

Relation between the chiral and deconfinement phase transitions

Yoshitaka Hatta

(Kyoto U. and RIKEN)

Abstract

We argue that the chiral phase transition and the deconfiement phase transitions in finite temperature QCD are continuously connected by the glueball-sigma mixing.

QCD in the non-perturbative regime

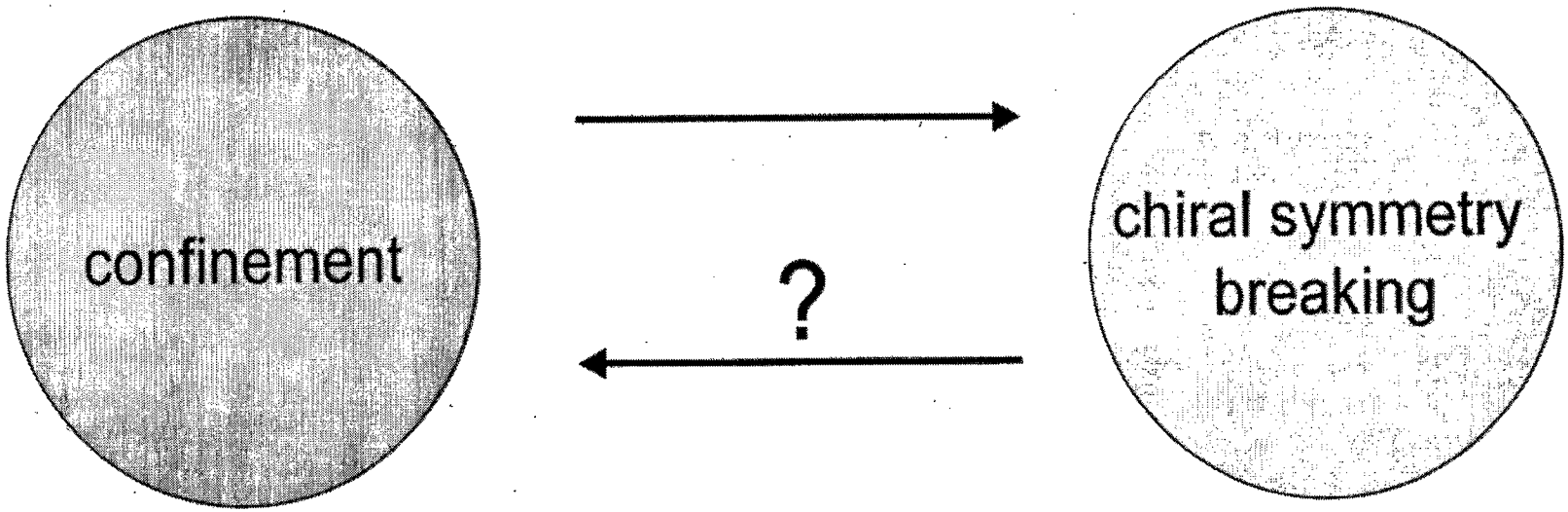

$$\Lambda_{QCD} < 4\pi f_\pi,\ m_\rho$$

chiral phase transition

$\boxed{m = 0}$ chiral symmetry $q \to e^{i\gamma_5 t_F^a \theta^a} q$

quark condensate

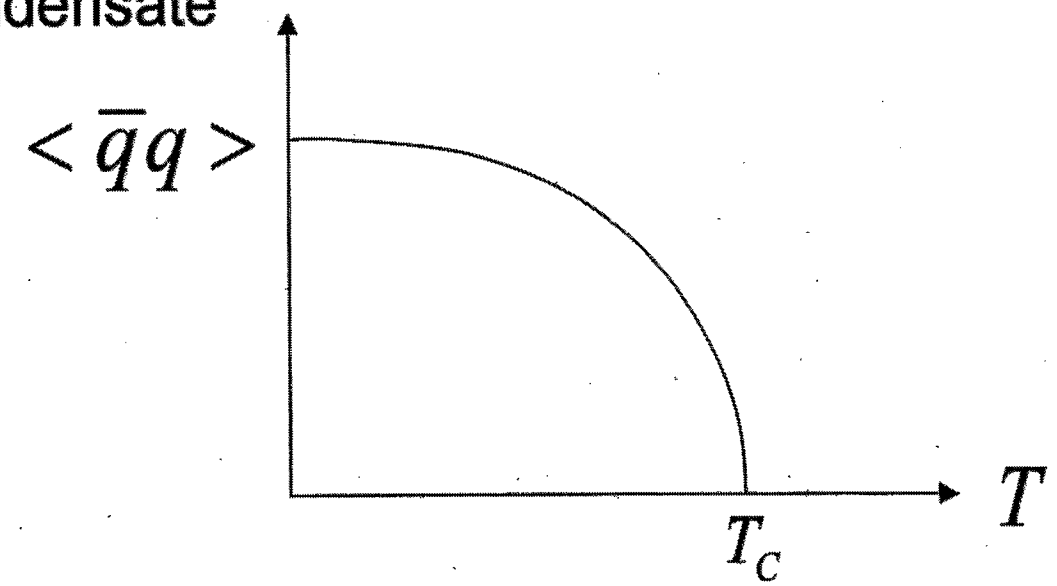

$N_f = 2$ second order

$N_f \geq 3$ first order

deconfinement phase transition

$\boxed{m = \infty}$ center symmetry $\Omega(\beta, \mathbf{x}) = e^{i\frac{2\pi}{N_C}n}\,\Omega(0, \mathbf{x})$

Polyakov loop

$$< L >$$
$$=< P\exp(-ig\int_0^\beta A_4(\mathbf{x},\tau)d\tau) >$$

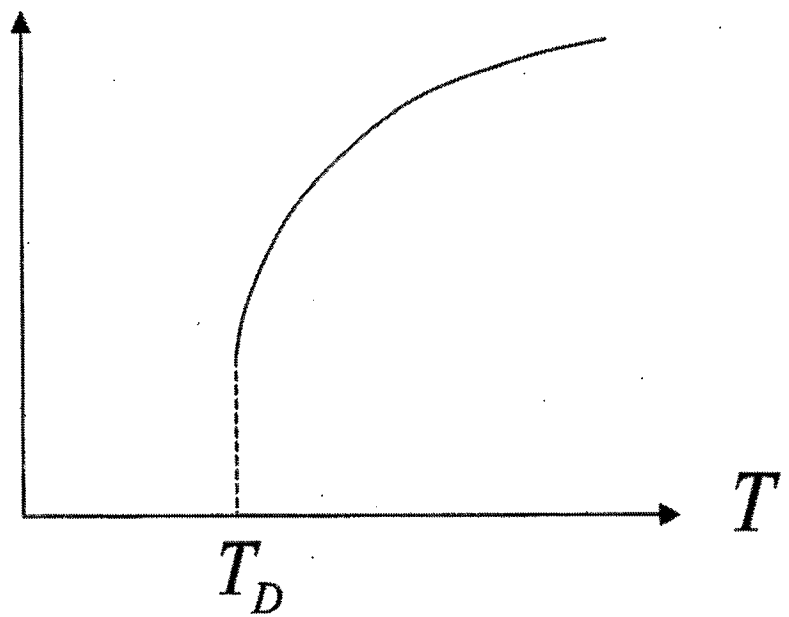

$N_C = 2$ second order

$N_C = 3$ first order

Lattice result:

—— an empirical fact

For all values of m ,

$$T_D(m) \approx T_C(m)$$

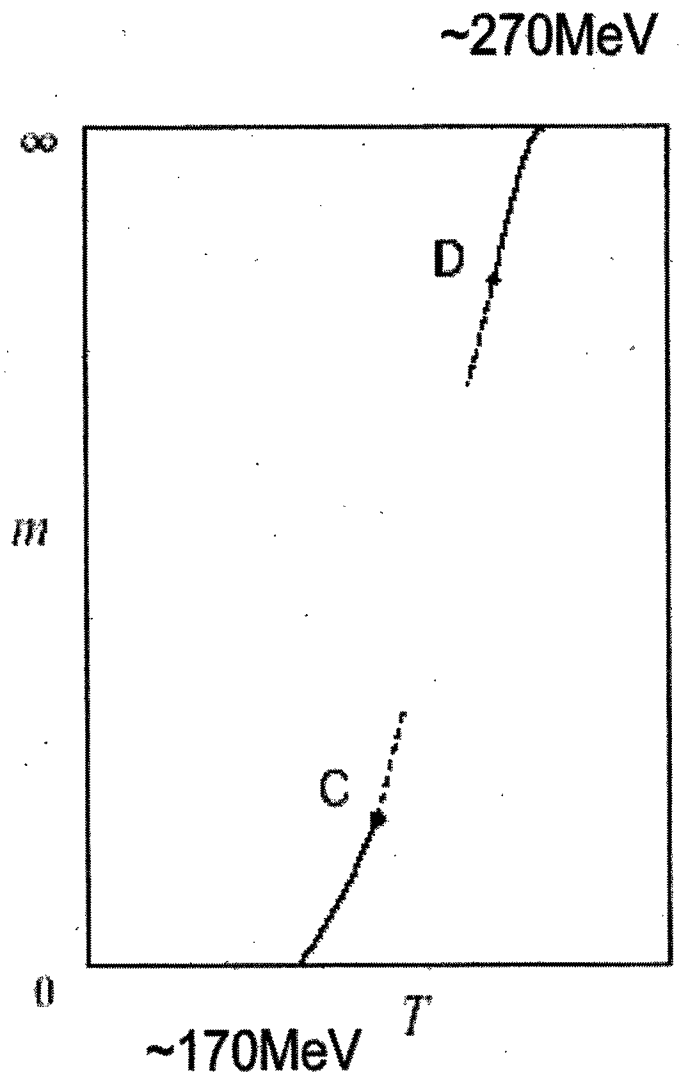

Deconfinement phase transition knows chiral phase transition.

—— Why?

Preceding works

Basic idea: What is responsible for the breaking of center symmetry is the constituent quark mass.

Gocksch & Ogilvie, '84
Digal, Laermann & Satz, '00
Fukushima, '02~

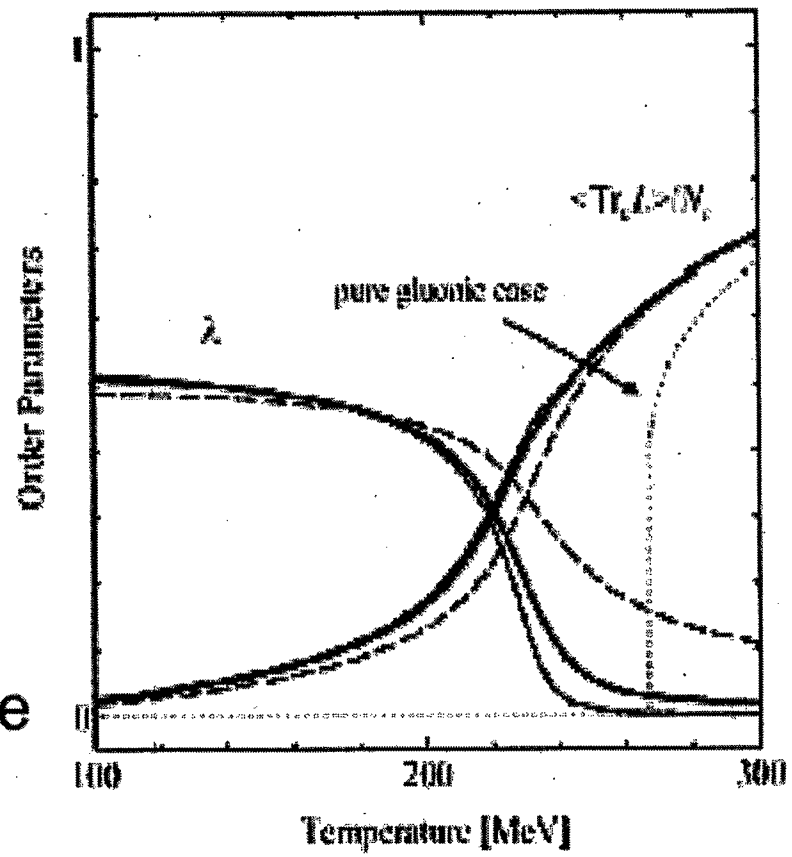

Jump of the Polyakov loop (deconfinement?) is a consequence of the chiral phase transition.

Fukushima, hep-ph/0209311

End-point —— existence of a massless excitation

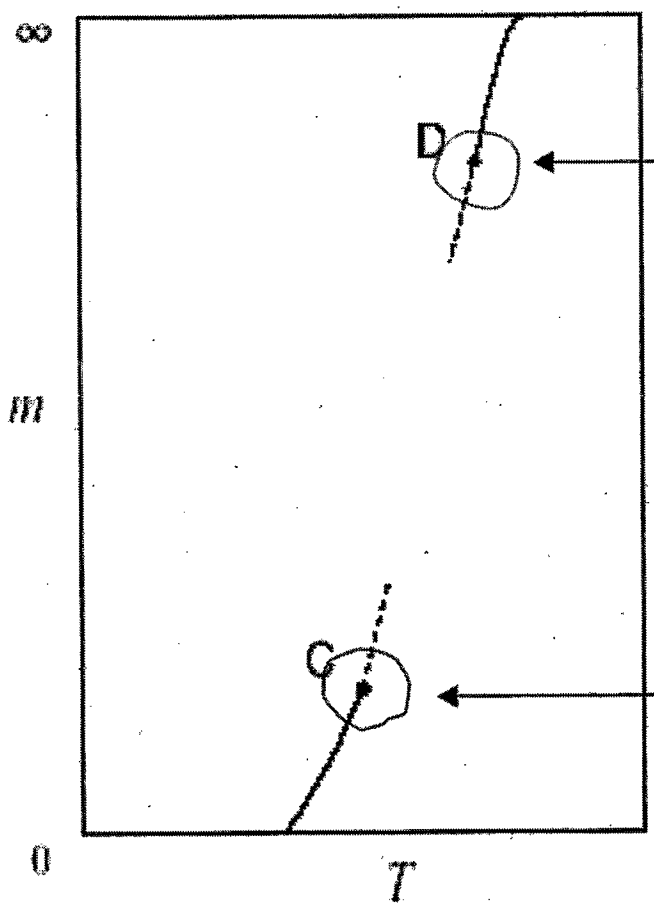

the shifted order parameter

$$L' = L - \langle L \rangle_D$$

$$\sigma' = \sigma - \langle \sigma \rangle_C$$

Gavin, Gocksch & Pisarski, '94

$SU_C(2)$ pure glue theory --- second order phase transition

Consider the specific heat

$$C_V \sim \frac{d^2\Omega}{dT^2}$$

$$\sim |t|^{-\alpha} \qquad (\alpha \approx 0.1) \qquad t = (T - T_C)/T_C$$

$$\sim < \sum_P \square \square >$$

$$\sim \int d^d\mathbf{x} < L^2(\mathbf{x}) L^2(\mathbf{0}) >_C$$

Explicit structure of the divergence

cf. $\int < LL > \sim |t|^{-\gamma}$

$$\int d^d\mathbf{x} < L^2(\mathbf{x})L^2(\mathbf{0}) >_C$$

$$\sim \int d^d\mathbf{x} \frac{\exp(-m_G|\mathbf{x}|)}{|\mathbf{x}|^{2(d-1/\nu)}} \sim |t|^{-\alpha}$$

scaling dimension

$$m_G \sim |t|^{\nu} \quad (\sim \xi^{-1})$$

The screening mass of the electric glueball goes to zero.

Lattice measurement Datta & Gupta, '98

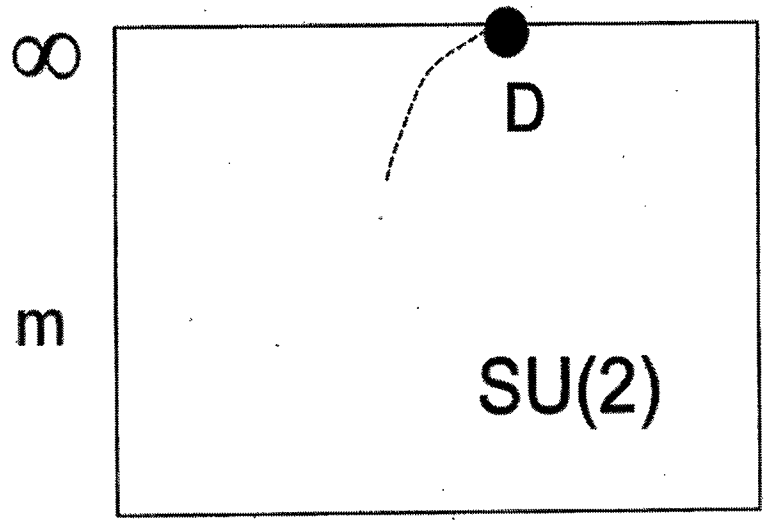

At $m = \infty$, a Polyakov loop and a glueball are distinct.

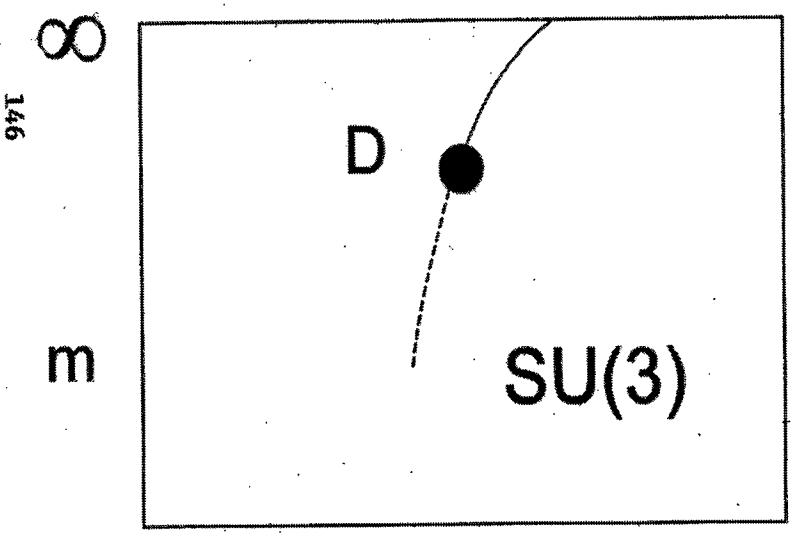

For $m < \infty$, a Polyakov loop is like a glueball.

$$G \sim |L|^2 = |L' + \langle L \rangle_D|^2$$

For $m < \infty$, a Polyakov loop is just one of many interpolating fields of the electric glueball.

Glueball-sigma mixing

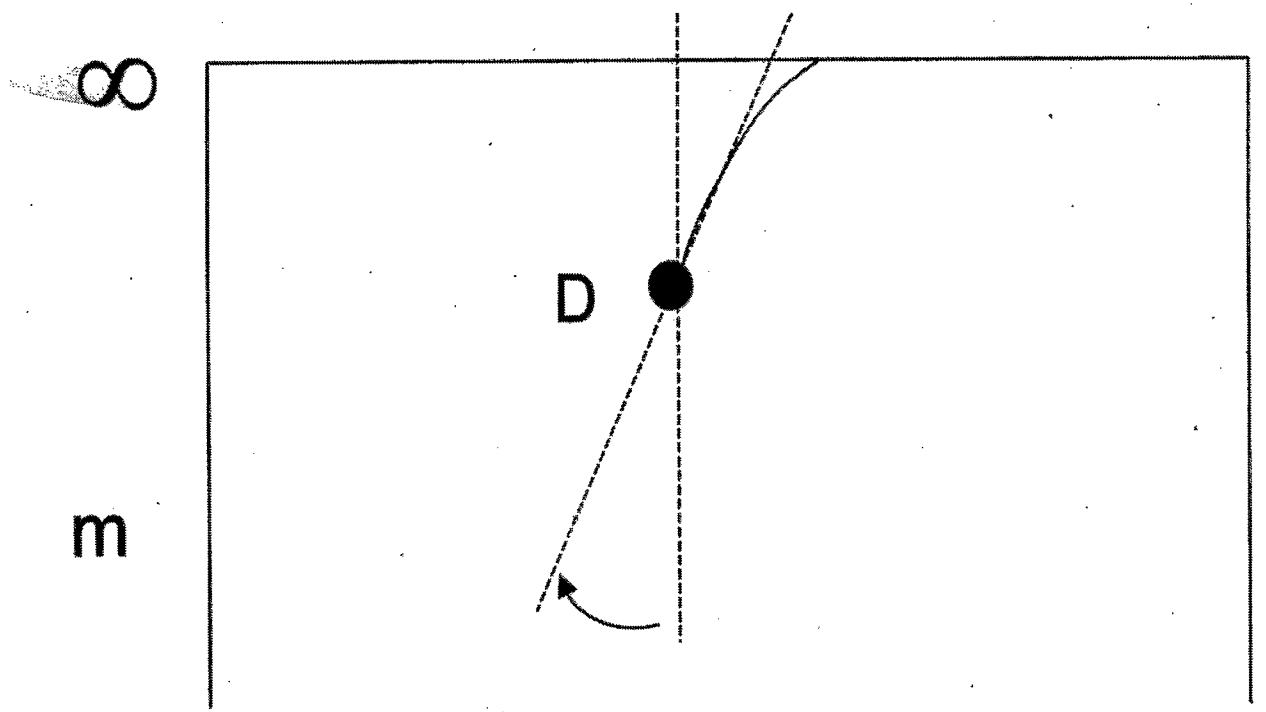

$$\int d^d\mathbf{x} < L'(\mathbf{x})L'(\mathbf{0}) >_C \sim \int d^d\mathbf{x} < \bar{q}q(\mathbf{x})\bar{q}q(\mathbf{0}) >_C$$

$$\sim \int d^d\mathbf{x} < G(\mathbf{x})G(\mathbf{0}) >_C \sim |t|^{-\gamma}$$

A bridge over the phase diagram

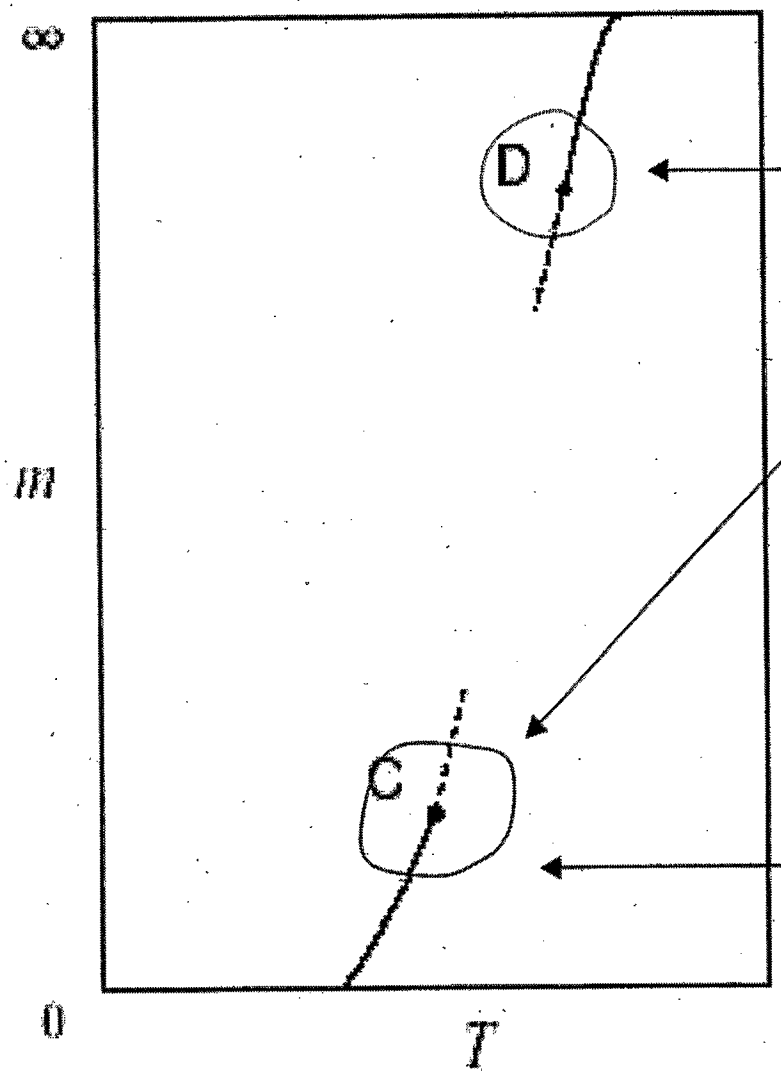

$$\phi = G\cos\theta + \sigma\sin\theta$$

$$\phi' = -G\sin\theta + \sigma\cos\theta$$

$$\theta \approx 0$$

$$\phi = G\cos\theta + \sigma\sin\theta$$

$$\theta \approx \frac{\pi}{2}$$

`Level repulsion' scenario

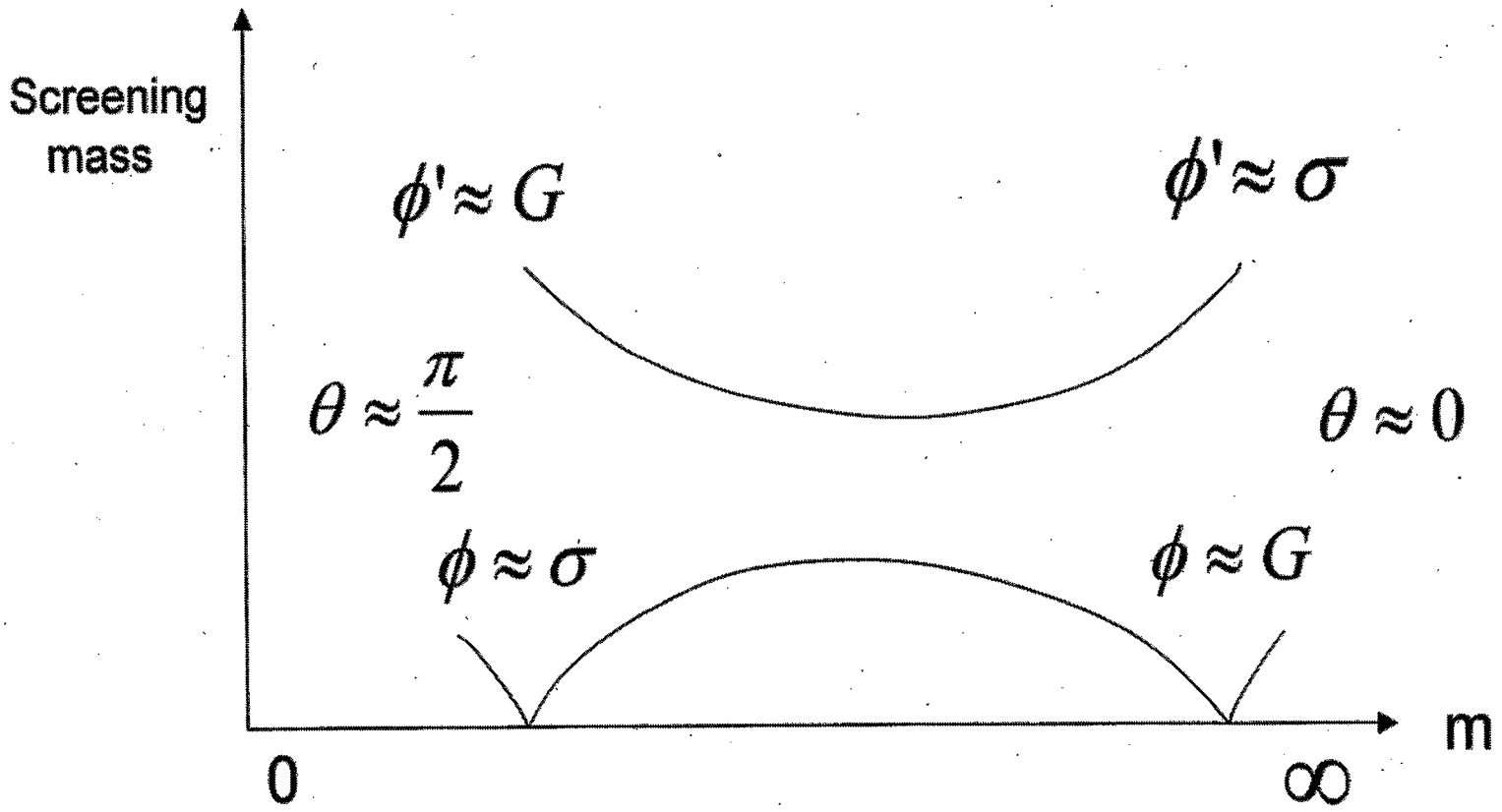

Single field describes the (crossover) phase transition for all values of m.

$\xrightarrow{\text{Naturally,}}$ $T_D(m) = T_C(m)$

Zero temperature QCD

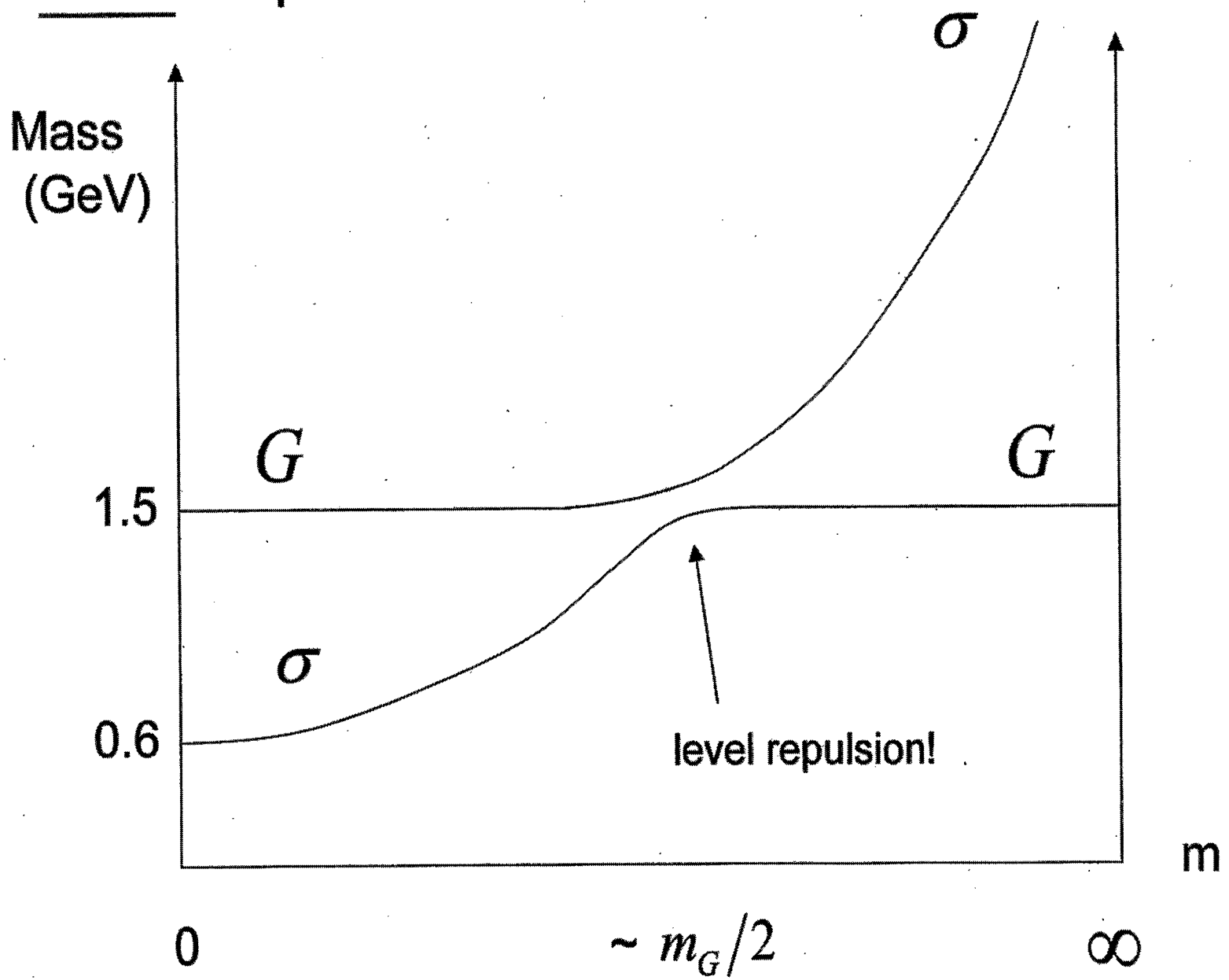

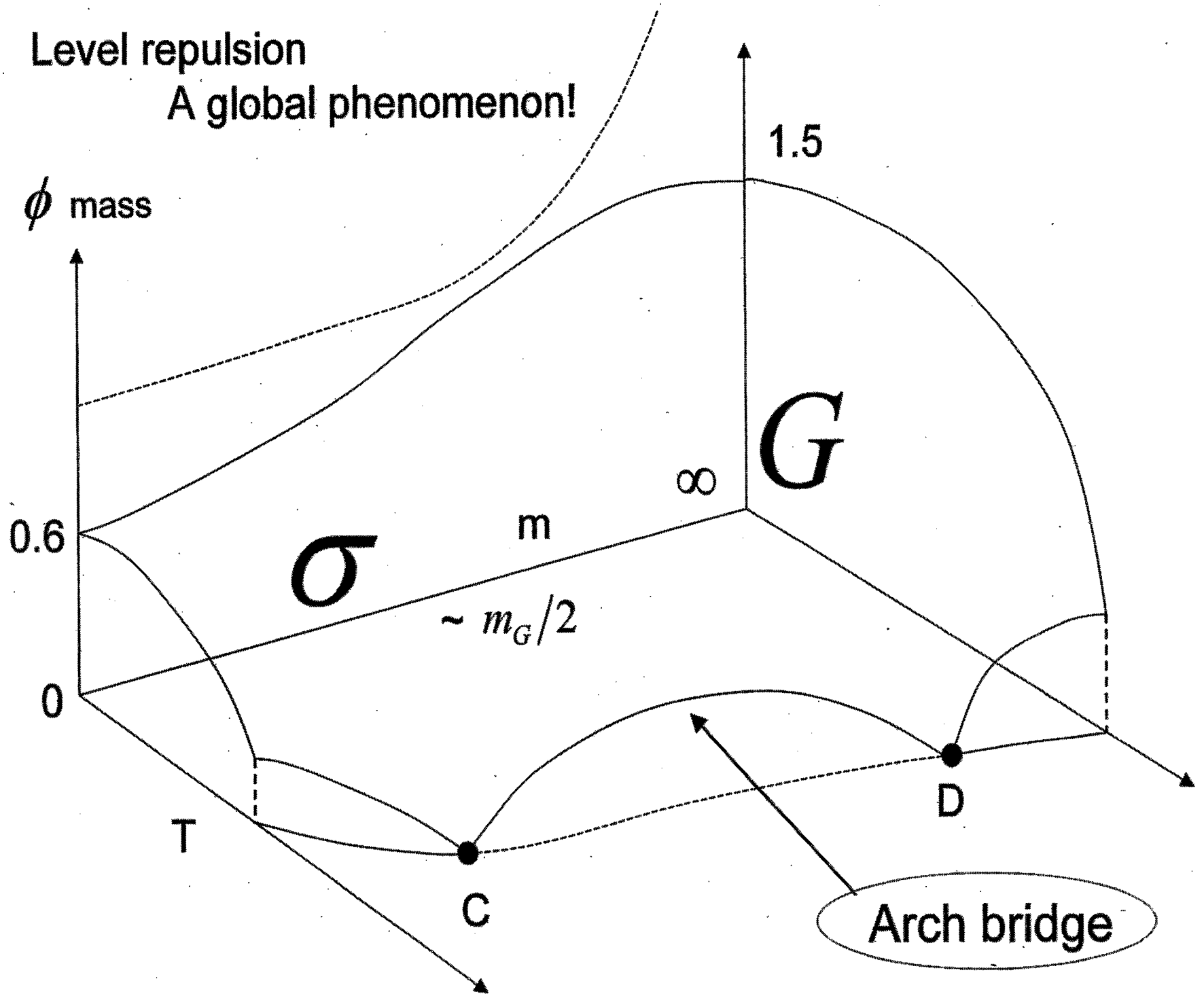
Level repulsion
A global phenomenon!
ϕ mass
1.5
G
∞
0.6
σ
m
$\sim m_G/2$
0
T
C
D
Arch bridge

Summary

2nd order ⟶ vanishing of a certain screening mass
Crossover ⟶ dropping of a certain screening mass

The two phase transitions are just different limits of a single (crossover) phase transition driven by the lightest screening state ϕ .

The glueball-sigma mixing and level repulsion provides not only a unified description of the QCD phase transitions, but also a consistent characterization of the entire phase diagram in the (T, m) plane.

Mode Coupling Theory for the Dynamic Aspect of the Chiral Phase Transition

K. Ohnishi

Mode coupling theory for the dynamic aspect of the chiral phase transition

K. Ohnishi (*Komaba, Univ. of Tokyo*)
with
K. Fukushima (*MIT*)
K. Ohta (*Komaba, Univ. of Tokyo*)

Abstract

We reanalyze the dynamic aspect of the chiral phase transition by means of the mode coupling theory. We point out the difference of the dynamic behaviors between the chiral phase transition and the antiferromagnet, which have been considered to belong to the same dynamic universality class. We also suggest reconsideration of Halperin and Hohenberg's rules for the classification of the dynamic universality class. By application of the mode coupling theory to the chiral phase transition, we derive the kinetic equation for it and find the dynamic critical exponent to be $z = 1 - \eta/2 \cong 0.98$. The value is contrasted with $z = d/2 = 1.5$ of the antiferromagnet. The difference explicitly shows the different dynamic behavior of the two systems.

Content

1. Introduction

2. Dynamic universality class of the chiral phase transition

3. Mode coupling theory for the linear sigma model

4. Summary

1. Introduction

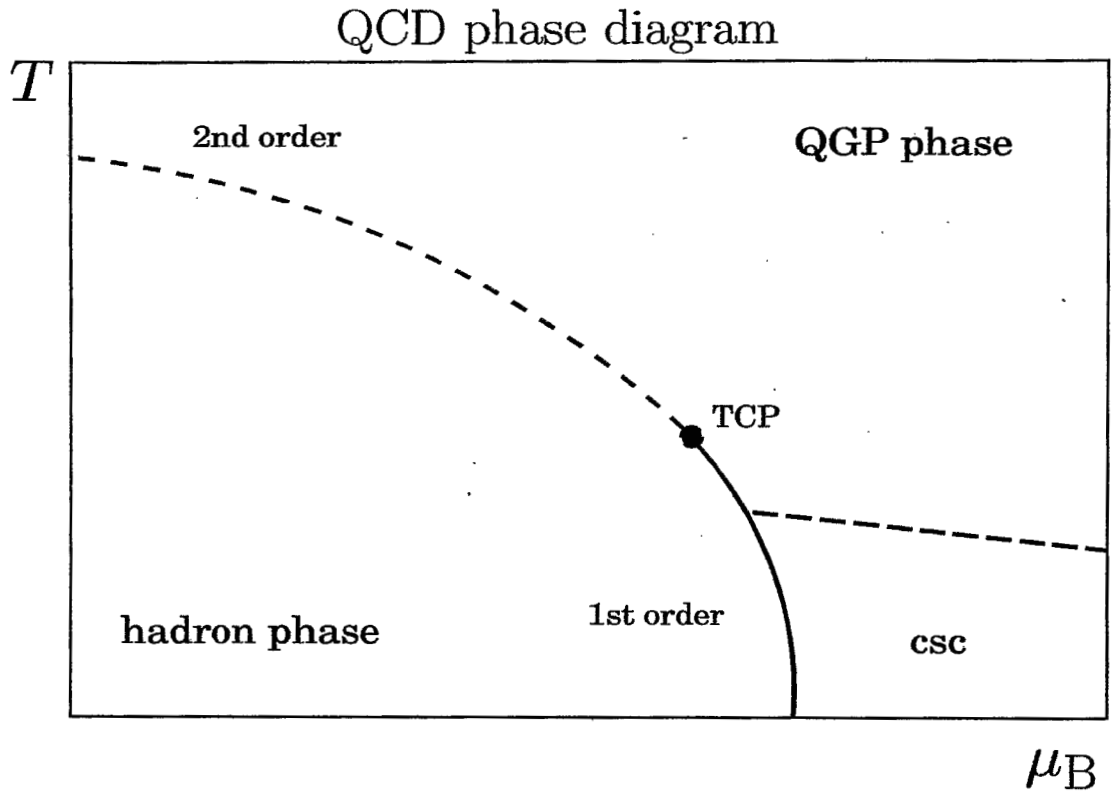

We are interested in the non-equilibrium or dynamic property of the 2nd order chiral phase transition.

Dynamic critical phenomena

· Critical slowing down

· Softening of propagating modes etc.

Degrees of freedom for describing the non-equilibrium behavior

$$\cdots \quad \text{Slow variables} \quad \Leftarrow \begin{cases} \text{Order parameter} \\ \text{Conserved quantities} \end{cases}$$

<u>Ex.</u> The magnetization M and the energy E are the slow variables for the ferromagnet.

The fluctuations of slow variables $\Rightarrow$ Slow modes

$$\text{Slow mode} \cdots \begin{cases} \text{Diffusive mode} \\ \text{Propagating mode} \end{cases}$$

Propagating mode $\cdots$ spin wave, sound wave, particle mode etc.

Slow modes appear in the (dynamic) spectral function as narrow peaks.

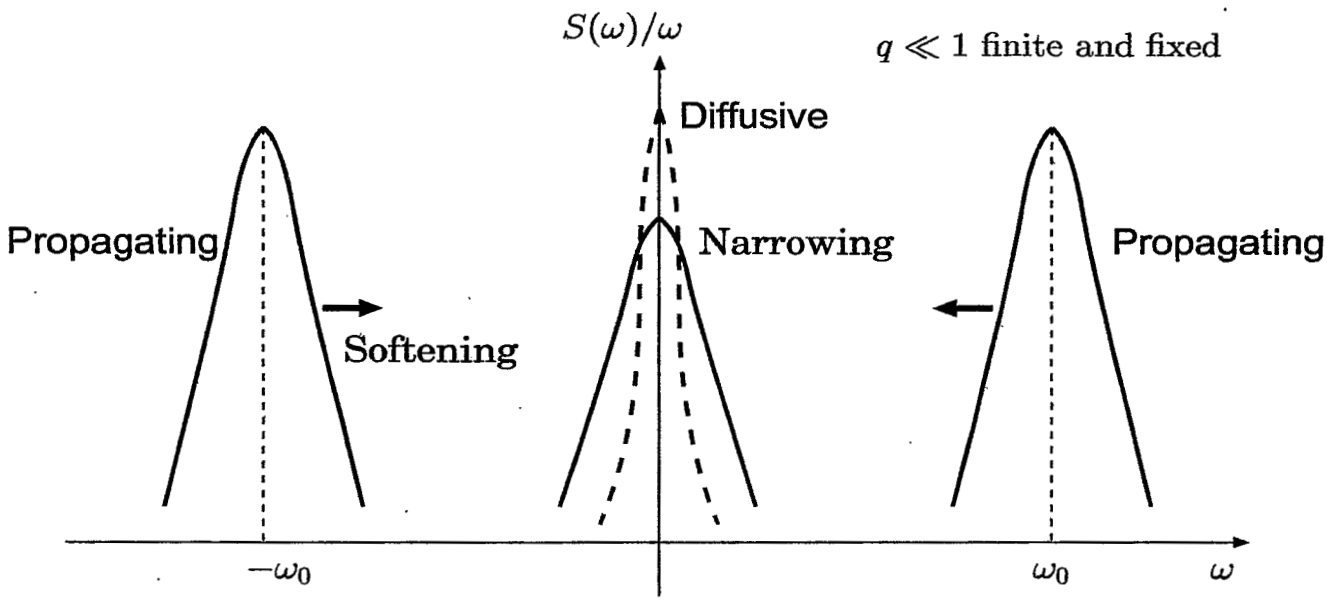

$$\begin{cases} \cdot\text{Diffusive mode} & \cdots \text{ Pole with only the imaginary part.} \\ \cdot\text{Propagating mode} & \cdots \text{ Pole with the imaginary part as well as the real part (frequency } \omega_0). \end{cases}$$

Example — Heisenberg Ferromagnet —

Slow variables $\cdots$

$$\begin{cases} \text{Magnetization} & \text{(order parameter)} \quad \vec{M} = (M_x, M_y, M_z) \\ \text{Energy} & \text{(conserved quantity)} \quad E \end{cases}$$

Slow modes

· Ordered phase ($T < T_c$)

$$\left.\begin{matrix} M_x \\ M_y \end{matrix}\right\} \cdots \text{ Propagating mode (Spin wave)}$$
$$M_z \quad \cdots \text{ Diffusive mode}$$
$$E \quad \cdots \text{ Diffusive mode}$$

· Disordered phase ($T_c < T$)

$$M_x \cdots \text{ Diffusive mode}$$
$$M_y \cdots \text{ Diffusive mode}$$
$$M_z \cdots \text{ Diffusive mode}$$
$$E \cdots \text{ Diffusive mode}$$

• Dynamic universality class

How to classify critical points:

⇐Halperin & Hohenberg (Rev.Mod.Phys. 49 (1977) 435)

(i) Whether or not the order parameter is a conserved quantity.

(ii) What kinds of conserved quantity are contained.

Observed critical points (ferromagnet, antiferromagnet, liquid-gas, superfluid etc) have been comprehensively classified.

2. Dynamic universality class of the chiral phase transition

Chiral phase transition belongs to the same dynamic universality class as that of the antiferromagnet.
$\Leftarrow$ Rajagopal & Wilczek (NPB 399 (1993) 395)

- Slow variables for the both systems

	antiferromagnet	chiral
order parameter	staggered magnetization N	meson field ϕ
conserved quantity	magnetization M energy E momentum P^i	chiral charge Q energy E momentum P^i

Rajagopal and Wilczek have analyzed the chiral phase transition by using the kinetic equation of the antiferromagnet.

They have obtained the dynamic critical exponent $z = d/2 = 3/2$.

However this is not the case.

- Slow modes in the disordered phase:

$$\begin{cases} \text{Staggered mag.} & \cdots \text{ diffusive mode} \\ \text{Meson field} & \cdots \text{ propagating mode (particle mode)} \end{cases}$$

Different slow modes apparently indicate the different dynamic behavior of the two systems.

The two systems cannot be in the same dynamic universality class.
$\Rightarrow$ The prescription of Halperin and Hohenberg for classifying the dynamic universality class does not work.

3. Mode coupling theory for the linear sigma model

- Mode coupling theory (Kawasaki, Ann.Phys.61 (1970) 1)

Kinetic equation for the slow variables A_j:

$$\frac{\mathrm{d}}{\mathrm{d}t}A_j(t) = \sum_l \left(\mathrm{i}\omega_{jl} - \frac{k_\mathrm{B}L^0_{jl}}{\chi_l}\right) A_l(t) + \frac{\mathrm{i}}{2}\sum_{lm}\Omega_{j;lm}\left(\chi_l\chi_m\right)^{-\frac{1}{2}}\left(A_lA_m - \langle A_lA_m\rangle\right) + f_j$$

where

$$\omega_{jl} = -\mathrm{i}\left(\dot{A}_j, A_l^\dagger\right)/\chi_l = -k_\mathrm{B}T\left\langle\left[A_j, A_l^\dagger\right]\right\rangle/\chi_l$$

$$\Omega_{j;lm} = -k_\mathrm{B}T\left\{\left\langle\left[A_j, A_l^\dagger A_m^\dagger\right]\right\rangle - \left\langle\left[A_j, A_p^\dagger\right]\right\rangle\chi_p{}^{-1}\left(A_p, A_l^\dagger A_m^\dagger\right)\right\}/\left(\chi_l\chi_m\right)^{\frac{1}{2}}$$

ω_{jl} gives the frequency matrix for the slow modes.

$$\begin{cases}\omega = 0 \rightarrow \text{diffusive mode}\\ \omega \neq 0 \rightarrow \text{propagating mode}\end{cases}$$

- O(2) linear sigma model

$$\mathcal{L} = \frac{1}{2}\left[(\partial_\mu\phi_1)^2 + (\partial_\mu\phi_2)^2\right] - \frac{1}{2}\mu^2\left(\phi_1{}^2 + \phi_2{}^2\right) - \frac{\lambda}{4}\left(\phi_1{}^2 + \phi_2{}^2\right)^2$$

$$\phi_a(\vec{x},t) = \frac{1}{\sqrt{V}}\sum_{\vec{k}}\frac{1}{\sqrt{2\omega_{a\vec{k}}}}\left(a^a_{\vec{k}}(t) + a^{a\dagger}_{-\vec{k}}(t)\right)e^{\mathrm{i}\vec{k}\cdot\vec{x}}$$

$$\pi_a(\vec{x},t) = \frac{1}{\sqrt{V}}\sum_{\vec{k}}(-\mathrm{i})\sqrt{\frac{\omega_{a\vec{k}}}{2}}\left(a^a_{\vec{k}}(t) - a^{a\dagger}_{-\vec{k}}(t)\right)e^{\mathrm{i}\vec{k}\cdot\vec{x}}$$

Commutation relation

$$\left[\phi^a(\vec{x},t), \pi^b(\vec{y},t)\right] = \mathrm{i}\delta_{ab}\delta(\vec{x}-\vec{y}),$$
$$\left[\phi^a(\vec{x},t)\phi^b(\vec{y},t)\right] = \left[\pi^a(\vec{x},t), \pi^b(\vec{y},t)\right] = 0$$

Slow variables A_j

$\cdots$ meson field, chiral charge, energy and momentum

$$\phi^a_{\vec{q}}(t) = \frac{1}{\sqrt{V}} \int \mathrm{d}^3x e^{-\mathrm{i}\vec{q}\cdot\vec{x}} \left(\phi^a(\vec{x},t) - \langle\phi^a\rangle\right)$$

$$Q_{\vec{q}}(t) = \frac{1}{\sqrt{V}} \int \mathrm{d}^3x e^{-\mathrm{i}\vec{q}\cdot\vec{x}} \epsilon^{ab}\pi^a\phi^b(\vec{x},t)$$

$$E_{\vec{q}}(t) = \frac{1}{\sqrt{V}} \int \mathrm{d}^3x e^{-\mathrm{i}\vec{q}\cdot\vec{x}} \left(\frac{1}{2}\left(\pi^a\right)^2 + \frac{1}{2}\left(\vec{\nabla}\phi^a\right)^2 + \frac{1}{2}\mu^2\left(\phi^a\right)^2 + \frac{\lambda}{4}\left(\left(\phi^a\right)^2\right)^2\right)(\vec{x},t)$$

$$P^i_{\vec{q}}(t) = \frac{1}{\sqrt{V}} \int \mathrm{d}^3x e^{-\mathrm{i}\vec{q}\cdot\vec{x}} \left(-\pi^a\nabla^i\phi^a\right)(\vec{x},t)$$

From these slow variables, the propagating mode for the meson mode does not appear.

$\Rightarrow$ Canonical momentum π is necessary.

The finite commutation relation $[\phi(\vec{x},t), \pi(\vec{y},t)] = \mathrm{i}\delta(\vec{x}-\vec{y})$ gives the finite frequency.

Frequency matrix in the disordered phase ($T > T_\mathrm{c}$)

$$\omega_{jl} = \begin{pmatrix} -\frac{k_\mathrm{B}T}{2\omega_{1\vec{q}}\chi_{1\vec{q}}} & 0 & 0 & 0 & 0 & 0 & 0 \\ 0 & \frac{k_\mathrm{B}T}{2\omega_{1\vec{q}}\chi_{1\vec{q}}} & 0 & 0 & 0 & 0 & 0 \\ 0 & 0 & -\frac{k_\mathrm{B}T}{2\omega_{2\vec{q}}\chi_{2\vec{q}}} & 0 & 0 & 0 & 0 \\ 0 & 0 & 0 & \frac{k_\mathrm{B}T}{2\omega_{2\vec{q}}\chi_{2\vec{q}}} & 0 & 0 & 0 \\ 0 & 0 & 0 & 0 & 0 & 0 & 0 \\ 0 & 0 & 0 & 0 & 0 & 0 & -\frac{D}{\chi_{p\vec{q}}}q^i \\ 0 & 0 & 0 & 0 & 0 & -\frac{D}{\chi_{e\vec{q}}}q^i & 0 \end{pmatrix}$$

$$\frac{k_\mathrm{B}T}{2\omega_{a\vec{q}}\chi_{a\vec{q}}} \equiv \omega_{a\vec{q}} \quad \Rightarrow \quad \omega_{a\vec{q}} = \sqrt{\vec{q}^2 + m^2} \qquad \left(2\chi_{a\vec{q}} = \frac{k_\mathrm{B}T}{\vec{q}^2 + m^2}\right)$$

Meson modes have appeared.

The microscopic equation of motion for the meson field

The Heisenberg equation for the meson field:

$$\mathrm{i}\frac{\mathrm{d}}{\mathrm{d}t}\phi(\vec{x},t) = [\phi(\vec{x},t), H]$$
$$\mathrm{i}\frac{\mathrm{d}}{\mathrm{d}t}\pi(\vec{x},t) = [\pi(\vec{x},t), H]$$

$\Rightarrow$ ϕ and π are necessary in order to describe the meson dynamics.

<u>cf.</u> Antiferromagnet
The Heisenberg equation is for the spin variables:

$$\mathrm{i}\frac{\mathrm{d}s_i^\alpha}{\mathrm{d}t} = [s_i^\alpha, H] \qquad (\alpha = x, y, z)$$
$$H = \sum_{jl} J_{jl}\vec{s}_j \cdot \vec{s}_l$$

$\Rightarrow$ The three staggered magnetization $N_{x,y,z}$ are the appropriate degrees of freedom for the antiferromagnet.

We can derive the full kinetic equation for the O(4) sigma model.
The dynamic critical exponent $z = 0.98$ is obtained.
$\Leftrightarrow$ $z = d/2$ for the antiferromagnet

4. Summary

- The chiral phase transition and the antiferromagnet are not in the same dynamic universality class.

  The slow modes are different in the two systems in spite of perfect coincidence of the slow variables (the order parameter and conserved quantities).
  $\Rightarrow$ Halperin and Hohenberg's prescription for classification of the dynamic universality class does not work.

- We reanalyzed the chiral phase transition by means of the mode coupling theory.
  $\Rightarrow$The canonical momentum π is necessary in order for the meson mode (particle mode) to appear.

- It is necessary to analyze the critical points that involves the particle mode, such as

  · Critical end point

  · Tricritical point

  · Color superconductor

  · Confinement-deconfinement transition

  · Elector-weak transition

  because they are not classified into any dynamic universality classes that have been considered in "Rev.Mod.Phys. 49 (1977) 435 Halperin & Hohenberg."

The Effect of Memory on Relation in ϕ^4 Theory

Takashi Ikeda

The effect of memory on relaxation in ϕ^4 theory

Takashi Ikeda
(RIKEN BNL Research Center)

Abstract

We derive a kinetic equation including a memory effect in ϕ^4 theory by using a generalized Kadanoff-Baym ansatz. Solving the kinetic equations with and without the memory effect, we found that, while relaxation of a single particle excitation is unaffected by that effect in the weak coupling regime, that effect leads to faster relaxation in the moderately large coupling and to slower relaxation in the strong coupling.

Motivation

- Nonequilibrium physics

> challenging problem in relativistic many-body theory
> motivated by Heavy-ion collisions, early universe, etc.....

Generalized kinetic equations beyond Boltzmann eq.
are necessary for
strongly correlated and/or dense plasmas !

- (Classical) Boltzmann equations;

Including scattering effect, but independent collisions

→ ~~strongly correlated plasmas~~

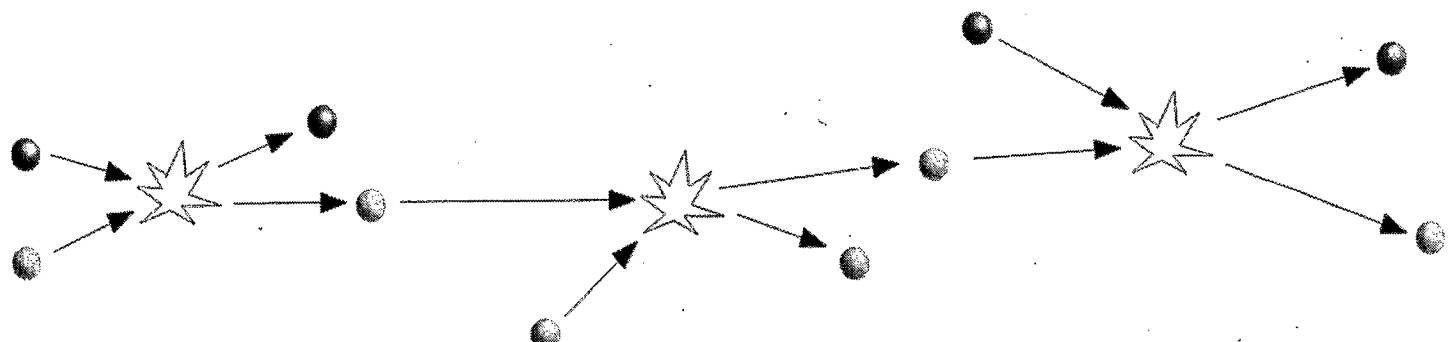

Strategy

- Starting point ····· **Kadanoff-Baym (KB) equations**

↓ designed to study nonequilibrium phenomena

One-particle distribution function, mean field, scattering effect, ~~memory effect~~, ~~dynamical spectral function~~

KB equations

↓ Equal time limit

Generalized KB ansatz for two-time Green's functions
(PRB34(1986),P.Lipavsky et al.)

↓ Quasiparticle approximation

Kinetic equations including memory effect
(non-Markovian collision term)

↓ neglecting memory effect

Boltzmann-type equation with Markovian collision term

Model : ϕ^4 theory

- Lagrangian : $\mathcal{L} = \frac{1}{2}(\partial_\mu \phi)^2 - g^2 \phi^4$

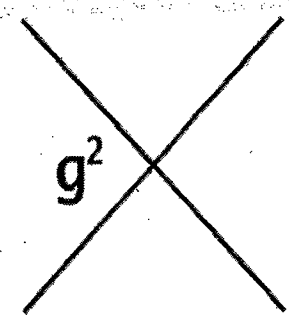

  - In 3+1 dimensions and spatially homogeneous case
  - Selfenergies as in thermal equilibrium, temperature T

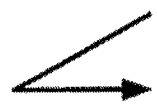

Single particle excitation

- Self-energies from 3-loop order of 2PI effective action

  - Leading order

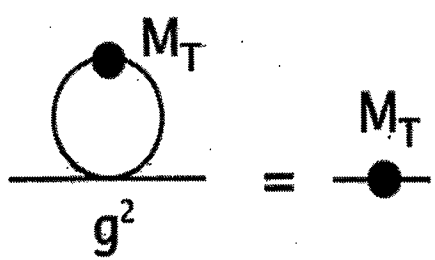

generating effective mass M_T by solving gap eq. self-consistently (Mean field)

  - Next-to Leading order

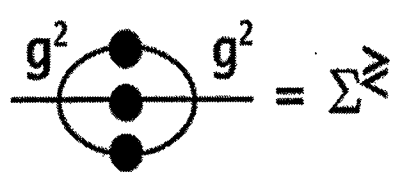

leading to damping of excitation (Scattering effect)

Thermal Mass

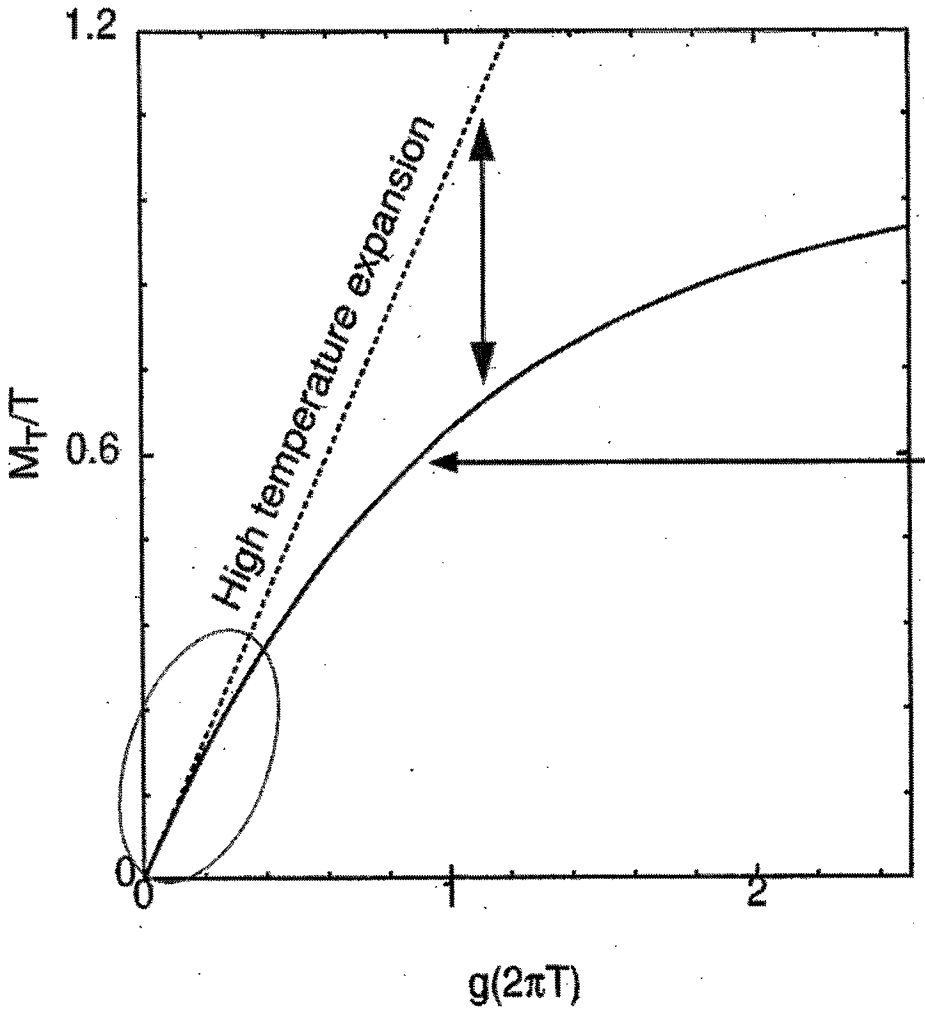

Gap equation

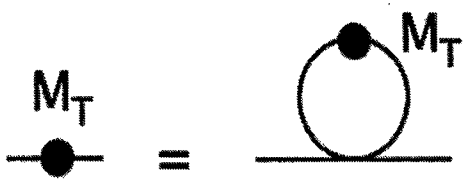

$$M_T^2 = 12g^2 \int \frac{d^3k}{(2\pi)^3} \frac{N_{eq}(\omega_k)}{\omega_k} + \frac{3g^2 M_T^2}{4\pi^2}\left(\ln\frac{M_T^2}{\bar{\mu}^2} - 1\right)$$

($\omega_p^2 = \mathbf{p}^2 + M_T^2$, modified MS scheme)

High temperature expansion
(Leading order of HTL)

$$M_T^2 = g^2 T^2$$

Result agrees with PRD63 065003 by J.-P.Blaizot et al.

From KB eq. to Boltzmann eq.

- KB eq. in equal-time limit

$$\boxed{\begin{array}{c} x_0=y_0=t \\ s\equiv x_0-y_0 \end{array}}$$

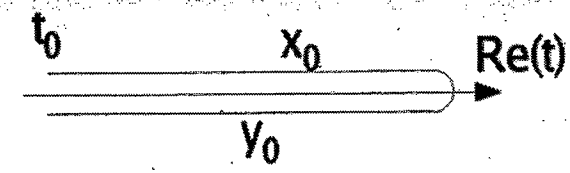

$$2\,\partial_t\partial_s G^<(\mathbf{p},s,t)\big|_{s=0} = -i\int_{t_0}^{t} dz_0[\,\Sigma^>(\mathbf{p},t,z_0)G^<(\mathbf{p},z_0,t)-\Sigma^<(\mathbf{p},t,z_0)G^>(\mathbf{p},z_0,t)$$
$$+G^<(\mathbf{p},t,z_0)\,\Sigma^>(\mathbf{p},z_0,t)-G^>(\mathbf{p},t,z_0)\,\Sigma^<(\mathbf{p},z_0,t)]$$

Reconstruction Problem :

- Kadanoff-Baym (KB) ansatz: $G^{\gtrless}(k,t)=\rho\,(k,t)N^{\gtrless}(k,t)$, $(N^<=N,\ N^>=1+N)$

  → lead to inconsistencies in time argument of memory effect

- Generalized KB ansatz: $G^{\gtrless}(\mathbf{p},\mathbf{x};x_0,y_0)=1/i\big[G_R(\mathbf{p},\mathbf{x};x_0,y_0)N^{\gtrless}(\mathbf{p},\mathbf{x};y_0)$
  $-\,N^{\gtrless}(\mathbf{p},\mathbf{x};x_0)G_A(\mathbf{p},\mathbf{x};x_0,y_0)\big]$
  (PRB34(1986),P.Lipavsky et al.)

  → take into account memory effect properly

using quasiparticle approximation:
$\rho\,(\mathbf{p},p_0)=2\pi\varepsilon\,(p_0)\delta\,(p_0^2-\mathbf{p}^2-M_T^2)$

~~Dynamical spectral function~~

From KB eq. to Boltzmann eq. (cont'd)

Kinetic equation with memory effect for δN $(=N - N_{eq})$

$$\frac{\partial}{\partial t}\delta N(\mathbf{p},t) = 2\int_{t_0}^{t} dz_0 \left(\frac{\partial}{\partial z_0}\gamma(\mathbf{p},t-z_0)\right)\delta N(\mathbf{p},z_0)$$

Non-Markovian collision term

Time-dependent damping rate

Neglecting memory effect

$N(\mathbf{p},z_0) \rightarrow N(\mathbf{p},t)$

Finite-initial time generalization of Boltzmann eq.

$$\frac{\partial}{\partial t}\delta N(\mathbf{p},t) = -2\gamma(\mathbf{p},t-t_0)\delta N(\mathbf{p},t)$$

Markovian collision term

~~Memory effect~~

Complete collision limit $t_0 \rightarrow -\infty$

(Classical) on-shell Boltzmann eq.

$$\frac{\partial}{\partial t}\delta N(\mathbf{p},t) = -2\gamma_\infty(\mathbf{p})\delta N(\mathbf{p},t)$$

exponential damping !

Time-dependent Damping Rate

$$\gamma(\mathbf{p},t) \equiv \frac{1}{2\omega_p}\int\frac{dp_0}{2\pi}[\Sigma^<(p)-\Sigma^>(p)]\frac{\sin(p_0-\omega_p)t}{p_0-\omega_p} \xrightarrow[t\to\infty]{} \pi\delta(p_0-\omega_p)$$

On-shell limit
(Fermi's golden rule)

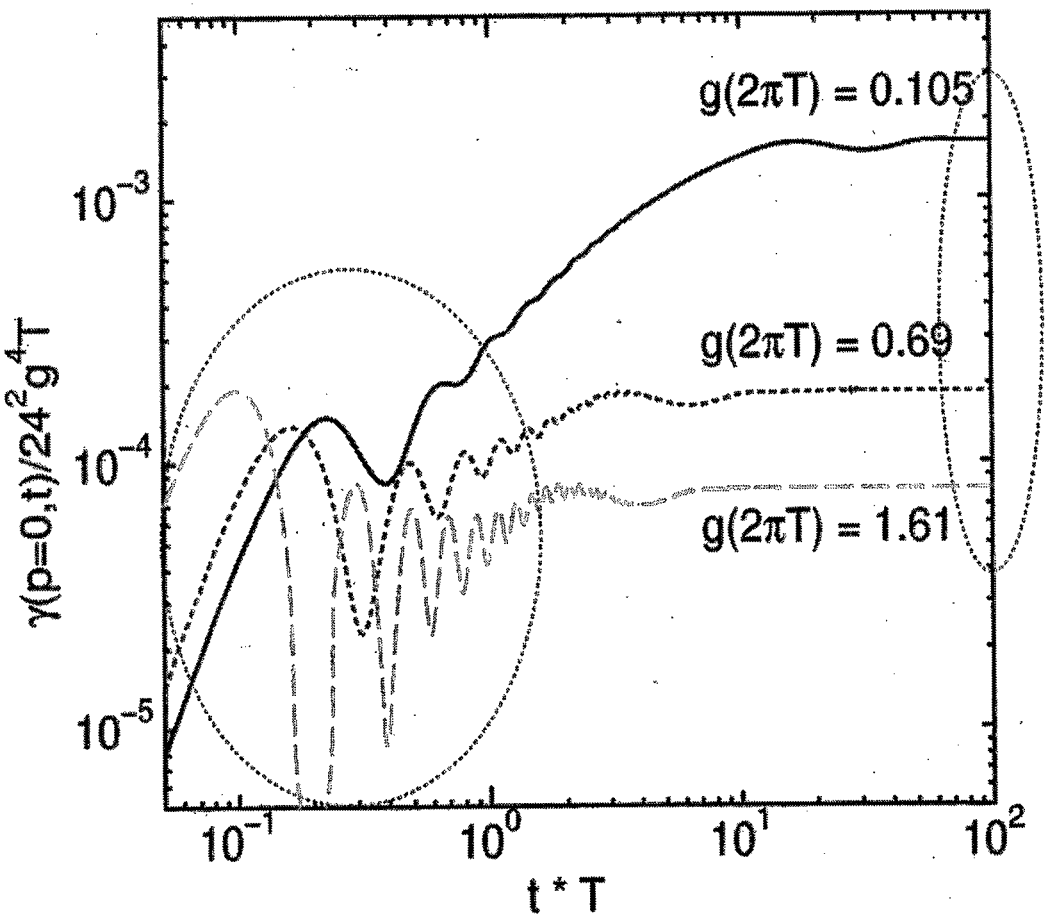

- In the early time ··· Oscillation

  More violently for stronger coupling

- In the late time

  Approach to some constant value

$$\gamma_\infty(\mathbf{p}=0) = \frac{1}{4M_T}[\Sigma^<(\mathbf{p},M_T)-\Sigma^>(\mathbf{p},M_T)]$$

Damping rate in on-shell Boltzmann eq.

Damping Processes

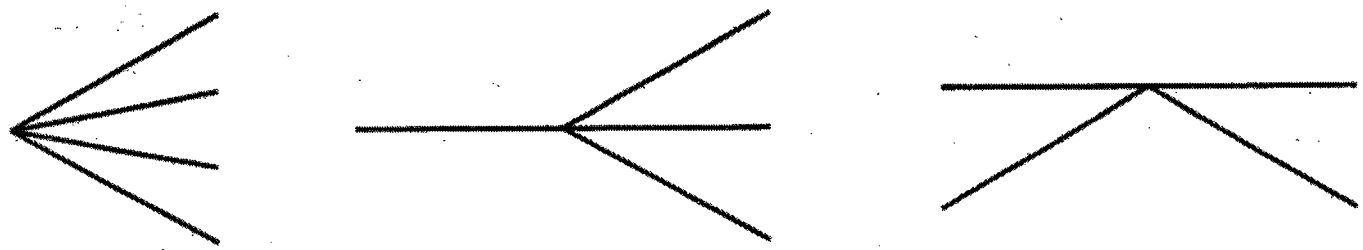

and inverse processes

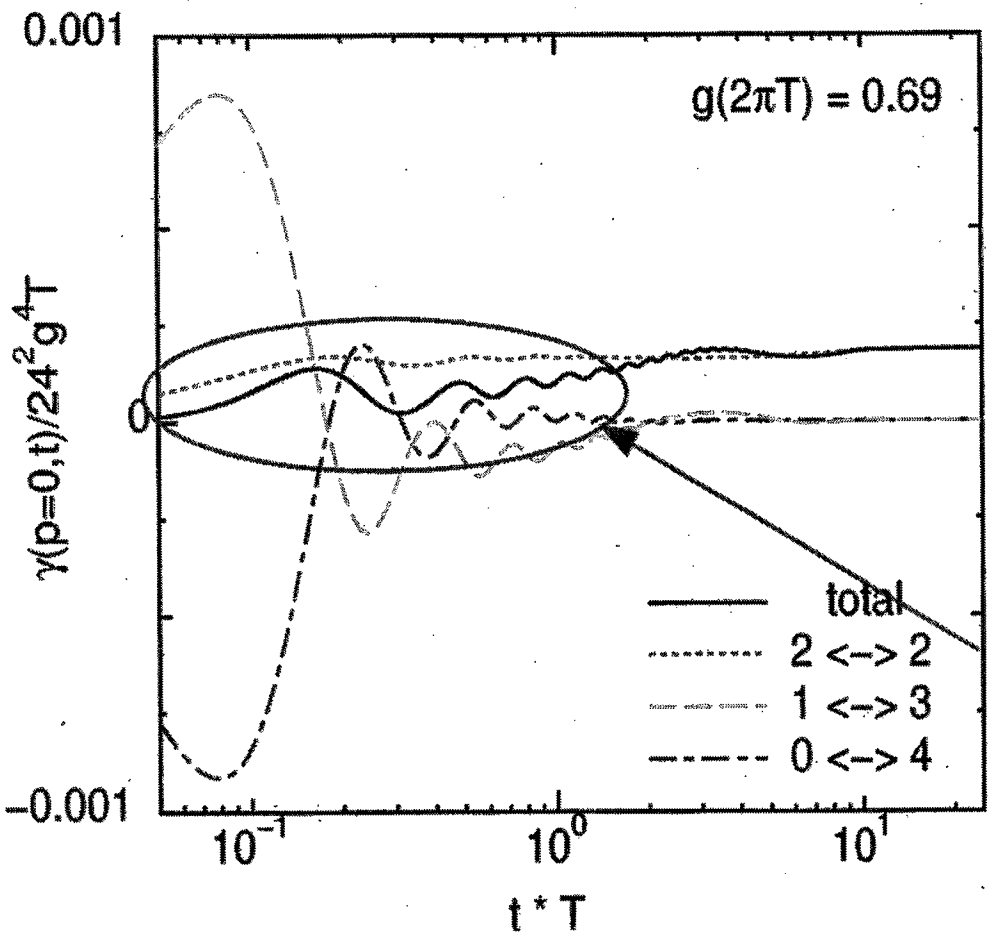

$$\frac{\partial}{\partial t}\delta N(\mathbf{p},t) \qquad \text{Non-Markovian solution}$$

$$= 2\int_0^t dz_0 \left(\frac{\partial}{\partial z_0}\gamma(\mathbf{p},t-z_0)\right)\delta N(\mathbf{p},z_0)$$

Solve these equations
&
compare solutions

$$\frac{\partial}{\partial t}\delta N(\mathbf{p},t) = -2\gamma(\mathbf{p},t)\delta N(\mathbf{p},t)$$

Markovian solution

Decay of Single Particle Excitation : I

- Weak coupling regime

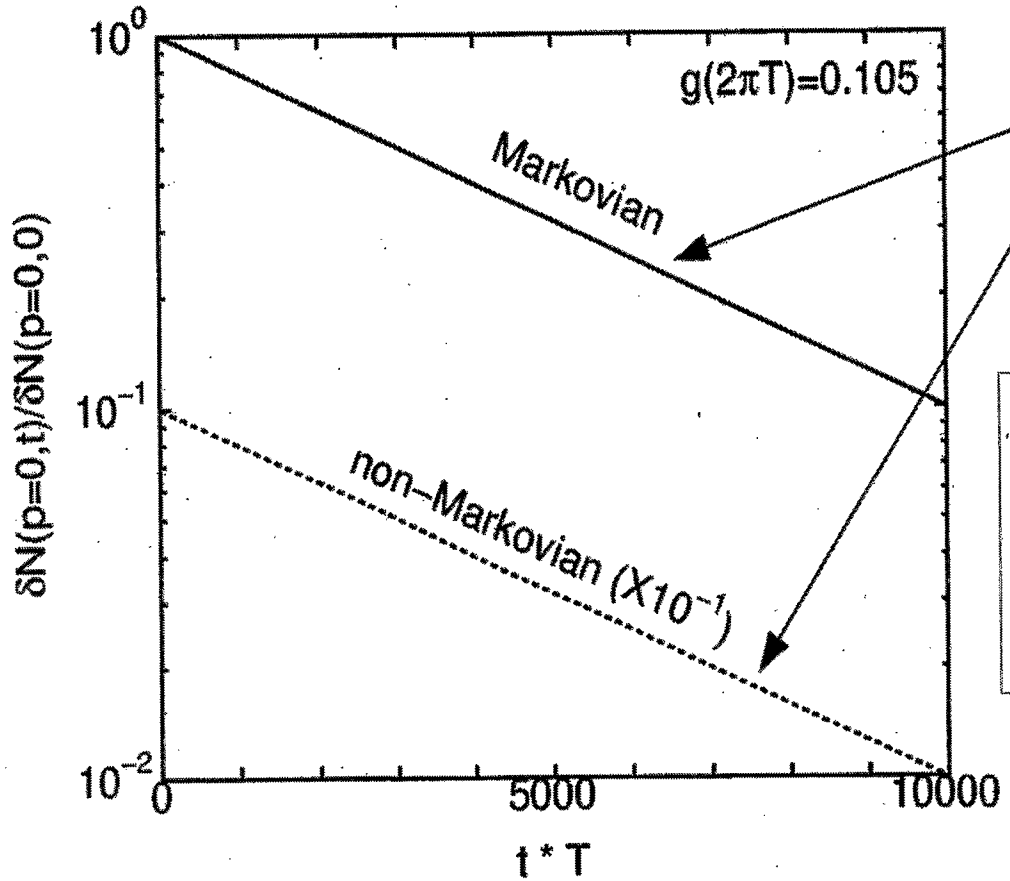

- In complete agreement
- Exponential damping

Why ?

Relaxation time (tT~4300)

⋙

time (tT~20) : oscillation of γ (t) ends
(separation of scales)

In this case, kinetic equations essentially coincide with on-shell Boltzmann eq.

Memory effect doesn't influence relaxation in weak coupling regime.

Decay of Single Particle Excitation : II

- Moderately large coupling regime

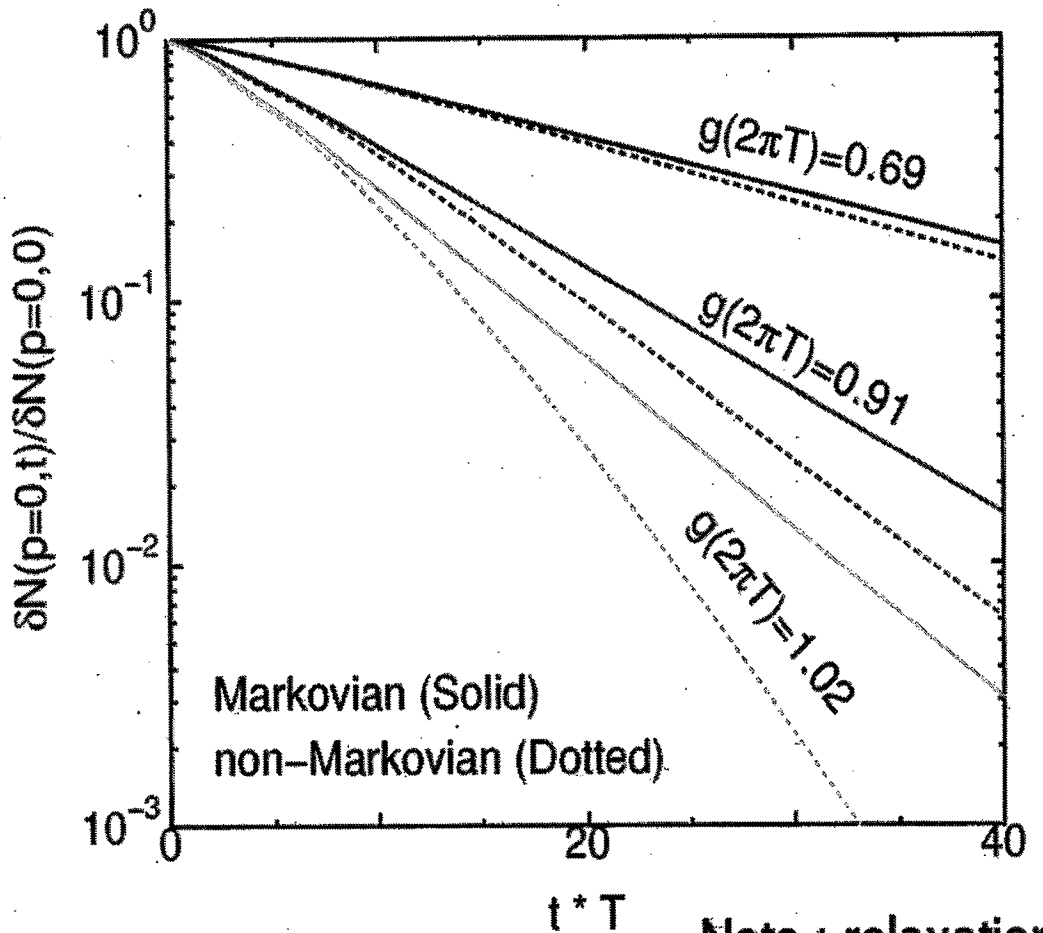

Memory effect leads to faster relaxation !!

Consistent with results of KB equations in 2+1 dimensions. (Cassing, et.al: PRD69,025006(2004))

Note : relaxation with memory effect seems to represent exponential damping in late times.

Decay of Single Particle Excitation : III

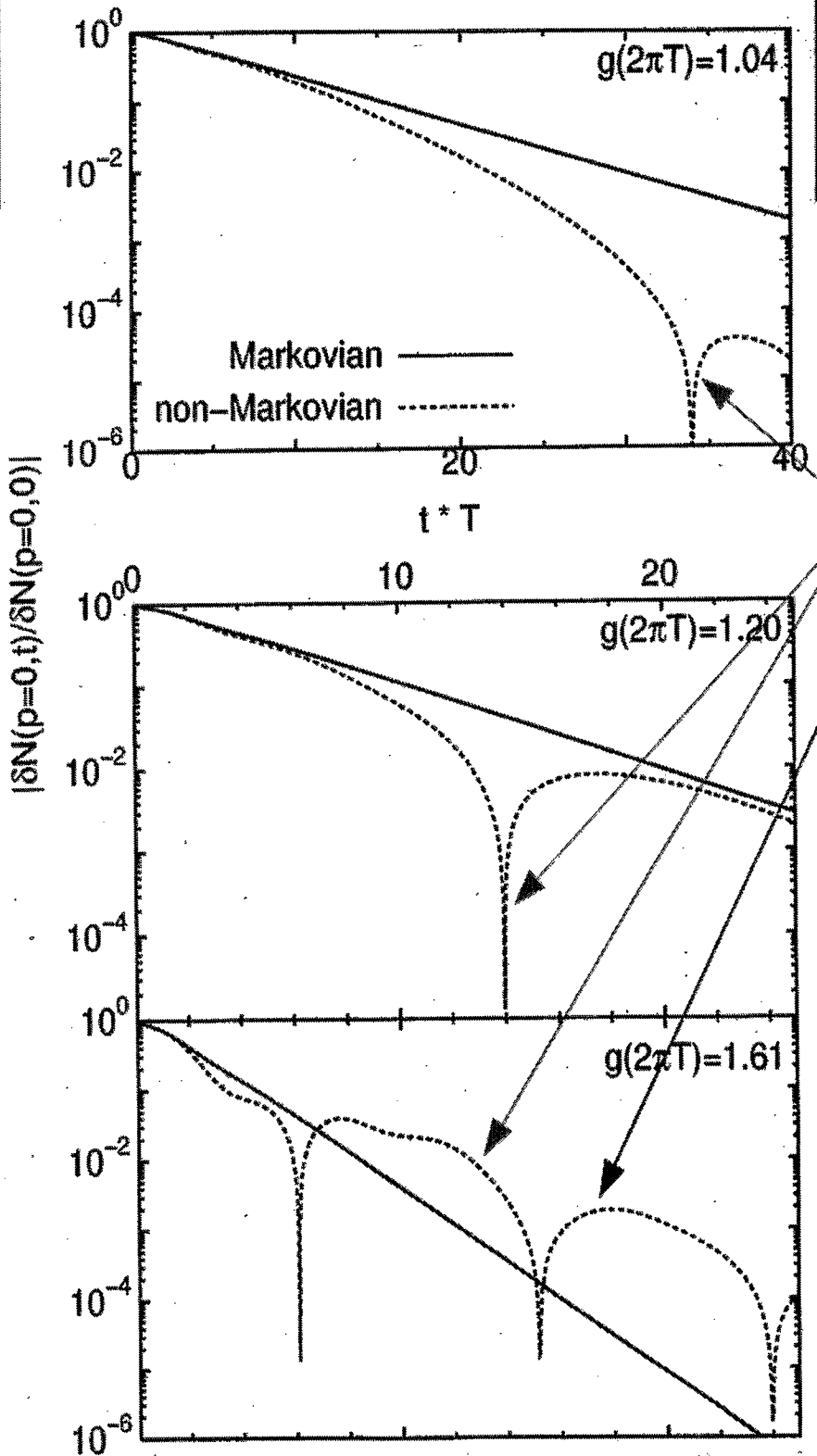

- Strong coupling regime

Memory effect leads to

- Oscillation around thermal value
- Slower relaxation of amplitude

This never occurs without memory effect.
Damping rate is always positive !

Summary and Outlooks

- Construct kinetic equation including memory effect from KB eqs. by generalized Kadanoff-Baym ansatz.
- Memory effect doesn't influence relaxation in weak coupling regime, due to separation of scales.
- As coupling increases, memory effect leads to ;

Faster relaxation for moderately large coupling

↓

oscillating around thermal value and slower relaxation for strong coupling

- Outlooks ·····
  - Totally nonequilibrimu situation
  - directly solve KB equation
  - Fermionic system (NJL model)
  - Non-abelian gauge theory

Glueball Properties Near the QCD Phase Transition

Noriyoshi Ishii

Glueball properties near the QCD phase transition

Noriyoshi Ishii (TITECH)
in collaboration with
Hideo Suganuma (TITECH)

We have reported glueball properties near the critical temperature Tc of QCD phase transition using quenched SU(3) anisotropic lattice QCD Monte Carlo calculation. We have first reviewed the effective model results, which support the pole mass reduction of the scalar glueball near Tc. We have then constructed the glueball correlators from 5,000-9,900 gauge field configurations generated with the quenched lattice QCD with $\beta = 6.25$ and the renormalized anisotropy $\gamma_G = a_S / a_T = 4$ at finite temperature. In addition to the ordinary pole-mass analysis, where the narrowness of the glueball peak is assumed, we have analyzed the glueball correlators with an advanced analysis, which can take into account the effects of thermal width of the glueball peak. We have found that the scalar glueball receives a huge thermal effect near Tc, and that this thermal effect can be understand as a significant thermal width broadening of the glueball peak as $\Gamma(T_C) \approx 300\,\mathrm{MeV}$ together with a modest reduction in the peak center as $\Delta\omega_0(T_C) \approx 100\,\mathrm{MeV}$. We finally make a comment on the origin of such a large thermal width and a possible physical implication of our results.

Glueball properties near the QCD phase transition

Noriyoshi Ishii (TITECH)
in collaboration with
Hideo Suganuma (TITECH)

Plan of the talk

1. Motivation / Background
2. Lattice QCD formalism
3. Numerical Results
4. Summary / Discussion

START

Motivation / Background

At T > 0, QCD vacuum is expected to change its structure

Low Temperature — Tc — **High Temperature**

Confinement (hadron) phase

- color confinement
- spontaneous chiral symmetry breaking (⇒ massive constituent quarks)

QGP Phase

- deconfined quarks and gluons
- chiral symmetry restoration (massless current quark)

The onset of phase transition

- Partial restoration of the chiral symmetry
- Reduction of the string tension

inter quark potential

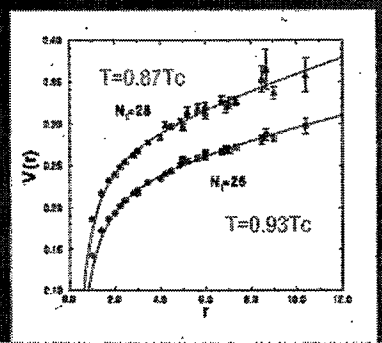

Hadron = bound state of quarks & gluons

⇩

Properties(mass, width, etc.) of some hadrons are expected change as a result of the change of QCD vacuum.

- charmonium
- light q qbar
- glueball

- T.Hatsuda et al., PRL55,158('85)
- T.Hashimoto et al., PRL57,2123('86)
- T.Hatsuda et al., PRD47,1225('93)
- H.Ichie et al., PRD52,2944('95)

Lattice studies of thermal hadrons near Tc

at quenched level

Lattice QCD simulations are performed to observe these phenomena.

1. QCD-TARO Collaboration, PRD63,054501('01) ⟺ light q qbar
2. T.Umeda et al., Int. J. Mod. Phys. A16,2215('01) ⟺ charmonium

⇩

Unfortunately, no significant changes are observed below Tc.

We are interested in **glueball** at finite temperature, due to

1. The significance of the nonperturbative gluon condensate <GG> suggests
   ⇨ condensation of the 0++ glueball in the vacuum like Higgs particle.
   ⇨ **the 0++ glueball may be sensitive to the change of QCD vacuum**.
2. The large difference between the glueball mass and Tc in quenched QCD.

Glueballs

$$L = -\mathrm{tr}\, G_{\mu\nu} G^{\mu\nu} + \sum \bar{q}_f \left(i\gamma^\mu D_\mu - m_f \right) q_f$$

$$D_\mu \equiv \partial_\mu - igA_\mu^a T^a$$

$$G_{\mu\nu}^a \equiv \partial_\mu A_\nu^a - \partial_\nu A_\mu^a + gf^{abc} A_\mu^b A_\nu^c$$

Glueballs are the hadrons which mainly consist of gluons only. Their existence is a prediction of QCD.

Non-Abelian natrure of the gauge group

↓

self-interaction of gluons

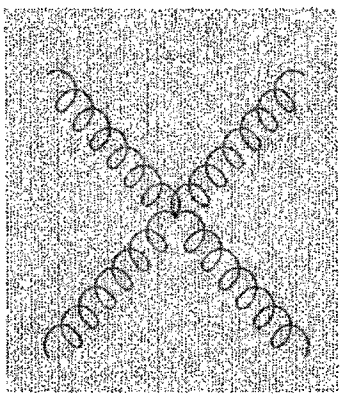

↓

glueball = bound state of gluons

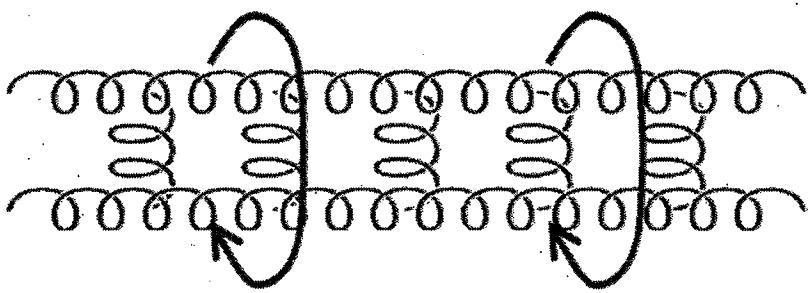

glueball

Theoretical studies of glueball

There have been a lot of theoretical studies on the glueball:

- ✓ **MIT bag model**
  T.Barnes et al., NPB224('83)241., etc.
- ✓ **Constituent gluon model**
  D.Hom et al., PRD17('78)898., etc.
- ✓ **Flux tube model**
  N.Isgur et al., PLB147('84)169., etc.
- ✓ **Instanton liquid model**
  T.Schaefer et al., PRL75('95)1707.
- ✓ **QCD sum rule**
  M.Shifman, Z.Phys.C9('81)347.
- ✓ **Lattice QCD**
  - ➢ **quenched level**
    C.J.Morningstar et al., PRD66('99)034509.
    J.Sexton et al., PRL75('95)4563., etc.
  - ➢ **full QCD**
    K.M.Bitar et al., PRD44('91)2090.
    A.Hart et al., PRD65('02)034502., etc.

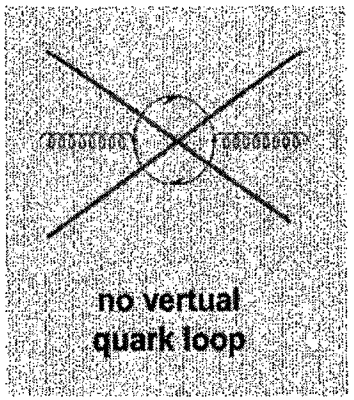

The most systematic study of glueball in quenched lattice QCD

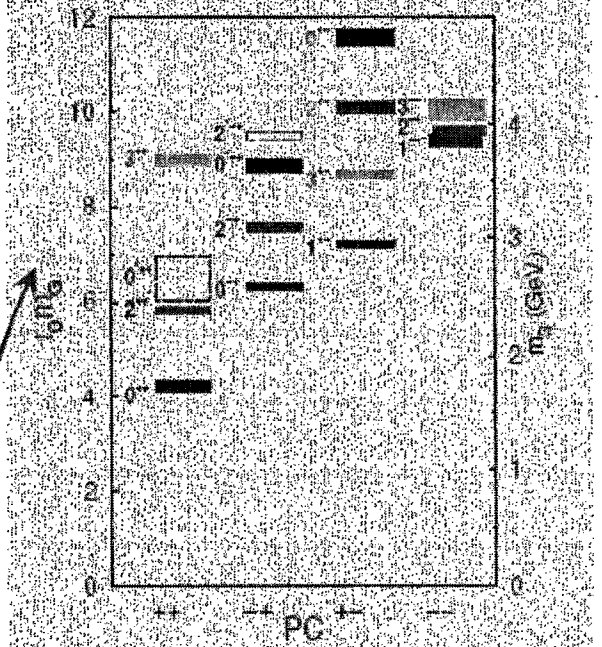

FIG. 8. The mass spectrum of glueballs in the pure SU(3) gauge theory. The masses are given in units of the hadronic scale r_0 along the left vertical axis and in units of GeV along the right vertical axis (assuming $r_0^{-1} = 410$ MeV). The mass uncertainties indicated by the vertical extents of the boxes do not include the uncertainty in setting r_0. The lattice artefacts whose interpretation requires further study are indicated by the dashed hollow boxes.

Except for minor variations, quenched lattice QCD predicts

$$m(0^{++}) \cong 1500-1700\ \mathrm{MeV}$$

$$m(2^{++}) \cong 2000-2400\ \mathrm{MeV}$$

The glueball in experiment

The glueball can mix with flavor-singlet q qbar.

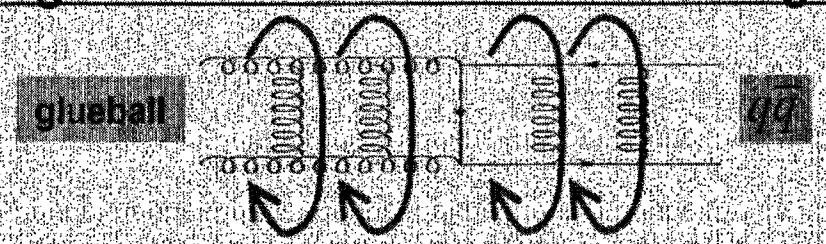

⇨ Careful considerations are necessary to determine **which flavor-singlet meson is a glueball** !

We need criterion to determine which one is a glueball:

- ✓ Glueballs are created in the **glue-rich process**
- ✓ Glueballs should be **exotic** mesons
- ✓ Their **decay width** shoud be **narrower** than ordinary mesons (**OZI rule**)
- ✓ **Flavor-blind decay**
- ✓ Glueballs should **not decay into two photons.**

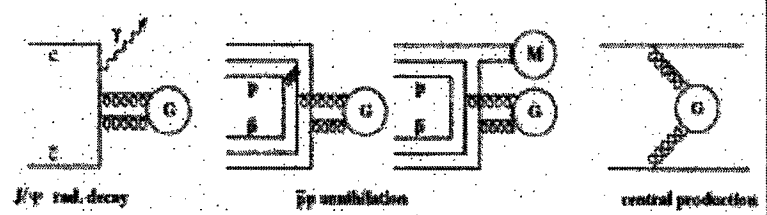

FIG. 3. Glue-rich processes for glueball production.

from K.Seth, Nucl.Phys.A675(2000)25c.

Serious glueball candidates:

$$f_0(1500),\ f_0(1710)$$

The large difference between the **glueball mass** and **Tc** in quenched QCD

In quenched QCD,

$$T_C \cong 260\text{–}280\,\text{MeV} \ll m_G \cong 1500\text{–}1700\,\text{MeV}$$

⇨ Thermal excitation of the glueball is suppressed in the confinement phase by a **very strong statistical factor** as

$$\exp\left(-\sqrt{m_G^2+\vec{p}^2}/T\right) < e^{-m_G/T_C} \cong 0.00207$$

The **glueball density** is very small even near Tc:

$$\rho(T_C) = \frac{N(T_C)}{V} = \int \frac{d^3k}{(2\pi)^3} \frac{1}{e^{\sqrt{m_G^2+\vec{k}^2}/T_C}-1} \cong 1/(4.0\,\text{fm})^3$$

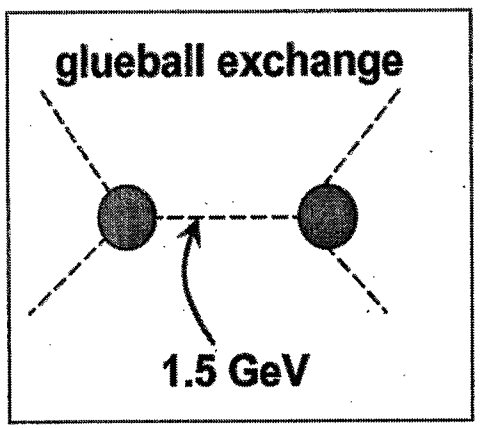

This density is considered to be **TOO SMALL:**

- The glueball is considered to have a rather **small size** !

  $r \leq 0.2-0.4$ fm

- The interactions among glueballs are expected to be **very short-ranged**, since the interaction is mediated by rather heavy glueball ($m_G > 1.5$ GeV) exchanges.

One possible answer would be

glueball (pole) mass reduction (and/or **swelling of the glueball size**)

near the critical temperature T_C

In fact, the glueball mass reduction near T_C is suggested by

H. Ichie et al., PRD52, 2944 (1995)

based on an effective model studies (dual Ginzburg-Landau model).

In this talk, we report the anisotropic lattice QCD study of the thermal glueball near the critical temperature.

References:

- N. Ishii et al., PRD66,014507(2002)
- N. Ishii et al., PRD66,094506(2002)
- N. Ishii et al., EPJA17,77(2003)

Dual Ginzburg-Landau(DGL) model

From H.Ichie et al., PRD52,2944('95)

(an effective model of confinement based on the dual Higgs Mechanism)

$$L=-\tfrac{1}{4}\left(\partial_\mu \vec{B}_\nu-\partial_\nu \vec{B}_\mu\right)^2+\sum_{\alpha=1}^{3}\left[\left|(i\partial_\mu-g\vec{\varepsilon}_\alpha\cdot\vec{B}_\mu)\chi_\alpha\right|^2-\lambda\left(\left|\chi_\alpha\right|^2-v^2\right)^2\right]$$

$B_\mu=(B_\mu^3,B_\mu^8)$ dual gauge field

$\chi_\alpha\,(\alpha=1,2,3)$ QCD monopole field

$\varepsilon_1=(1,0),\varepsilon_2=(-\tfrac{1}{2},-\tfrac{\sqrt{3}}{2}),\varepsilon_3=(-\tfrac{1}{2},\tfrac{\sqrt{3}}{2})$

Higgs phase of DGL
electric flux is squeezed due to dual Meissner mechanism

⟺

confinement phase of QCD

Effective Potential

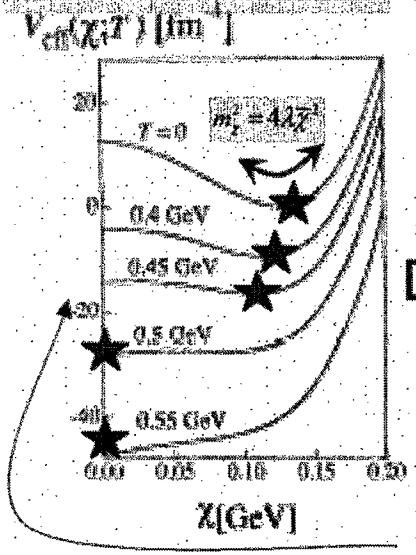

Vacuum expectation value

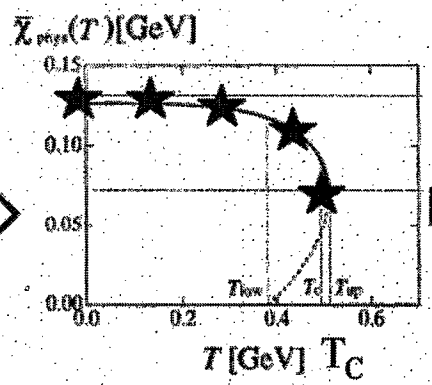

1st-order phase transition

The glueball mass redutin near T_C

A paticular combination:

$$\phi\equiv\chi_1+\chi_2+\chi_3$$

satisfies gauge-invariance condition, and becomes observed as a physical particle, i.e., the 0^{++} glueball

cf. H.Ichie et al., PRD60, 077501 ('99)

$$m_G^2=4\lambda\bar{\chi}^2$$

30-40 % pole mass redution of glueball near T_C

IMPORTANT: We use the DGL argument only in the section of motivation. Our main results are nothing to do with it.

Lattice QCD formalism

continuum QCD

$$L = -\mathrm{tr}\, G_{\mu\nu} G^{\mu\nu} + \sum \bar{q}_f \left(i\gamma^\mu D_\mu - m_f \right) q_f$$

$$D_\mu \equiv \partial_\mu - igA_\mu^a T^a$$

$$G_{\mu\nu}^a \equiv \partial_\mu A_\nu^a - \partial_\nu A_\mu^a + ig f^{abc} A_\mu^b A_\nu^c$$

Weak coupling at short distance (asympototic freedom)
But strong coupling at long distance !

discretization

lattice QCD

$$S = S_G + S_F$$

$$S_G = -\frac{1}{2g^2} \sum_{x,\mu\nu} \mathrm{tr}\left(U_{\mu\nu}(x) \right)$$

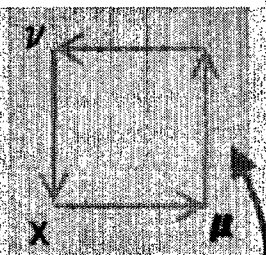

$$U_{\mu\nu}(x) \equiv U_\mu(x) U_\nu(x+\hat{\mu}) U_\mu^\dagger(x+\hat{\nu}) U_\nu^\dagger(x)$$

S_F : Fermionic part

$$S_G \cong -\tfrac{1}{2} \sum \mathrm{tr}\left(\exp\left(ia^2 g^2 G_{\mu\nu}(x) \right) \right)$$

$$\rightarrow \tfrac{1}{4} \int d^4x\, G_{\mu\nu}^a G^{a\mu\nu}$$

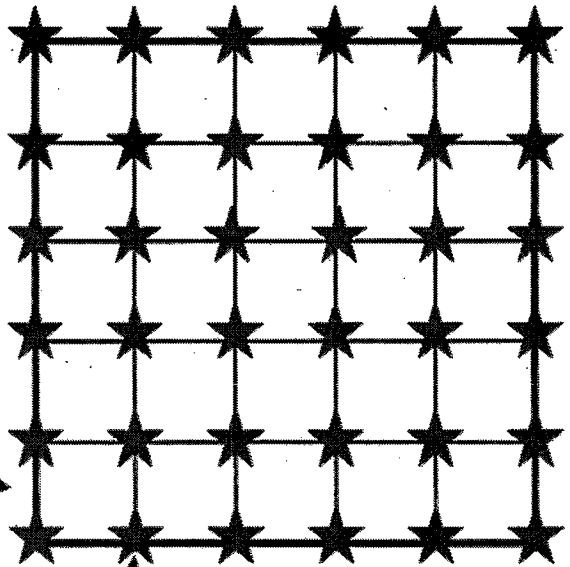

site

quark fields live on sites.

link

gluon fields live on the links in the form of

$$U_\mu(x) \equiv \exp\left[iagA_\mu^a(x) T^a \right] \in \mathrm{SU}(3)_c$$

.

The glueball correlation

glueball operator

$\phi(\tau) \equiv$ 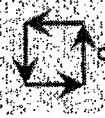 $\propto G^a_{ij} G^a_{ij}$

The glueball temporal correlator:

$$G(\tau) \equiv Z(T)^{-1} \mathrm{Tr}\left(e^{-H_{QCD}/T} \phi(\tau)\phi(0)\right)$$

The spectral function:

$$\rho(\omega) = \sum_{m,n} \frac{|\langle n|\phi|m\rangle|^2}{Z(\beta)} e^{-\beta E_m} \times 2\pi\left[\delta(\omega - \Delta E_{nm}) - \delta(\omega + \Delta E_{mn})\right]$$

The correlator

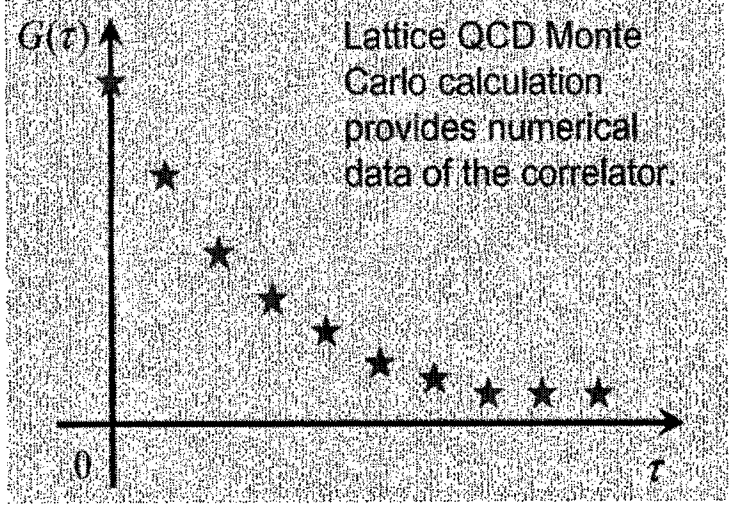

The spectral function

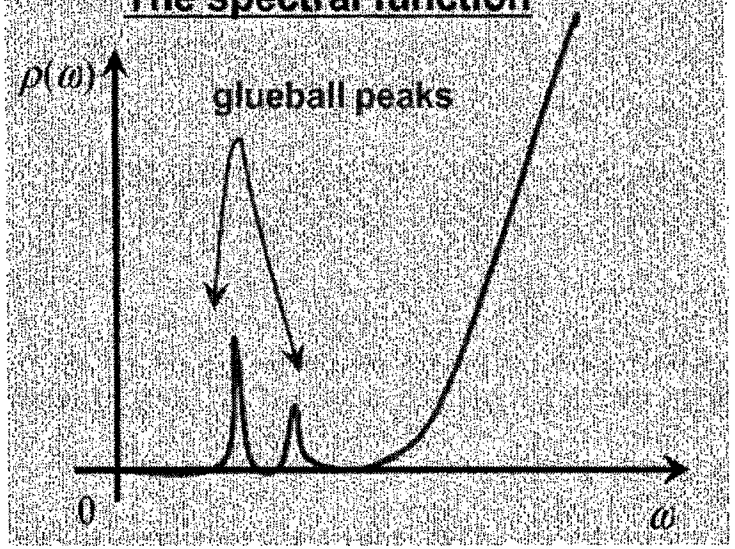

The spectral representation

$$G(\tau) = \int_0^\infty \frac{d\omega}{2\pi} \frac{\cosh[\omega(1/\beta - \tau)]}{\sinh[\beta\omega/2]} \rho(\omega)$$

- We adopt some **Ansatz** on ρ(ω) and **fit** the lattice QCD data of G(τ) to extractd the physical observables such as mass, width, etc.
- **Maximal Entropy Method** to extract ρ(ω) from G(τ) directly. (no Ansatz is needed)

Narrow peak ansatz

If we assume the **narrowness of the peak**, the spectral function can be approximated by introducing a temperature dependent "**pole mass**" m(T)

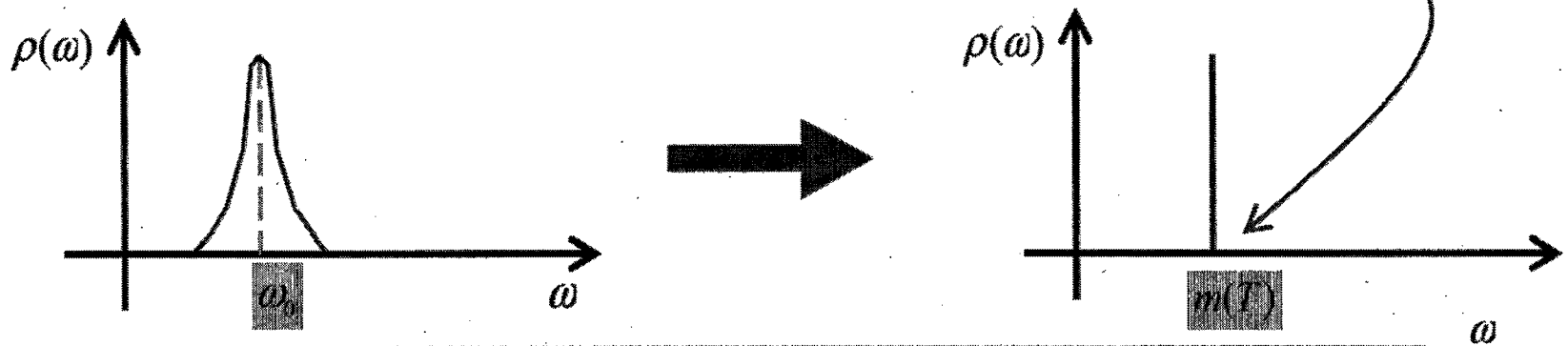

$$\rho(\omega) \cong 2\pi A\left[\delta(\omega - m(T)) - \delta(\omega + m(T))\right]$$

At T>0, each peak acquires a **thermal width** through the **interaction with the heat bath**. → ≠ **decay width**

→ It is desirable to respect the presence of thermal width at T>0.

Ansatz with thermal width

- What is the **appropriate functional form** ?
  - With increasing T (>0), bound state poles of $G_R(\omega)$ are moving off the real ω axis into complex ω plane.

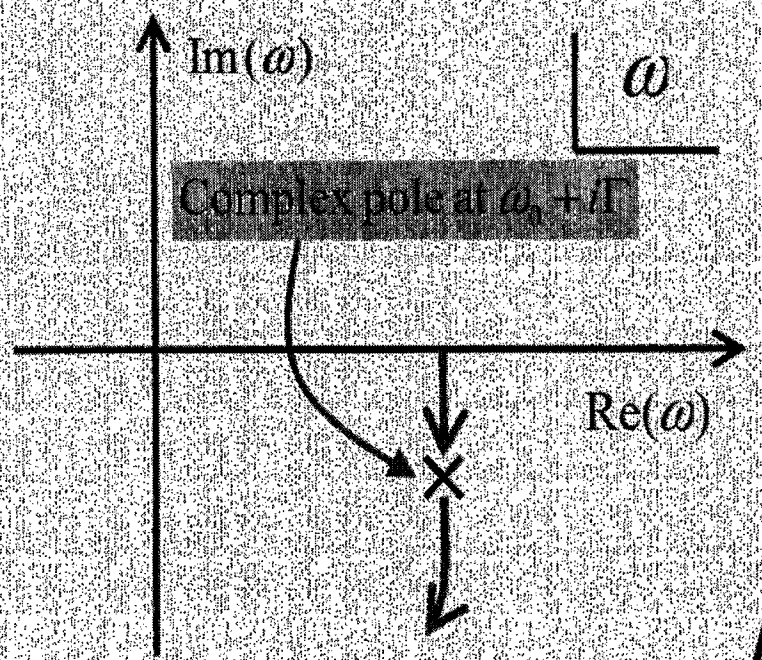

$$G_R(\omega) = \frac{A}{\omega - \omega_0 + i\Gamma} + \cdots$$

$$\rho(\omega) = -2\mathrm{Im}(G_R(\omega))$$
$$= 2\pi A[\delta_\Gamma(\omega-\omega_0) - \delta_\Gamma(\omega+\omega_0)] + \cdots$$

Lorentzian at ω_0 with width Γ

$$\delta_\Gamma(\omega-\omega_0) \equiv \frac{1}{\pi}\mathrm{Im}\left[\frac{1}{\omega-\omega_0+i\Gamma}\right]$$
$$= \frac{1}{\pi}\frac{\Gamma}{(\omega-\omega_0)^2+\Gamma^2}$$

- The appropriate functional form is "**Breit-Wigner type**".

$$g(t) \equiv \int_{-\infty}^{\infty} \frac{d\omega}{2\pi} \frac{\cosh[\omega(\beta/2-t)]}{\sinh[\beta\omega/2]}$$
$$\times 2\pi A[\delta_\Gamma(\omega-\omega_0) - \delta_\Gamma(\omega+\omega_0)]$$

A, Γ, ω fit parameters

What happens if the thermal width is broad ?

The spectral representation

$$G(t) = \int_{-\infty}^{\infty} \frac{d\omega}{2\pi} \frac{\rho(\omega)}{2\sinh(\beta\omega/2)} \cosh[\omega(\beta/2 - t)]$$

G(t) is an **average** of $\cosh[\omega(\beta/2-t)]$ with the **weight** $\dfrac{\rho(\omega)}{2\sinh(\beta\omega/2)}$

In the narrow peak ansatz, the weight is approximated by the δ function.

The role of the denominator $\left[2\sinh(\beta\omega/2) \cong e^{\beta\omega/2}\right]$

small ω region $\Leftarrow$ enhanced, large ω region $\Leftarrow$ suppressed

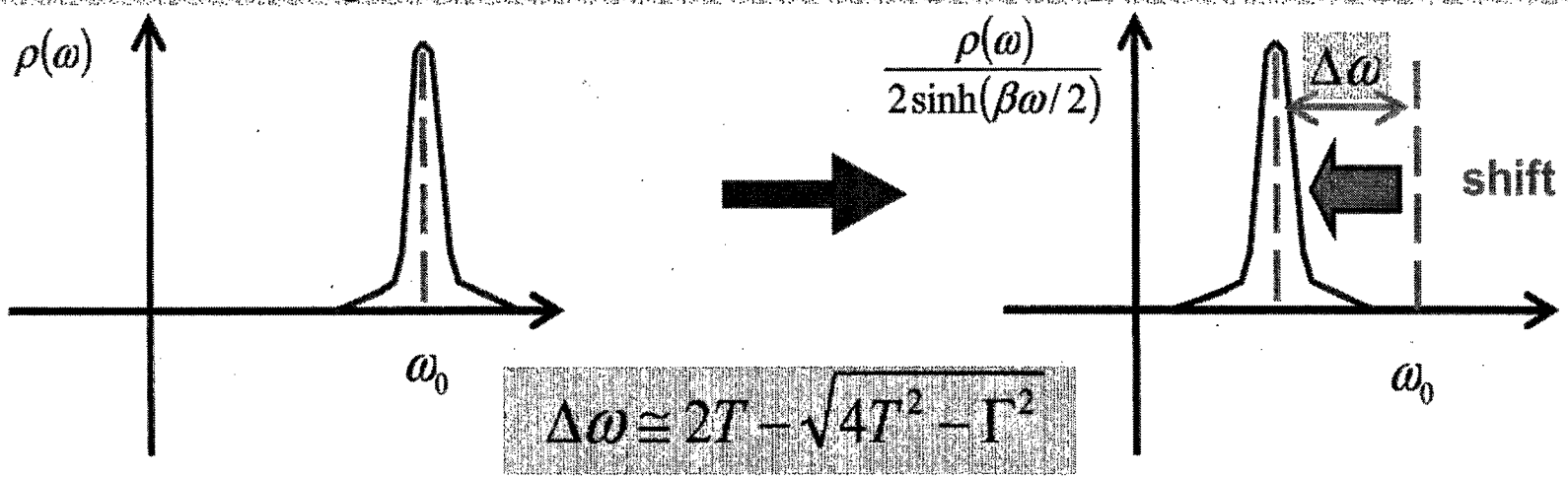

$$\Delta\omega \cong 2T - \sqrt{4T^2 - \Gamma^2}$$

The peak position is shifted to below !

Numerical Results

$a_s^{-1} = 2.341(16)\,\mathrm{GeV},\ a_t^{-1} = 9.365(66)\,\mathrm{GeV}$

The lattice parameter setup:

1. Gauge config. by **anisotropic Wilson action** with $\beta_{\mathrm{lat}} = 2N_C / g^2 = 6.25$
2. **Lattice spacings** are determined from the **string tension** as $\sqrt{\sigma} = 440\,\mathrm{MeV}$

   $a_s = 0.084\,\mathrm{fm},\ a_t = 0.021\,\mathrm{fm}$ $\Longrightarrow$ renormalized lattice anisotropy $a_s / a_t = 4$
3. **The Lattice size:** $20^3 \times N_t (N_t = 24, \cdots, 72)$ $\Longleftrightarrow$ $T = 390, \cdots, 130\,\mathrm{MeV}$
4. For each T, we pick up gauge configs every 100 sweeps after skipping 20,000 sweeps for thermalization.
5. **Number of gauge configs**: 5,500-9,900 (bin size: 100)
6. We adopt **APE smearing** to improve the glueball operator to have a better overlap to the lowest glueball peak.
7. **The critical temperature** is determined from the Polyakov loop susceptibility as

   $T_C \cong 280\,\mathrm{MeV}$

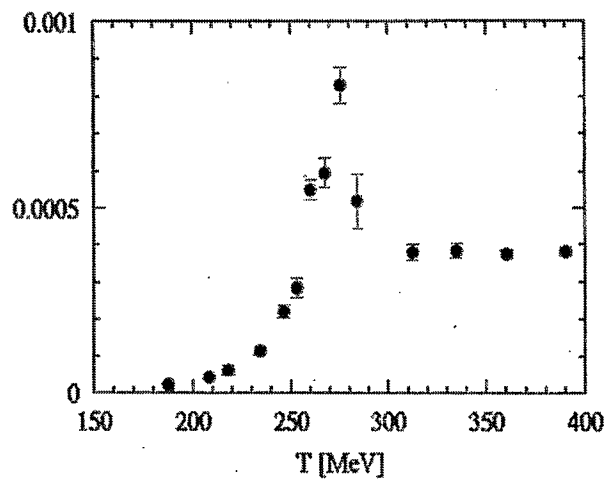

The glueball correlator at low temperature (T=130MeV)

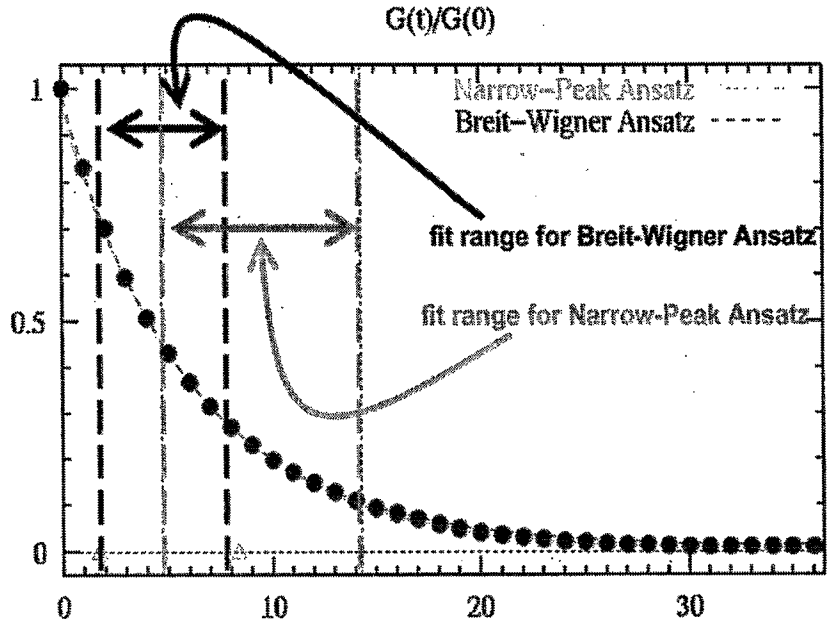

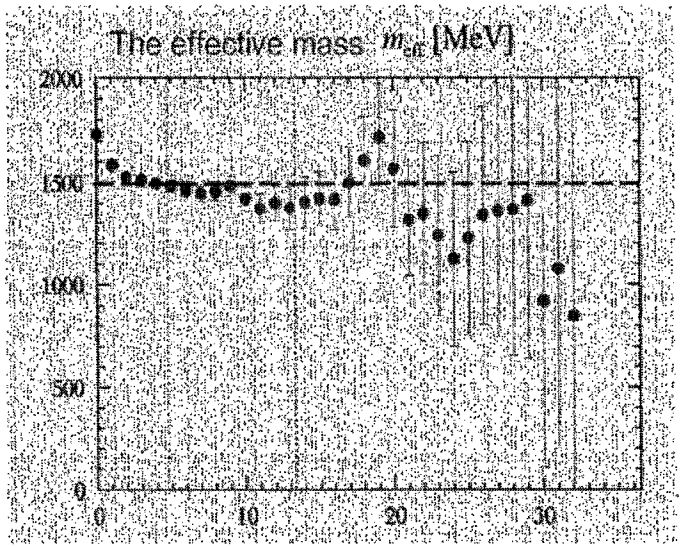

Spatially extended operator is used to enhance the lowest-lying glueball peak.

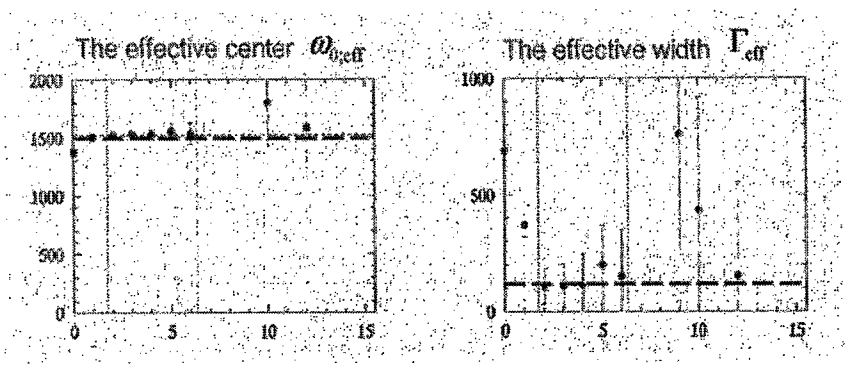

The both ansatz fit the lattice QCD data very well.

It is natural, since the thermal width is still narrow at low temperature.

The **effective mass**, the **effective center** and the **effective width**

The **effective mass**

$$\frac{G(t)}{G(t+1)} = \frac{\cosh[(t-\beta/2)m_{\mathrm{eff}}(t)]}{\cosh[(t+1-\beta/2)m_{\mathrm{eff}}(t)]}$$

The existence of the **plateau** is a necessary condition for the **single pole saturation**.

The **effective center** and the **effective width**

$$\frac{G(t)}{G(t+1)} = \frac{g(t,\omega_{\mathrm{eff}}(t),\Gamma_{\mathrm{eff}}(t))}{g(t+1,\omega_{\mathrm{eff}}(t),\Gamma_{\mathrm{eff}}(t))}$$

$$\frac{G(t+1)}{G(t+2)} = \frac{g(t+1,\omega_{\mathrm{eff}}(t),\Gamma_{\mathrm{eff}}(t))}{g(t+2,\omega_{\mathrm{eff}}(t),\Gamma_{\mathrm{eff}}(t))}$$

The existence of the **simultaneous plateau** is a necessary condition for the **single peak saturation**.

$$g(t,\omega_0,\Gamma) \equiv \int_{-\infty}^{\infty} \frac{d\omega}{2\pi} \frac{\cosh[\omega(\beta/2-t)]}{2\sinh(\beta\omega/2)} \times 2\pi\{\delta_\Gamma(\omega-\omega_0)-\delta_\Gamma(\omega+\omega_0)\}$$

The glueball correlator at high temperature (T=253MeV<Tc) ■

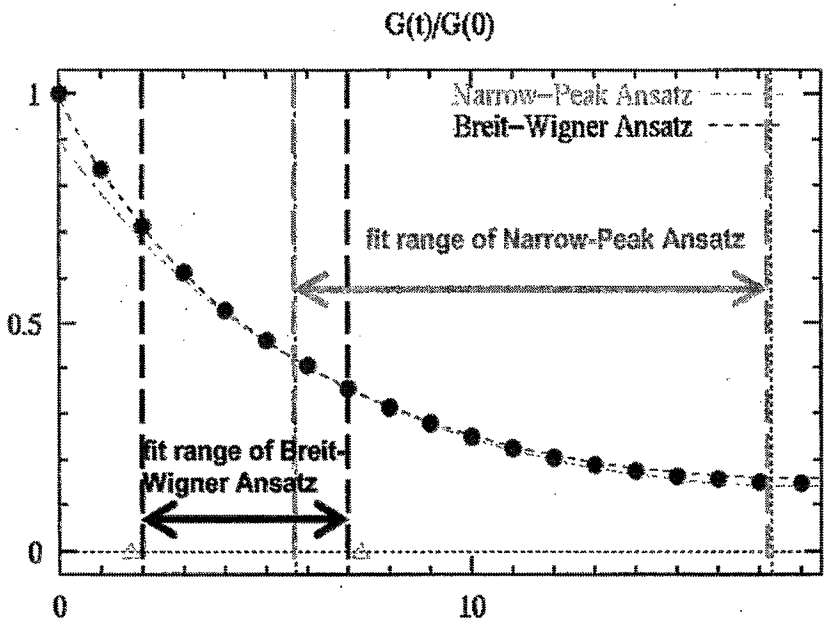

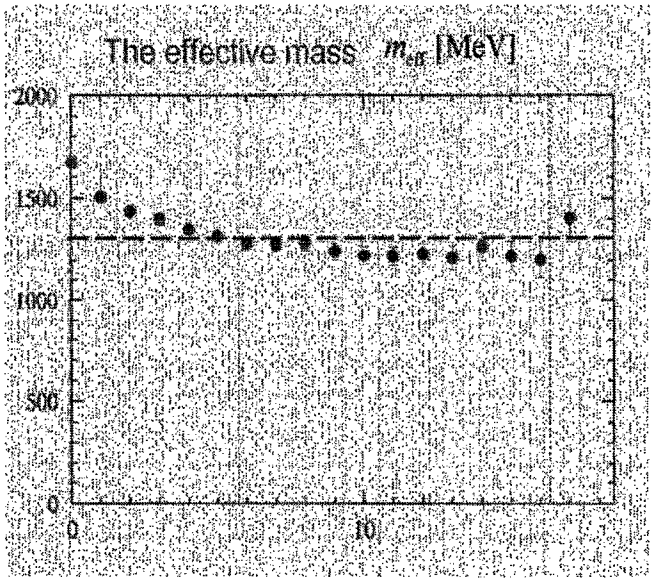

Spatially extended operator is used to enhance the lowest-lying glueball peak.

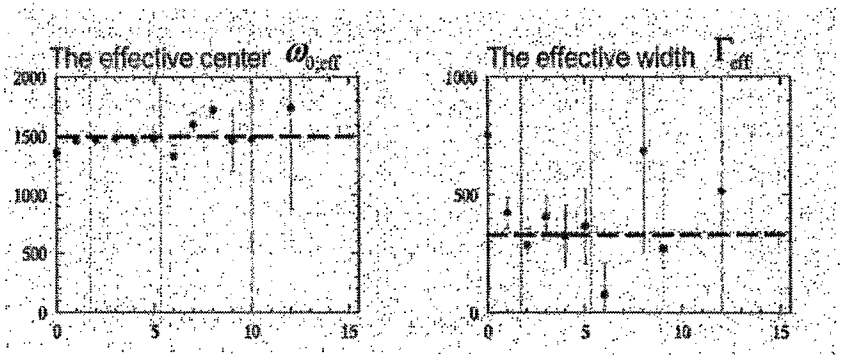

The **narrow-peak ansatz** fails to fit the lattice QCD data around t=0.

The **Breit-Wigner ansatz** fits the lattice QCD data in the whole region rather well.

The smearing dependence (T<Tc)

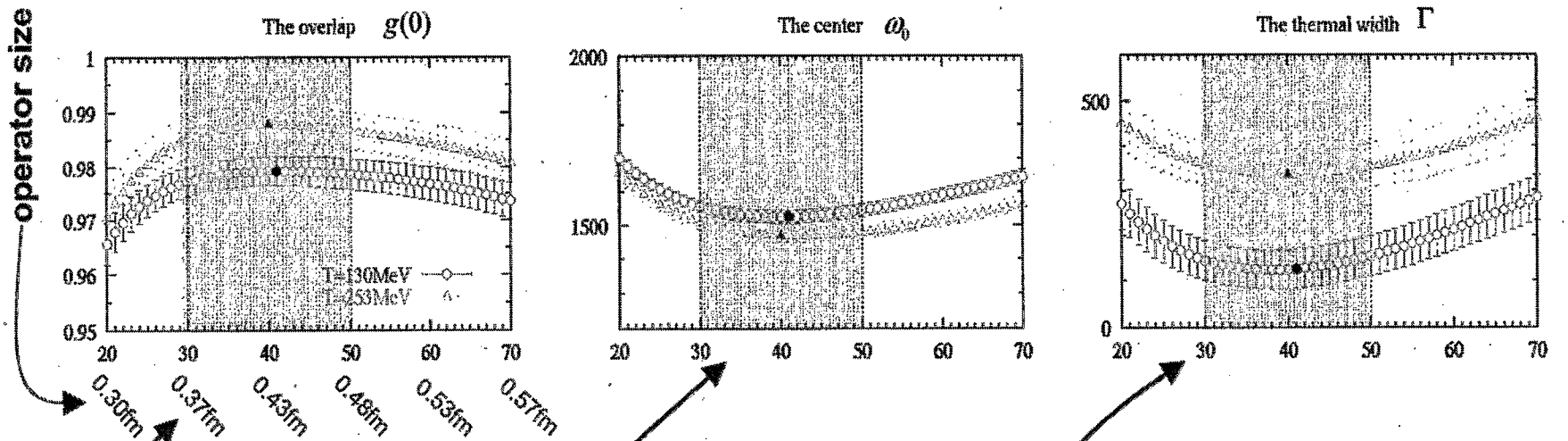

$g(0) \cong 1$

the single-peak saturation of G(t).

ω_0 minimum

contributions from higher spectral components are suppressed.

Γ minimum

contributions from higher spectral components are suppressed.

The lowest peak contribution seems to be <u>maximally enhanced</u> in this region.

From the operator size of the best smearing operator at various T,

we find **<u>no significant thermal effect on the glueball size below Tc</u>**.

$r \approx 0.43$ fm for all T < Tc.

The glueball correlator above Tc (T=390 MeV)

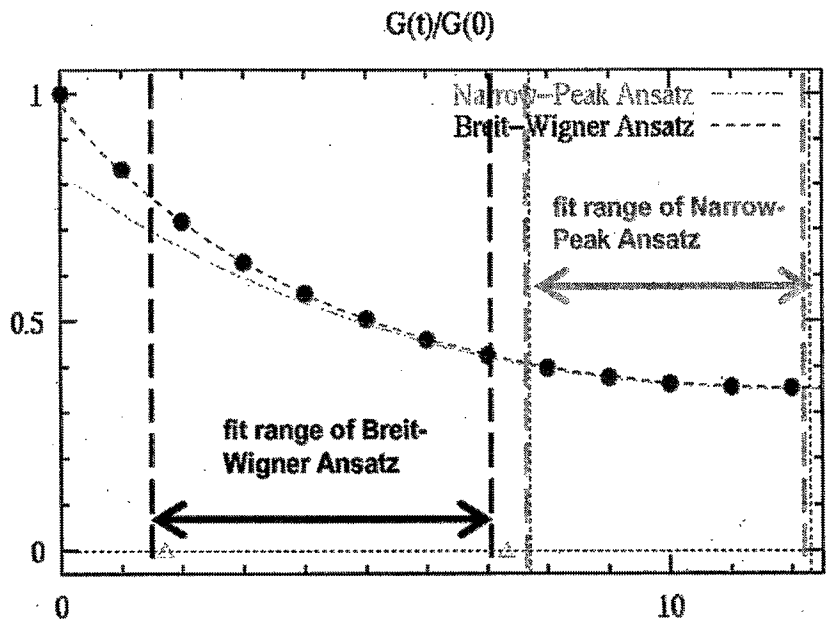

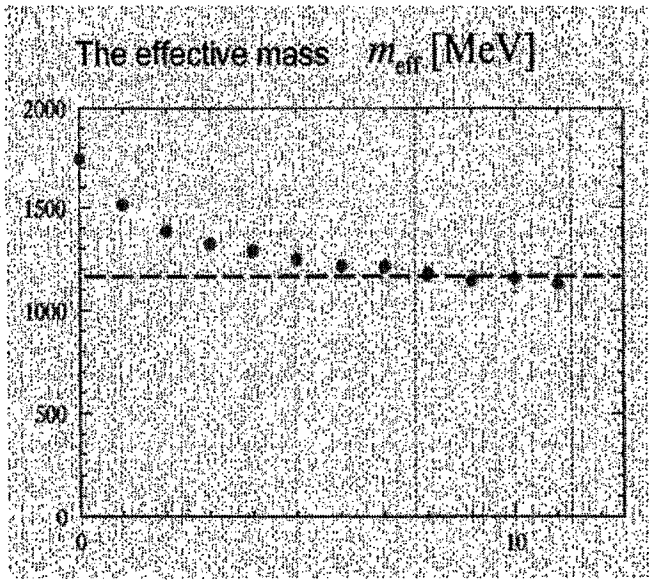

Spatially extended operator is used to enhance the lowest-lying glueball peak.

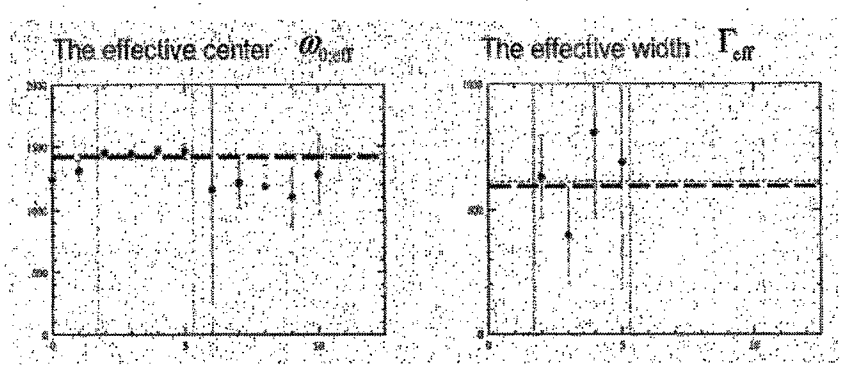

The peak center

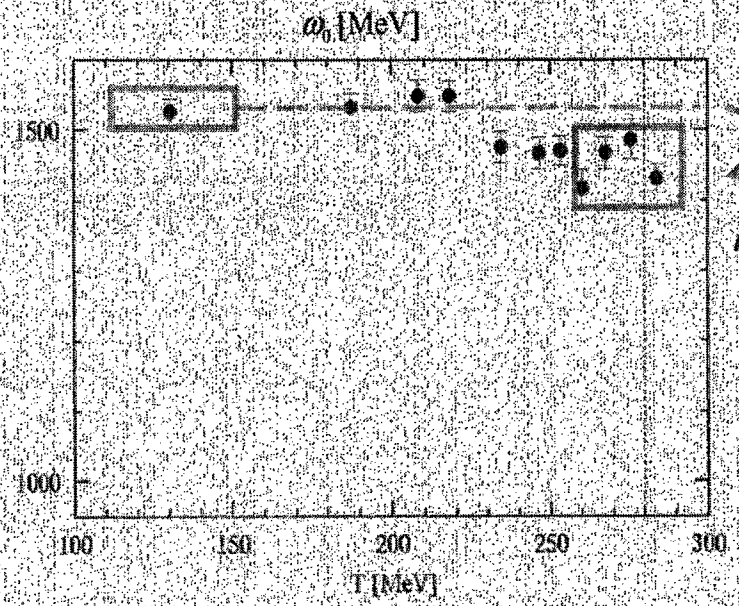

The thermal width

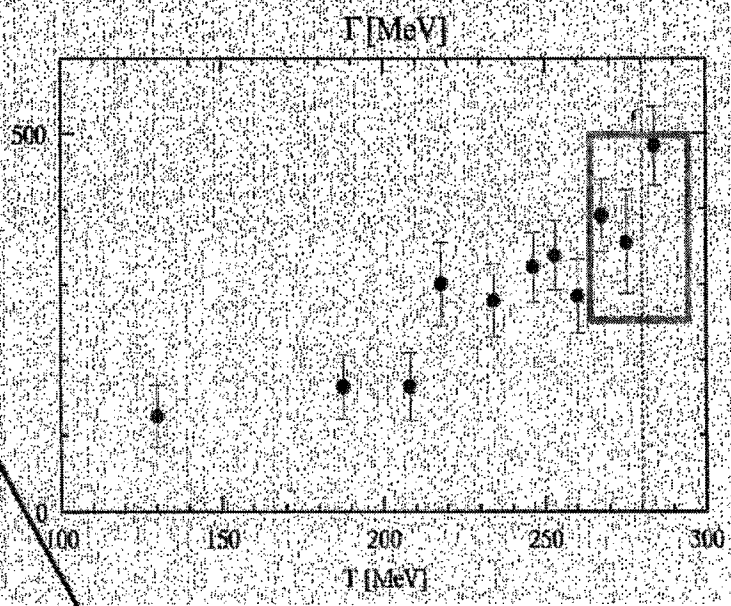

The **polemass** from narrow peak ansatz

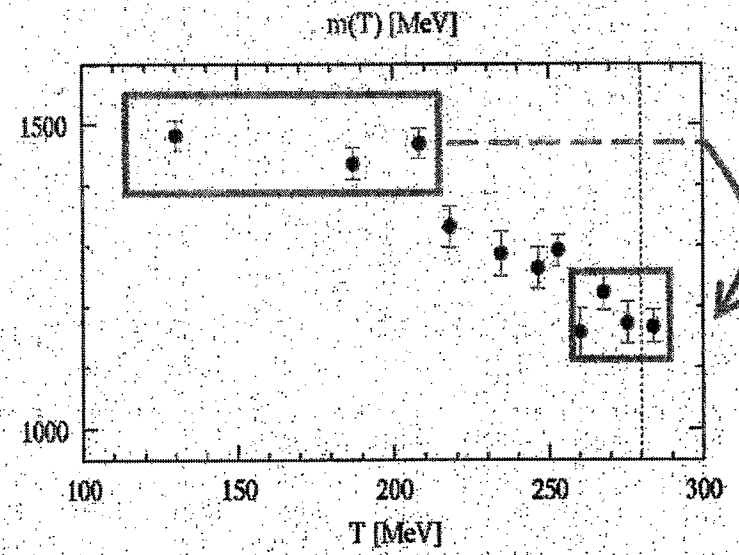

- **The Breit-Wigner ansatz**
  - thermal width broadening near Tc

$$\Gamma(T_c) \cong 300\,\mathrm{MeV}$$

  - modest reduction in peak center

$$\Delta\omega_0 \leq 100\,\mathrm{MeV}$$

- **The narrow peak ansatz**
  - polemass reduction near Tc

$$\Delta m \cong 300\,\mathrm{MeV}$$

The low lying glueball peak(0++)

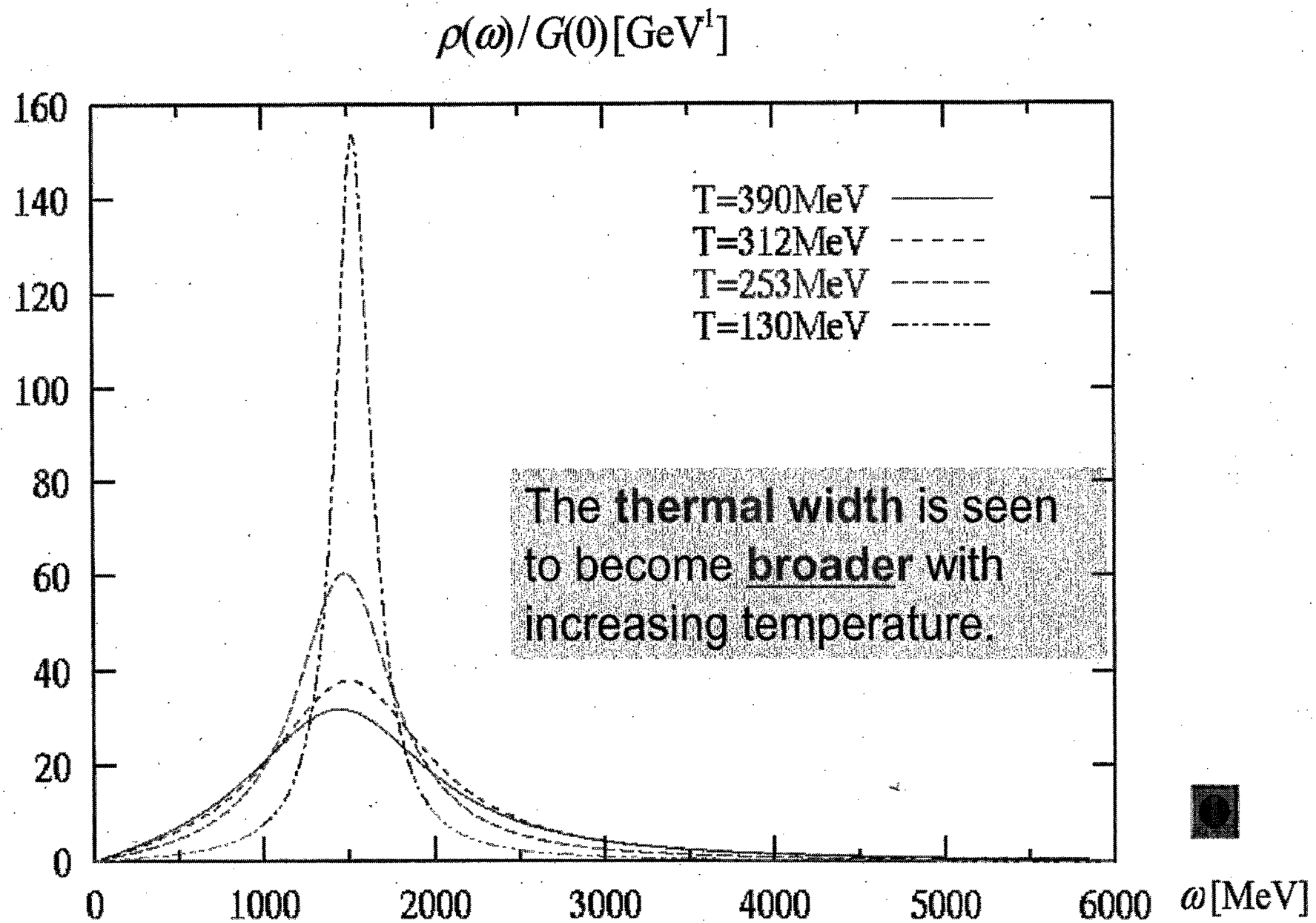

The thermal width is seen to become broader with increasing temperature.

Maximum Entropy Method

A method to directly obtain the spectral function **without adopting a paticular Ansatz.**

"Maximize":

$$Q = \alpha S - \frac{1}{2}\chi^2$$

where

$$\chi^2 \equiv \sum_{i,j} \left(\overline{G}(\tau_i) - G_A(\tau_i)\right) C^{-1}_{i,j} \left(\overline{G}(\tau_j) - G_A(\tau_j)\right)$$

$$G_A(\tau) \equiv \int_0^\infty d\omega\, K(\tau,\omega) A(\omega)$$

$$K(\tau,\omega) \equiv \frac{\cosh\left[\omega(\beta/2-\tau)\right]}{\cosh\left[\beta\omega/2\right]}$$

Shannon-Jaynes entropy:

$$S \equiv \int_0^\infty d\omega \left[A(\omega) - m(\omega) - A(\omega)\log\left(\frac{A(\omega)}{m(\omega)}\right)\right]$$

$$m(\omega) \propto \omega^4 \exp\left(-(\omega\rho)^2/4\right)$$

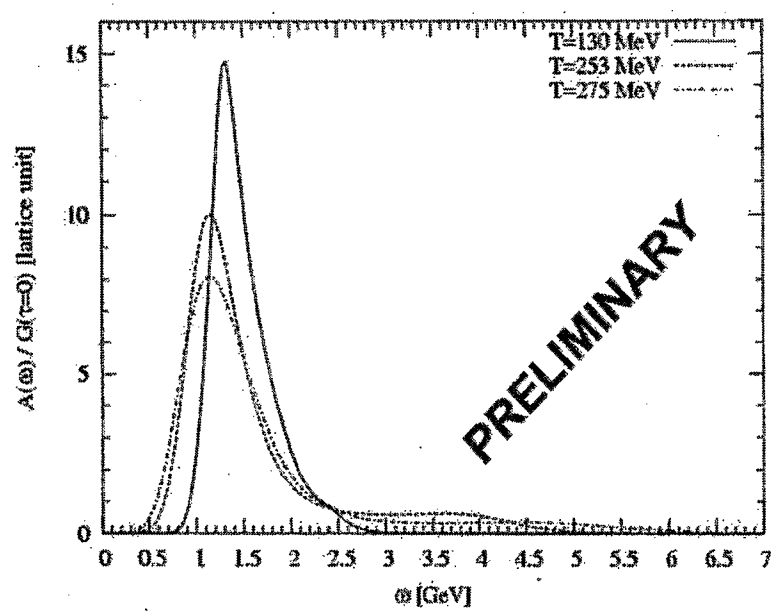

Summary / Discussion

1. We have constructed the **temporal 0^{++} glueball correlators** at finite temperature using 5,500-9,900 gauge configurations generated by SU(3) anisotropic lattice QCD at quenched level.

2. We have performed an advanced analysis adopting **Breit-Wigner ansatz** for the spectral function in order to take into account the possible appearance of the thermal width at finite temperature.

   a. **A significant thermal width broadening near Tc:** $\Gamma(T_c) \cong 300\,\mathrm{MeV}$

   b. **A modest reduction in peak center near Tc:** $\Delta\omega_0(T_c) \cong 100\,\mathrm{MeV}$

   [c. No significant thermal effects in the glueball size.]

3. What is the origin of such a huge thermal width ?

   $\rho \cong 1/(4.0\,\mathrm{fm})^3$

   a. It is not thermally excited lowest-lying glueballs. (Too small glueball density even at Tc)

   b. The contributions of bound state glueballs listed in C.J.Morningstar et al., PRD60,034509('99) is estimated to be not significant. (They are too heavy.)

   c. We have to resort to **higher energy resonace modes** trusting in the sufficient increase in the number of modes. ⟹ Hagedorn's picture, Resonance gas model, ... ?

4. Future Plans:
   Glueball correlations above Tc, Experimental observability, Extension to the unquenched QCD calculations, etc.

Contributions from higher resonances

$$Z = \sum_n e^{-E_n/T}$$

$$= \int_0^\infty dE\, e^{-E/T}\, D(E)$$

$D(E) \equiv \sum_n \delta(E - E_n)$ is the density of states.

If D(E) increases rapid enough so that it can compensate the statistical suppression factor $e^{-E/T}$, **higher energy states** have a chance to **contribute to the thermodynamic quantity.**

For example,

$$D(E) \approx e^{bE} \quad \Longrightarrow \quad T_C = 1/b$$

Glueball spectrum in quenched SU(3) lattice QCD

Most systematic result of glueball spectra from the quenched lattice QCD

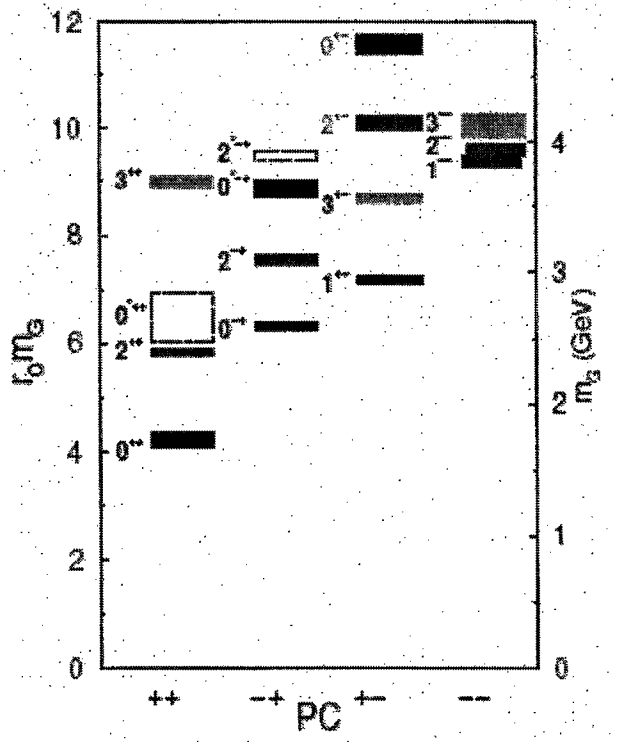

FIG. 8. The mass spectrum of glueballs in the pure SU(3) gauge theory. The masses are given in terms of the hadronic scale r_0 along the left vertical axis and in terms of GeV along the right vertical axis (assuming $r_0^{-1} = 410$ MeV). The mass uncertainties indicated by the vertical extents of the boxes do *not* include the uncertainty in setting r_0. The locations of states whose interpretation requires further study are indicated by the dashed hollow boxes.

from C.J.Morningstar et al., Phys.Rev.D60 (1999) 034509.

Thermal Effects on Quark-Gluon Mixed Condensate $g\langle\bar{q}\sigma_{\mu\nu}G_{\mu\nu}q\rangle$ From Lattice QCD

Takumi Doi

Thermal effects on quark-gluon mixed condensate $g\langle\bar{q}\sigma_{\mu\nu}G_{\mu\nu}q\rangle$ from lattice QCD

Takumi Doi, Noriyoshi Ishii, Makoto Oka and Hideo Suganuma

Department of Physics, Tokyo Institute of Technology, Ohokayama 2-12-1, Meguro, Tokyo 152-8551, Japan

The thermal effects on the quark-gluon mixed condensate $g\langle\bar{q}\sigma_{\mu\nu}G_{\mu\nu}q\rangle$ are investigated in $\mathrm{SU}(3)_c$ lattice QCD at the quenched level. We discuss the importance of $g\langle\bar{q}\sigma_{\mu\nu}G_{\mu\nu}q\rangle$, as it behaves as another chiral order parameter and has the large contribution to the operator product expansion in QCD. We calculate $g\langle\bar{q}\sigma_{\mu\nu}G_{\mu\nu}q\rangle$ as well as $\langle\bar{q}q\rangle$ in the chiral limit for $0 \lesssim T \lesssim 500$MeV, using the lattices at $\beta = 6.0, 6.1, 6.2$ in high statistics. Except for the sharp decrease of both the condensates around $T_c \simeq 280$MeV, the thermal effects are found to be weak below T_c. We also find that the ratio $m_0^2 \equiv g\langle\bar{q}\sigma_{\mu\nu}G_{\mu\nu}q\rangle/\langle\bar{q}q\rangle$ is almost independent of the temperature even in the very vicinity of T_c, which indicates nontrivial similarity in the critical behaviors of the two different condensates.

1 Contents

- Motivation

  The condensates and hadron physics

  Condensates represent
  non-perturbative nature of QCD

- Quark gluon mixed condensate $g\langle\bar{q}\sigma_{\mu\nu}G_{\mu\nu}q\rangle$

  Physical importance of
  the mixed condensate $g\langle\bar{q}\sigma_{\mu\nu}G_{\mu\nu}q\rangle$

  ▷ **chiral order parameter**
  ▷ strong relation to hadron phenomenology

- The Lattice formalism

  $\mathrm{SU}(3)_c$ lattice at the quenched level
  KS fermion

- Lattice results at finite temperature

  ○ **chiral restoration of the QCD vacuum**

- Summary and Outlook

2 Motivation

QCD $\Longleftrightarrow$ hadron physics

How to understand ?

The condensate is key concept.

The condensates embody the non-perturbative properties of QCD.

e.g.

$$\begin{array}{ccl} \langle \bar{q}q \rangle & \longleftrightarrow & \text{spontaneous chiral-symmetry breaking} \\ \langle G_{\mu\nu}G^{\mu\nu} \rangle & \longleftrightarrow & \text{trace anomaly} \\ \Downarrow & \Downarrow & \Downarrow \quad \Downarrow \quad \Downarrow \end{array}$$

These vacuum structures of QCD are reflected on the hadronic properties.

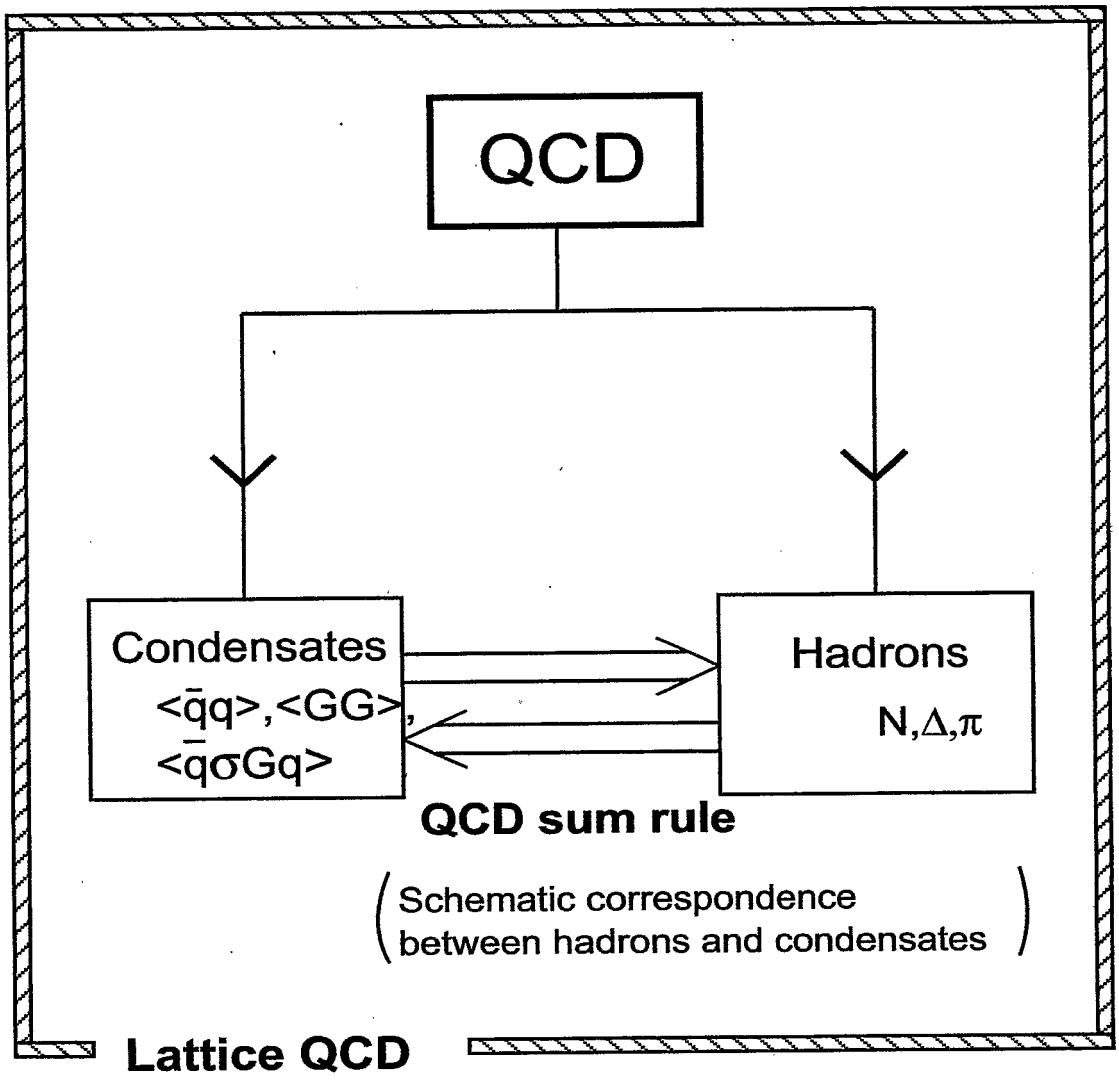

Physical parameters
are under control
(Temperature, quark mass, ...)

3 Quark-gluon mixed condensate

— $g\langle\bar{q}\sigma_{\mu\nu}G_{\mu\nu}q\rangle$ —

- Chirality flipping operator

$$g\langle\bar{q}\sigma_{\mu\nu}G_{\mu\nu}q\rangle$$
$$= g\langle\bar{q}_L\,(\sigma_{\mu\nu}G_{\mu\nu})\,q_R\rangle + g\langle\bar{q}_R\,(\sigma_{\mu\nu}G_{\mu\nu})\,q_L\rangle$$

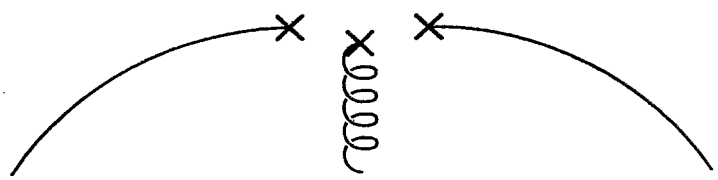

$\Downarrow \quad \Downarrow \quad \Downarrow \quad \Downarrow \quad \Downarrow$

Another **order parameter** of
spontaneous chiral symmetry breaking

- Direct correlation between quarks and gluons

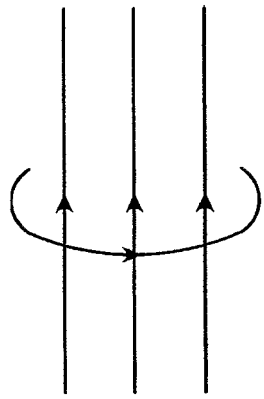

c.f. $\langle G_{\mu\nu}G^{\mu\nu}\rangle$: gluonic sector
$\langle \bar{q}q\rangle$: quark sector

$g\langle \bar{q}\sigma_{\mu\nu}G_{\mu\nu}q\rangle$ represents the <u>color-octet components</u> of quark-antiquark pairs in the vacuum.

$$g\langle \bar{q}\sigma_{\mu\nu}G_{\mu\nu}q\rangle \Longleftarrow \underset{\text{color } \mathbf{8}}{(q\bar{q})} \otimes \underset{\text{color } \mathbf{8}}{(gG_{\mu\nu}\sigma_{\mu\nu})}$$

$$\langle \bar{q}q\rangle \Longleftarrow \underset{\text{color } \mathbf{1}}{(q\bar{q})}$$

$g\langle \bar{q}\sigma_{\mu\nu}G_{\mu\nu}q\rangle$ and $\langle \bar{q}q\rangle$ characterizes different aspect of the QCD vacuum.

- Large contribution to hadron spectrum

QCD sum rules for baryon masses

B.L. Ioffe,
Nucl.Phys.B**188** (1981) 317

W-Y.P. Hwang and K.-C. Yang,
Phys. Rev. **D49** (1994) 460

$$\lambda_N^2 m_N e^{-m_N^2/M^2}$$
$$= \frac{1}{(2\pi)^2} M^4(-\langle\bar{q}q\rangle) \quad + \quad 0 \qquad\qquad + \cdots$$

$$\lambda_\Delta^2 m_\Delta e^{-m_\Delta^2/M^2}$$
$$= \frac{4}{3(2\pi)^2} M^4(-\langle\bar{q}q\rangle) - \frac{2}{3(2\pi)^2} M^2(-g\langle\bar{q}\sigma_{\mu\nu}G_{\mu\nu}q\rangle) + \cdots$$

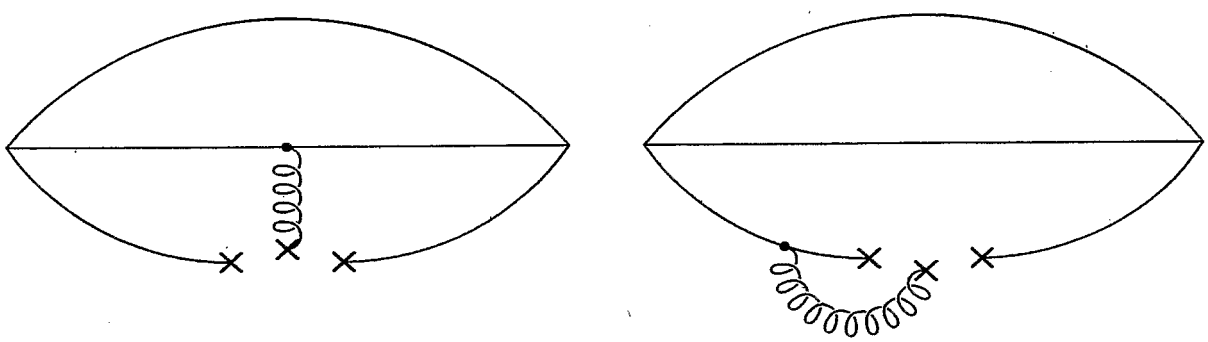

QCD sum rule for penta-quark system Θ^+

J. Sugiyama, T. Doi and M. Oka,
Phys. Lett. **B581** (2004) 167

$$\eta(x) = \epsilon^{abc}\epsilon^{def}\epsilon^{cfg}\{u_a^T C d_b\}\{u_d^T C\gamma_5 d_e\}C\bar{s}_g^T$$

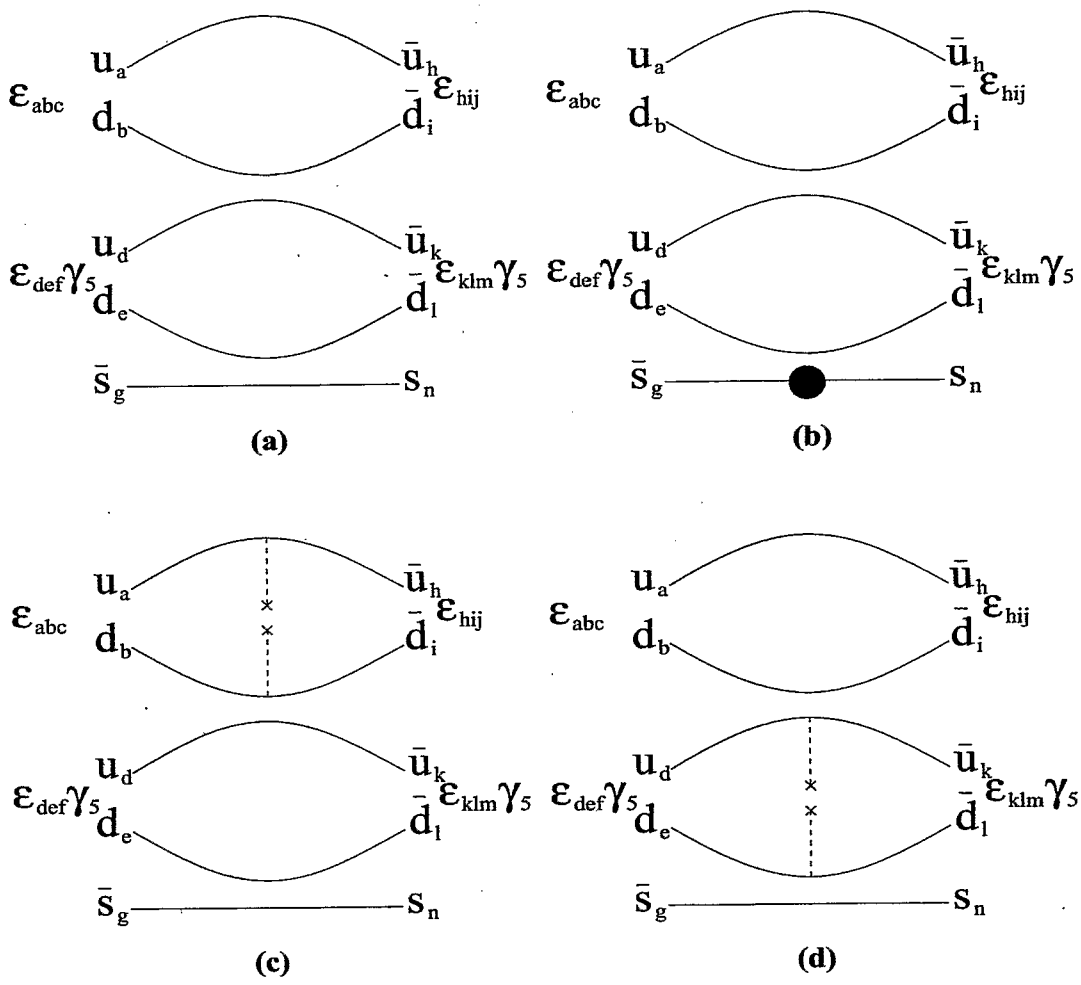

$m_0^2(s) \equiv g\langle\bar{s}\sigma\cdot Gs\rangle/\langle\bar{s}s\rangle$
is a key parameter to determine the parity of Θ^+.

Quark-gluon mixed condensate
— $g\langle\bar{q}\sigma_{\mu\nu}G_{\mu\nu}q\rangle$ —

- <u>The order parameter of chiral symmetry breaking</u>
- Direct correlation between quarks and gluons
- Large contribution to hadron spectrum

$\Downarrow \quad \Downarrow \quad \Downarrow \quad \Downarrow \quad \Downarrow$

Thermal effects on $g\langle\bar{q}\sigma_{\mu\nu}G_{\mu\nu}q\rangle$
is interesting to investigate !!

Physics at RHIC (Finite temperature QCD)

In spite of the importance of this quark-gluon mixed condensate $g\langle\bar{q}\sigma_{\mu\nu}G_{\mu\nu}q\rangle$, there is only preliminary (but pioneering) lattice result.

M.Kremer and G.Schierholz, Phys.Lett.B**194** (1987) 283.

· KS-fermion, 8^4, $\beta = 5.7(a \simeq 0.18[\text{fm}])$,
· only 1 point $\times$ 5 configs
· [**only at zero temperature**]

4 Our Lattice formalism

Keeping chiral symmetry is important because $g\langle\bar{q}\sigma_{\mu\nu}G_{\mu\nu}q\rangle$ is a chiral order parameter.

$\Downarrow \quad \Downarrow$

We use **KS-fermion**.

KS fermion

Doublings are assigned as SU(N_f=4) flavors

Explicit chiral symmetry is preserved.

- **KS fermion**

$$S_F = \frac{1}{2}\sum_{s,\mu}\eta_\mu(s)\bar{\chi}(s)\left[U_\mu(s)\chi(s+\mu) - U_\mu^\dagger(s-\mu)\chi(s-\mu)\right]$$
$$+ma\sum_s \bar{\chi}(s)\chi(s)$$

$\chi, \bar{\chi}$: single-component Grassmann fields

SU($N_f = 4$) spinor field q is composed of χ as

$$q_i^f(x) = \frac{1}{8}\sum_\rho (\gamma_1^{\rho_1}\gamma_2^{\rho_2}\gamma_3^{\rho_3}\gamma_4^{\rho_4})_{if}\ \chi(x+\rho)$$
$$\rho = (\rho_1, \rho_2, \rho_3, \rho_4), \quad \rho_\mu \in \{0, 1\}$$

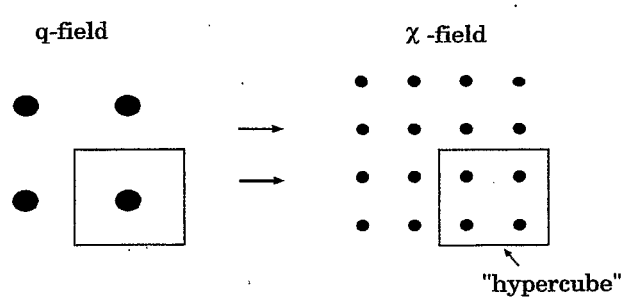

Spinor DoF (4) $\times$ Flavor DoF SU($N_f = 4$)
are assigned to the $2^4 = 16$ sites on the hypercube.

S_F is invariant under

$$q \longrightarrow e^{i\alpha(\gamma_5\otimes\gamma_5^f)}\ q$$
$$\bar{q} \longrightarrow \bar{q}\ e^{i\alpha(\gamma_5\otimes\gamma_5^f)}$$

Explicit chiral symmetry is preserved.

$$\langle \bar{q}q \rangle \equiv -\left\langle \mathrm{Tr}[\, S_F(x,x)\,] \right\rangle_{\text{average}}$$

$$g\langle \bar{q}\sigma_{\mu\nu}G_{\mu\nu}q \rangle \equiv -\left\langle \mathop{\mathrm{Tr}}_{\text{color}}[\, gG_{\mu\nu} \mathop{\mathrm{Tr}}_{\text{spinor}}[\sigma_{\mu\nu}\, S_F(x,x)\,]\,] \right\rangle_{\text{average}}$$

<u>In terms of the KS fermion,</u>

$$a^3\langle \bar{q}q \rangle = -\frac{1}{2^8}\sum_{\rho} \mathrm{Tr}\,[\langle \chi(x+\rho)\bar{\chi}(x+\rho)\rangle]$$

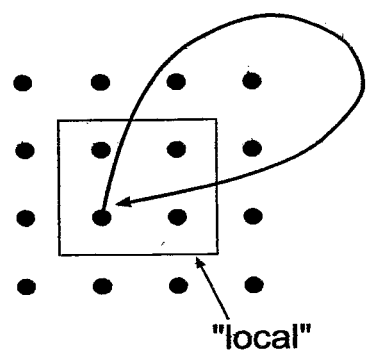

Tr [$q\bar{q}$]

$$g\langle\bar{q}\sigma_{\mu\nu}G_{\mu\nu}q\rangle \equiv -\left\langle \operatorname*{Tr}_{\text{color}}\left[\, gG_{\mu\nu} \operatorname*{Tr}_{\text{spinor}}[\sigma_{\mu\nu}\, S_F(x,x)\,]\,\right]\right\rangle_{\text{average}}$$

<u>In terms of the KS fermion,</u>

$$a^5 g\langle\bar{q}\sigma_{\mu\nu}G_{\mu\nu}q\rangle$$
$$= -\frac{1}{2^8}\sum_{\mu,\nu,\rho}\mathrm{Tr}\,\Big[\,\mathcal{U}'_{\mu,\nu}(x+\rho)\,\langle\chi(x+\rho+\mu+\nu)\bar{\chi}(x+\rho)\rangle$$
$$\sigma_{\mu\nu}\, G^{\text{lat}}_{\mu\nu}(x+\rho)\,\Big]$$

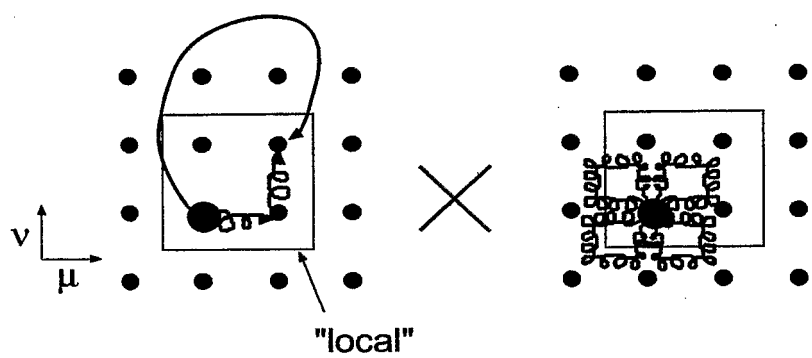

Tr [$\sigma_{\mu\nu}q\bar{q}$ $\times$ $G_{\mu\nu}$ **]**

We generate gauge configurations with the standard Wilson action under the quenched approximation. We take **16 point sources** ($\beta = 6.0$) or **2 point sources** ($\beta = 6.1, 6.2$) to calculate the condensates.

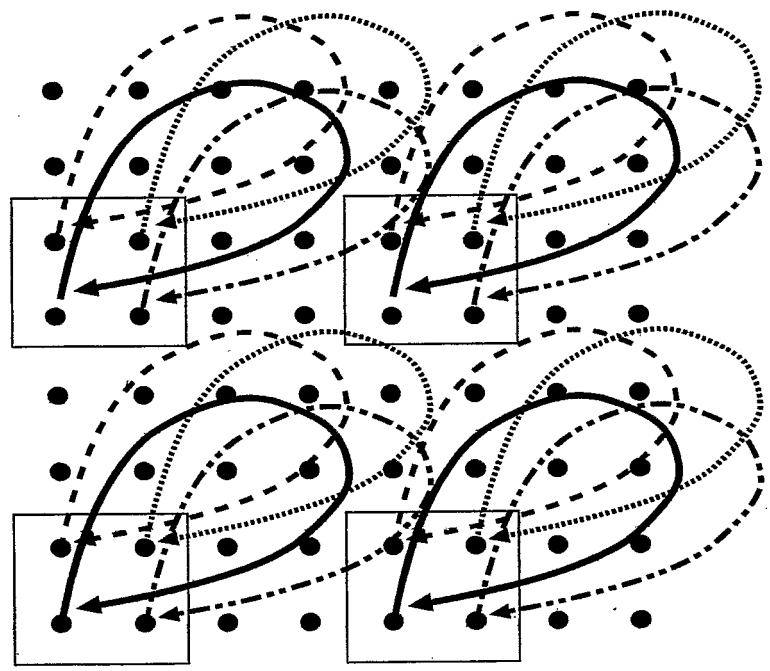

Finite temperature lattice QCD

(a) $\mathbf{16^3 \times 16, 12, 10, 8, 6, 4}$ at $\boldsymbol{\beta = 6.0}$
$(\boldsymbol{a \simeq 0.1}[\mathbf{fm}])$

16 points $\times$ 100 configs $\Rightarrow$ **1600 data**

(b) $\mathbf{20^3 \times 20, 12, 10, (8), 6}$ at $\boldsymbol{\beta = 6.1}$
$(\boldsymbol{a \simeq 0.09}[\mathbf{fm}])$

2 points $\times$ 100 configs $\Rightarrow$ **200 data**

(c) $\mathbf{24^3 \times 24, 16, 12, (10), 8}$ at $\boldsymbol{\beta = 6.2}$
$(\boldsymbol{a \simeq 0.07}[\mathbf{fm}])$

2 points $\times$ 100 configs $\Rightarrow$ **200 data**

(b')(c') **For** $\boldsymbol{T \sim T_c}$, $\mathbf{20^3 \times 8}$ $(\boldsymbol{\beta = 6.1})$
and $\mathbf{24^3 \times 10}$ $(\boldsymbol{\beta = 6.2})$,

2 points $\times$ 1000 configs $\Rightarrow$ **2000 data**

large & fine lattices, and large statistics !

First study of $g\langle\bar{q}\sigma_{\mu\nu}G_{\mu\nu}q\rangle$ at finite temperature

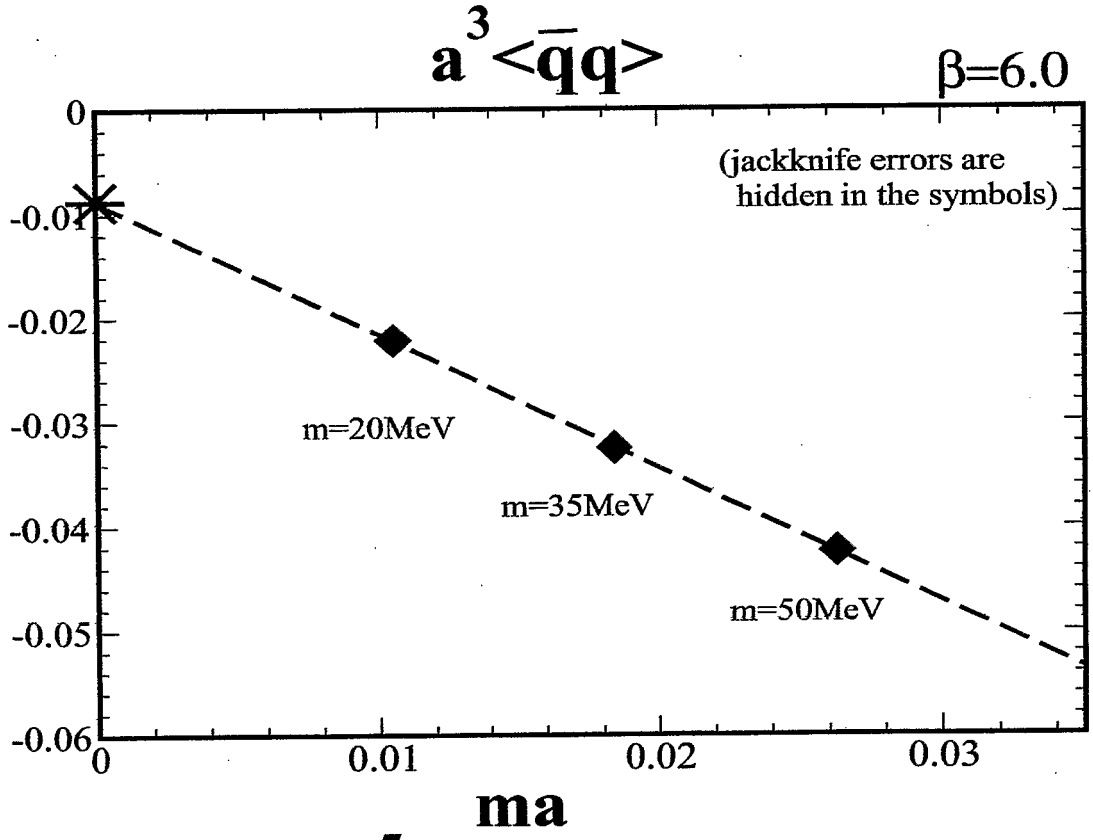
a^3<q̄q>
β=6.0
(jackknife errors are hidden in the symbols)
m=20MeV
m=35MeV
m=50MeV
0
-0.01
-0.02
-0.03
-0.04
-0.05
-0.06
0
0.01
0.02
0.03
ma

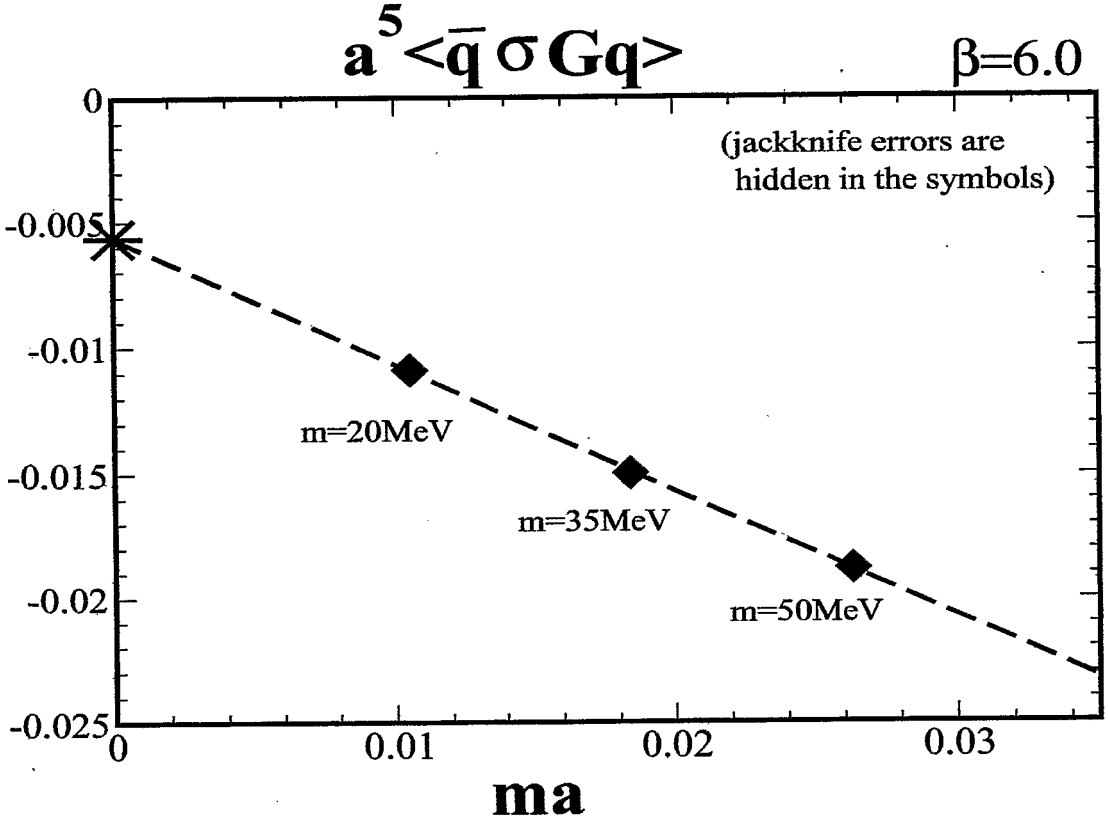
a^5<q̄σGq>
β=6.0
(jackknife errors are hidden in the symbols)
m=20MeV
m=35MeV
m=50MeV
0
-0.005
-0.01
-0.015
-0.02
-0.025
0
0.01
0.02
0.03
ma

Results for finite temperature

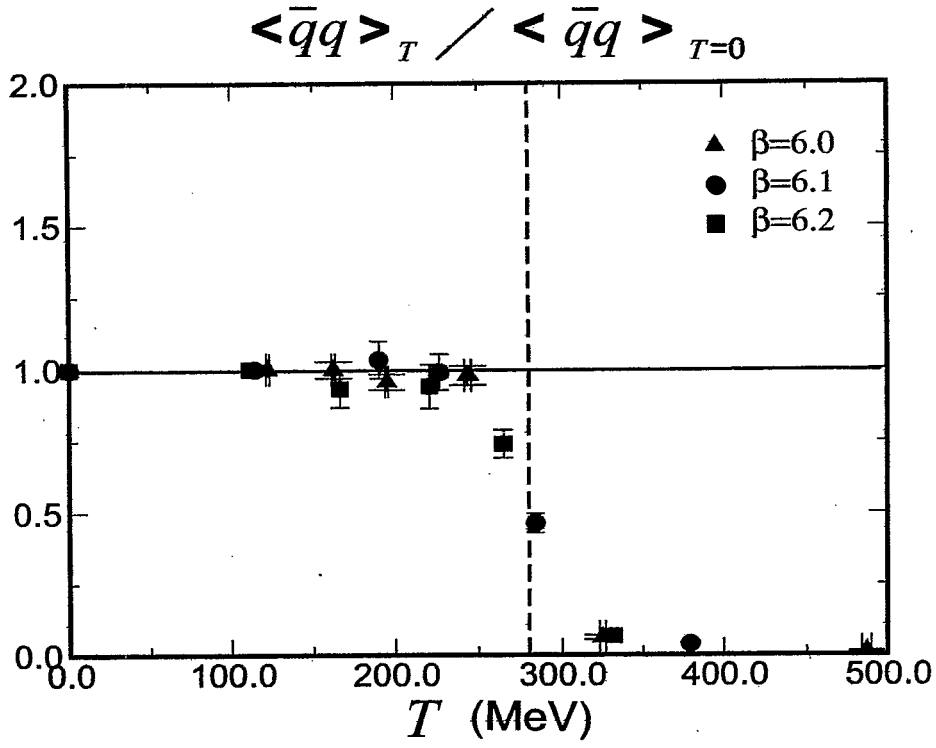

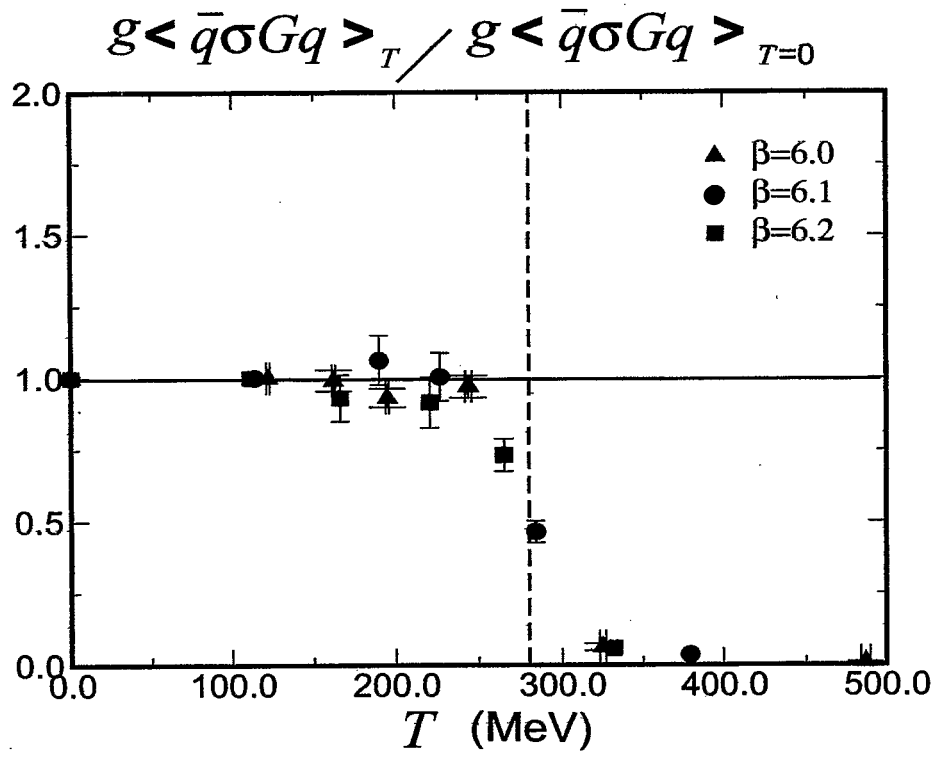

$$m_0^2 \equiv g\langle\bar{q}\sigma_{\mu\nu}G_{\mu\nu}q\rangle/\langle\bar{q}q\rangle$$

$$\frac{m_0^2(T)}{m_0^2(T=0)} = \frac{g\langle\bar{q}\sigma_{\mu\nu}G_{\mu\nu}q\rangle_T/g\langle\bar{q}\sigma_{\mu\nu}G_{\mu\nu}q\rangle_{T=0}}{\langle\bar{q}q\rangle_T/\langle\bar{q}q\rangle_{T=0}}$$

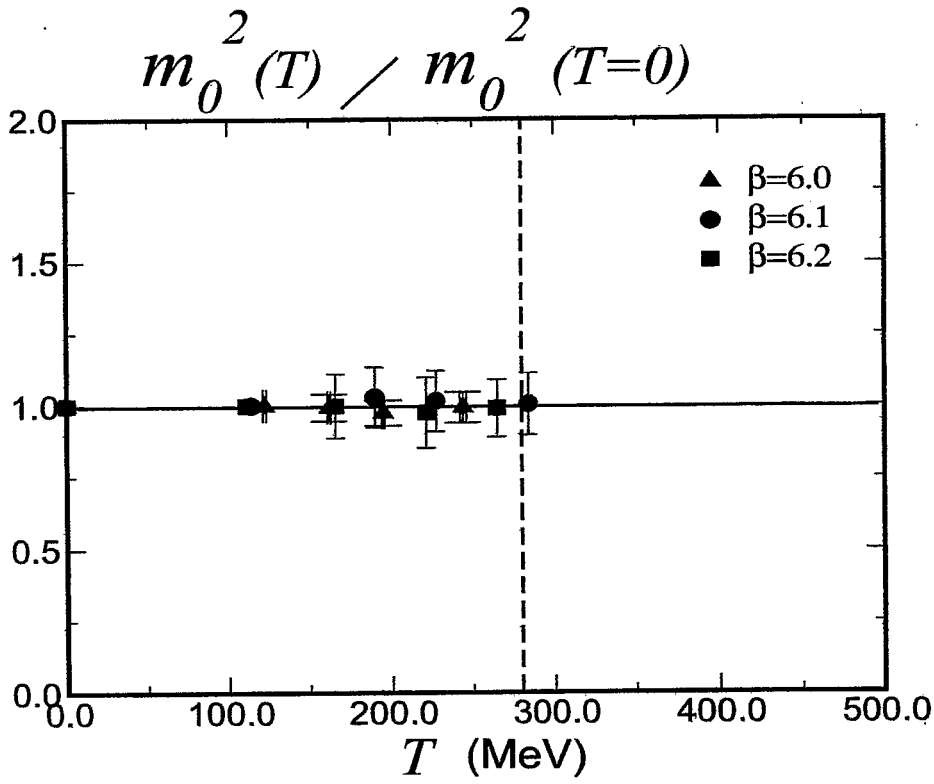

$m_0^2 \equiv g\langle\bar{q}\sigma_{\mu\nu}G_{\mu\nu}q\rangle/\langle\bar{q}q\rangle$

is almost independent of the temperature.

(Very nontrivial results !)

Universality in the critical behavior of the chiral order parameters ?

Electric/Magnetic components of $g\langle\bar{q}\sigma_{\mu\nu}G_{\mu\nu}q\rangle$

$$R_{E/B}(T) \equiv \frac{\sum_i g\langle\bar{q}\sigma_{4i}G_{4i}q\rangle_T}{\sum_{j<k} g\langle\bar{q}\sigma_{jk}G_{jk}q\rangle_T}$$

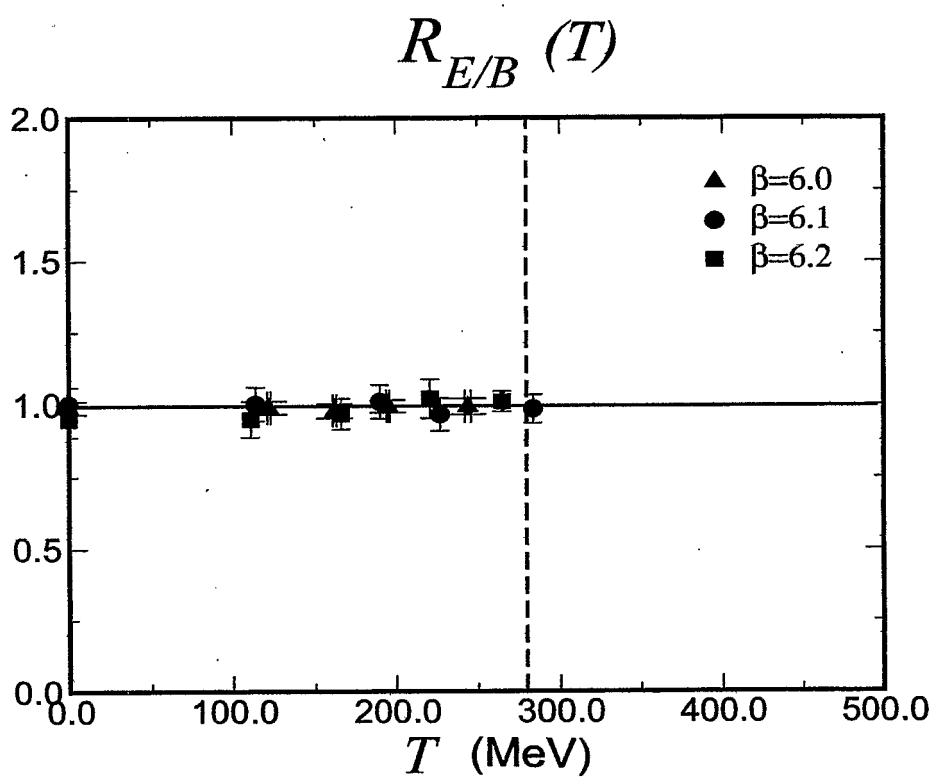

Common critical behavior !

Relation to the chiral zero modes:

$$\langle \bar{q}q \rangle \qquad \Longleftrightarrow \frac{1}{V}\int d\lambda' \frac{m\rho(\lambda')}{\lambda'^2 + m^2}$$

$$g\langle \bar{q}\sigma_{\mu\nu}G_{\mu\nu}q \rangle \Longleftrightarrow \frac{1}{V}\int d\lambda' \frac{m\rho(\lambda')}{\lambda'^2 + m^2}\langle \lambda' | \sigma_{\mu\nu}G_{\mu\nu} | \lambda' \rangle$$

$$i\not{D}|\lambda\rangle = \lambda|\lambda\rangle$$

$\rho(\lambda)$: the spectral density

$g\langle \bar{q}\sigma_{\mu\nu}G_{\mu\nu}q \rangle$:

Critical behavior is mainly governed by $\rho(\lambda)$

The correlation between gluon field and zero modes $\langle \lambda | \sigma_{\mu\nu}G_{\mu\nu} | \lambda \rangle \Big|_{\lambda=0}$ is insensitive to the temperature.

5 Summary and Outlook

- We have investigated the thermal effects on the quark-gluon mixed condensate $g\langle\bar{q}\sigma_{\mu\nu}G_{\mu\nu}q\rangle$ using KS-fermion in SU(3) lattice.

$0 \lesssim T \lesssim 500\text{MeV}$

$$\left(\begin{array}{l} 16^3 \times 16, 12, 10, 8, 6, 4 \text{ lattice, } \beta = 6.0, \\ \quad 16 \text{ points * } 100 \text{ configs} = 1600 \text{ data} \\ 20^3 \times 20, 12, 10, (8), 6 \text{ lattice, } \beta = 6.1, \\ \quad 2 \text{ points * } 100 \text{ configs} = 200 \text{ data} \\ 24^3 \times 24, 16, 12, (10), 8 \text{ lattice, } \beta = 6.2, \\ \quad 2 \text{ points * } 100 \text{ configs} = 200 \text{ data} \\ 20^3 \times 8 \ (\beta = 6.1) \text{ and } 24^3 \times 10 \ (\beta = 6.2) \text{ lattice,} \\ \quad 2 \text{ points * } 1000 \text{ configs} = 2000 \text{ data} \end{array}\right)$$

▷ Chiral restoration has been studied in terms of $g\langle\bar{q}\sigma_{\mu\nu}G_{\mu\nu}q\rangle$ as well as $\langle\bar{q}q\rangle$.

▷ The thermal effects of $g\langle\bar{q}\sigma_{\mu\nu}G_{\mu\nu}q\rangle$ and $\langle\bar{q}q\rangle$ have been found to be remarkably weak for $T \lesssim 0.9\,T_c$.

▷ We have obtained $m_0^2 = g\langle\bar{q}\sigma_{\mu\nu}G_{\mu\nu}q\rangle/\langle\bar{q}q\rangle$ is almost independent of temperature.

▷ We have found $g\langle\bar{q}\sigma_{4i}G_{4i}q\rangle$ and $g\langle\bar{q}\sigma_{jk}G_{jk}q\rangle$ also have the same critical behavior.

New aspects of the chiral structure of QCD ?

⋆ Universality of the chiral order parameters

⋆ The correlation between gluon and chiral zero modes

Phys. Rev. **D67** (2003) 054504.
hep-lat/0402005 (2004).

Future plan:

- Full QCD calculation (dynamical quark effects) (in progress)
- Complementary use of
  - Lattice QCD and the QCD sum rule
    (Hadron spectroscopy at finite temperature)

Detailed Lattice QCD Study of the Three-quark Potentials: The Ground-state and the Excited-state of the Static 3Q System

Toru T. Takahashi

RIKEN-TODAI Mini-Workshop on
"Topics in Hadron Physics at RHIC"

Detailed lattice QCD study of the three-quark potentials: the ground-state and the excited-state of the static 3Q system

Toru T. Takahashi (Yukawa Institute for Theoretical Physics)
with H.Suganuma (Tokyo Institute of Technology)

We study the ground-state three-quark (3Q) potential and the excited-state 3Q potential using SU(3) lattice QCD. From the accurate and thorough calculation for more than 300 different patterns of 3Q systems, the static ground-state 3Q potential is found to be well described by the Coulomb plus Y-type linear potential(Y-ansatz) within 1%-level deviation. With lattice QCD, we calculate also the excited-state potential in the 3Q system, and find the gluonic excitation energy to be about 1 GeV. This large gluonic-excitation energy would play an essential role to the success of the quark model for the low-lying hadrons in terms of the absence of the gluonic mode. Finally, we give a functional form which reproduces the gluonic-excitation energy in the 3Q system.

Introduction

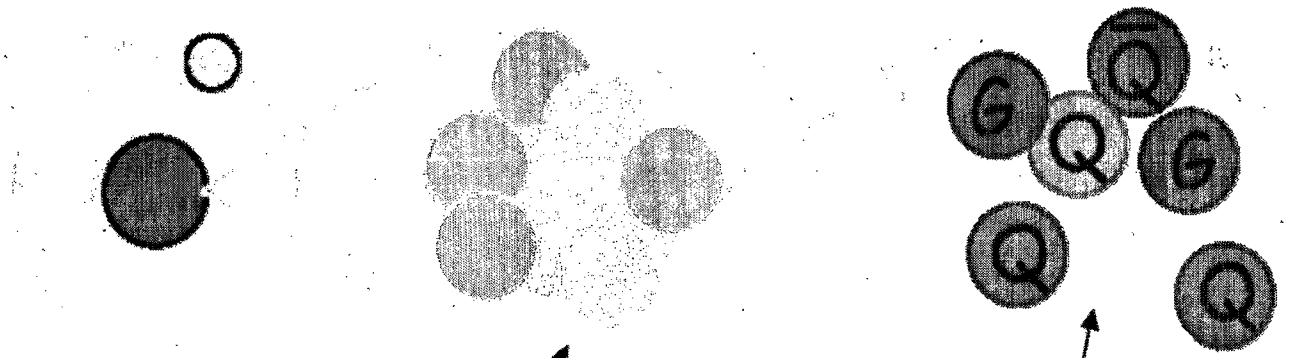

Interested in hadron dynamics

QCD is the fundamental theory of the Dynamics.

$$\mathcal{L}_{QCD} = -\frac{1}{2}\mathrm{tr}\, F_{\mu\nu}F^{\mu\nu} + \sum_f \bar{\psi}(i\gamma^\mu D_\mu - m_f)\psi$$

Lattice QCD to Hadron Physics

In practical,

Coupling g >>1 at the hadronic scale.

~~Perturbative calculation~~

The large coupling constant leads to rich nonperturbative nature

- chiral symmetry breaking
- color confinement

→Lattice QCD calculations

Reliable nonperturbative method

Lattice QCD

Lattice QCD calculation is a powerful tool
for the hadron spectroscopy.

↕

The calculation itself says almost nothing
about the internal structure of hadrons.

It is important to investigate the interquark potential
using lattice QCD.

Interquark Potentials

The quark-antiquark potential is well known.

$$V_{Q\bar{Q}} = -\frac{A}{r} + \sigma r + C$$

Coulomb type term

Linear confinement term

Color confinement & MESON properties

The flux-tube formation among quarks
can be observed using lattice QCD.

Flux-tube formation in the ground-state quark-antiquark system

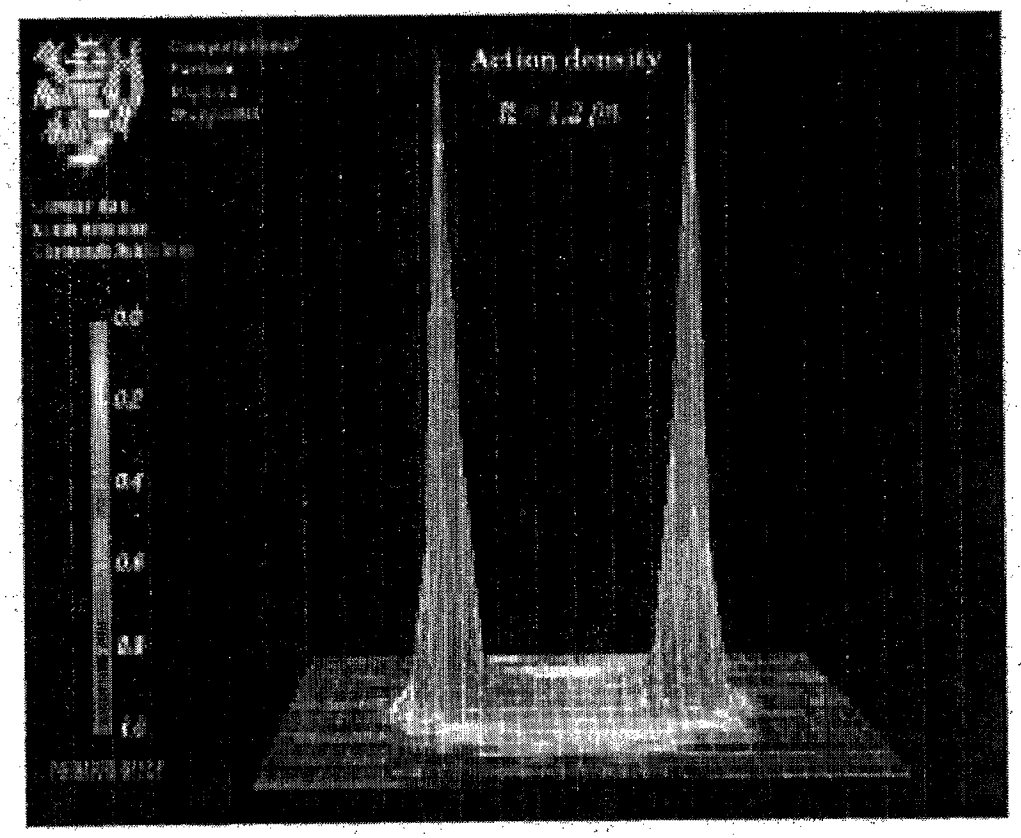

Figure in hep-ph/09809263
Prof.Nora Brambilla,
(figure provided byProf.G.S.Bali)

3Q potentials

3Q potential is important for the BARYONS.

However,
in spite of its importance,

Until the end of the 20th century,
The 3Q potential form was not settled.

3Q potentials

Roughly, there were 2 candidates for long-distance behavior of the 3Q potential form.

2-body sum

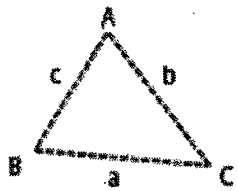

$L_\Delta = a+b+c$

For its simplicity,
used in quark model calculations

3-body

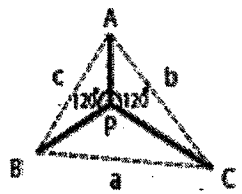

$L_{min} = \overline{AP} + \overline{BP} + \overline{CP}$

Supported by …

Center vortex model

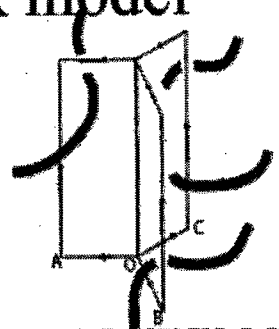

THE BARYON WILSON LOOP AREA LAW IN QCD.
John M. Cornwall (UCLA) **Phys.Rev.D54:6527(1996)**
(However, in hep-th/0305101, he re-calculated and found that Y-law is supported.)

Dual superconductor picture of the QCD vacuum

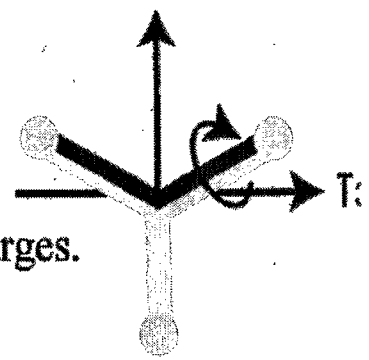

There appear 2 abelian charges.

3Q potentials

Lattice QCD studies

Sommer and Wosiek,
Phys.Lett.B149(1984)497, Nucl.Phys.B267(1986)531

Thacker, Eichten and Sexton,
Lattice '87

C.Alexandrou et.al.
Phys.Rev.D65(2002)054503

Even lattice QCD studies were controversial.

Contaminations of excited-state components
→ Smearing technique to enhance the G.S. component

Too few different patterns of quark configurations
→ 300 different patterns of quark configurations

3Q potentials

We have studied 3Q potential,
which is responsible for baryon properties.

We have found that the 3Q potential obeys
the following form.

$$V_{3Q} = -\sum \frac{A}{|r_i - r_j|} + \sigma L_{min} + C$$

2-body Coulomb 3-body linear

L_{min} is the length of Y-shaped flux-tube.

- universality of the string tension
- reproduction of OGE result

Phys.Rev.Lett.86:18-21,2001
Phys.Rev.D65:114509,2002

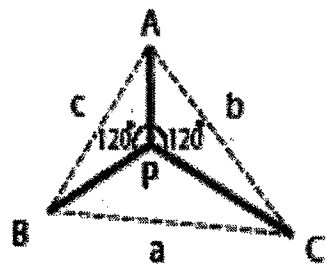

$L_{min} = \overline{AP} + \overline{BP} + \overline{CP}$

Flux-tube formation in the ground-state 3Q System

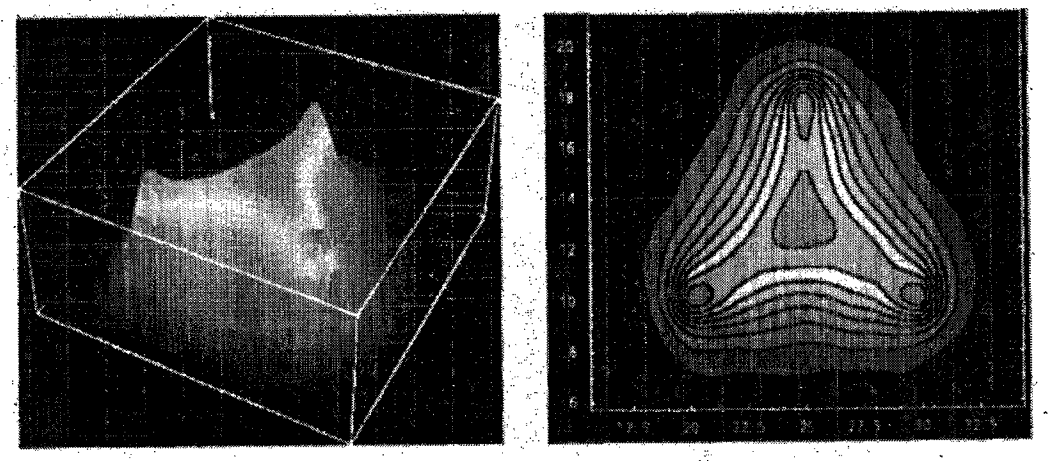

Action density in the static 3 quark system
in the Abelian-projected QCD.

H.Ichie, V.Bornyakov, T.Streuer, G.Schierholtz
Nucl.Phys.A721:887-890,2003

Gluonic Excitations of the 3Q System

Excitation induced by the massless GLUONS

Massive
Due to χSB

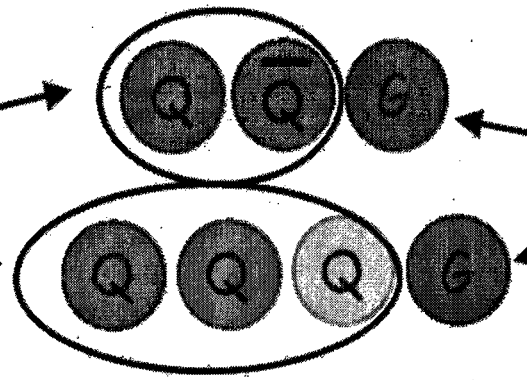

Massless
Gauge-boson

Hybrid Hadrons

In spite of its masslessness,
we find no HYBRIDS in the low-lying hadron spectra

Simple quark model well works. ONLY

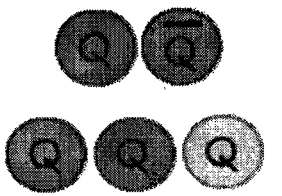

→Lattice QCD study about the excited-state potential

Excitation modes of the gluons

Gluonic Excitations of the 3Q System

β =5.8

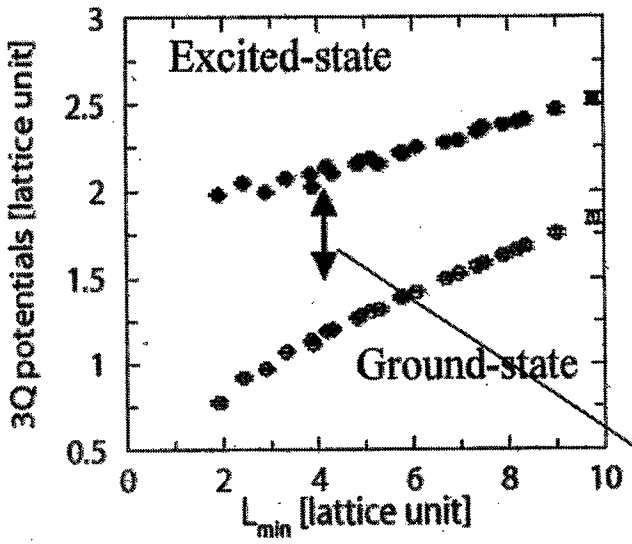

β =6.0 (finer lattice)

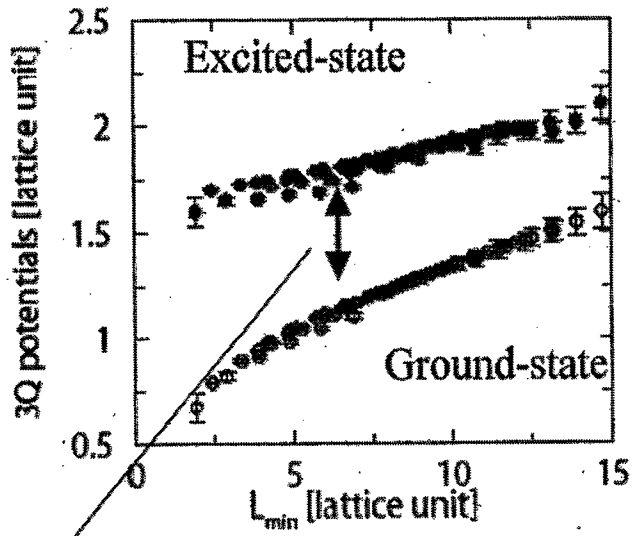

The excitation energy ΔE between ground state and excited state is about [illegible] of the typical hadronic scale.

ΔE is large in comparison with the excitation of quark origin.

→ It leads to the absence of the hybrid hadrons in the low-lying mass spectra.

→This supports the success of the quark model, which does not have the explicit gluonic degrees of freedom and has gluons as an instantaneous interaction among quarks.

Gluonic Excitations of the 3Q System

What is it?

Vibrational modes of the flux tube?

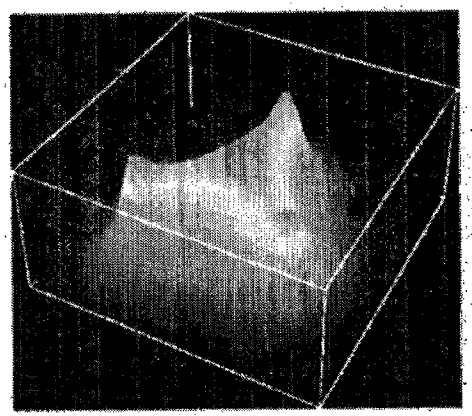

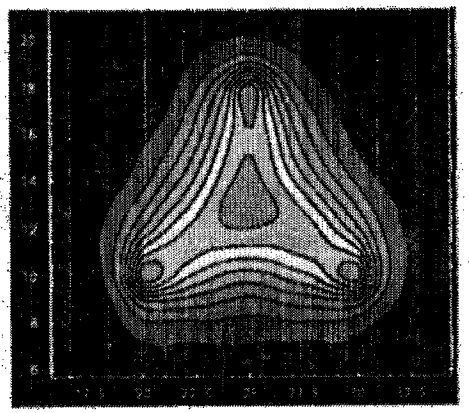

H.Ichie, V.Bornyakov, T.Streuer, G.Schierholtz
Nucl.Phys.A721:887-890,2003

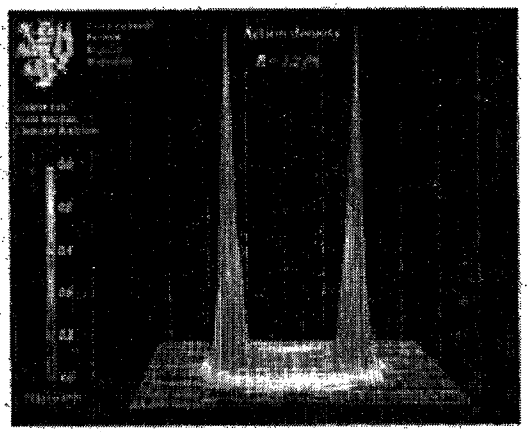

Figure in hep-ph/09809263
Prof.Nora Brambilla,
(provided byProf.G.S.Bali)

Gluonic Excitations of the 3Q System

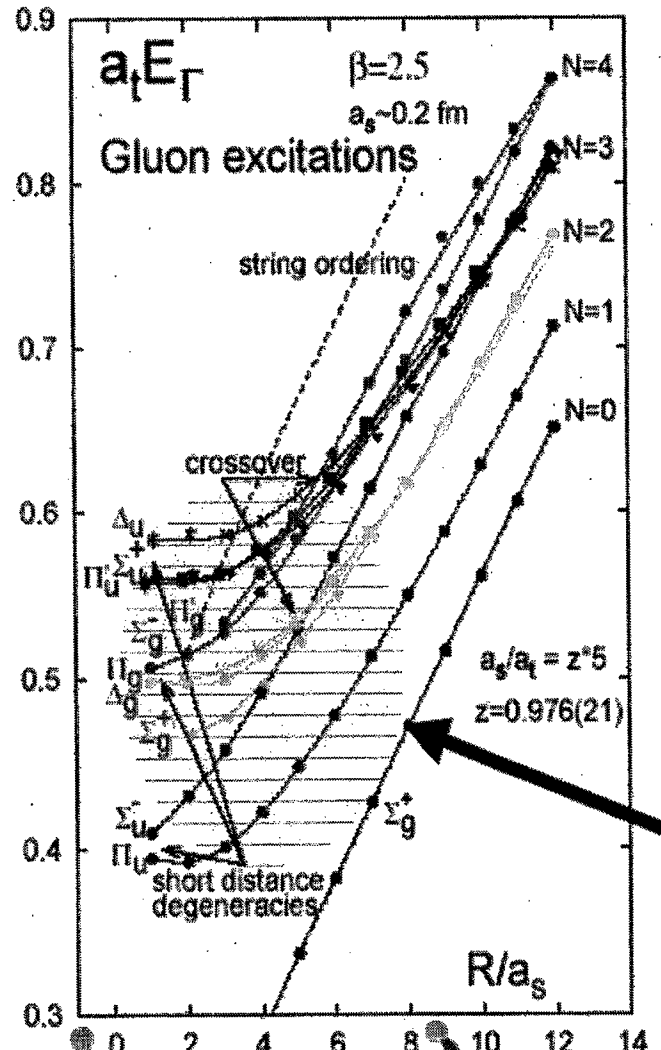

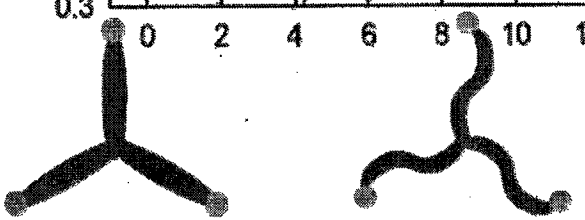

?

Static Quark-Antiquark system

Phys.Rev.Lett.90 161601(2003)
K.J.juge, J.kuti, C.Morningstar

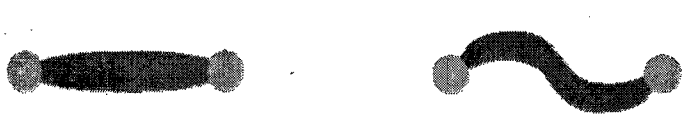

?

Naïve estimation using NG-string action

$$\sigma \quad \int_0^{r/2} dx \int_0^{r/2} dy \sqrt{\det\left(\partial_\alpha X^\mu \partial_\beta X_\mu\right)}$$

Fails to reproduce the excitation at the hadronic scale

Finite radius effect….?

More complicated in the 3Q system

Gluonic Excitations of the 3Q System

Phenomenologically,

we have found the functional form which describe ΔE in the static 3 quark system.

$$\Delta E = \frac{A}{L_{\bar{Y}}} + C$$

$$L_{\bar{Y}} \equiv \frac{1}{2}\left|\ \right|$$

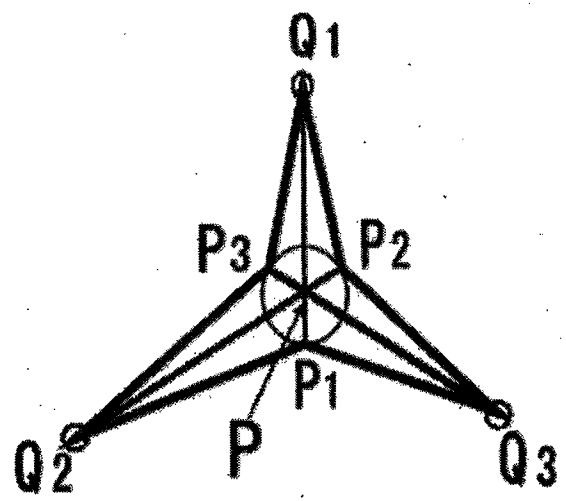

Gluonic Excitations of the 3Q System

β =5.8

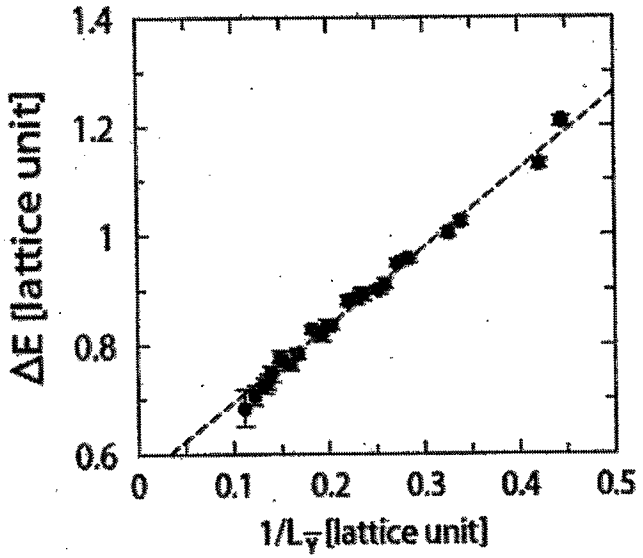

β =6.0 (finer lattice)

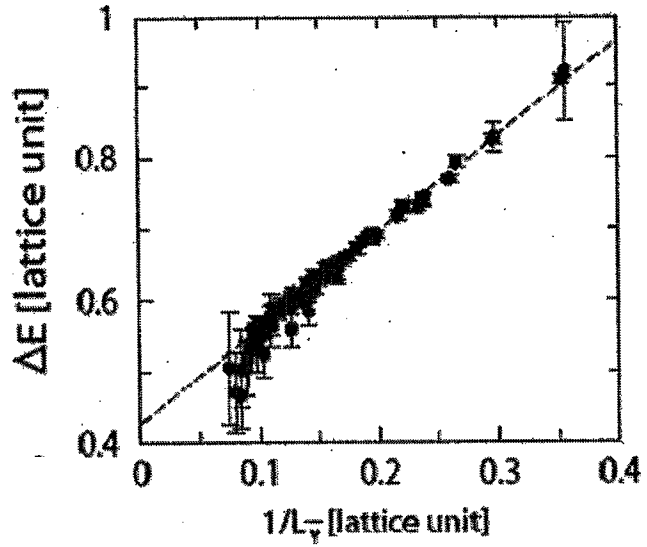

$$\Delta E_{3Q} = \frac{A}{L_{\bar{Y}}} + C$$

This form can reproduce ΔE_{3Q} with $\chi^2/N_{DF} \sim 1$ for about 100 Patterns of 3 quark spatial configurations

Gluonic Excitations of the 3Q System

We stress that this result can be applied to the 3Q system where 0～Lmin～1.5 fm. The infrared asymptotic behavior should be investigated carefully.

$$\Delta E = \frac{A}{L_Y} + C$$

$$L_Y = \frac{1}{2}\Big|$$

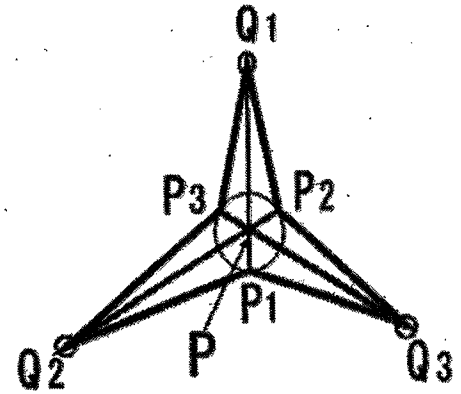

This may represent global oscillations of the 3 quark system.

For further study, we need modeling of the coupled vibrations of the Y-type Flux-tube. At that time, this Lattice QCD result will be useful.

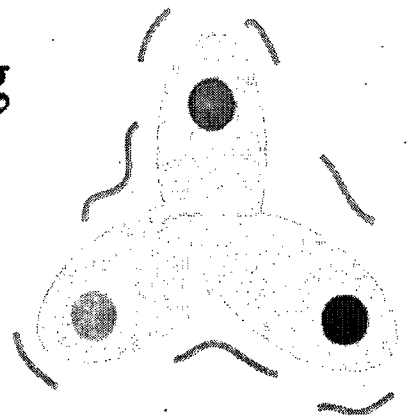

Summary

Ground-state of the static 3Q system

$$V_{3Q}^{(g.s.)} = -\sum \frac{A}{|r_i - r_j|} + \sigma L_{min} + C$$

2-body Coulomb 3-body linear

L_{min}: the length of Y-shaped flux tube

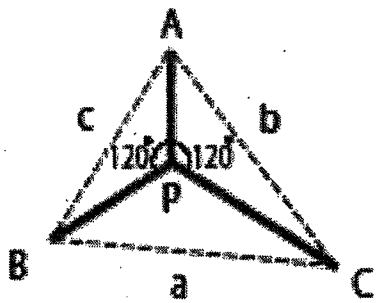

$L_{min} = \overline{AP} + \overline{BP} + \overline{CP}$

- universality of the string tension
- reproduction of OGE result

Phys.Rev.Lett.86:18-21,2001
Phys.Rev.D65:114509,2002

Summary

Excited-state of the static 3Q system

$$\Delta E = \frac{A}{L_Y} + C$$ (excitation energy)

L_Y: the length of ***vibrating*** flux tube ?

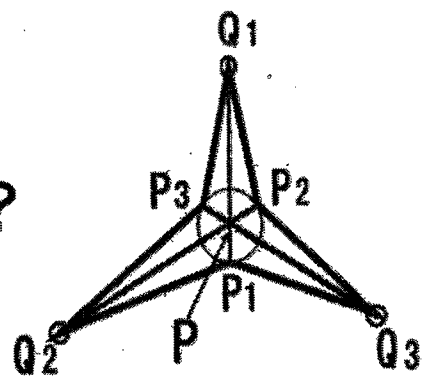

$L_Y = \frac{1}{2}$

$E_{1st} - E_{gs} > 1$ GeV

Phys.Rev.Lett:90(2003)182001

→ Gluonic excitations do not contribute to the low-lying hadron spectra

Polarized Parton Distributions and Their Uncertainties

M. Hirai

Polarized parton distributions and their uncertainties

M. Hirai

(Asymmetry Analysis Collaboration)

Radiation Laboratory, RIKEN

I discussed new AAC analysis of the polarized parton distributions by using current polarized deep inelastic scattering data and uncertainty estimation for these distributions by the Hessian method. Moreover, I discussed determination of the polarized gluon distribution from prompt photon data which will be measured by the RHIC experiments.

http://spin.riken.bnl.gov/aac/

Mar 24 2004, RIKEN

RIKEN

Polarized deep inelastic scattering

- **Cross section**

$$\frac{d^2\sigma}{d\Omega\, dE'} = \frac{\alpha^2}{2Mq^4}\frac{E'}{E}L_{\mu\nu}W^{\mu\nu}$$

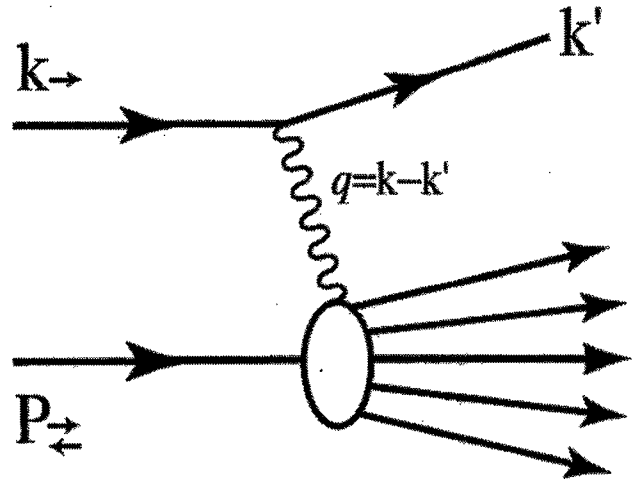

$$\begin{cases} Q^2 = -q^2, & \nu = \dfrac{P\cdot q}{M} \\ x = \dfrac{Q^2}{2M\nu}, & (0 \le x \le 1) \end{cases}$$

- **Hadron tensor (asymmetric part)**

$$W_A^{\mu\nu} = \varepsilon^{\mu\nu\rho\sigma}\frac{q_\rho}{\nu}\left\{ s_\sigma M^2 \nu G_1\left(\nu, Q^2\right) + \left[s_\sigma - \frac{(s\cdot q)P_\sigma}{M\nu}\right] M\nu^2 G_2\left(\nu, Q^2\right)\right\}$$

- **$Q^2 \to \infty$, x fixed**

$$\boxed{M^2\nu G_1\left(\nu, Q^2\right) \to g_1(x), \quad M\nu^2 G_2\left(\nu, Q^2\right) \to g_2(x)}$$

Polarized structure function g_1

- **Structure function g_1**

$$g_1(x)=\frac{1}{2}\sum_{i=1}^{n_f}e_i^2\left[\Delta C_q(x)\otimes\left(\Delta q_i(x)+\Delta\overline{q_i}(x)\right)+\Delta C_g(x)\otimes\Delta g(x)\right]$$

ΔC_q , ΔC_g (coefficient function)

$$\Delta q(x)=q_\uparrow(x)-q_\downarrow(x),\quad q(x)=q_\uparrow(x)+q_\downarrow(x)$$

$$(f\otimes g)=\int_x^1\frac{dy}{y}f\left(\frac{x}{y}\right)g(y)$$

- **DGLAP evolution equation**

$$\frac{d}{d\ln Q^2}\begin{pmatrix}\Delta\Sigma(x,Q^2)\\ \Delta g(x,Q^2)\end{pmatrix}=\begin{pmatrix}\Delta P_{qq}(x,\alpha_s) & \Delta P_{qg}(x,\alpha_s)\\ \Delta P_{gq}(x,\alpha_s) & \Delta P_{gg}(x,\alpha_s)\end{pmatrix}\otimes\begin{pmatrix}\Delta\Sigma(x,Q^2)\\ \Delta g(x,Q^2)\end{pmatrix}$$

$$\left(\Delta\Sigma=\Delta u^+ +\Delta d^+ +\Delta s^+\right)$$

Spin asymmetry $A_1(x,Q^2)$

$$A = \frac{d\sigma(\uparrow\downarrow) - d\sigma(\uparrow\uparrow)}{d\sigma(\uparrow\downarrow) + d\sigma(\uparrow\uparrow)}$$

$$\approx \frac{g_1}{F_1} = g_1 \frac{2x(1+R)}{F_2}$$

$$\left[R(x,Q^2) = \frac{\sigma_T}{\sigma_L} \right]$$

- L. W. Whitlow et al., Phys. Lett. B 250 (1990) 193

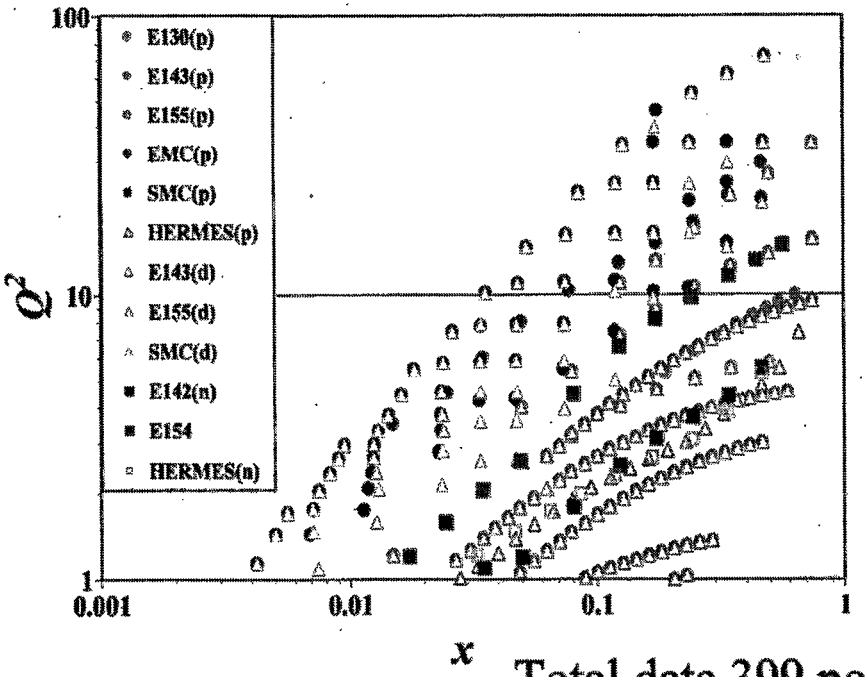

Total data 399 points (Q^2>1GeV^2)

- **Polarized DIS experiments**
  - Proton : E130, E143, EMC, SMC, HERMES, E155
  - Deuteron: E143, E155, SMC
  - Neutron : E142, E154, HERMES, JLab

RIKEN

Uncertainty estimation

- Functional form of polarized PDF

$$\Delta f_i(x,Q_0^2) = N\, x^{\alpha}(1-\gamma x)^{\beta}\ f_i(x,Q_0^2), \quad i = u_v, d_v, \bar{q}, g$$

- Hessian method

$$\left[\delta\Delta f(x)\right]^2 = \Delta\chi^2 \sum_{i,j} \frac{\partial \Delta f(x)}{\partial a_i} H_{ij}^{-1} \frac{\partial \Delta f(x)}{\partial a_j}$$

- Hessian matrix H_{ij}
  - parameter error
  - correlation between each parameters

- $\Delta\chi^2$ is relevant to the confidence level of uncertainty, and depend on χ^2 distribution K(s) with N degree of freedom
  - $\int_0^{\Delta\chi^2} K(N,s)\, ds = 0.683$ (N: the number of parameter)
  - AAC03, N=11: $\Delta\chi^2 = 12.64$

RIKEN

Result

- **Constraint condition**
  - Antiquark $SU(3)_f$ symmetry: $\Delta\bar{u}(x) = \Delta\bar{d}(x) = \Delta\bar{s}(x) = \Delta\bar{q}(x)$
  - Positivity condition: $|\Delta f(x)| \leq f(x)$
- **Total χ^2**
  - χ^2(/d.o.f.)=346.5 (0.893)
- **1st moment** $\left(\Delta\Sigma = \Delta u_v + \Delta d_v + 6\Delta\bar{q}\right)$

	Δg	$\Delta\Sigma$
AAC03	0.499 ± 1.268	0.213 ± 0.138
AAC00	0.532 ± 1.848	0.241 ± 0.220

  - AAC03: M.Hirai et al., Phys. Rev. D69 (2004) 054021
  - AAC00: Y.Goto et al., Phys. Rev. D62 (2000) 034017

- Unpol PDF:GRV98
- $Q_0^2 = 1$ GeV^2
- $N_f = 3$
- $\Lambda_{QCD} = 299$ MeV
- Data : 399

RIKEN

Polarized PDFs from DIS data (AAC03)

- PDF uncertainties reduced by including precise data
- Well determined valence quark distribution
  - Small uncertainty of Δu_v, Δd_v
- Antiquark uncertainty is significantly reduced
  - $g_1^p \propto 4\Delta u_v + \Delta d_v + 12\Delta\bar{q}$
- Undetermined $\Delta g(x)$
  - Large uncertainty
  - Indirect contribution to g_1^p
  - Correlated with $\Delta g(x)$

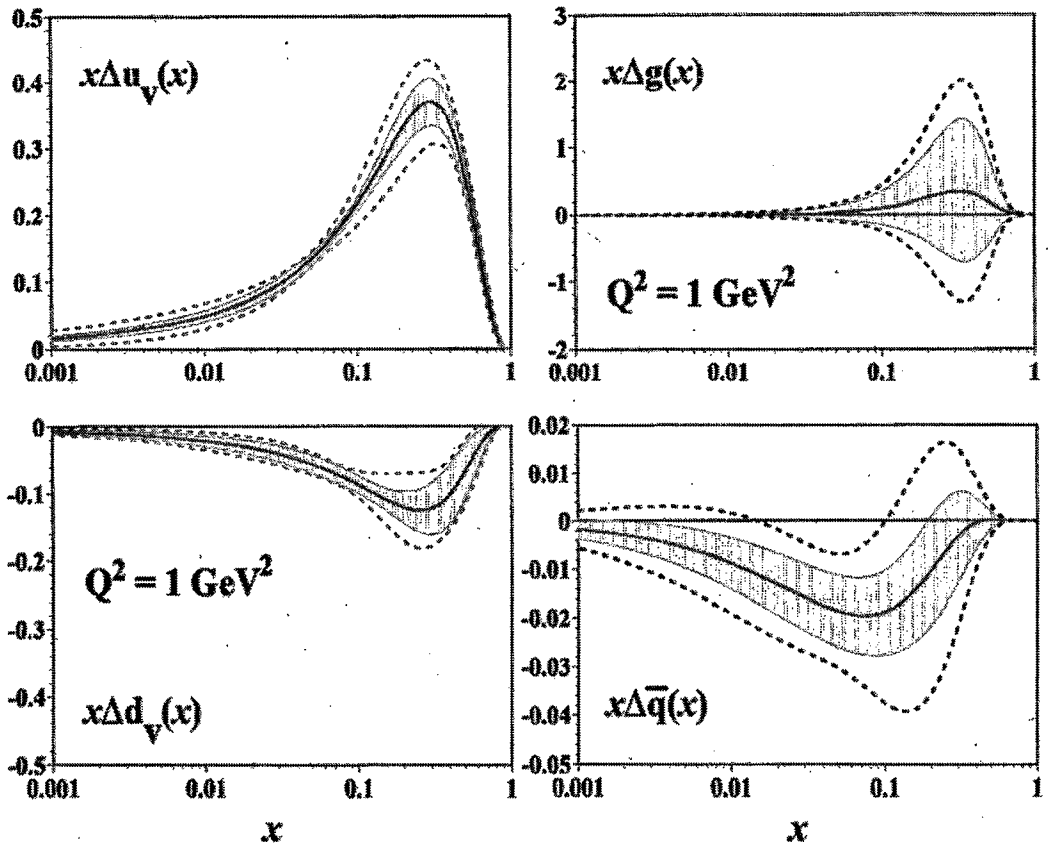

RIKEN

Correlation between $\Delta\bar{q}(x)$ and $\Delta g(x)$

- Fixed $\Delta g(x)=0$
  - χ^2(/d.o.f.)=355.0 (0.915)
- $\Delta q_v(x)$ uncertainties are scarcely changed
- Antiquark uncertainty is reduced
  - Strong correlation with $\Delta g(x)$
- Well determined $\Delta g(x)$
  - Eliminating correlation effect
  - Flavor decomposition $\Delta\bar{q}(x)$

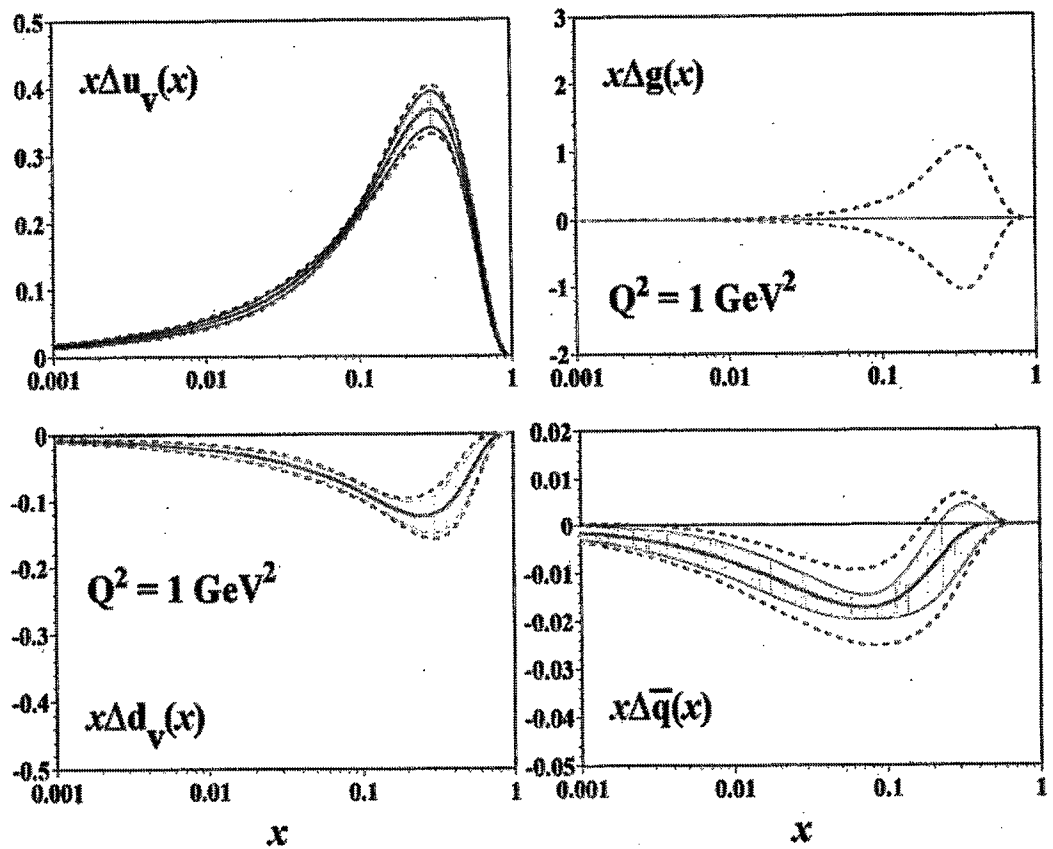

RIKEN

Spin asymmetry A_1^p

- Precise data improve asymmetry uncertainty
- Good agreements with polarized DIS data
  - Quark and antiquark distributions are constrained
  - Gluon distribution need other constraint

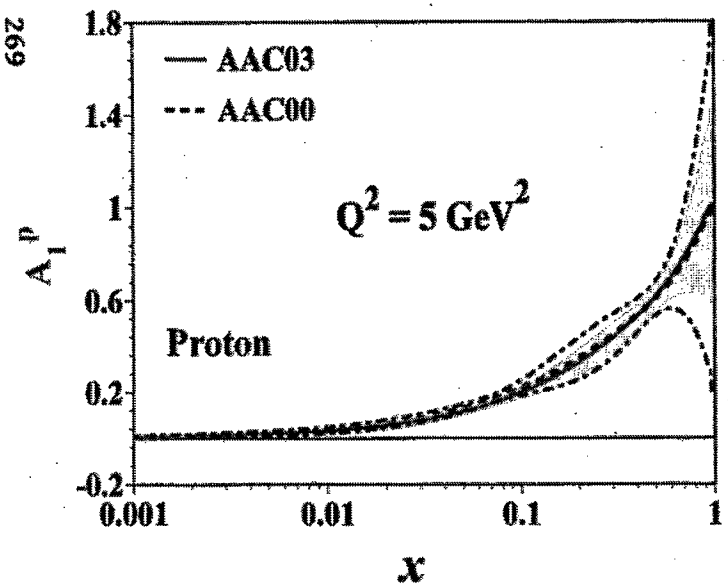

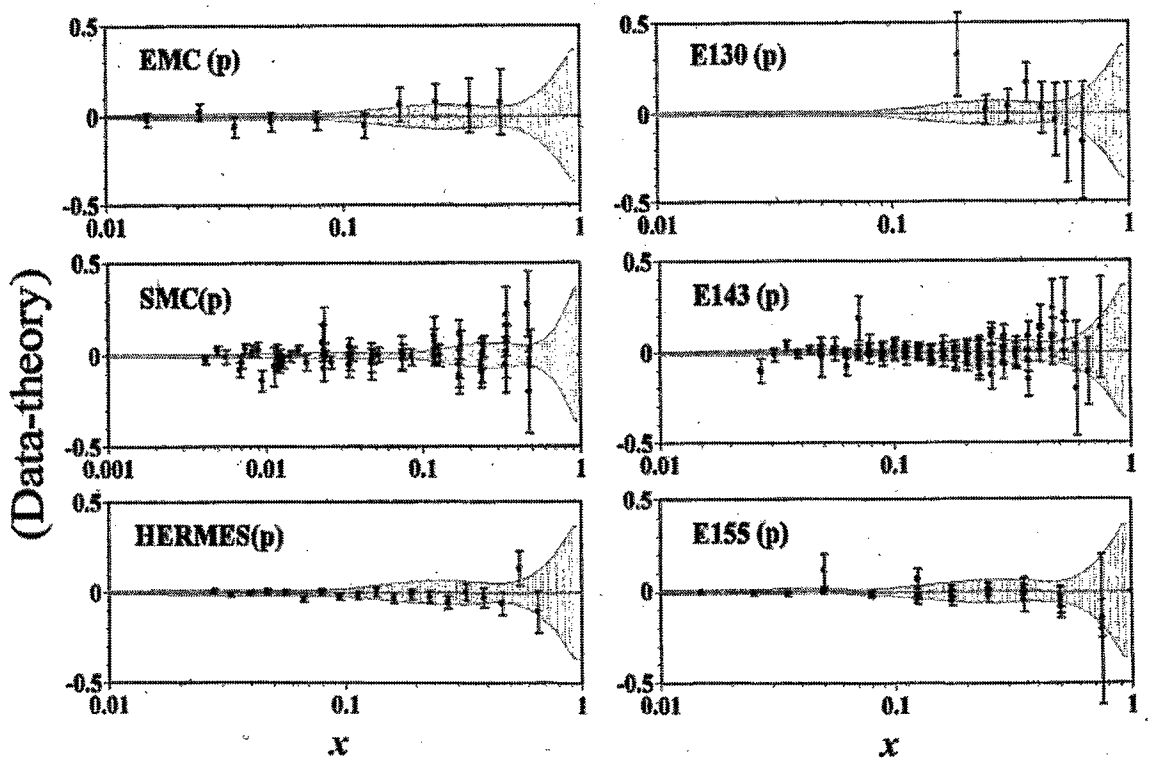

RIKEN

Prompt photon production

- **Polarized prompt photon cross section**
  - $qg \to \gamma q, q\bar{q} \to \gamma g$
  - NLO: L.E. Gordon and W. Vogelsang, Phys. Rev. D48, 3136 (1993)

$$\frac{d\Delta\sigma^{pp\to\gamma X}}{dp_T} = \sum_{a,b} \int_{\eta\, bin} d\eta \int_{\xi_1}^{1} dx_1 \int_{\xi_2}^{1} dx_2\, \Delta f_a^A(x_1,\mu)\Delta f_b^B(x_2,\mu) \frac{d\Delta\hat{\sigma}^{ab}}{dp_T d\eta}(x_1, x_2, \sqrt{s}, \eta, p_T, \mu)$$

$$\left(\xi_1 = \frac{x_T e^{\eta}}{2 - x_T e^{-\eta}},\quad \xi_2 = \frac{x_1 x_T e^{-\eta}}{2x_1 - x_T e^{\eta}},\quad x_T = \frac{2p_T}{\sqrt{s}},\quad \mu = p_T\right)$$

- **Fragmentation contribution is neglected**
  - Isolation cut (Reduction of $\pi^0 \to \gamma\gamma$, collinear photon)

- **Spin asymmetry and statistical error**

$$A_{LL}^{\gamma} = \frac{d\Delta\sigma^{\gamma}/dp_T}{d\sigma^{\gamma}/dp_T},\quad \delta A_{LL}^{\gamma} = \frac{1}{P_1 P_2 \sqrt{L_{\text{int}}\sigma^{\gamma}\varepsilon}}$$

P : beam polarization
L_{int} : integrated luminosity
σ^{γ} : unpolarized cross section
ε : detection efficiency ($\varepsilon \le 1$)

Uncertainty of $A_{LL}^{\gamma}(P_T)$

- Large uncertainty of A_{LL}^{γ} is mainly composed of gluon uncertainty $\delta\Delta g(x)$
  - Small uncertainty except $\delta\Delta g(x)$
- Weak constraint on quark and antiquark distributions
  - Off $\delta\Delta g(x)$ uncertainty is composed of quark and antiquark uncertainty
  - The off $\delta\Delta g(x)$ is smaller than expected statistical errors
- Prompt photon data mainly constricts the gluon uncertainty

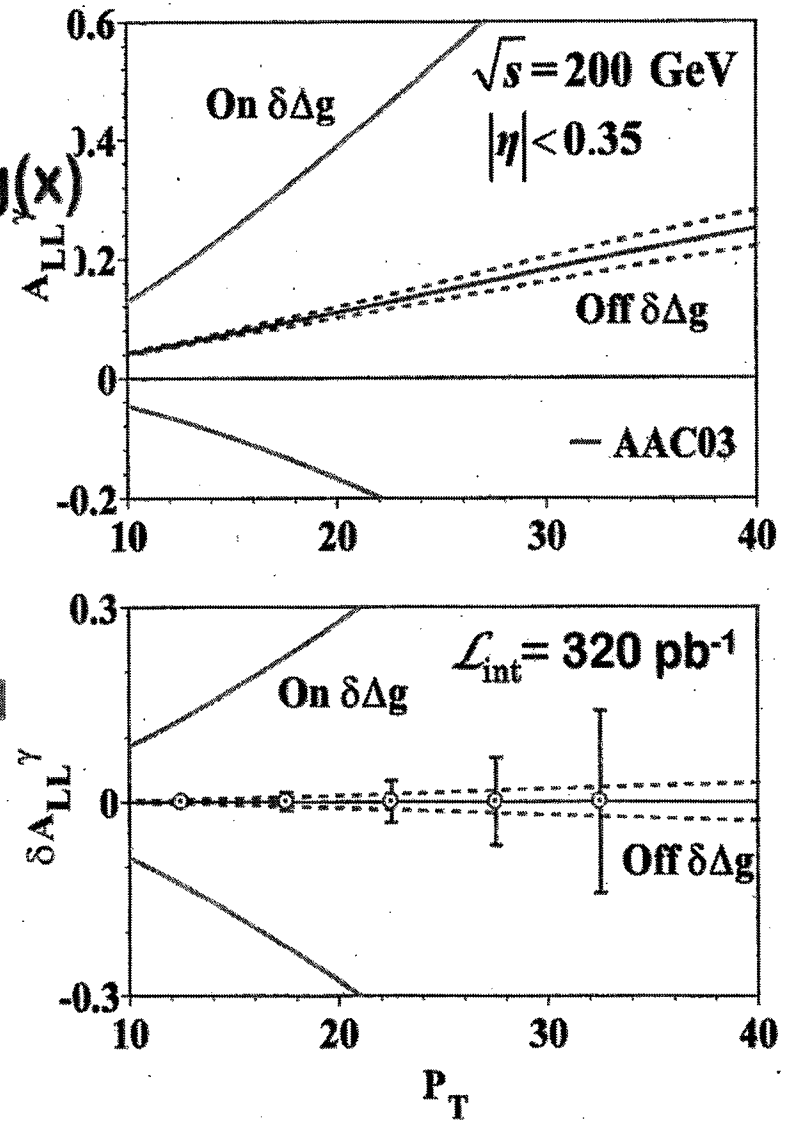

RIKEN

Comparison with statistical error

- Overhaul factor for gluon uncertainty $\delta\Delta g(x)$
  - 1/18 (P_T=10~20 GeV)
- Constricting $\delta\Delta g(x)$ in different x_T (=$2P_T/\sqrt{s}$) region
  - X_T = 0.1~0.2 ($\sqrt{s}$= 200 GeV)
  - X_T = 0.04~0.08 ($\sqrt{s}$= 500 GeV)
- Gluon contribution: $\Delta g = \int_0^1 dx\, \Delta g(x)$
  - Covering wide range of x_{BJ}

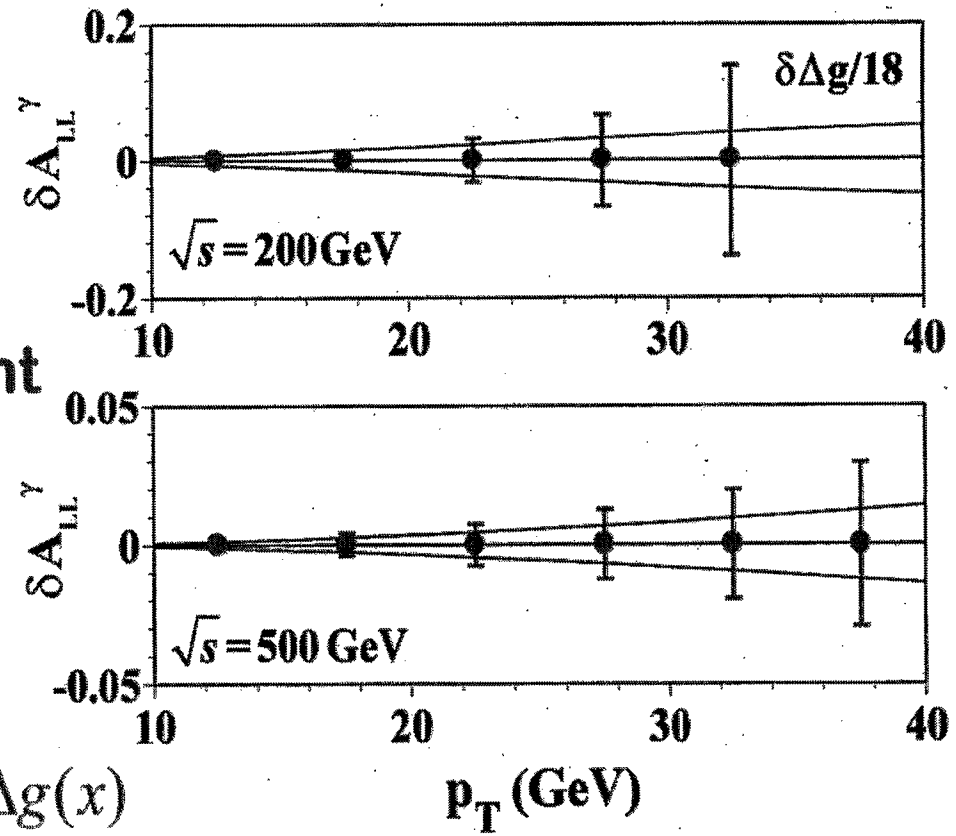

- $\mathcal{L}_{int}$= 320 pb^{-1} (200 GeV)
  800 pb^{-1} (500 GeV)
- $|\eta| < 0.35$
- P=0.7
- $\Delta\phi = \pi$

RIKEN

Δg(x) uncertainty from prompt photon

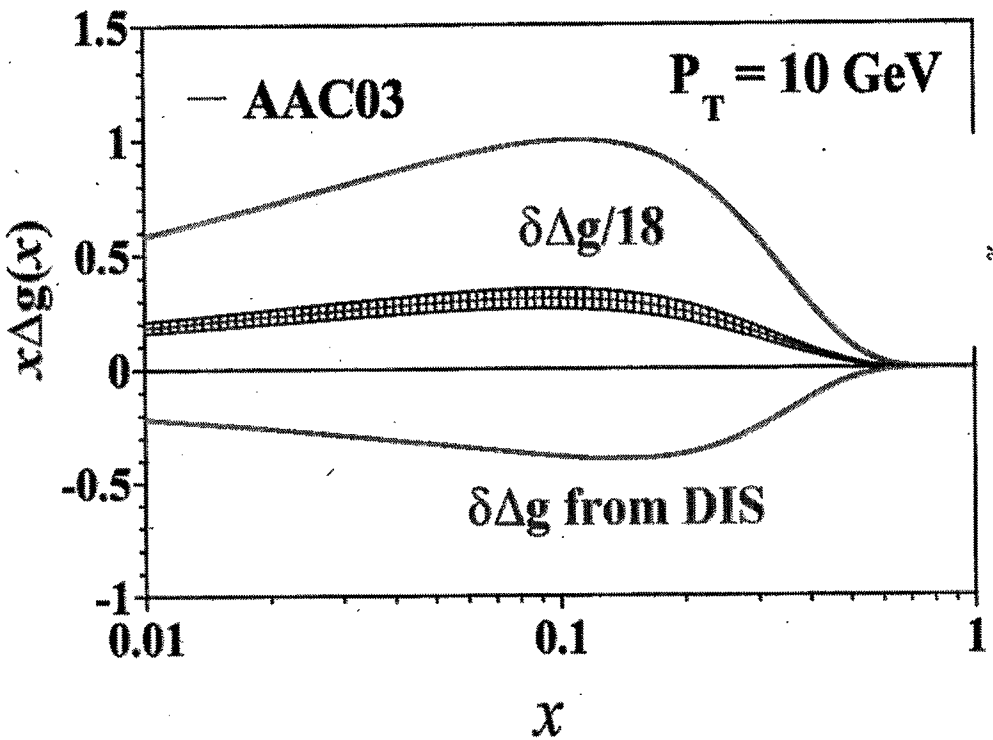

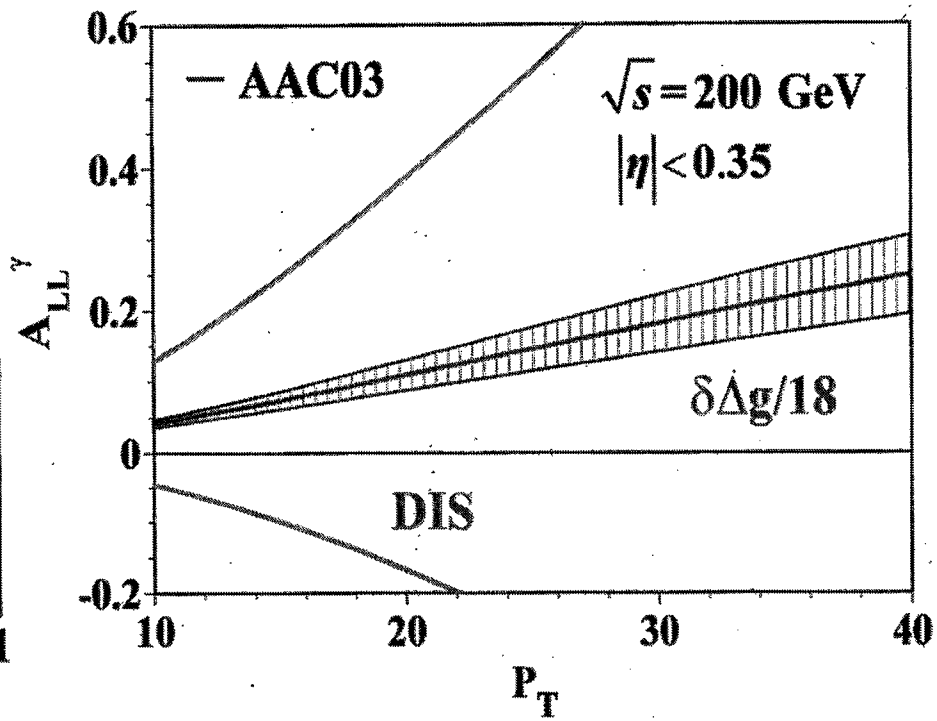

RIKEN

Summary

- **Polarized PDF from polarized DIS data**
  - $\Delta u_v(x)$, $\Delta d_v(x)$ are determined well
  - $\Delta\Sigma = 0.213 \pm 0.138$ ($Q^2 = 1$ GeV^2)
  - $\Delta g(x)$ could not be constrained
- **$\Delta g(x)$ uncertainty can be reduced by prompt photon data**
  - A_{LL}^{γ} uncertainty is composed of the Δg uncertainty
  - Current A_{LL}^{γ} uncertainty quite larger than expected statistical errors
- **Comparison A_{LL}^{γ} uncertainty with expected statistical errors**
  - Effective region (P_T=10~20 GeV)
  - X_T=0.1~0.2 ($\sqrt{s}$= 200 GeV), 0.04~0.08 ($\sqrt{s}$= 500 GeV)

RIKEN

Comment on π^0 Double Spin Asymmetry at RHIC

K. Sudoh

Comment on π^0 double spin asymmetry at RHIC

K. Sudoh (RIKEN)
RIKEN-TODAI Mini-Workshop
24 March 2004

hep-ph/0403102, with M. Hirai

Abstract

Double spin asymmetry for π^0 production has been measured by the PHENIX. The preliminary data indicate negative asymmetry at low p_T, whereas the theoretical prediction is positive asymmetry.

We study effects of polarized gluon distribution on the spin asymmetry, and suggest the possibility to obtain sizable negative asymmetry in larger p_T regions.

RIKEN

Contents

I. Introduction

II. Inclusive π^0 Production in $\vec{p}\vec{p}$ Collisions

$$\vec{p} + \vec{p} \rightarrow \pi^0 + X$$

III. Correlation to $\Delta g(x)$

IV. Summary

I. Introduction

- Uncertainty of the polarized gluon distributions $\Delta g(x)$ is still large, since the gluon contribution appears in NLO in polarized DIS.

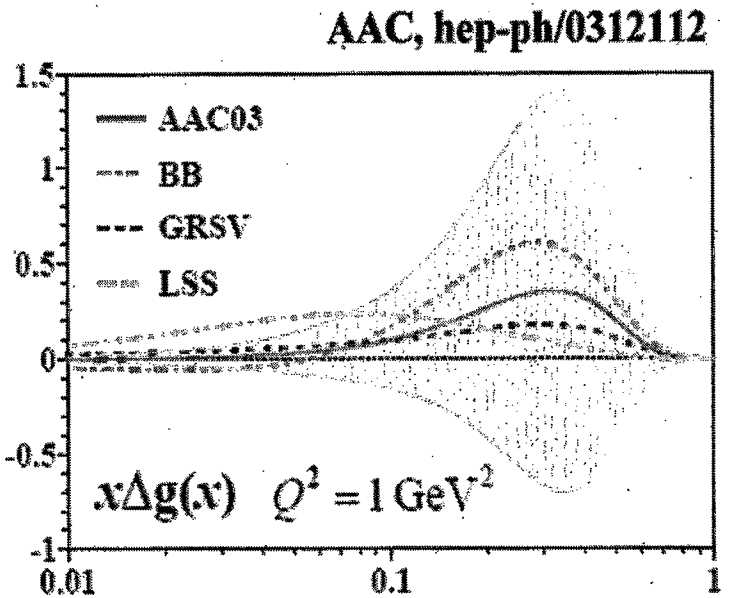

➡ RHIC has started!!

- The π^0 spin asymmetry A_{LL}^{π} has been measured by the PHENIX.
  - The data suggest significant negative asymmetry!!!

Effects of $\Delta g(x)$ on the π^0 spin asymmetry

Negative Asymmetry

- **Comparison A_{LL}^{π} with the PHENIX data**

  $\sqrt{s} = 200\ \text{GeV}, \quad |\eta| \le 0.38$

- **pQCD prediction indicates positive asymmetry.**

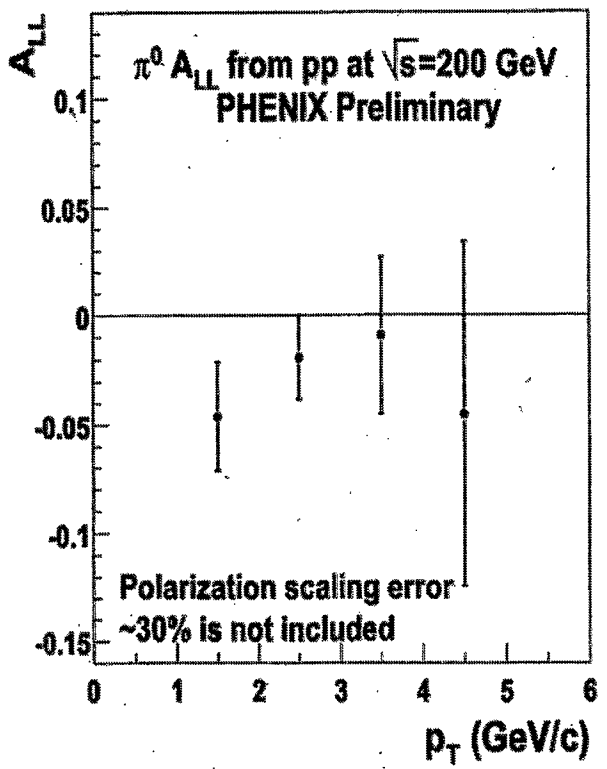

A. Bazilevsky, talk at Spin-03, Dubna

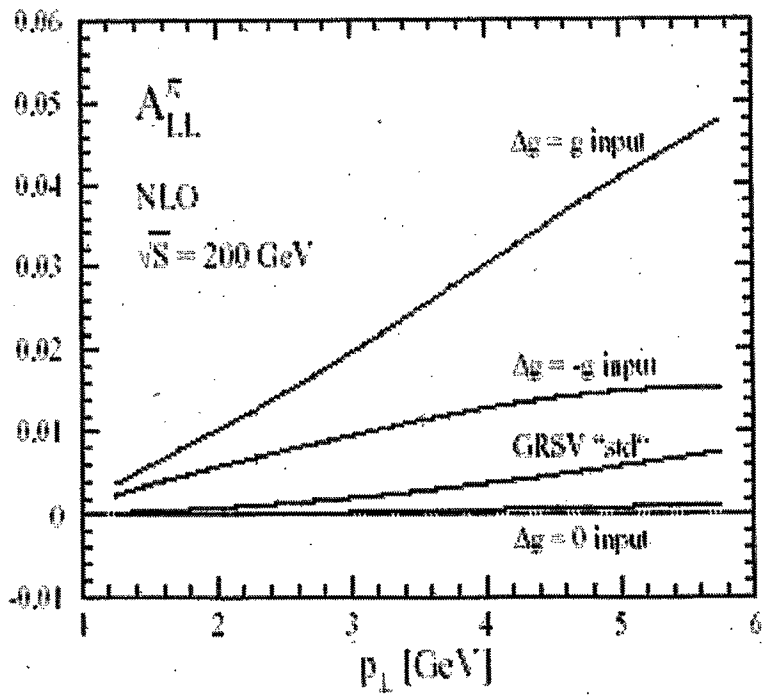

B. Jagar *et al.*, PRD67, 054005 (2003)

Inclusive π^0 Production @RHIC

- **Subprocesses for π^0 production**
  - **$O(\alpha_s^2)$ 2→2 tree-level channels in LO**

$$gg \to q(g)X, \quad qg \to q(g)X, \quad qq \to qX,$$
$$q\bar{q} \to q(g,q')X, \quad qq' \to qX, \quad q\bar{q}' \to qX$$

  - **Dominant contribution:**

$gg \to q(g)X$ **: in small p_T**

$qg \to q(g)X$ **: in large p_T**

- **π^0 spin asymmetry is sensitive to $\Delta g(x)$.**

⇒ **Determined by a balance between *gg* and *qg* contributions.**

Double Spin Asymmetry

Longitudinal Double Spin Asymmetry:

$$A_{LL}^{\pi^0} \equiv \frac{[d\sigma_{++} - d\sigma_{+-}]/dp_T}{[d\sigma_{++} + d\sigma_{+-}]/dp_T} = \frac{d\Delta\sigma/dp_T}{d\sigma/dp_T}$$

$$\frac{d\Delta\sigma}{dp_T} \equiv \frac{1}{2}\left[\frac{d\sigma_{++}}{dp_T} - \frac{d\sigma_{+-}}{dp_T}\right] \qquad : \ |\eta| \le 0.38, \quad Q^2 = p_T^2$$

$$= \sum_{a,b,c} \int d\eta \int dx_a \int dx_b \int dz \ \underline{\Delta f_a(x_a, Q^2)\Delta f_b(x_b, Q^2)} \underline{\frac{d\Delta\hat{\sigma}}{dp_T d\eta}} \underline{D_c^{\pi}(z, Q^2)}$$

PDF and FF: Determined using experimental data

Amplitude: Calculable in pQCD

Where does the inconsistency come from?

Where does ambiguity come from?

- **Fragmentation function: $D^{\pi}(z)$**
  - Unpolarized π^0 cross section by the PHENIX is consistent with pQCD calculation.

$$\sqrt{s} = 200 \text{ GeV}, \quad |\eta| \le 0.35$$

  - Determined from e^+e^- data

- **Pol. quark distribution: $\Delta q(x)$**
  - Flavor blind reaction
  - Depends on the sum $\Delta q(x)+\Delta\bar{q}(x)$.

⇨ **Ambiguity comes from $\Delta g(x)$**

PHENIX Collab. PRL91, 241803 (2003)

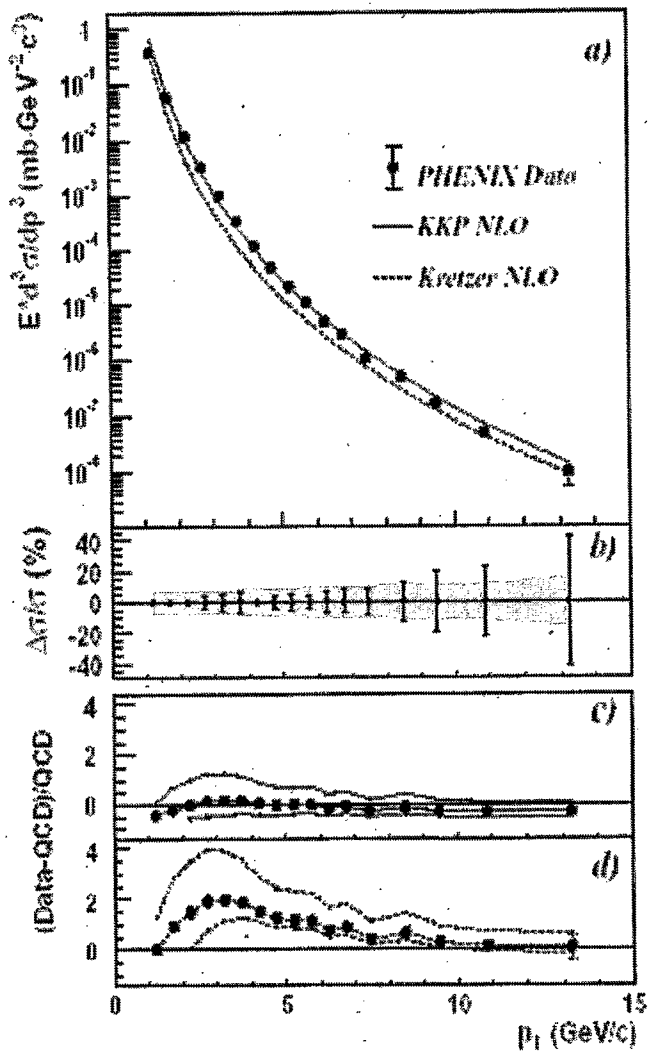

Modification of $\Delta g(x)$

Can we obtain negative asymmetry by modifying $\Delta g(x)$?

3 configurations of $\Delta g(x)$ within their uncertainty

- Scen.1 standard Δg
  - global analysis with pol. DIS
  - A_{LL} does not become negative.
- Scen.2 Δg with a node
  - possibility $gg<0$ ($\Delta g(x_a)\cdot\Delta g(x_b)<0$)
  - $|x_a-x_b|$ is small in $\eta<0.38$
- Scen.3 negative Δg
  - $gg>0$, $qg<0$
  - $|\Delta g(x)|$ is small in low x
  - $|\Delta g(x)|$ is large in high x

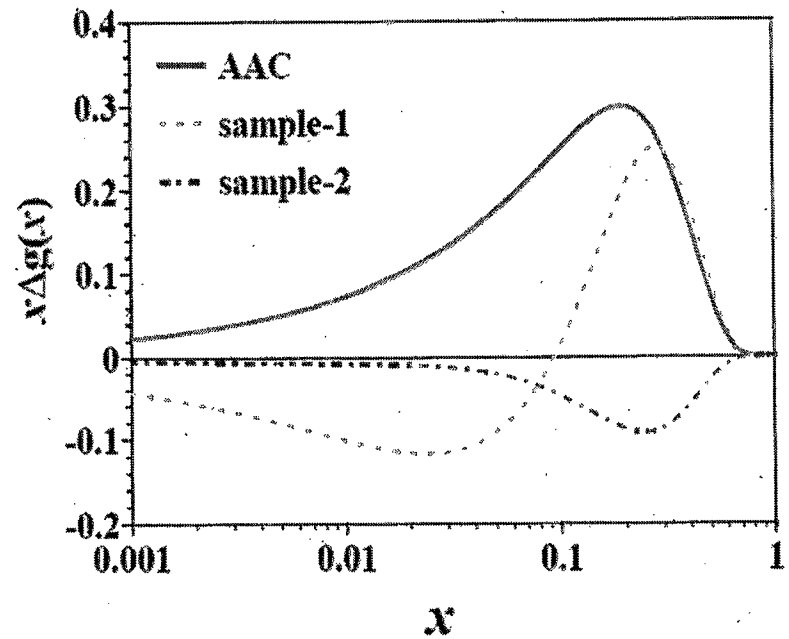

$\Delta g(x)$ has Q^2 dependence by DGLAP equation.

A_{LL}^{π} with modified $\Delta g(x)$

- AAC $\Delta g(x)$
  - Both gg and qg >0
  - A_{LL} is positive and increases with p_T
- Sample-1
  - In low p_T
    - Both gg and qg <0
    - Slight negative A_{LL} in η<0.38
  - In large p_T
    - Both gg and qg >0
    - A_{LL} becomes large positive
- Sample-2
  - gg>0, qg<0, A_{LL}<0 in whole p_T
  - $|A_{LL}|$ becomes larger to negative

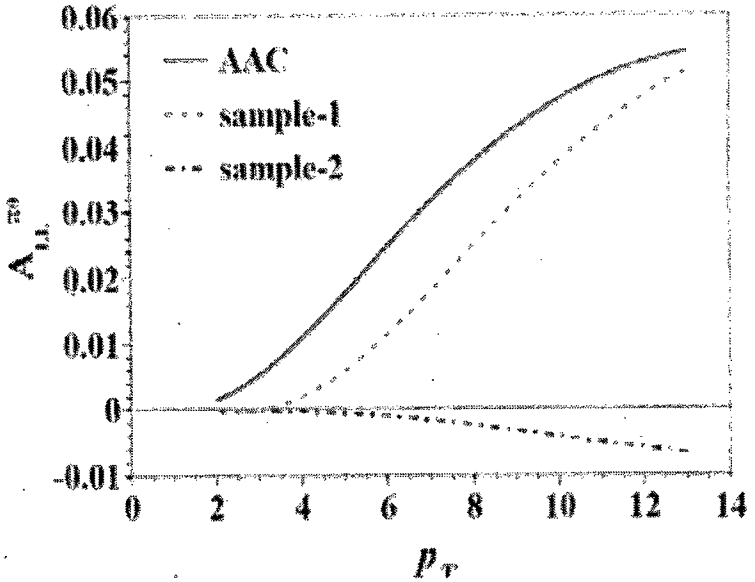

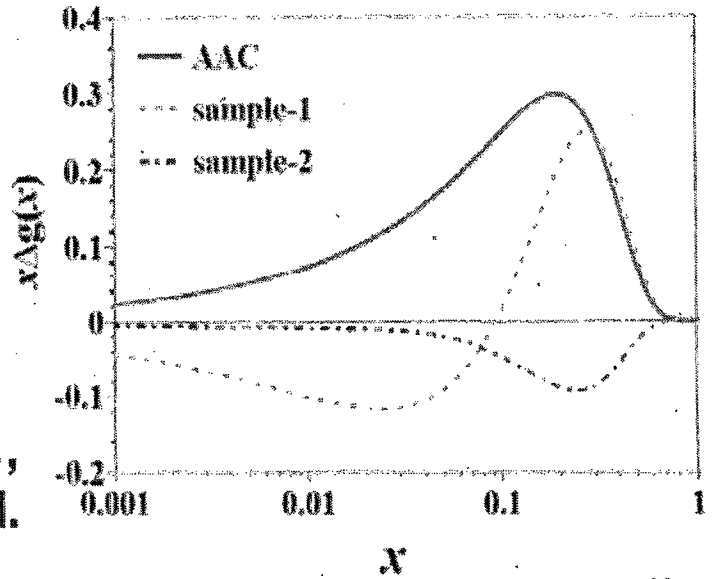

Difficult to obtain sizable asymmetry in low p_T, since partonic cross section itself is too small.

Uncertainty of A_{LL}^{π}

- Comparison A_{LL} uncertainty with errors of PHENIX data
- A_{LL} uncertainty comes from the gluon uncertainty
- The same constriction as the polarized DIS data

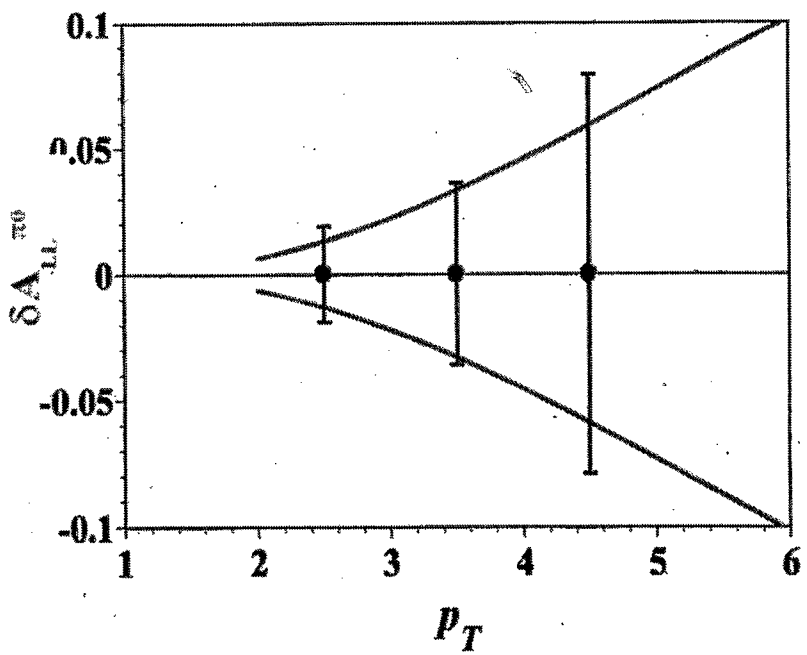

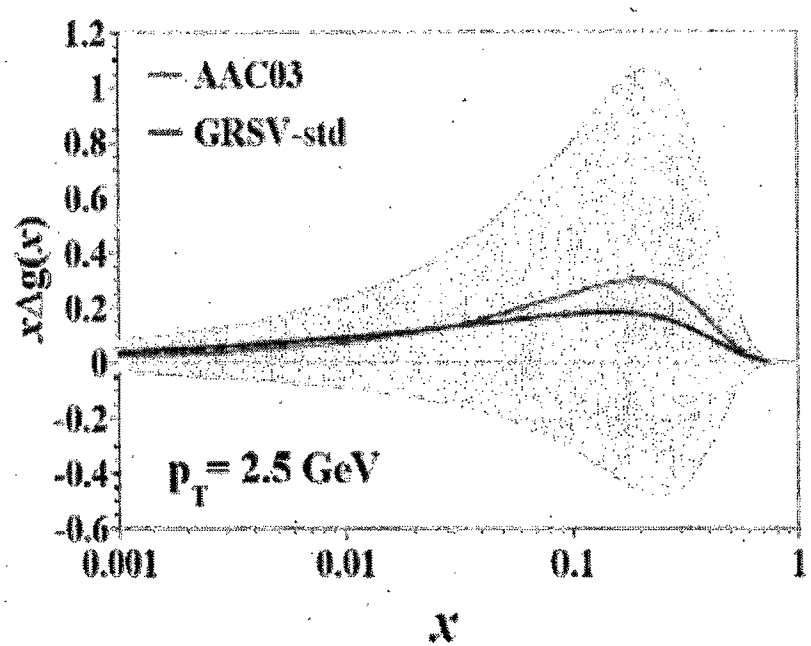

IV. Summary

- **Correlation between π^0 spin asymmetry and $\Delta g(x)$ is studied.**

  ☆ **It is extremely difficult to derive sizable A_{LL} in a few % level in low p_T.**

  – **Slight negative asymmetry at low p_T can be obtained.**
  – **It is premature to conclude that pQCD is not applicable to π^0 asymmetry.**
  – **Existence of $\Delta g(x)$ which keeps A_{LL} to be negative in whole p_T.**

- **PHENIX data motivate us to modify $\Delta g(x)$ drastically?**
  – **Negative asymmetry suggests negative polarization of $\Delta g(x)$.**

⇨ **Precise data in wide p_T regions is needed to determine the gluon spin content.**

Chiral Doubling of Heavy-Light Hadrons in the Vector Manifestation

Chihiro Sasaki

Chiral Doubling of Heavy-Light Hadrons in the Vector Manifestation [1]

Chihiro SASAKI

Department of Physics, Nagoya University, Nagoya, 464-8602, Japan

Abstract

Starting with a hidden local symmetry Lagrangian at the vector manifestation fixed point that incorporates heavy-quark symmetry, we calculate the splitting of chiral doublers of heavy-light mesons proposed by Nowak, Rho and Zahed [Phys. Rev. D **48**, 4370 (1993)] and Bardeen and Hill [Phys. Rev. D **49**, 409 (1994)], and show, in the three-flavor chiral limit, that the splitting is proportional to the light-quark condensate $\langle\bar{q}q\rangle$ and comes out to be ~ 0.37 GeV $\sim \frac{1}{3}m_N$ where m_N is the nucleon mass. This is to be compared with the recently measured BaBar result for the splitting between $D_s^+(2316.8 : 0^+)$ and $D_s^+(0^-)$ of 348 MeV and the CLEO result for that between $D_s^{*+}(2463 : 1^+)$ and $D_s^*(1^-)$ of 352 MeV.

[1]This talk is based on the work done in hep-ph/0312182 by M. Harada, M. Rho and C. Sasaki.

Chiral Doubling of Heavy-Light Hadrons in the Vector Manifestation

Chihiro SASAKI (Nagoya University)

based on
M. Harada, M. Rho and C.S., hep-ph/0312182.

Contents

1. Introduction
   - Heavy quark symmetry & chiral symmetry, "Chiral doubling"
   - Our approach
2. Wigner Realization of Chiral Symmetry
3. Our Effective Field Theory
4. Matching to the Operator Product Expansion
5. Quantum Correction
6. Mass Splitting
7. Summary

Introduction

D-meson : heavy-light system
(c) (u,d,s)

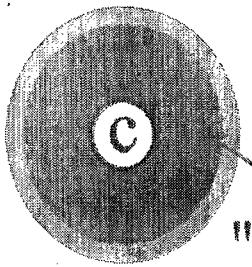

"Light–quark cloud"
surrounds the heavy–quark.

- Heavy quark sector $\cdots$ Heavy quark symmetry
  M_Q (heavy quark mass) $\rightarrow \infty$ limit $\Rightarrow$ Spin-flavor symmetry :
  Dynamics of the heavy quark Q is independent of its mass and spin.

  Ground state : $D(0^-)$, $D(1^-)$ $\Leftarrow$ spin partner $(s_{\rm light} = \frac{1}{2})$

- Light quark sector $\cdots$ Chiral symmetry

Recent discoveries ($c\bar{s}$-system)

$$D(0^+) \,:\, 2317\,\text{MeV} \quad \text{[BaBar (03)]}$$
$$D(1^+) \,:\, 2463\,\text{MeV} \quad \text{[CLEO (03)]}$$

$$\begin{pmatrix} D(0^-) \,:\, 1969\,\text{MeV} \\ D(1^-) \,:\, 2112\,\text{MeV} \end{pmatrix} \;:\; \text{known}$$

$$\star\,\text{mass shifts} \quad \left.\begin{matrix} m(0^+) - m(0^-) \\ m(1^+) - m(1^-) \end{matrix}\right\} \sim 350\,\text{MeV}$$

- Prediction : "Chiral doubling"

$D(0^+)$ (or $D(1^+)$) is chiral partner of $D(0^-)$ (or $D(1^-)$).

$$\left.\begin{array}{l} m(0^+) - m(0^-) \\ m(1^+) - m(1^-) \end{array}\right\} \sim m_{\text{constituent}}$$

[Nowak, Rho and Zahed (92), Bardeen and Hill (93).]

$\cdots$ based on the manifestation of chiral symmetry restoration
á la linear sigma model

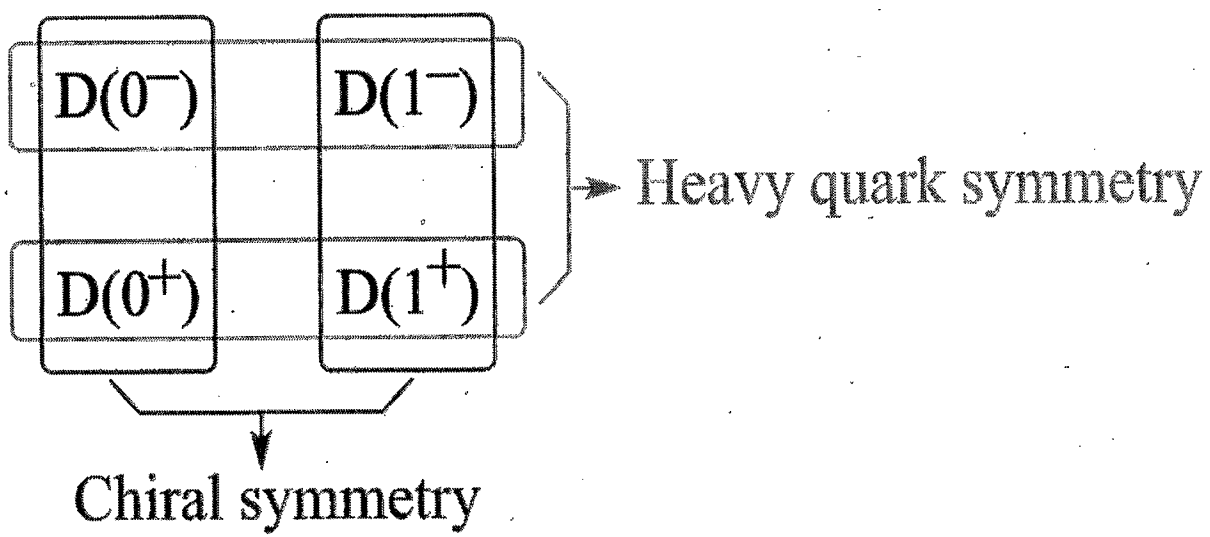

- Our approach :

$$\text{Chiral symmetic phase} \Rightarrow \text{Chiral broken phase}$$

- The main assumption :
  At the chiral symmetry restoration point, the vector manifestation (VM) is realized.

$$\Uparrow$$

Massless ρ-meson becomes chiral partner of π.

- formulated in the framework of hidded local symmetry (HLS) theory.

$\cdots$ dynamical d.o.f. $= \pi, \rho$

- characterized by the fixed point of RGEs.

[Harada and Yamawaki (01).]

⋆ We start from the Lagrangian at the VM fixed point and include the effect of chiral symmetry breaking.

Wigner Realization of Chiral Symmetry

Chiral representations of low-lying mesons (zero helicity)

- In broken phase, the eigenstate of the chiral representation under $SU(3)_L \times SU(3)_R$ symmetry does not agree with the mass eigenstate.

$$
\begin{aligned}
|s\rangle &= |(3,3^*) \oplus (3^*,3)\rangle, \\
|\pi\rangle &= |(3,3^*) \oplus (3^*,3)\rangle \sin\psi + |(1,8) \oplus (8,1)\rangle \cos\psi, \\
|V\rangle &= |(1,8) \oplus (8,1)\rangle, \\
|A_1\rangle &= |(3,3^*) \oplus (3^*,3)\rangle \cos\psi - |(1,8) \oplus (8,1)\rangle \sin\psi.
\end{aligned}
$$

mixing angle $\psi \simeq 45^\circ$

F. J. Gilman and H. Harari, PR 165, 1803 (1968);

S. Weinberg, PR 177, 2604 (1969).

- Chiral symmetry restoration

  $\longrightarrow$ Representation mixing is dissolved at critical point.

  $\longrightarrow$ There are 2 possibilities for pattern of chiral symmetry restoration.

<u>One possibility</u> $(\cos\psi \to 0)$

$$|\pi\rangle = |(3,3^*) \oplus (3^*,3)\rangle,$$
$$|s\rangle = |(3,3^*) \oplus (3^*,3)\rangle.$$

$\cdots$ Standard scenario

<u>Another possibility</u> $(\sin\psi \to 0)$

$$|\pi\rangle = |(1,8) \oplus (8,1)\rangle,$$
$$|V\rangle = |(1,8) \oplus (8,1)\rangle.$$

$\cdots$ Vector Manifestation

Our Effective Field Theory

- Restoration point of chiral symmetry :
  - Light sector
    $M_\rho = 0$: Massless ρ-meson is chiral partner of π.
  - Heavy sector
    $\Delta M \equiv M(0^+) - M(0^-) = M(1^+) - M(1^-) = 0$:
    $D(0^+)$ (or $D(1^+)$) is chiral partner of $D(0^-)$ (or $D(1^-)$).
- Terms expressing chiral symmetry breaking :
  - Light sector
    $M_\rho \neq 0$: Massive ρ-meson
  - Heavy sector
    Chiral symmetry breaking generates $\Delta M \neq 0$.

Concept of the Matching in the Wilsonian Sense

- The bare Lagrangian of the EFT is defined at a suitable matching scale Λ.

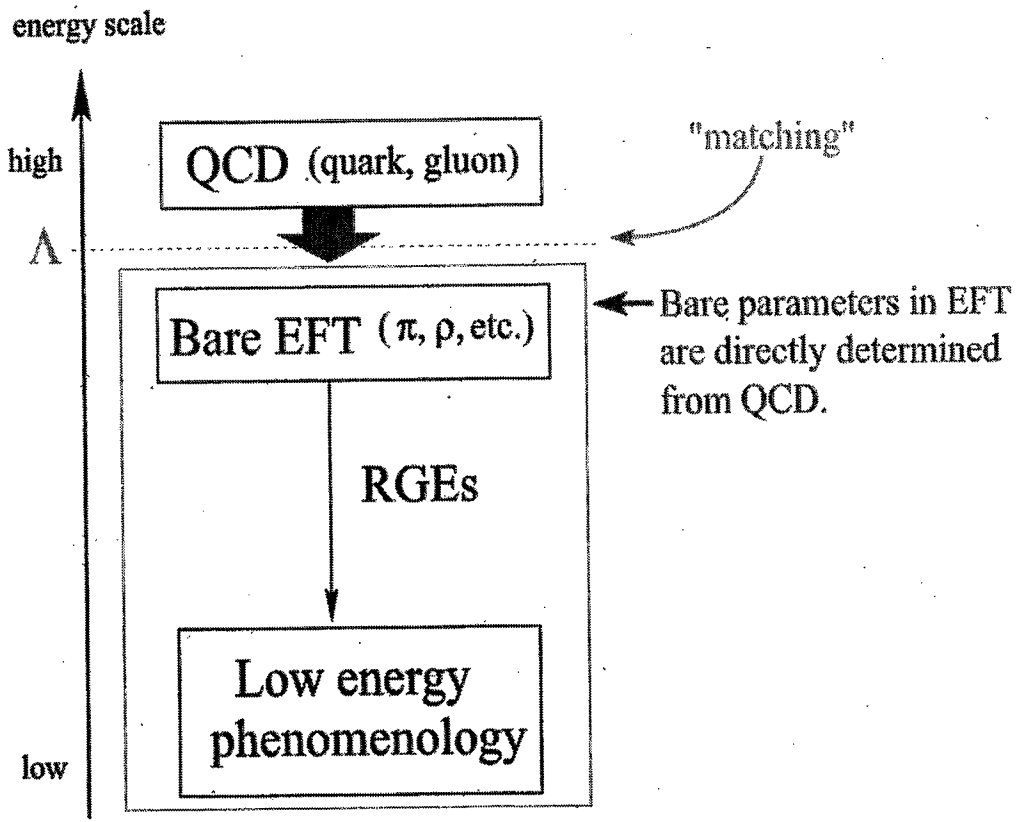

$\Rightarrow$ We obtain the bare Lagrangian of the EFT after integrating out the high energy modes.

i.e, the quarks and gluons above Λ

Matching to the Operator Product Expansion

$$\Delta_{\rm SP}(Q^2) \equiv G_{\rm S}(Q^2) - G_{\rm P}(Q^2)$$

where

$G_{\rm S}(Q^2)$: Scalar correlator for $D(0^+)$

$G_{\rm P}(Q^2)$: Pseudoscalar correlator for $D(0^-)$

302

EFT sector

$$\Delta_{\rm SP}^{\rm (EFT)}(Q^2) = \frac{3F_D^2 M_D^2}{M_D^2 + Q^2}\Big(M(0^+) - M(0^-)\Big)$$

OPE sector [Narison (03)]

$$\Delta_{\rm SP}^{\rm (OPE)}(Q^2) = -\frac{2m_H^3}{m_H^2 + Q^2}\langle\bar{q}q\rangle$$

$\Rightarrow$ Equating $\Delta_{\rm SP}^{\rm (EFT)}$ and $\Delta_{\rm SP}^{\rm (OPE)}$ at the matching scale Λ.

$\Rightarrow$ Bare mass splitting

$$\Delta M(\Lambda) \equiv M(0^+) - M(0^-) = -\frac{2}{3}\frac{\langle \bar{q}q \rangle}{F_D^2}$$

Parameters : estimated by using QCD sum rule [Narison (88)]

D-meson decay constant $F_D = 0.205\,\text{GeV}$

Light quark condensate $\langle \bar{q}q \rangle = -(0.243\,\text{GeV})^3$

$$\Delta M_{\rm bare} = \Delta M(\Lambda) = 0.23\,\text{GeV}$$

$$\Downarrow$$

Enhanced by quantum correction of ρ-meson

Quantum Correction

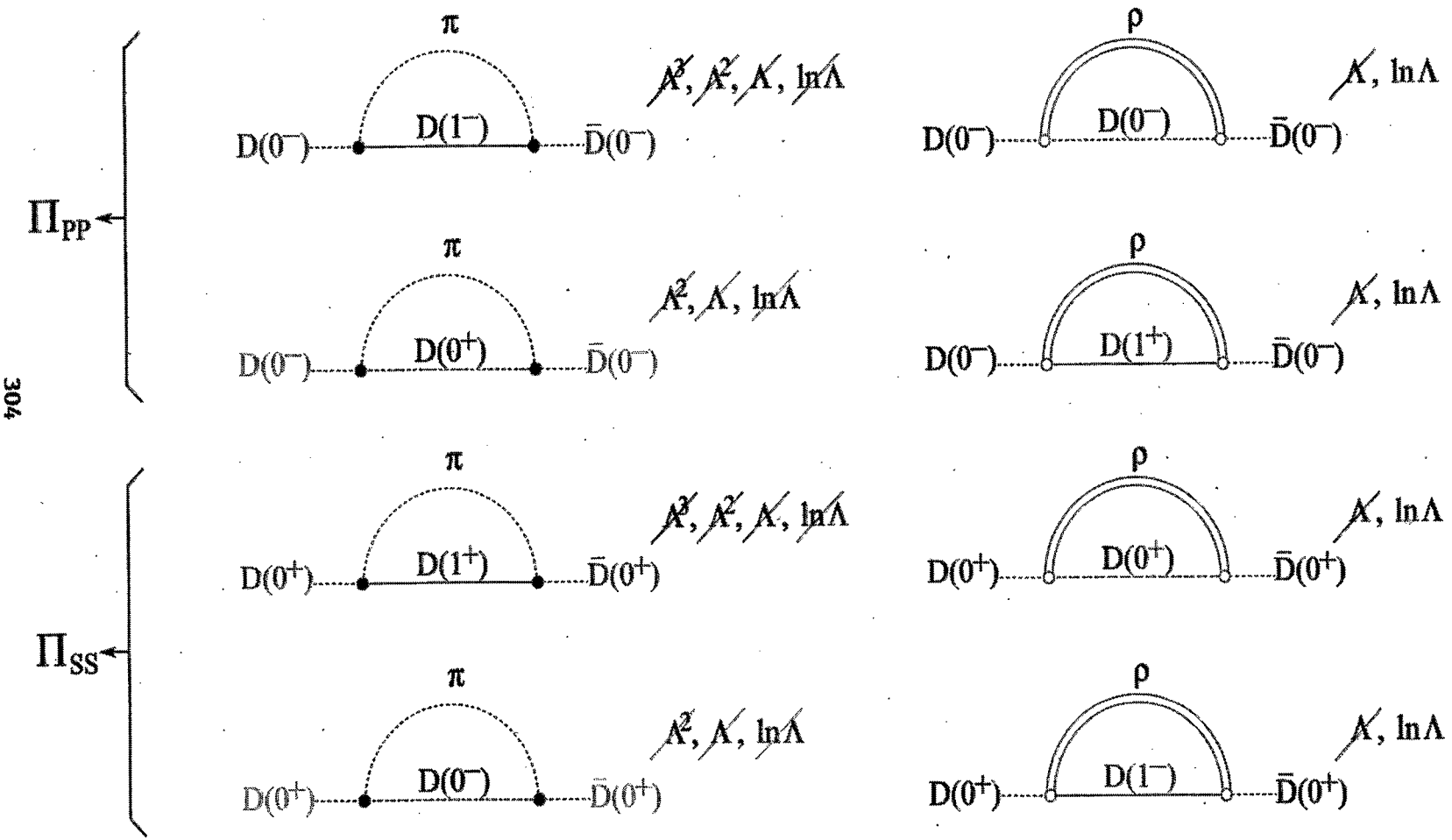

$$\Delta M = \Delta M_{\rm bare} \times C_{\rm quantum} \quad \propto \langle \bar{q}q \rangle$$
$$= \Delta M_{\rm bare} \exp\left[-\mathcal{C}_2(N_f) \frac{g^2}{2\pi^2} (1 - 2k - k^2) \ln \frac{\Lambda}{\mu} \right]$$

Parameters, e.g.,

$\mathcal{C}_2(N_f = 3) = 4/3,$
$g = 6.27,$ [← HLS gauge coupling constant]
$k = 0.59,$ [← extracted from $D^* \to D\pi$]
$\mu = m_\rho = 771\,$MeV,
$\Lambda = 1.1\,$GeV.

$$\Rightarrow \quad C_{\rm quantum} \simeq 1.6$$

The quantum effect increases $\Delta M_{\rm bare}$ by $\sim 60\%$.

Mass Splitting

$$\Delta M_{\rm bare} = 0.23\,\text{GeV}$$

$\Downarrow$ enhanced by ρ-loop effect

$$\Delta M = 0.37\,\text{GeV} \sim m_{\rm constituent}$$

Good agreement with experiment

306

Summary

- We started from the premise that at the critical point, the VM is realized.
- We included the effect of chiral symmetry breaking and matched our EFT to the OPE.
  - $\Delta M_{\rm bare} \propto \langle \bar{q}q \rangle$
  - Due to the quantum effect of ρ-meson, $\Delta M_{\rm bare}$ was enhanced by about 60%.

$$\Rightarrow \Delta M \propto \langle \bar{q}q \rangle$$

- This suggests that
  - identifying the chiral symmetry restoration as the VM
  - the chiral doubling as a signal of spontaneous chiral symmetry breaking

308 are mutually consistent.

- What is the characteristic feature of the VM?

  $\Rightarrow$ Decay process

Additional RIKEN BNL Research Center Proceedings:

Volume 60 – Lattice QCD at Finite Temperature and Density – BNL –72083-2004
Volume 59 – RHIC Spin Collaboration Meeting XXI, XXII, XXIII, January 22, 2004, February 27, 2004, March 19, 2004– BNL-
Volume 58 – RHIC Spin Collaboration Meeting XX – BNL-71900-2004
Volume 57 – High pt Physics at RHIC, December 2-6, 2003 – BNL-72069-2004
Volume 56 – RBRC Scientific Review Committee Meeting – BNL-71899-2003
Volume 55 – Collective Flow and QGP Properties – BNL-71898-2003
Volume 54 – RHIC Spin Collaboration Meetings XVII, XVIII, XIX – BNL-71751-2003
Volume 53 – Theory Studies for Polarized *pp* Scattering – BNL-71747-2003
Volume 52 – RIKEN School on QCD "Topics on the Proton" – BNL-71694-2003
Volume 51 – RHIC Spin Collaboration Meetings XV, XVI – BNL-71539-2003
Volume 50 – High Performance Computing with QCDOC and BlueGene – BNL-71147-2003
Volume 49 – RBRC Scientific Review Committee Meeting – BNL-52679
Volume 48 – RHIC Spin Collaboration Meeting XIV – BNL-71300-2003
Volume 47 – RHIC Spin Collaboration Meetings XII, XIII – BNL-71118-2003
Volume 46 – Large-Scale Computations in Nuclear Physics using the QCDOC – BNL-52678
Volume 45 – Summer Program: Current and Future Directions at RHIC – BNL-71035
Volume 44 – RHIC Spin Collaboration Meetings VIII, IX, X, XI – BNL-71117-2003
Volume 43 – RIKEN Winter School – Quark-Gluon Structure of the Nucleon and QCD – BNL-52672
Volume 42 – Baryon Dynamics at RHIC – BNL-52669
Volume 41 – Hadron Structure from Lattice QCD – BNL-52674
Volume 40 – Theory Studies for RHIC-Spin – BNL-52662
Volume 39 – RHIC Spin Collaboration Meeting VII – BNL-52659
Volume 38 – RBRC Scientific Review Committee Meeting – BNL-52649
Volume 37 – RHIC Spin Collaboration Meeting VI (Part 2) – BNL-52660
Volume 36 – RHIC Spin Collaboration Meeting VI – BNL-52642
Volume 35 – RIKEN Winter School – Quarks, Hadrons and Nuclei – QCD Hard Processes and the Nucleon Spin – BNL-52643
Volume 34 – High Energy QCD: Beyond the Pomeron – BNL-52641
Volume 33 – Spin Physics at RHIC in Year-1 and Beyond – BNL-52635
Volume 32 – RHIC Spin Physics V – BNL-52628
Volume 31 – RHIC Spin Physics III & IV Polarized Partons at High Q^2 Region – BNL-52617
Volume 30 – RBRC Scientific Review Committee Meeting – BNL-52603
Volume 29 – Future Transversity Measurements – BNL-52612
Volume 28 – Equilibrium & Non-Equilibrium Aspects of Hot, Dense QCD – BNL-52613

Additional RIKEN BNL Research Center Proceedings:

Volume 27 – Predictions and Uncertainties for RHIC Spin Physics & Event Generator for RHIC Spin Physics III – Towards Precision Spin Physics at RHIC – BNL-52596

Volume 26 – Circum-Pan-Pacific RIKEN Symposium on High Energy Spin Physics – BNL-52588

Volume 25 – RHIC Spin – BNL-52581

Volume 24 – Physics Society of Japan Biannual Meeting Symposium on QCD Physics at RIKEN BNL Research Center – BNL-52578

Volume 23 – Coulomb and Pion-Asymmetry Polarimetry and Hadronic Spin Dependence at RHIC Energies – BNL-52589

Volume 22 – OSCAR II: Predictions for RHIC – BNL-52591

Volume 21 – RBRC Scientific Review Committee Meeting – BNL-52568

Volume 20 – Gauge-Invariant Variables in Gauge Theories – BNL-52590

Volume 19 – Numerical Algorithms at Non-Zero Chemical Potential – BNL-52573

Volume 18 – Event Generator for RHIC Spin Physics – BNL-52571

Volume 17 – Hard Parton Physics in High-Energy Nuclear Collisions – BNL-52574

Volume 16 – RIKEN Winter School - Structure of Hadrons - Introduction to QCD Hard Processes – BNL-52569

Volume 15 – QCD Phase Transitions – BNL-52561

Volume 14 – Quantum Fields In and Out of Equilibrium – BNL-52560

Volume 13 – Physics of the 1 Teraflop RIKEN-BNL-Columbia QCD Project First Anniversary Celebration – BNL-66299

Volume 12 – Quarkonium Production in Relativistic Nuclear Collisions – BNL-52559

Volume 11 – Event Generator for RHIC Spin Physics – BNL-66116

Volume 10 – Physics of Polarimetry at RHIC – BNL-65926

Volume 9 – High Density Matter in AGS, SPS and RHIC Collisions – BNL-65762

Volume 8 – Fermion Frontiers in Vector Lattice Gauge Theories – BNL-65634

Volume 7 – RHIC Spin Physics – BNL-65615

Volume 6 – Quarks and Gluons in the Nucleon – BNL-65234

Volume 5 – Color Superconductivity, Instantons and Parity (Non?)-Conservation at High Baryon Density – BNL-65105

Volume 4 – Inauguration Ceremony, September 22 and Non -Equilibrium Many Body Dynamics –BNL-64912

Volume 3 – Hadron Spin-Flip at RHIC Energies – BNL-64724

Volume 2 – Perturbative QCD as a Probe of Hadron Structure – BNL-64723

Volume 1 – Open Standards for Cascade Models for RHIC – BNL-64722

For information please contact:

Ms. Pamela Esposito
RIKEN BNL Research Center
Building 510A
Brookhaven National Laboratory
Upton, NY 11973-5000 USA

Phone: (631) 344-3097
Fax: (631) 344-4067
E-Mail: pesposit@bnl.gov

Ms. Tammy Heinz
RIKEN BNL Research Center
Building 510A
Brookhaven National Laboratory
Upton, NY 11973-5000 USA

(631) 344-5864
(631) 344-2562
theinz@bnl.gov

Homepage: http://www.bnl.gov/riken

RIKEN BNL RESEARCH CENTER

RIKEN-TODAI Mini-Workshop on "Topics in Hadron Physics at RHIC"

March 23-24, 2004

Li Keran

Nuclei as heavy as bulls
Through collision
Generate new states of matter.
T.D. Lee

Copyright©CCASTA

Speakers:

H. Abuki	T. Doi	H. En'yo	Y. Hatta	M. Hira
T. Ikeda	N. Ishii	S. H. Lee	L. McLerran	K. Ohnishi
M. Ohtani	C. Sasaki	K. Sudoh	M. Tachibana	T. Takahashi

Session Chairs: H. Fujii, T. Hatsuda, K. Iida, and K. Yazaki
Organizers: H. En'yo, H. Hamagaki, T. Hatsuda, Y. Watanabe, and K. Yazaki